Development of a High-Strength Radial-Flow HEPA Filter

W. Bergman[1], G. Garcia[2] and C. Waggoner[3]

[1]Aerosol Science LLC, Stanwood, WA 98292
[2] Bechtel National Inc., Richland WA, (Retired)
[3] ICET, Mississippi State University, Starkville, MS

ABSTRACT

Bechtel National Inc (BNI) and its team of filter and media manufacturers, Aerosol Science (AS) and Mississippi State University (MSU) developed and tested a high-strength radial-flow HEPA filter that can withstand a differential pressure up to 50 inches W.C. by replacing the standard HEPA medium with a glass-cloth-reinforced HEPA filter medium from Lydall Inc. (Cambo et al, 1987) as was previously done with axial-flow HEPA filters (Reudinger et al., 1990; Gilbert et al., 1992). The project was sponsored by the Department of Energy (DOE) to address deficiencies found in the radial-flow HEPA filters using conventional HEPA filter designs and materials (Giffin et al., 2012).

Initially the goal was to develop a HEPA filter that can fit into existing filter housings at the Waste Treatment Plant (WTP) in Hanford, WA and also withstand pressures of 225 inches W.C. based on maximum fan pressures in the WTP. Two high-strength filter technologies were considered: a steel fiber HEPA filter and a reinforced glass fiber HEPA filter. However, the steel fiber HEPA was eliminated due to the high pressure drop from overcrowding the required amount of steel fiber medium into the defined filter dimensions. The initial prototypes of the reinforced glass fiber HEPA filter also failed for one or more of the following: high pressure drop due to overcrowding of the pleats from not using separators , structural failures from using insufficiently strong metal components, and low efficiency from insufficient medium area. Adding corrugated separators along with sufficient area of the reinforced glass fiber medium corrected two of the three problems, but the new prototypes used the standard AG-1 filter design components and not higher strength metal components and thus were not reliable at 225 inches WC. In addition, the gel-seal failed above 70 inches W.C., and although higher strength gels worked, they required much greater force to seal and would potentially introduce operational problems when installing and removing filters.

BNI re-evaluated the requirement of 225 inches W.C. for the maximum pressure drop and found that with typical mitigation strategies, the maximum pressure drop requirement for HEPA filters could be reduced to 50 inches W.C. This change allowed BNI to use the glass-cloth-reinforced HEPA filter medium in the standard AG-1 FK design with corrugated separators and added straps connecting the filter endcaps and the standard gel-seal. The resulting high-strength HEPA filter was qualified to all of the AG-1 required tests for the filter and medium with two exceptions: the remote-change filter had a pressure drop of 1.9 inches WC instead of the required 1.3 inches WC, and the high-strength HEPA medium had a combustible material of 8% by weight instead of the limit of 7%. Both of these exceptions were allowed in WTP.

BNI and AS worked closely with MSU to develop the test facilities and procedures for filter testing such as the high viscosity water flow system for testing filters at 225 inches WC. AS also provided the detailed design and test procedure for dioctyl phthalate (DOP) aerosol filter efficiency measurements for MSU to comply with DOE and AG-1 test standards. Other testing details involving particle loading and aerosol measurements were given in the BNI testing specifications.

A unique aspect of this filter development project was the development and use of test systems to measure the differential pressure, efficiency and particle loading capacity of the filter medium in addition to the filter. These additional tests enabled the project team to determine the effect of the pleat spacing and separators on the differential pressure, efficiency and particle loading capacity of the filter and also to determine the extent of filter leakage in the filters. This information was used in designing the filters to ensure a minimum efficiency of 99.97% for 0.3 microns DOP while striving for the lowest possible differential pressure and a particle loading capacity of 830 g for 2.5 micron particles which is comparable to commercial radial-flow HEPA filters (Loughborough, 1991).

INTRODUCTION

Background leading to the Development of High-Strength Radial-Flow HEPA Filters

The high-strength radial-flow HEPA filters were developed to address newly found deficiencies in commercial radial-flow HEPA filters that were planned for installation in a new facility to vitrify the radioactive waste at the Hanford Site in the state of Washington. This development evolved from the different approaches used by the various contractors over the years to process the waste and with the introduction of radial-flow HEPA filters by the British firm, BNFL

The Hanford Site in south-central Washington has accumulated about 53 million gallons of liquid and sludge waste stored in 177 tanks from the production of

Plutonium for nuclear weapons from 9 nuclear reactors beginning in 1944. Since the last of the reactors was shut down in 1987, the Hanford Site has had several contractors with different approaches for processing the tank waste and the associated off-gas treatment (Dagk et al, 2012). The initial approach examined by Westinghouse Hanford in 1989 was to vitrify the high level waste and grout the low level waste (Van Beek, 1990, Okemgbo, 2009, Dahl et al, 2012). The off gas from the proposed vitrification plant would use standard nuclear grade HEPA filters followed by deep bed sand filters, the default exhaust treatment system at Hanford at the time.

In 1991, DOE, Westinghouse Hanford, and Flour-Daniel conducted a study that indicated replacing the standard glass fiber HEPA filters and deep bed sand filter with steel HEPA filters was technically superior and cost effective (Flour Daniel, 1991). This study was initiated and based on the development of steel HEPA filters at the Lawrence Livermore National Laboratory (LLNL) for nuclear defense applications (Bergman et al, 1991). Although metal powder filters have been widely used in industry for many years, the Livermore Lab development was the first to demonstrate filters made from sintered steel fibers can be made to function like HEPA filters. Following this development, DOE began funding LLNL to further develop steel HEPA filters for applications in DOE facilities (Bergman et al, 1993a, 1993b, 1995, 1996, 1997a). Figure 1 shows a photo of the partially disassembled view of the two-stage steel HEPA filter that led to the Hanford steel HEPA study. Note that two stages of HEPA filter were used to meet health and safety requirements in a simple configuration.

Figure 1. Photograph of partially disassembled 2-stage, steel HEPA filter manufactured by Pall Corp. to LLNL specifications (Bergman et al, 1991). Air enters from the right inlet and flows through the outer side of the larger, first HEPA, then through the outer side of the smaller, second HEPA and exits at the left outlet. Two stages of HEPA filter are required by health and safety requirements for the intended application.

Westinghouse Hanford and Flour Daniel proceeded to design the exhaust ventilation system for the proposed vitrification plant using steel filter elements from Pall Corp. modeled after that shown in Figure 1, but with a diameter of 6 inches and a length of 16 inches (Grenwal et al, 1993). Three of the steel HEPA elements were joined to make a 6 inch diameter filter tube that was 48 inches long, and five of the filter tubes were mounted in a filter housing as shown in Figure 2. The resulting filter assembly is rated at 1,000 cfm with 2 inches WC DP. In contrast, the 1,000 cfm steel HEPA filter developed by LLNL has the standard HEPA dimensions, 24" x 24" x 12" and has a measured DP= 3.1 inches WC (Bergman et al, 1993a).

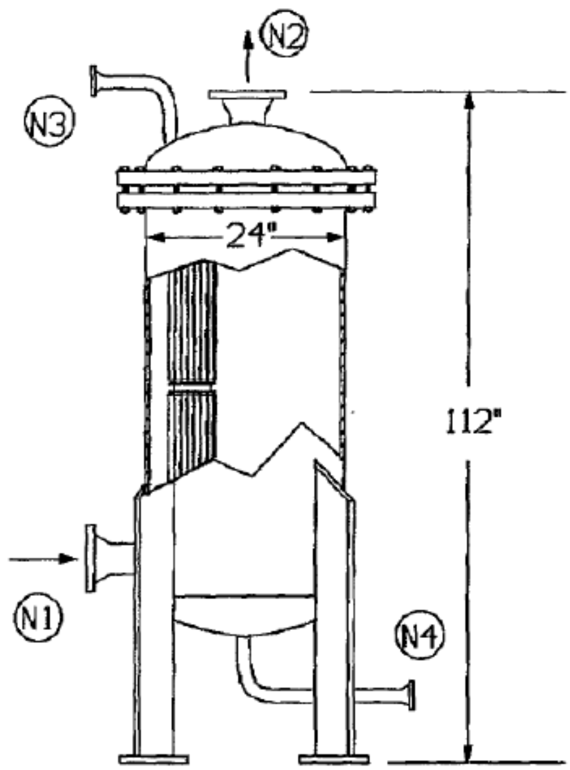

Figure 2. 1,000 cfm steel HEPA filter tube sheet assembly consisting of 5 filter tubes, 6" diameter and 48" long (Flour Daniel, 1991; Grenwal et al, 1993). N1: air inlet, N2: exhaust, N3: washing fluid inlet, N4: washing fluid drain. Design DP = 2 inches WC.

The plan for the Hanford vitrification plant and the steel HEPA off gas system was terminated in 1993 due to DOE budget limitations and the need to treat additional waste from the single-shell tanks (Dahl et al, 2012). A larger vitrification plant was then planned that required additional pre-treatment plant and vitrification facilities to process high level and low level waste in all 177 tanks. However, DOE soon began looking at privatizing the waste treatment and finally awarded the contract to British Nuclear Fuels Limited (BNFL) in 1996.

The replacement of Westinghouse Hanford with BNFL in 1996 resulted in major changes in the proposed vitrification design and in the off gas treatment. BNFL had incorporated the radial flow glass HEPA filters used in the British Sellafield Plant (ter Kuile et al,1999). However, in May 2000, after BNFL estimated they would spend more than $14 billion to complete the project, despite an earlier cost estimate of $7 billion, the DOE ended the BNFL contract. In December 2000, through a competitive contract bid, DOE awarded Bechtel National Inc. (BNI) a contract to design and construct the WTP project at DOE's Hanford Site in Washington State. Following the transfer of management, technical reviews of the BNFL design were favorable, and DOE therefore instructed BNI to continue with the same design (Dahl et al, 2012; Hedges, 2009) using commercially available glass-fiber radial-flow HEPA filters.

Bechtel used the BNFL design of a submerged bed scrubber, a wet electrostatic precipitator, a preheater, and HEPA filters to treat the exhaust from the low activity waste (LAW) vitrification melters (Anderson et al, 2000). The high level waste (HLW) vitrification melter used a similar exhaust system except a high efficiency mist eliminator (HEME) was used in place of the preheater (Rouse, 2000). The HEPA filters used in the offgas are modeled after the Vokes Air (Burnley Cancashire, UK) radial flow glass HEPA filters in two configurations: a remote-change design for HLW remote filter replacement and a safe-change design for LAW manual filter replacement (Navennti, 2002). Bechtel had contracted Flanders to develop the remote change and safe change filter housings and the two radial flow HEPA filter designs (i.e., safe change and remote change filter designs). Flanders did not use the Vokes design in which glass fiber ribbons were used to separate the filter pleats; rather, Flanders used embossed media to form dimples that separate the pleats as shown in Figure 3.

Although Flanders had conducted multiple informal ASME AG-1 type qualification tests using in-house test equipment and had shown the filters would meet all DOE requirements, the official tests were not yet conducted. DOE also had concerns that there was insufficient experimental data and field experience to ensure the new radial flow HEPA filters would perform their intended safety function in the WTP exhaust systems with actual temperatures and relative humidities that were higher than those parameters used in the ASME AG-1 qualification tests. As a result, DOE, with extensive input from Bechtel, Flanders, academia, users within the DOE complex, and the Defense Nuclear Facilities Safety Board contracted the Institute for Clean Energy Technology at Mississippi State University (MSU) to conduct an experimental study of the filter performance with particle loading under high temperature and relative humidity conditions expected in the WTP (Diaz, 2010).

The MSU tests were completed in December, 2011 and showed the Flanders filters suffer from pleat collapse and rapid increase in pressure drop on exposure to 130°F and elevated relative humidity (Giffin et al 2012). Reversible pleat collapse occurs when the pressure drop overcomes the medium stiffness and increasingly narrows the pleat channel until it closes. The narrowing of the pleat channels increases the pressure drop, which in turn narrows the channel ever further in a highly non-linear fashion and leads to the rapid increase in pressure drop as seen in Figure 4. The rapid increase in pressure drop in Figure 4 leads to filter medium rupture when the filter DP exceeded about 30 inches WC.

(A) (B) (C)

Figure 3. Flanders (A) 2,000 cfm remote change filter (top flange OD=21", filter OD=19 3/8" , inlet ID = 11.0", total L=25 ½", effective area =308 ft2), (B) close-up of outside pleats and (C) cut out portion of filter pack showing the 3" deep pleat with embossed dimples (Giffin et al, 2012).

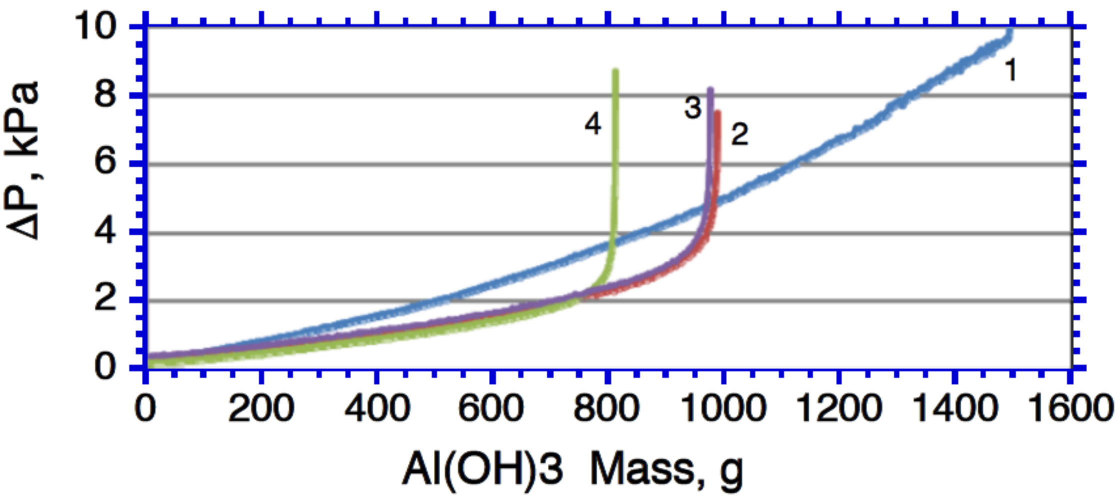

Figure 4. Loading of Al(OH)3 aerosols on different radial flow HEPA filters at 2,000 cfm and ambient laboratory conditions. (1) Vokes with ribbon separators, (2) Flanders remote-change with dimple pleats, (3) Flanders remote-change with dimple pleats, and (4) Flanders safe-change with dimple pleats. Pleat collapse in the Flanders filters is seen as the rapid increase in pressure drop with increasing particle load. (Giffin et al, 2012)

Pleat collapse and non-linear increase in filter pressure drop also occur with slightly loaded Flanders filters that are exposed to increased temperature and relative humidity as seen in Figure 5.

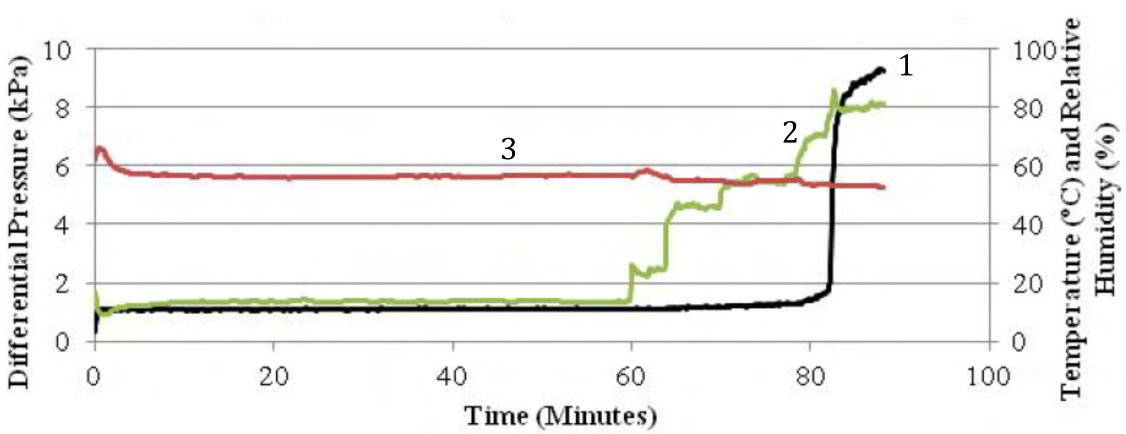

Figure 5. Temperature and relative humidity exposure to Flanders safe-change radial flow HEPA filter partially loaded with Al(OH)3 aerosols. (1) filter differential pressure, (2) relative humidity, (3) temperature. Pleat collapse occurs due to the softening of the medium at elevated temperature and higher relative humidity. (Giffin et al, 2012)

No pleat collapse or rapid increase in pressure drop was observed under similar conditions for the radial flow Vokes filter where the pleats are separated with ribbons of filter media (Giffin et al 2012). Waggoner (2012) showed that the pleat collapse and rapid increase in filter pressure drop also occurs for axial flow HEPA filters with no separators but does not occur for HEPA filters with separators. These studies confirm the early studies that show separatorless HEPA filters are significantly weaker than HEPA filters with separators (Gregory et al, 1982, 1983; Horak et al, 1982)

The DOE filter performance study alerted Bechtel to a major operational problem with the filters that would not have been detected until the WTP project became operational. Bechtel had assumed that the HEPA filter qualification tests specified in ASME AG-1 would be sufficient to ensure the Flanders filters would function properly up to 10 inches WC differential pressure. Unfortunately, the ASME AG-1 qualification tests cannot determine pleat collapse and the rapid DP increase seen in the DOE filter study. The DNFSB recognized the significance of Elaine (Diaz) Porcaro's work (DNFSB, 2012).

Formation of Project Team

Bechtel contracted two filter companies to help develop the high-strength radial-flow HEPA filters: Kurion, a small filtration service company in cooperation with Roome Technologies, a small filter fabricator and Porvair Filtration Group, an intermediate size filter company specializing in metal filters. Bechtel also issued a contract to the Institute for Clean Energy Technology, Mississippi State University (MSU) to develop the test facilities and to conduct the filter tests. And lastly, Bechtel contracted Aerosol Science LLC to provide technical advice on filter design and testing to its engineers and to the two filter companies and to MSU for filter testing.

METHOD

The development of the high-strength radial-flow HEPA filter required a detailed project plan to design, build and test the filter and to direct the work of two filter companies, Kurion and Porvair, and the filter test facility, MSU. In addition to using established test methods, several new filter test methods were developed and/or improved for this project. Although MSU had existing test facilities that were used to conduct the DOE sponsored tests of particle loading under elevated temperature and relative humidity conditions (Giffin et al, 2012), the following modifications and additions were required for the Bechtel project: the development of a high pressure liquid test system; the installation of a rough handling machine; the development of three different flat media testers for pressure drop, efficiency and particle loading; the development an ASME AG-1 test system for measuring filter efficiency and pressure drop; the development of a test system for particle loading under elevated temperature and moisture conditions and procedures for characterizing aerosol mass as a function of diameter and for characterizing particle deposits on the filters (Garcia, 2012b) . In addition Bechtel required that the MSU personnel, test equipment and procedures meet the requirements of NQA-1 (Phillips, K et al, 2016).

Project Plan

Following the findings from the MSU tests (Giffin et al, 2012) that showed the intended HEPA filters for the WTP plant were unacceptable, Bechtel developed separate plans to develop (Garcia, 2012a) and to test (Garcia, 2012b) the required HEPA filters. The first step in this effort was to establish the filter performance requirements and the test parameters by assessing the unmitigated, non-accident operating conditions in the WTP to which the HEPA filters could be exposed. The results from an extensive review are tabulated into three filter types shown in Table 1 (Weamer, 2012a).

Table 1. Summary of WTP maximum environmental conditions for HEPA filters.

	Filter 1-High RH, High T	Filter 2- Moderate RH, High T	Filter 3-Moderate RH, High T
Flow Rate, (acfm)	150-2000	300-2000	300-2000
Temperature, (°F)	90-150	50-170	50-200
Relative Humidity, (RH%)	70-100	2-80	2-80
Particle loading[1], (grams)	830	830	
Static Pressure[2] (negative, inches WC)	80-120	130-180	20

[1] Based on loading carbon black test aerosols on British radial flow HEPA filter to 10 inches WC from Loughborough (1990)
[2] The static pressure values are taken from the maximum values of the air blowers.

A common approach in nuclear facility design is to design the process with sufficient features (e.g., heaters, air treatment systems, etc.) to mitigate severe conditions at their source sufficiently to minimize degradation of the HEPA filters located downstream and thereby allow standard ASME AG-1 HEPA filters to be used. Alternatively, high strength HEPA filters (e.g., steel HEPA filters like those initially proposed for the Hanford vitrification plant, or HEPA filters using media with reinforced glass cloth) could be used to survive the unmitigated upstream conditions in Table 1. Bechtel chose the conservative approach of developing the high strength HEPA filter to accommodate uncertainties in the WTP operation (Weamer, 2012b). This approach also allows for greater flexibility in the WTP design and off-gas treatment systems.

The strategy for developing and testing the high strength HEPA filters was to contract filter manufactures to build HEPA filters to Bechtel's specifications and to contract a testing laboratory to conduct the required tests. Bechtel developed a specification for the HEPA filters modeled after the ASME AG-1, Section FK and included an appendix for steel HEPA filters adapted from the draft section FI of ASME AG-1 and an appendix for the high strength HEPA filter adapted from the draft section FM of ASME AG-1 (Garcia, 2012a). A key feature of the filter specification is that the filters had to fit into existing remote-change and safe-change filter housings. The HEPA filter specification document was revised multiple times as new issues arose with the filter development by the manufacturers and with testing by the testing agency.

Bechtel had recognized that the steel HEPA filter option as a disposable filter in the fixed ventilation design of the WTP would be far more expensive than the reinforced glass fiber HEPA filter, but no specific analysis was conducted. The use of steel HEPA filters in the 1992 design of the Hanford vitrification plant used in-situ filter cleaning to greatly reduce the high initial cost of the steel HEPA filers (Grenwal et al, 1993). The small waste stream from the cleaning would be added to the input to the vitrification process. A break-even analysis showed that steel HEPA filters were only economically viable in ventilation systems if the filters can be periodically cleaned and reused (Bergman et al, 1997a). Since in-situ cleaning was not possible in the WTP, then off-line cleaning would be required if the steel HEPA filter option were used.

Bechtel also developed a companion filter test specification for conducting tests that met both the standard ASME AG-1 requirements plus the additional requirements imposed by the conditions in Table 1 (Garcia, 2012b). Since the high pressure requirements in Table 1 imposed on a particle loading test at high temperature and high humidity in a single test system would require developing an expensive and complex test system, the environmental filter challenge was split into two separate tests: a high pressure liquid test and a particle loading test at elevated temperature and relative humidity.

A review of the test conditions in Table 1 also showed that the maximum pressures could be reduced with small changes in the WTP exhaust system to 30 inches WC in the safe-change filter system and 150 inches WC in the remote-change filter system. Adding a 50% safety margin yields 45 and 225 inches WC for the safe-change and remote-change systems, respectively. With these changes, Table 1 is converted into Table 2 for conducting tests. Note that 225 inches WC is also the maximum pressure rating for the filter housings.

Table 2. Pre-Qualification Tests

Filter	Liquid Pressure Test
Safe-Change	20[3] inches WC
Safe-Change	45[1] inches WC
Remote-Change	225[2] inches WC

[1] Value based on a maximum 30 inches WC in safe-change systems plus 50% margin.
[2] Value based on the maximum 150 inches WC for the remote change system plus 50% margin.
[3] An additional filter category of 20 inches WC was added for the Safe-Change filters after the testing had been underway for a number of months.

Filter testing was divided into two phases: a pre-qualification phase using the RLPTS to validate the manufacture filter design (Table 2) and a qualification phase that included the standard ASME AG-1 qualification tests plus the tests shown in Table 2 (Garcia, 2012b). Manufacturers were required to successfully pass the Phase 1 tests in Table 1 prior to commencing with Phase 2 tests. Phase 2 also included additional particle loading tests at ambient temperature and relative humidity conditions up to 50 inches WC plus an additional test of a filter preloaded with $Al(OH)_3$ powder and tested at elevated temperature and relative humidity to duplicate the loading tests conducted by MSU on the original Flanders filter (Giffin et al 2012). Initially the three test aerosols were $Al(OH)_3$, carbon black, and Arizona road dust; but the carbon black was later replaced with acetylene soot since the carbon black was about the same size as the $Al(OH)_3$ powder. The three test aerosols allowed for a variation in both particle size and particle morphology and density to bracket the range of potential normal, off-normal and accident conditions and to provide input for modeling filter loading.

A separate test requirement was added later to the test plan to measure the efficiency and particle loading on flat media, thus, enabling Bechtel and filter manufacturers to separate the performance of the filter medium from the filter design. Electron micrographs of the test aerosols and the particle deposits on the filter were planned to support the development of engineering model of the filter loading. These specifications were updated and revised as new information became available from the filter development and testing activities during the nearly 5 years of the project. DOE officials and their consultants took an active role and provided valuable contributions to the development of the two specifications and in the review of the test result.

A key aspect of the project plan was to measure and use fundamental filtration parameters to guide the engineering development (Garcia, 2012b). The fundamental parameters consisted of (1) the efficiency and pressure drop of the flat filter media as a function of velocity for air flow and pressure drop as a function of velocity for liquid flow, (2) particle loading on flat filter media to yield pressure drop vs particle mass deposits, (3) the number and mass size (sphere equivalent) distribution and the morphology (by electron micrographs) of the three test aerosols used for filter loading, and (4) characterization of the particle deposits on the flat filter media to determine the density of the deposits, the deposit thickness, and the morphology via electron micrographs of the deposits. The electron micrographs of the particles and filter deposits were needed to relate particle size measurements and macroscopic measurements (mass, pressure drop) to the microscopic nature of three different test aerosols used in this project. An inertial impactor was used to obtain the particle mass distribution as a function of size and validate the computed mass size distributions from aerosol instruments. In addition to guiding the engineering development, these fundamental parameters were intended for the development of an engineering model of the filter performance for use by Bechtel operational and safety engineers.

Figure 6 shows hypothetical examples of the pressure drop from different filter designs using the same filter medium (Garcia, 2012b). Filter A represents the ideal filter design where the filter pressure drop is primarily due to the medium. Filter B represents a filter where the filter design configuration has added additional flow resistance, e.g. due to narrow pleats that restrict the flow. Filter C represents a filter with significant inertial flow due to restrictive filter openings or filters that have pleat collapse and/ media compression. The flat filter media and full scale filters would be tested in different test stands.

Flat filter media tests were also planned for optimizing the filter design for maximum particle loading. The optimum filter design represents a compromise between the opposing factors of increasing surface area and decreasing pleat spacing. The particle loading capacity increases with increasing filter medium area. However, when the filter area is increased for the same exterior filter dimensions, the pleat spacing decreases and thus decreases the filter volume available for particle deposits. In the extreme example of maximum filter area, the pleats are in contact with each other (zero pleat separation); and, consequently, there is no space for particle deposits (zero particle loading capacity). In the other extreme of minimum filter area, there are no pleats and particle loading is limited to the small filter area. The maximum particle loading occurs between these two limits.

The filter test plan required that multiple filter holders having an isokinetic inlet tube should be installed inside the test duct and upstream of the large-scale filter so that the same aerosol used to load the large filter also loads the small filters (Garcia, 2012b). Each particle loading test consists of measuring the ΔP across the pleated filter and the flat medium. By having four separate flat medium samples weighed at different times during the loading test, one can generate the $\Delta P/V$ versus M/A line for the flat medium. The two $\Delta P/V$ versus M/A curves (filter and medium) can be used to optimize the particle loading by determining the optimum pleat spacing. Figure 7 shows a hypothetical case of three different filter designs have different pleat spacing.

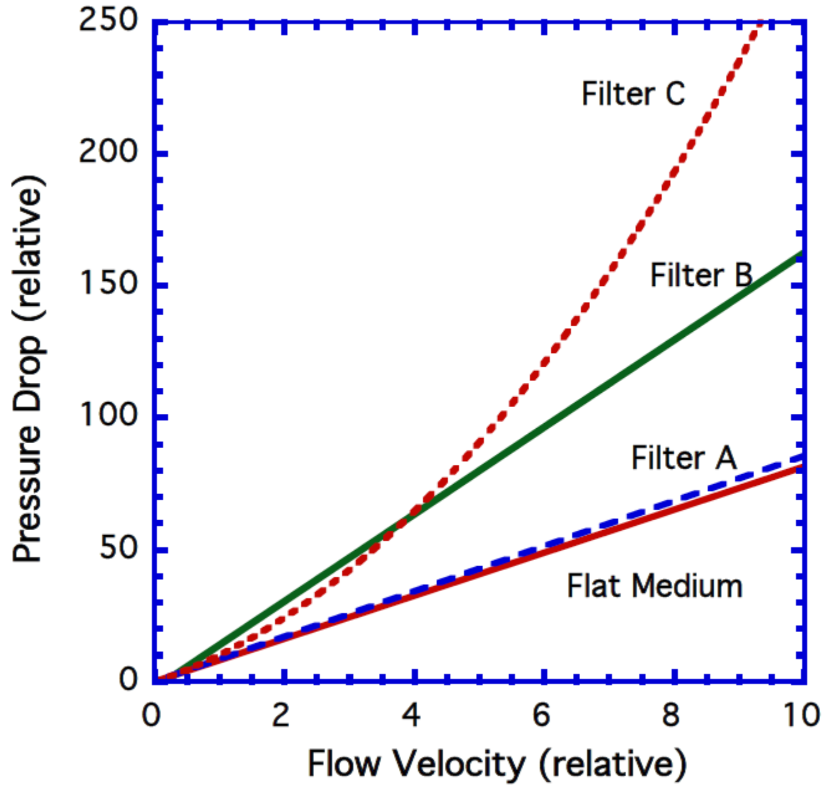

Figure 6. Example of potential test results of pressure drop measurements as a function of the flow velocity for flat medium and three different filters. Using flow velocity allows the pressure drop for filter medium and full-scale filters to be compared. (A) ideal filter design, (B) filter with additional flow resistance, e.g. due to narrow pleat spaces, (C) filter with inertial flow restrictions or pleat collapse and/or media compression. (Garcia, 2012b)

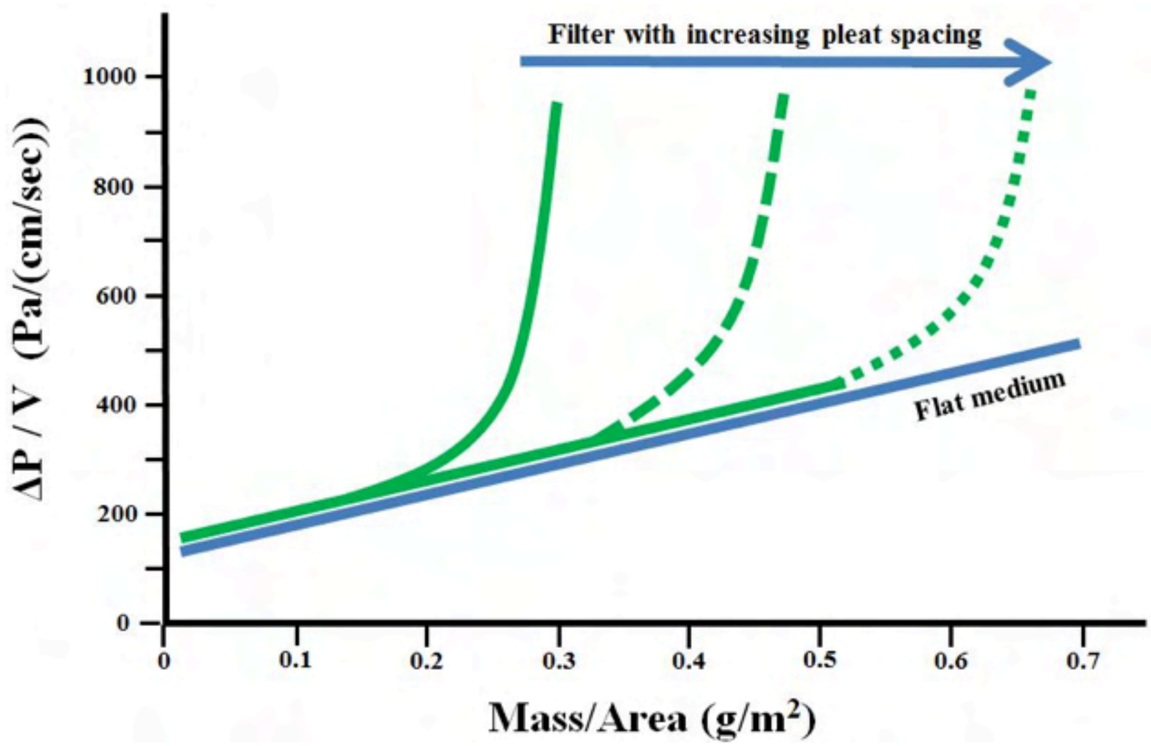

Figure 7. Filter loading on filters with three different pleat spacing and on flat medium. The pressure drop is normalized with respect to velocity (ΔP/V) and the particle loading with respect to filter area (M/A) to allow for direct comparisons of filter and medium loading (Hettkkamp et al, 2012; Garcia, 2012b)

Method for Measuring Resistance to Liquid Pressure Test System (RLPTS)

The development of the RLPTS shown as a schematic in Figure 8 was described by Garcia et al (2014), Unz et al (2014) and Wilson et al (2016). High pressure air systems are not practical because the low viscosity of air requires very large and expensive equipment. The RLPTS is modeled after widely used ISO Standards for testing hydraulic filter and is analogous to the current ASME AG-1 resistance to air pressure test, whereby the filter is exposed to 10 inches WC DP at 95% RH and 95°F for one hour. (Garcia, 2012b). Inspiration for the RLPTS was also provided by the early work of Dr. Ricketts on high pressure filter testers based on constant water flow systems (Ricketts et al, 1998, 2006). Figure 9 shows a photograph of the tester in the liquid test configuration with the inlet and outlet air ducts removed.

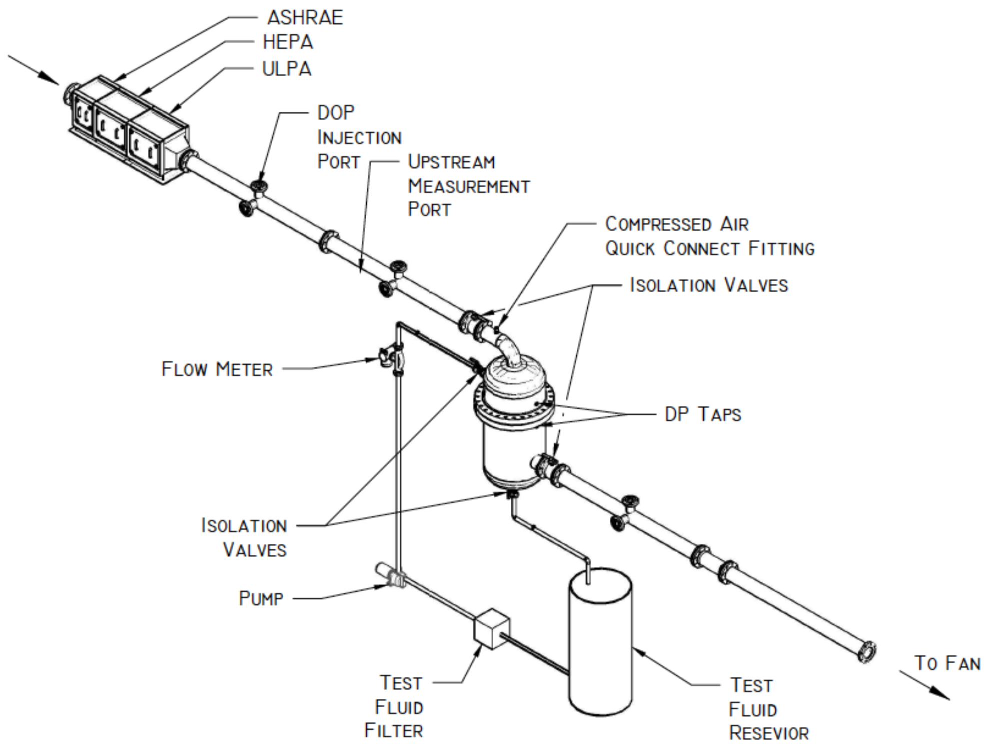

Figure 8. Schematic of the MSU full-scale resistance to liquid pressure test system (RLPTS) with water flow system for generating filter pressure and an air flow system for drying the filter and measuring DOP efficiency. (Unz et al, 2014)

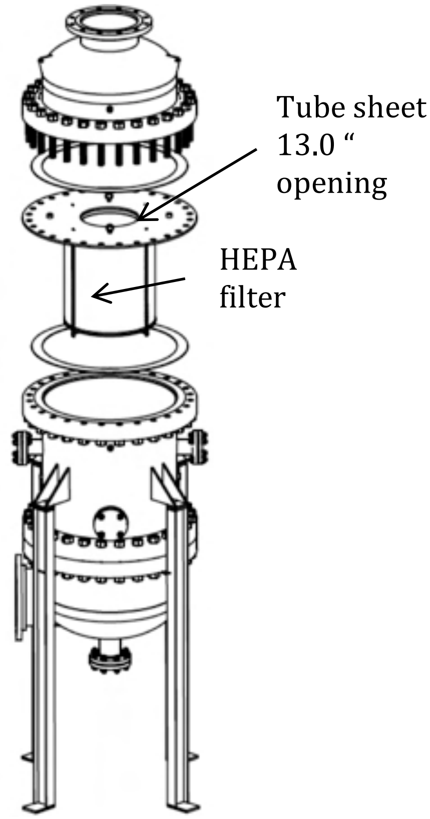

(A) (B)

Figure 9 Full-scale resistance to liquid pressure test system (RLPTS) (A) photograph of tester in the liquid test configuration with the inlet and exhaust air ducts removed, (B) schematic of filter holder disassembled showing the HEPA filter attached to a tube sheet with 13.0 inch inlet diameter. (Unz et al, 2014)

Ricketts et al (19998, 2006) had previously examined the use of a flowing water test system to apply high pressure to HEPA filters. Although the viscosity of water is much higher than that of air, it is not sufficient for higher pressures. Ricketts et al (2006) estimated that a water flow of 500 gallons per minute would only yield a filter differential pressure of 30 inches WC, and they abandoned the approach in favor of dropping a slug of water to obtain higher pressure pulses (Ricketts et al, 2008, 2010, 2012). Ricketts et al (1998, 2006) did not consider adding a high viscosity polymer to the flowing water test to increase the viscosity.

Bechtel and MSU had explored various options for the working fluid in the liquid pressure tester and had converged on a 50-50 weight percent solution of water/PEG8000 (Polyethylene Glycol-8000, Dow Chemical Co.), (Perry, 2013a). It was important to have water as a major component of the fluid to relate to the ASME AG-1 resistance to pressure test where the filter is subjected to 95% RH and 95°F and a differential pressure of 10 inches WC for one hour. ASME AG-1 also requires a tensile strength of the water soaked medium.

The temperature of the PEG-8000/water solution was initially intended to be 170°F to correspond to the WTP environment shown in Table 2, but MSU calculations showed that the housing heat capacity and heat loss would require an extremely large heater to bring the system to 170°F within one hour (Norton, 2013b). As a result, the liquid and system are heated to 95°F to match the ASME AG-1 conditions.

The procedure for testing the HEPA filter in the RLPTS evolved as new issues arose. Initially, the tester was used only to apply pressure to the filter, and a separate test duct was used for filter efficiency measurements as is done in the ASME AG-1 tests. However, the process of installing and removing the filter in two different systems was complicated using an overhead crane, time consuming, and prone to developing gasket leaks. Incorporating a separate air duct inlet and outlet greatly improved the testing efficiency and allowed measurements of air flow resistance and DOP efficiency to be determined before and after the high-pressure, liquid test. A test for verifying air leakage around the filter seal based on the ASME AG-1 pressure decay test was also added as the first test in the sequence of tests using the RLPTS (Unz et al, 2014). This test is described in greater detail later in this report.

The final procedure for testing the filter consisted of the following steps: install the filter using separate gaskets rather than the gel seal, perform a leak test on the gasket using the ASME AG-1 pressure decay test, measure the air flow DP versus flow from 250 cfm to 2000 cfm in 250 cfm increments, measure the DP and DOP efficiency at 2000 cfm, convert the test system from air to liquid with the filter still sealed to the housing, fill the chambers with the PEG/water solution, increase the liquid flow in increments to obtain a DP versus flow curve to the maximum 45 inches or 225 inches, maintain the filter DP at the maximum DP for one hour, drain the PEG/water solution, fill the tank with heated (100°F) clean water and rinse the filter , drain the water, convert the test system to air, pass heated air through the filter to dry the filter until the DP of the slightly wet filter at 20% flow is twice the initial dry filter DP at 20% flow, and measure the filter DP and DOP efficiency at 20% flow.

The pressure drop criterion (DP of the wetted filter is twice that of the dry filter) for the filter drying at 20% flow is based on 24 measured DP values for a variety of filters tested according to ASME AG-1 at the US Army Filter Test Facility at Aberdeen Maryland (Stillo, 2015). Although this criterion would provide a reasonable comparison with the ASME AG-1 test on resistance to pressure, it assumes that all the PEG has been removed from the filter, which was not observed in the initial tests. The residual PEG deposits on the filter effectively loads the filter and results in a higher DP and decreased efficiency due to increased effective medium velocity. Weighing the dried filter before and after the high pressure liquid test indicated the residual PEG that was not rinsed off the filter. The first test showed a residual mass of 730 grams, but with increased rinse, the residual mass was reduced to 74, 53, 257 and 147 grams in four subsequent tests. Tests on small scale flat media samples show deposits of PEG-8000 accumulated on the filter surface as seen in Figure 10. Although small scale tests on flat sheets show that all of the PEG can be removed from the filter and the filter pressure drop returned to the original value, the rinse procedure was not optimized for the full scale filter tests.

Figure 10. Photograph of metal fiber media after testing in the bench-scale tester with PEG/water solution and following drying. The PEG deposits are seen on the medium surface.

Another issue in the early tests with the PEG/water solution was the large variation in the measured viscosity as seen in Figure 11. The viscosity of the PEG/water solution would vary greatly with different preparations in the early tests prior to implementing adequate quality control, but the variation also occurs due to changes in molecular weight of different batches of PEG. The very low viscosity in Figure 11 for the full-scale preliminary test was due to improper tare measurements that resulted in low PEG concentration. The slightly higher viscosity in the 1st BSTS batch is probably due to water evaporation that increased the PEG concentration. Measurements of the viscosity using a Brookfield DV-E instrument showed the initial viscosity at 95 °F was about 212 cP while the measurement 3.5 months later in Figure 11 was about 220 cP. The cause for much higher viscosity in the 2nd BSTS solution is unknown. To mitigate the variation in viscosity, the procedure for testing flat media and full scale filters was modified to take a sample of the PEG/water solution before and after every full-scale and a single sample for each bench-scale filter test. The viscosity of the sample was measured with an Anton Paar viscometer over a range of temperature from 85°F to 105°F. By measuring the viscosity in the full-scale and bench-scale filter tests, the pressure drop measurements could be normalized with respect to the viscosity.

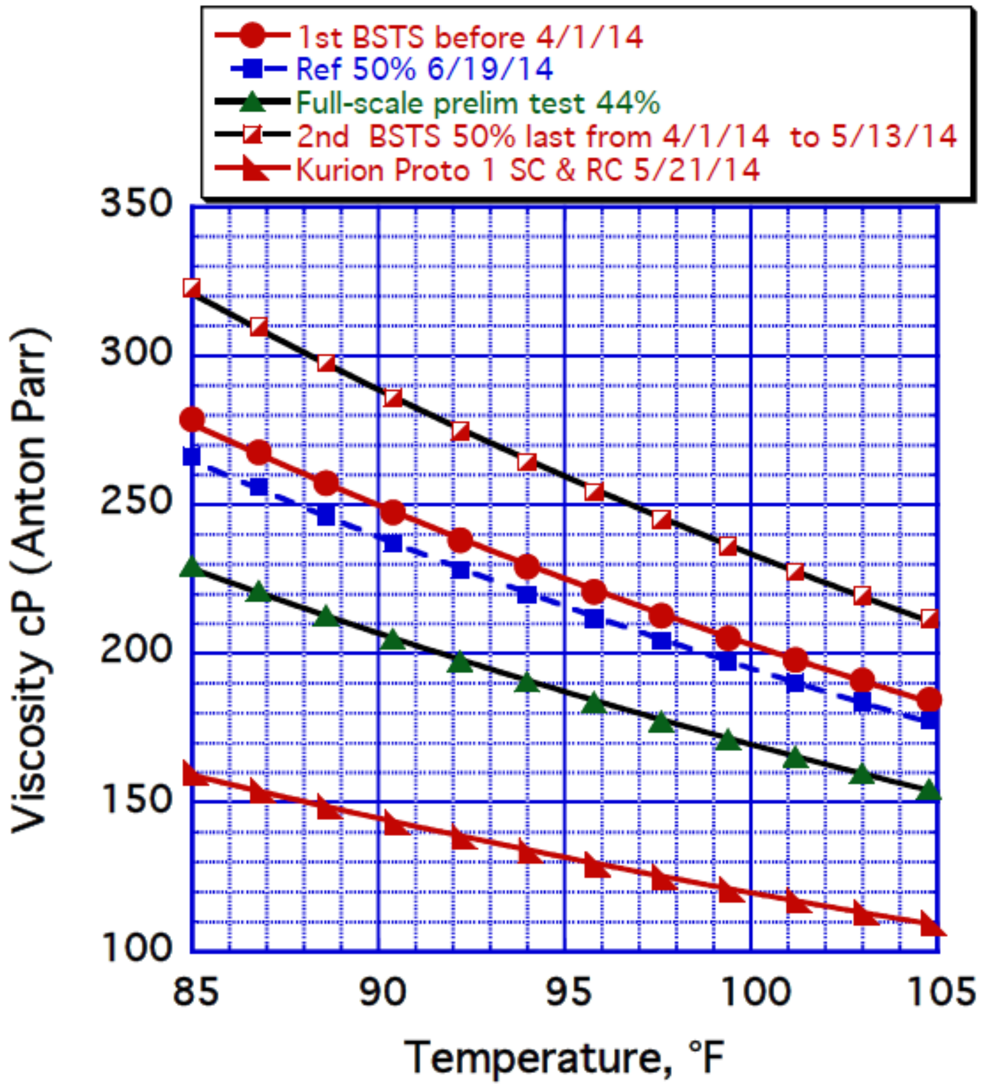

Figure 11. Variability in the PEG/water viscosity used in bench-scale tests for flat media and in full-scale tests for preliminary Kurion filters.

Note that MSU used the measured viscosity at the filter test temperature (typically 95°F) to correct the liquid flow for changes in viscosity due to temperature variations. Although this approach is correct when the filter pressure drop is directly proportional to the volumetric flow, this does not hold when the medium compresses or when the filters have an inertial contribution (e.g. due grab rings in the RC filter). Note that inertial effects due to liquid flow is negligible compared to air flow. To allow for direct comparisons for different filter designs and different fluids (air, water, PEG) the actual flows (and velocities) are used, and the pressure drop is corrected for viscosity changes.

Although the RLPTS was successful in testing prototype high strength HEPA filters, the test system has not been optimized for avoiding precipitation of PEG on the filters and the requirement for rinsing and for the prolonged drying time. Decreasing the PEG concentration from the current 50% to a level that avoids significant precipitation would require greater liquid flows and larger pumps to compensate for the decreased viscosity. This optimization effort could be conducted as part of an active filter test program.

Filter Seal Test Method

There are no separate performance standards for qualifying filter seals for leakage in the ASME AG-1 code (ASME AG-1, 2019) or in the DOE standards 3020 (DOE-3020-2105) and 3025 (DOE-STD-3025, 2022): the standards either state explicitly or imply that gasket leakage is measured in the efficiency tests. Tests conducted at the US Army test facility in Edgewood, MD and at DOE's ATI test facility in Baltimore, MD comply with these standards for gasket seals but not for gel seals. The ATI facility uses a neoprene seal against the HEPA filter gasket or gel seal channel in their test fixture but does not use a knife edge on any of the gel seals since that would be a destructive test. The Edgewood facility generally tests gel seals with a knife edge for HEPA filters since the tests are destructive tests. However, the Edgewood qualification tests on the radial-flow HEPA filters in this study were conducted using supplemental gaskets. In contrast, filter leak tests including gel-seals or gaskets are conducted for HEPA filters after installation in user facilities according to ASME AG-1 (2019) Mandatory Appendix TA-VI and ASME N-511 (2017) Mandatory Appendix III.

Previous tests conducted by Flanders using a special fixture shown in the schematic in Figure 12 (A) with two steel plates, one with a circular knife edge and a second with a circular channel containing the Blu-Jel, showed the gel seal is not effective beyond 70 inches WC since the gel blows out of the gel channel. (Peebles, 2003). The two steel plates in Figure 12 (A) were clamped together, and compressed air was increased in increments of 10 inches WC for 5 minutes and the pressure measured. At 80 inches the pressure could not be maintained, and the gel was partly blown out of the channel.

Flanders used the test fixture in Figure 12 (B) for testing the gel seal in radial-flow HEPA filters with the remote-change design, and the results showed there were no leaks over 16 hours at 16 inches WC vacuum (Urton, 2005). The gel-seal in a safe-change filter can be tested in a similar fashion using a different top plate with an integral knife edge and a vacuum or pressure port between the inner gel channel and an outer gasket.

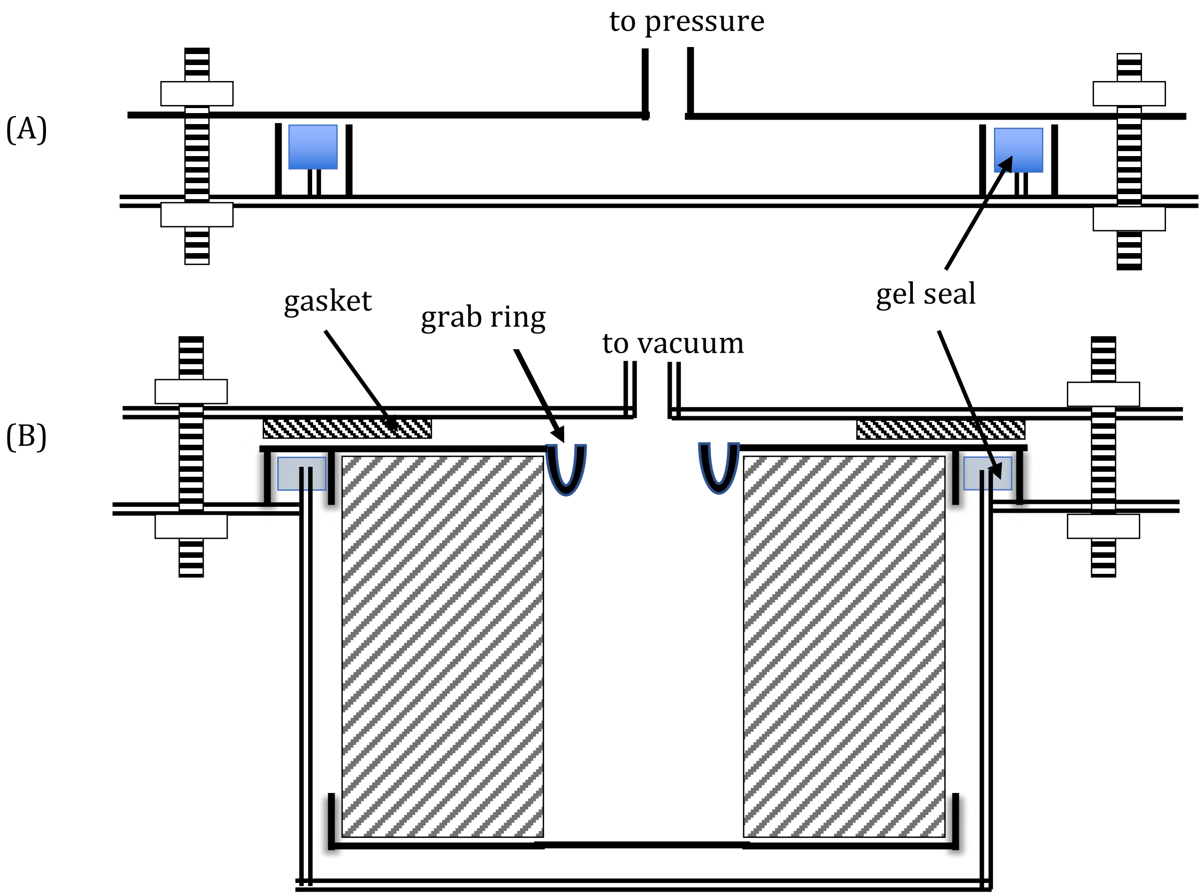

Figure 12. Drawings of test fixtures used by Flanders for determining leakage around the gel seals for (A) testing the gel material itself (Peebles, 2003) and for (B) testing the leakage in a radial-flow HEPA filter with the remote-change design.(Urton, 2005)

MSU proposed testing the gel-seal as an independent test using the general concept in Figure 12 (A) but using actual filter end plates with the integral gel-seals for the safe-change and the remote-change filters. However, BNI requested that the gel-seal leak test be performed on the complete filters as part of a sequence of tests in the RLPTS so that the seal would not be damaged when moving the filter to different test stands. This led to MSU developing and using an inflatable plug that blanked off the inlet throat of the radial-flow HEPA filter so that only the filter seal is exposed to the rated filter pressure. (Unz et al 2014). Figure 13 shows photographs of the inflatable filter plug unit that is inserted into the throat of the radial-flow filters. A metal tube inserted over a portion of the plug to prevent the filter pack from damage. The sleeved plug is inserted into the filter (Figure 13 (B)) and then inflated so that it touches the inner wall of the filter housing but not the tube sheet to which the filter is attached (Figure 13 (C)). This blinds the filter pack and isolates the filter seal to be tested for leaks at high pressure. Figure 14 shows a drawing of the inflatable plug used for testing the gel seal of a safe-change HEPA filter.

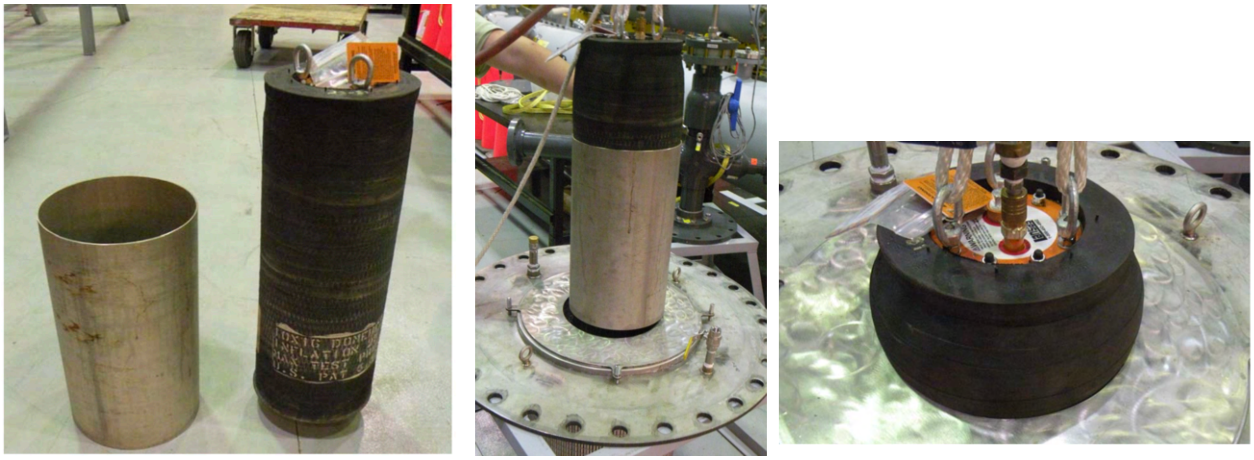

(A) (B) (C)

Figure 13. Photographs of the filter plug used to seal the throat of the remote-change radial-flow filter in test K-GFR-RC-001-Pre. (A) the inflatable plug with a protective steel sleeve, (B) filter plug with sleeve being inserted into throat of the remote-change filter (C) final installation with the plug sealed against the inside of the filter.

The leak test for the gel seal evolved as more experiments were conducted. Initially, the leak test illustrated in Figure 14 used an additional enclosure (top housing of the RLPTS in Figure 9 B) over the test section, and the top enclosure was filled with compressed air to the desired pressure and the pressure decay measured for one hour. Using the inflatable plug on a remote-change filter and applying 244 inches WC to the seal in test, K-GFR-RC-001-PRE, resulted in structural damage to the filter and caused the filter pack to separate from the top filter plate. In. a subsequent teston a safe-change filter, K-GFR-SC-001-PRE, the applied pressure deflated the filter plug and allowed the compressed air to by-pass the plug seal, thus invalidating the test. Following these tests, the approach using the filter plug was abandoned and alternative procedures were adapted.

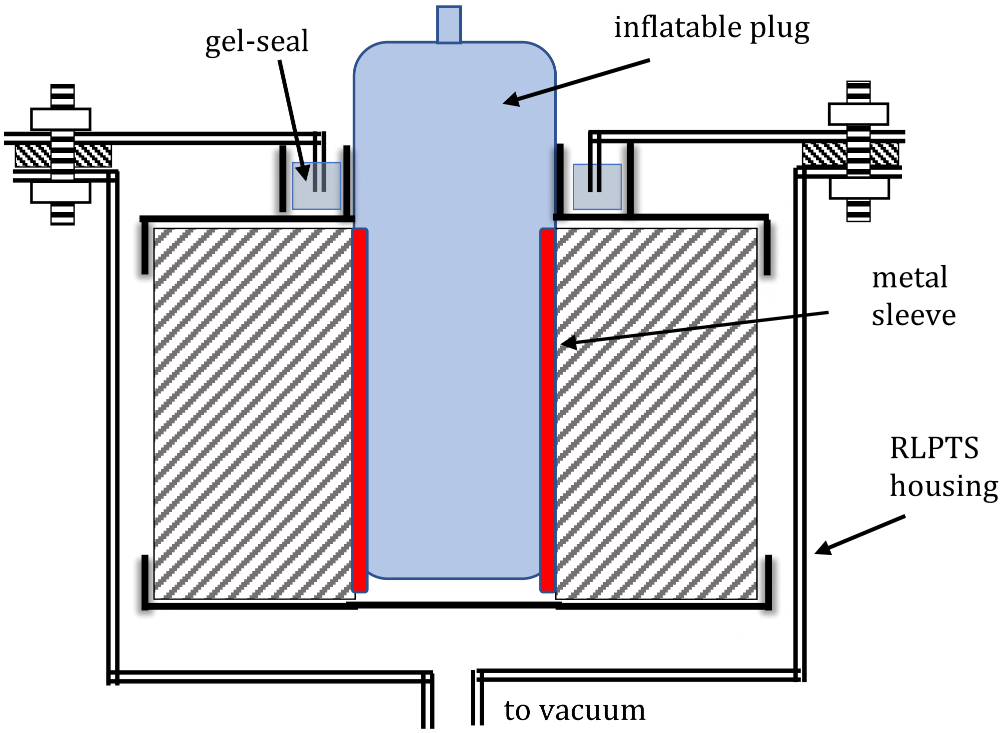

Figure 14. Drawing of inflatable plug inserted into the throat of a safe-change filter for testing gel-seal leak testing. The metal sleeve around the lower portion of the plug prevents damaging the filter pack.

Subsequent tests for the both the safe-change and the remote-change filter eliminated the top housing and used vacuum instead of pressure. For remote-change filters, the gel seal was tested using the test configuration shown in Figure 15. where a metal disk was sealed to the filter inlet using silicone and/or vinyl tape. For safe-change filters, the test configuration in Figure 14 was used, but the inflatable plug was replaced with the filter blank shown in Figures 16 and 17. The filter blank is inserted into the inlet throat of the safe-change filter, and the adjustable expansion seal tightened against the outside surface of the gel-seal channel. The leak rate for a prescribed vacuum was determined using the procedure in AME AG-1 TA-III-4200 for both the safe-change and remote-change HEPA filters.

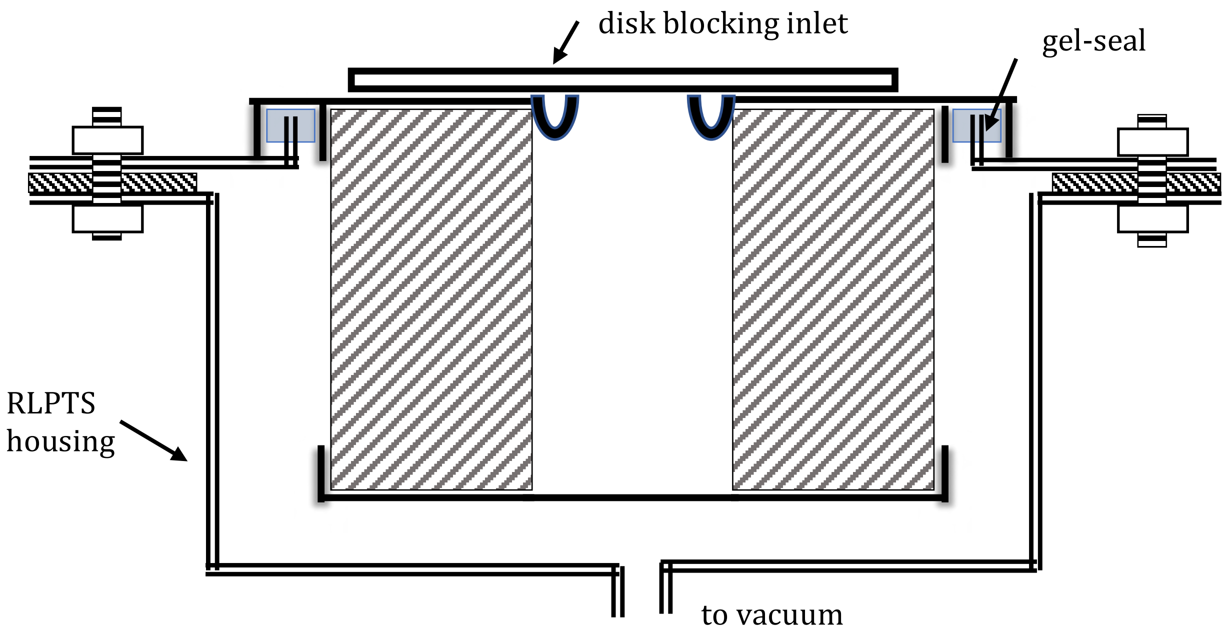

Figure 15. Drawing of test configuration for testing the leakage of the gel-seal of the remote-change HEPA filter with the filter inlet throat blocked with a metal disc sealed to the filter with silicone and/or viny tape.

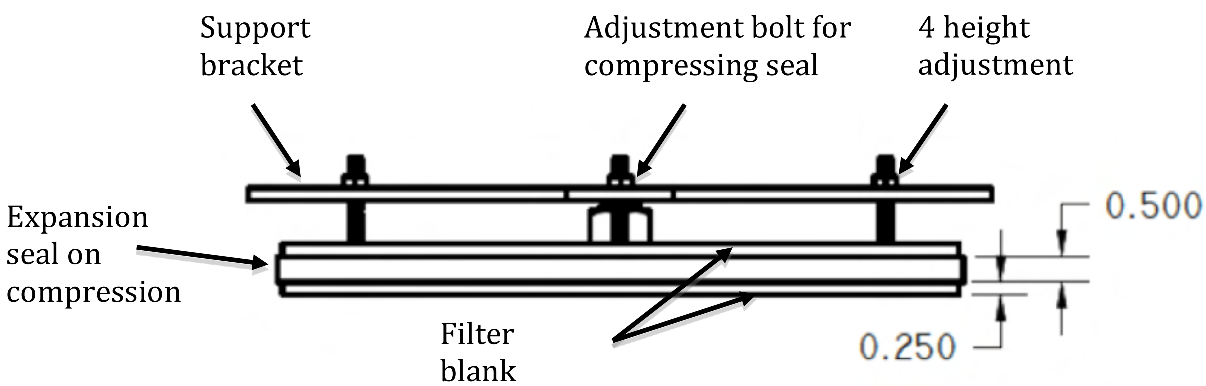

Figure 16. Side view of the filter blank used to blank off the inlet air flow to the remote-change HEPA filter. The expansion seal is compressed and expands to seal the filter blank against the inside surface of the HEPA filter by turning the adjustment bolt. Height adjust bolts are used to position the blank plates within the annular opening of the HEPA filter.

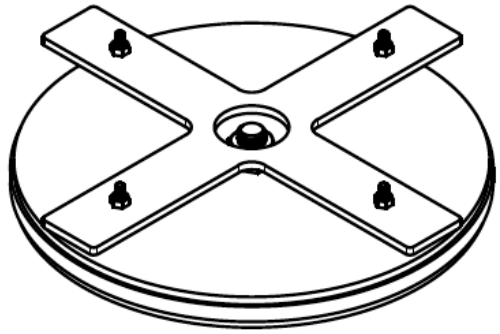

Figure 17. Perspective view of the filter blank used to blank off the flow to the remote-change HEPA filter.

Rough Handling Test

MSU installed a commercial rough handling machine in a sound-proof enclosure shown in Figure 18. The machine follows the requirements of ASME AG-1 Section FK 5130 to shake the filter in a vertical amplitude of ¾ inch at 200 cycles per minute for 15 minutes.

Figure 18. Photograph of Kurion K1-GFR-RC-001 filter mounted on the MSU rough handling machine.

Bench Scale Test System (BSTS) for Pressure Drop Measurements in Liquid and Gas Flows

The first of the three different flat media testers developed in this project was the bench-scale test system (BSTS) shown in the photographs in Figure 19 and in the schematic in Figure 20.

The BSTS shown in Figure 19 (A) consists of a filter holder with associated equipment and sensors for measuring the pressure drop across flat filter samples as a function of flow rate for liquids and gases and is mounted in an enclosure that can be heated to allow for tests at elevated temperature at 95°F. Photograph (B) shows the open downstream side of the filter holder with a support screen (4.72 inches diameter) welded to the holder in a recessed notch (0.14 inches wide), a recessed section where a test filter (6.10 inches diameter) is placed over the support screen and the perimeter filter sealing surface (0.69 inches wide), and an O-ring (6.51 inches inside diameter). The O-ring in photographs (B) and (C) is used to seal the housing and not the filter medium. Photograph (C) shows a test filter placed in the filter holder with a superimposed compressible sealing gasket (0.063 inch thick and 6.10 inches OD and 4.44 inches ID). Although the filter holder was designed to have the effective filter test diameter be the same as the 4.44 inches ID bore of the filter holder, the welded section of the support screen allows for a small by-pass thus increasing the effective diameter of the filter to 4.70 inches, nearly the same as the support screen, 4.72 inches.

The BSTS in Figures 19 and 20 was initially used to obtain experimental parameters to support the design and operation of the high pressure liquid tester in Figures 8 and 9. Subsequently, BSTS was used to generate curves of DP versus medium velocity to support the development of the high strength HEPA filters and the analysis of their performance. Figure 21 shows the two initial measurements of the Lydall HEPA glass fiber medium 3398-L1W (one layer of glass cloth laminated to the standard 3398 HEPA medium) using the BSTS plus the average of many tests of the same filter on the vertical test stand (VTS).

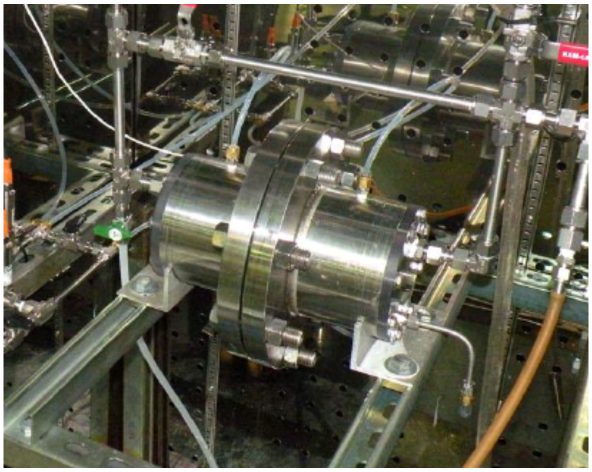

(A)

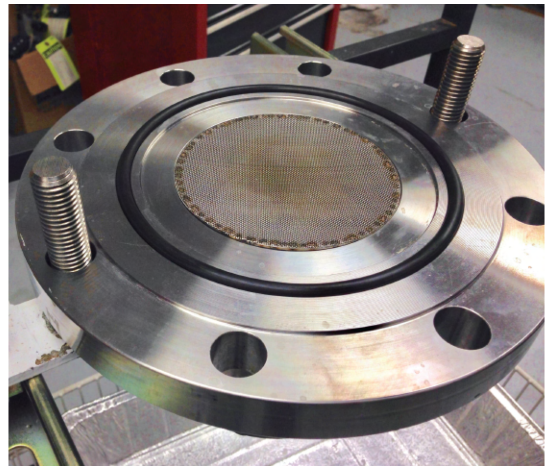

(B)

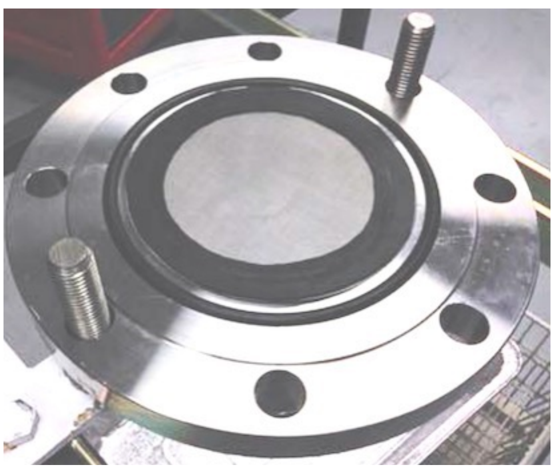

(C)

Figure 19. Photographs of (A) the bench-scale filter test system (BSTS) with a filter holder and connecting tubes for measuring the pressure drop through flat filter samples at various flow rates using liquids or air (B) the open filter holder (exit side) showing the screen filter support and O-ring and (C) the open filter holder (exit side) with a test filter with compressible sealing gasket (Unz et al, 2014)

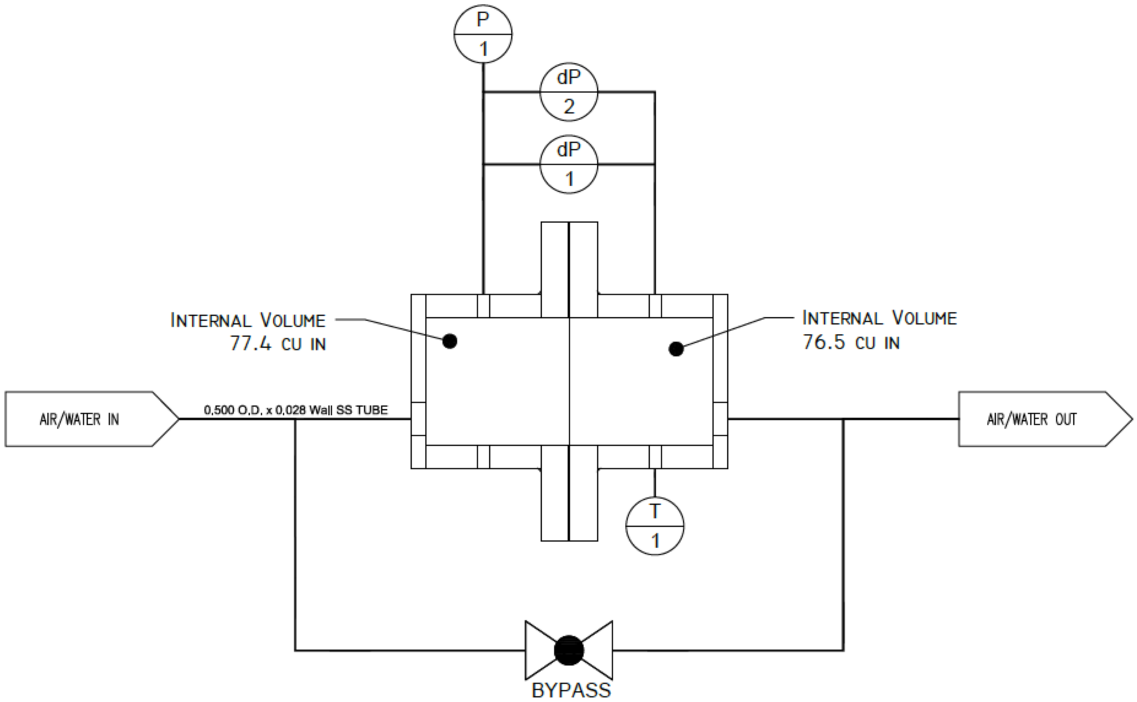

Figure 20. Schematic of the bench scale test system (BSTS) used for air and liquid pressure measurements at various flow rates. The ID and OD of the filter holder are 4.44 inches and 6.00 inches respectively.

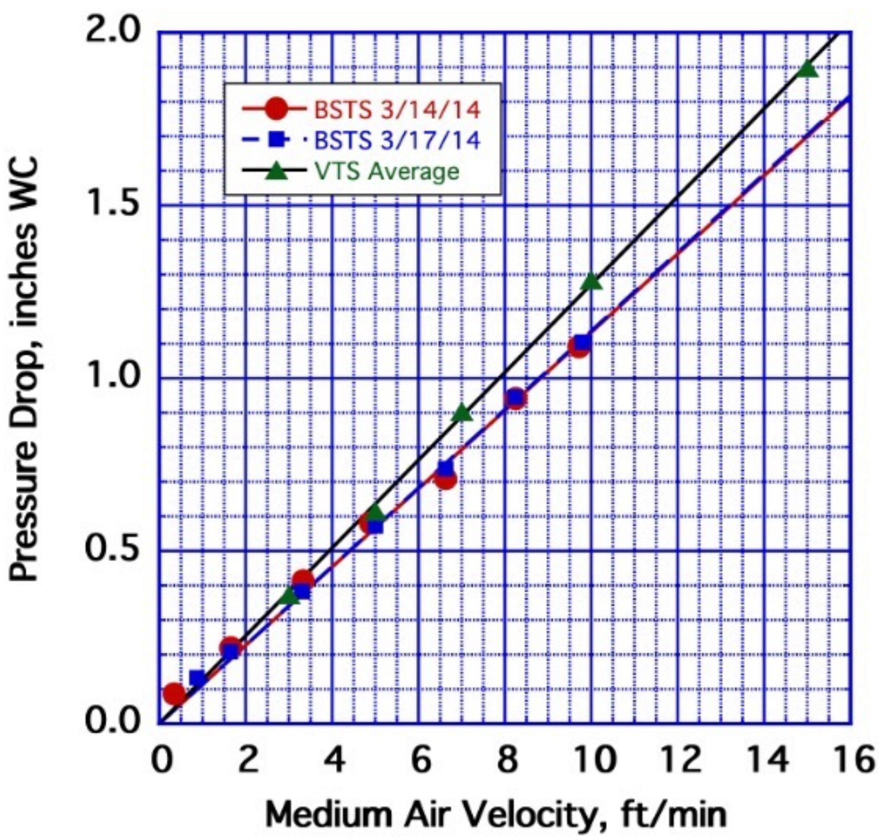

Figure 21. Pressure drop measurements of Lydall HEPA filter medium 3398-L1W as a function of medium air velocity for the BSTS and VTS. The BSTS pressure drop measurements are lower than the corresponding VTS measurements due to by-pass leakage around the support screen perimeter in Figure 19 (B). The scatter of 4 data sets for the VTS data is less than the symbol of the average.

Figure 21 shows excellent repeatability for the results from each of the two test systems; however, the BSTS has a lower pressure drop than the VTS. The deviation was found to be due to the different designs of medium clamping used in the two systems. The BSTS in Figure 19 (C) used a single compression gasket on the upstream side of the filter sample while the downstream side was compressed primarily against a flat surface of the flange plus a small portion of the support screen seen in Figure 19 (B). The lack of a gasket on the downstream side of the test filter allowed for leakage around the 0.14 inches perimeter of the support screen that is welded to the housing flange and does not provide a smooth surface for sealing. In contrast, the VTS system used Teflon gaskets on both sides of the test filter to ensure a good filter seal. It is possible that the single compression gasket in Figure 19 (C) could have prevented by-pass leakage if the gasket were on the downstream side of the filter against the support screen; however, no tests were conducted to confirm this. The preferred option is to use Teflon gaskets on both sides of the test filter as is done with the VTS. The filter air velocities in Figure 21 were computed from measured flow rates and the ID of the pipes (4.44 inches for the BSTS and 5.80 inches for the VTS). The use of double gaskets for the VTS ensured no by-pass leakage while the single gasket on the upstream side introduced a small leak. In addition, the BSTS data in Figure 21 had a small non-zero offset of 0.038 inches WC with no flow.

Since the pressure drop of the Lydall 3398-L1W medium in Figure 21 should be identical at the same air velocity for both the BSTS and VTS, the computed air velocity in the BSTS must be in error and the correct air velocity determined from Equation 1 using the VTS slope of 0.127 inches WC/ft/min as a reference. The slope of the BSTS data in Figure 21 is 0.113 inches WC/ft/min when the line is forced through 0 and not to the best fit.

$$\Delta P_M = 0.113\, V_{BSTS} = 0.127\, V_{X,BSTS} \tag{1}$$

where ΔP_M = pressure drop across medium
V_{BSTS} = computed medium velocity in the BSTS assuming D=4.44 in.
$V_{X,BSTS}$ = computed medium velocity in the BSTS assuming D= X in.

The coefficients, 0.113 and 0.127, in Equation 1 are the slopes of the graphs in Figure 21 for the BSTS and the VTS, respectively. Recognizing that V = Q/A, where Q= volumetric flow rate and A= filter area, and that Q is constant for both V_{BSTS} and $V_{X,BSTS}$, Equation 1 becomes.

$$\Delta P_M = 0.113\, \frac{4Q}{\pi D_{BSTS}^2} = 0.127\, \frac{4Q}{\pi D_{X,BSTS}^2} \tag{2}$$

Rearranging Equation 2 yields

$$D_{X,BSTS} = \sqrt{\frac{0.127}{0.113}}\, D_{BSTS} = \sqrt{\frac{0.127}{0.113}}\, 4.44 = 4.70 \tag{3}$$

Thus the effective diameter of the filter media tested in the BSTS is 4.70 inches, which is greater than the BSTS bore diameter of 4.44 inches and is nearly the diameter of the support screen of 4.72 inches, thus demonstrating that the increased effective diameter of the test filter is due to leakage around the edges of the support screen. The 4.70 inches diameter is used to re-compute the effective air velocity in the BSTS tests shown in Figure 21, and the results are plotted in Figure 22. The good agreement of the BSTS results with the VTS results verifies that the calculation of 4.72 inches for the effective BSTS medium diameter is correct and was therefore used in all of the BSTS tests. Figure 22 also shows additional pressure drop measurements on the Lydall 3398-L2W medium with glass cloth glued to both sides and additional screens on both sides. Future improvements of the BSTS design should include gaskets to define the effective medium diameter as the internal duct diameter of 4.44 inches and thereby avoid the ambiguity with velocity determination described here.

Another experimental issue with the BSTS was occasional non-zero values for the measured pressure drops at zero flow. These errors were corrected by adding or subtracting a small constant value to the experimental values. The cause of these intermittent errors was not determined.

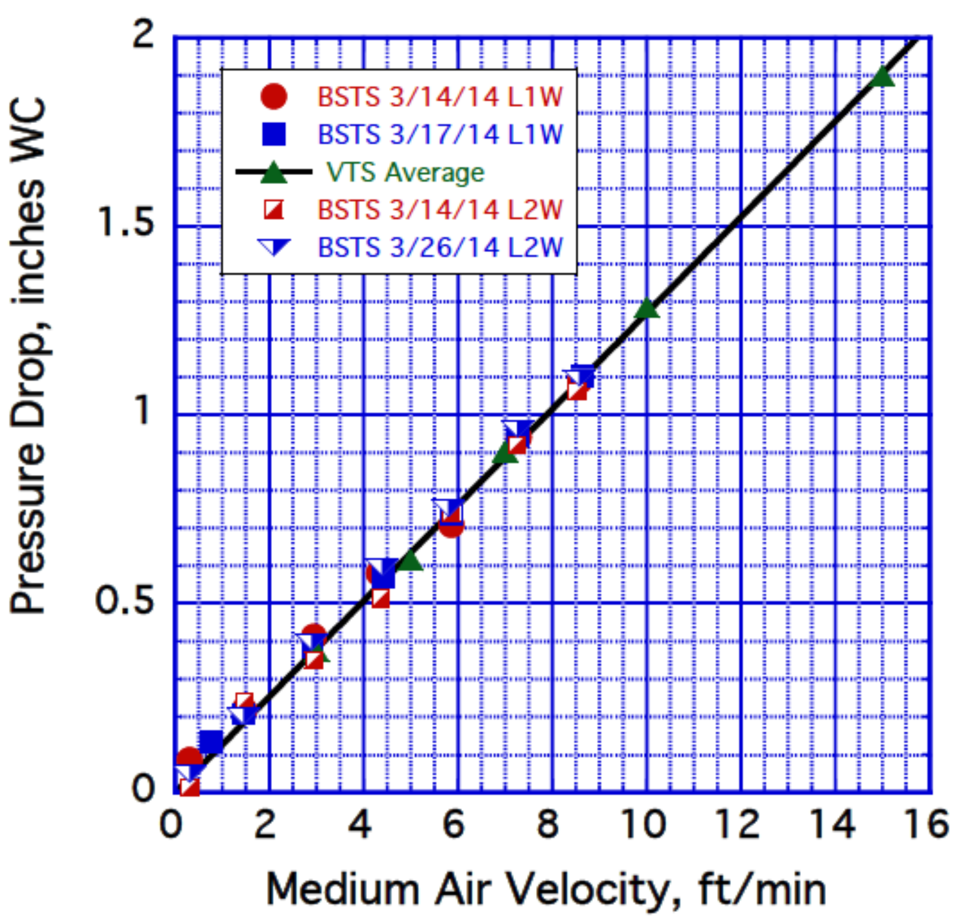

Figure 22. Pressure drop measurements for the Lydall HEPA filter medium 3398-L1W as a function of medium air velocity using the BSTS and VTS from Figure 21 plus the pressure drop measurements for the 3398-L2W medium sandwiched between screens using the BSTS. The BSTS velocity is computed assuming a medium diameter of 4.72 inches. The slope of the VTS average line is 0.127 in. WC/ft/min (6.23E3 Pa/m/s). Air viscosity is 0.0185 cP (1.85E-5 Pa s) at the average temperature of 23°C.

From Figure 22 it is observed that the pressure drops across the two filter media (3398-L1W without screens and the 3398-L2W with screens) in air are essentially equal and linear with velocity for the range of values tested and can be approximated by Equation 4. Although the added glass cloth of the 3398-L2W medium and additional wire screens should have a slightly higher pressure drop than the 3398-L1W medium, the increase is less than the experimental variability of the measurements.

$$\Delta P_M = K_M \, \eta V = \frac{\eta}{k_M} \, T V \qquad (4)$$

where ΔP_M = pressure drop across the filter medium
η = viscosity of the fluid in the medium test
V = velocity of the fluid
K_M = a constant depending on the filter structure (e.g., Thickness, fiber diameter, fiber packing density, etc.) Note $K_M = T/k_M$.
T = medium thickness
k_M = permeability of the medium

The value of k_M for the Lydall 3398-L1W and 3398-L2W media was determined using Equation 4 and the data in Figure 22 and the effective medium thickness of 0.0177 inches (4.50E-4 m) to yield 1.33E-12 m^2 after converting the units to metric.

Equation 4 is generally referred to as Darcy's Law and is found in the literature with the medium permeability, k_M , explicitly shown in the right hand side of the equation rather than lumped with the medium thickness, T, in the left hand side of the equation. However, since the HEPA filter media analyzed in this report is highly compressible, thereby changing both k_M and T when compressed, the two parameters are lumped together. It is not experimentally practical to measure the thickness of the compressed medium during the pressure drop measurements.

Equation 4 is based the assumption that the permeability of the medium, k_M, is independent of the fluid and only depends on the properties of the filter medium (e.g. fiber diameter distribution, fiber packing density, fiber packing inhomogeneity, etc). Although this has been demonstrated for liquids, it is not true for gases due to slip flow, whereby the filter has a reduced flow resistance (i.e. momentum transfer of the gas molecules with the filter fibers) due to the discontinuous nature of gas, especially for very small fibers as occur in HEPA filters. Recent studies on slip flow in HEPA filters (Choi et al, 2017; Bao et al, 2016) have used an empirical equation developed by Kirsch et al (1973) given in simplified form by Equation 5.

$$\Delta P_M = \frac{\eta T V}{k_M} = \frac{\eta T V}{f(\alpha, d_F)\left(1 + g(\alpha) Kn\right)} = \frac{\eta T V}{k_{M0}\left(1 + g(\alpha) Kn\right)} \tag{5}$$

where $f(\alpha,d_F)$, $g(\alpha)$ = functions of the filter medium structure
α = filter medium fiber volume fraction
d_F = filter medium fiber diameter
Kn = Knudsen number $= \lambda/d_F$
λ = mean free path of gas molecules
k_{M0} = filter medium permeability in liquids

Equation 5 shows that the medium permeability, k_M, is given by

$$k_M = k_{M0}\left(1 + g\, Kn\right) \tag{6}$$

Equation 6 shows that the permeability, k_M, increases with increasing Knudsen number due to gas slip.

The thickness of the medium, T, used in Equations 4 and 5 does not include the glass cloth since it has a negligible pressure drop, and the geometry of the cloth differs greatly from the Lydall 3398 medium. Thus the T in Equations 4 and 5 corresponds to the Lydall 3398 thickness of 0.0177 inches (Ricketts et al , 2008).

The functions $f(\alpha,d_F)$ and $g(\alpha)$ and the Knudsen number, Kn, are not required for the current analysis and are included here only for completeness with the literature and to illustrate the effect of slip. The mean free path of air under ambient temperature and pressure conditions is 0.066 microns (Jennings, 1988). Since a typical HEPA media uses a mixture of fibers having a range of diameters from 0.2 to 3 microns, with the submicron diameters used primarily for the higher efficiency, (e.g. see Clarenburg and Schiereck ,1968), the Kn value can vary from 0.03 to 0.3 with an average about 0.1. These small diameter fibers cause sufficient air slippage to increase the permeability and hence decrease the pressure drop.

Since liquid molecules are essentially in contact with each other, the mean free path for molecules in liquids is approximately the distance between their centers, or about 0.0001 microns. This value is so much smaller than the mean free path of air (0.066 microns) that the Knudsen number is essentially 0 and $k_M = k_{M0}$ for liquids.

The Lydall high-strength HEPA filter media, 3398-L1W and 3398-L2W, were also tested for resistance to water in the BSTS in Figures 19 and 20 and the results shown in Figure 23.

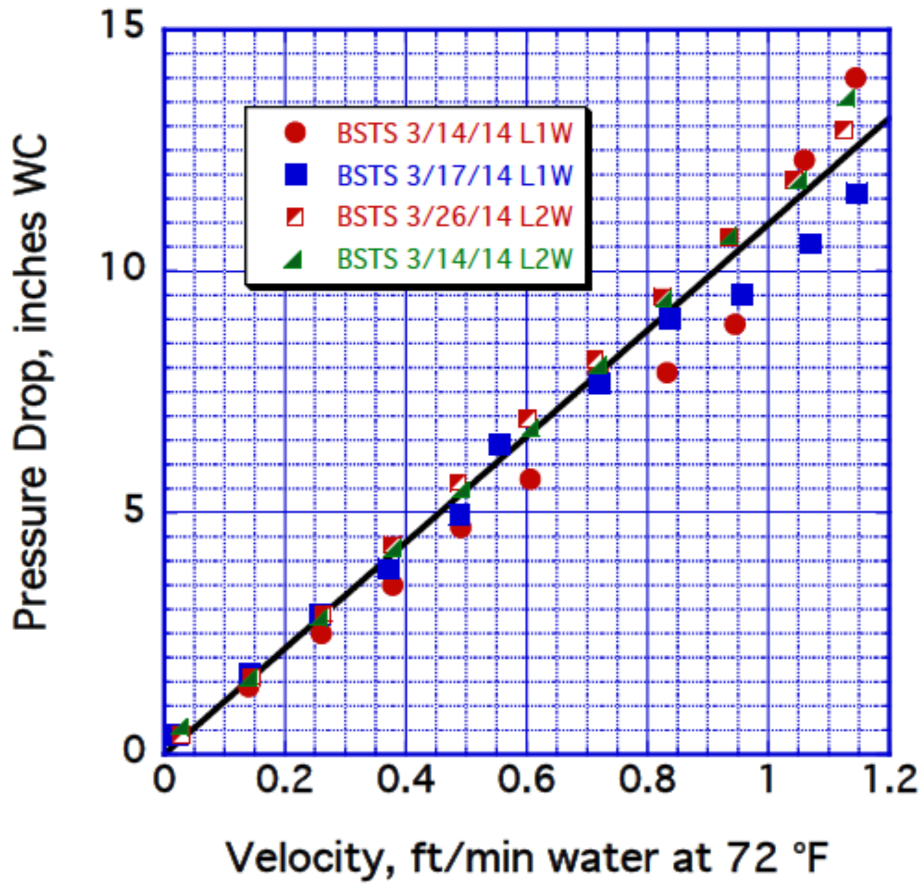

Figure 23. Pressure drop measurements of Lydall HEPA filter media 3398-L1W and 3398-L2W with front and back wire screens as a function of medium water velocity for the BSTS. The BSTS velocity is computed assuming a medium diameter of 4.72 inches. The slope is 10.98 in. WC/ft/min (5.38E5 Pa/m/s) and represents the best fit to all the data.

Using Equation 4 and the slope of the curve 10.98 in. WC/ft/min (5.38E5 Pa/m/s), from Figure 23; the viscosity of water at 72 °F, 0.953 cP (9.53E-4 Pa s); and the medium thickness, 0.0177 inches (4.50E-4 m); yields, k_M = 7.96E-13 m^2. The corresponding value for K_M = 11.52 in. WC/(ft/min)2/cP (Note that the permeability for the same medium in air (k_M= 1.33E-12 m^2) is 68% greater due to the effect of slip.

Air bubbles were encountered in the water and PEG/water tests and would confound the measured pressure drop. The presence of air bubbles in the water could accumulate on the filter and thereby increase the filter pressure drop due to decreased available medium area. To mitigate the problem with air bubbles, all pressure drops were measured only after the filter was completely wetted and no air bubbles were observed.

The final tests on the Lydall 3398-L1W and 3398-L2W media were with a 50% water solution of PEG-8000 and are shown in Figure 24. In contrast with the previous two tests, the tests with the PEG/water solution show a distinct non-linear response to the increased pressure drop. The data for the test, BSTS 3/14/14 L2W, was not included in Figure 24 because of irregularities in the procedure used to heat the PEG/water solution and the test hardware. These irregularities yielded significantly different results than the repeat test, BSTS 3/26/14 L2W, shown in Figure 24.

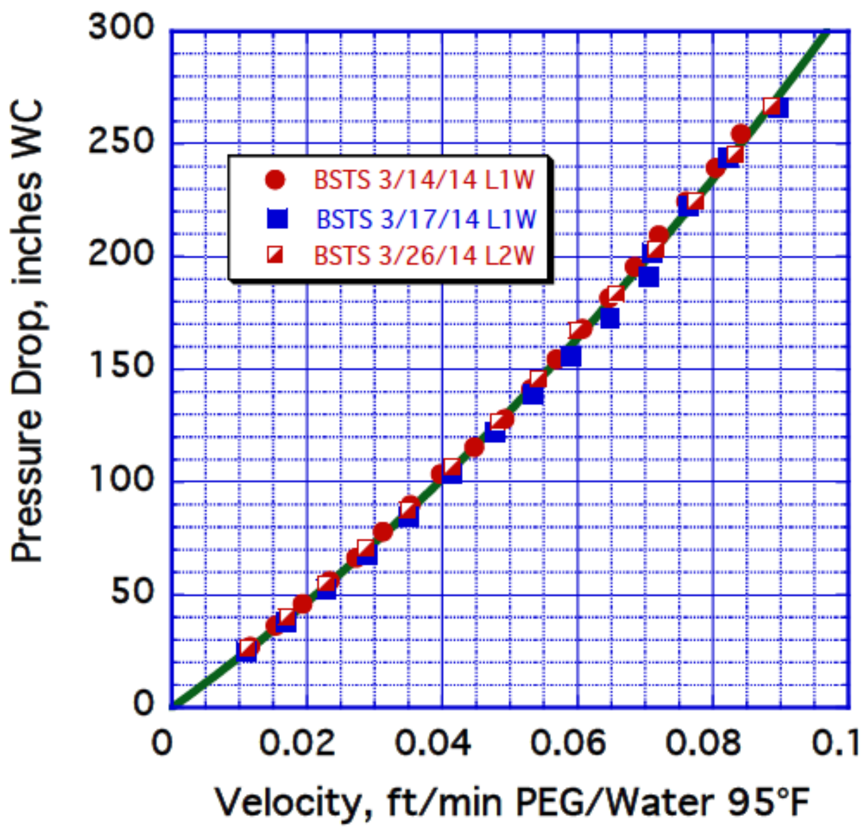

Figure 24. Pressure drop measurements of Lydall HEPA filter medium 3398-L1W (no screens) and 3398-L2W (with screens) as a function of medium PEG/water (186 cP computed from the water test in Figure 23) velocity for the BSTS. The BSTS velocity is computed assuming a medium diameter of 4.723 inches. The best fit curve through the data is given by Equation 7.

$$\Delta P_M = 2145\,V + 9832\,V^2 \qquad (7)$$

If the medium compresses with increasing differential pressure, then the medium constant, K_M, in Equation 4 increases with increasing velocity in the first approximation by the following equation:

$$K_M = K_{M0} + c_M V \qquad (8)$$

where K_{M0} = medium constant of uncompressed medium
c_M = coefficient of medium compression at increased velocity

Note that for low differential pressures as in Figures 22 and 23, the HEPA medium does not compress, and $K_M = K_{M0}$.

Substituting Equation 8 into Equation 4 for the filter medium yields

$$\Delta P_M = K_{M0}\,\eta V + c_M\,\eta V^2 \qquad (9)$$

The value of the filter medium constant, K_{M0}, and the coefficient of medium compression, c_M, can be determined using the coefficients of Equations 7 and 9 and the viscosity of the PEG/water solution. However, since the viscosity of the PEG/water test solution was not measured, the unknown viscosity can be computed using the K_{M0} value for water, since K_{M0} is a constant for the filter medium and independent of viscosity. Using the K_{M0} value for water (11.52 inch WC/ft/min/cP) and the first coefficient, 2145, in Equation 7 for the PEG test, yields a viscosity of 186.2 cP (2145/11.52) for the test in Figure 24. The value of c_M is then determined using the 186.2 cP viscosity and the second coefficient, 9832, in Equation 7 to yield c_M= 52.80 inch WC/(ft/min)^2/cP. (9832/186.2). The computed viscosity value of 186 cP falls within the middle of the measured viscosity values in Figure 11.

The magnitude of the increased pressure drop due to medium compression can be seen in Figure 25 where only the first term of Equation 7 is graphed along with the experimental data from Figure 24.

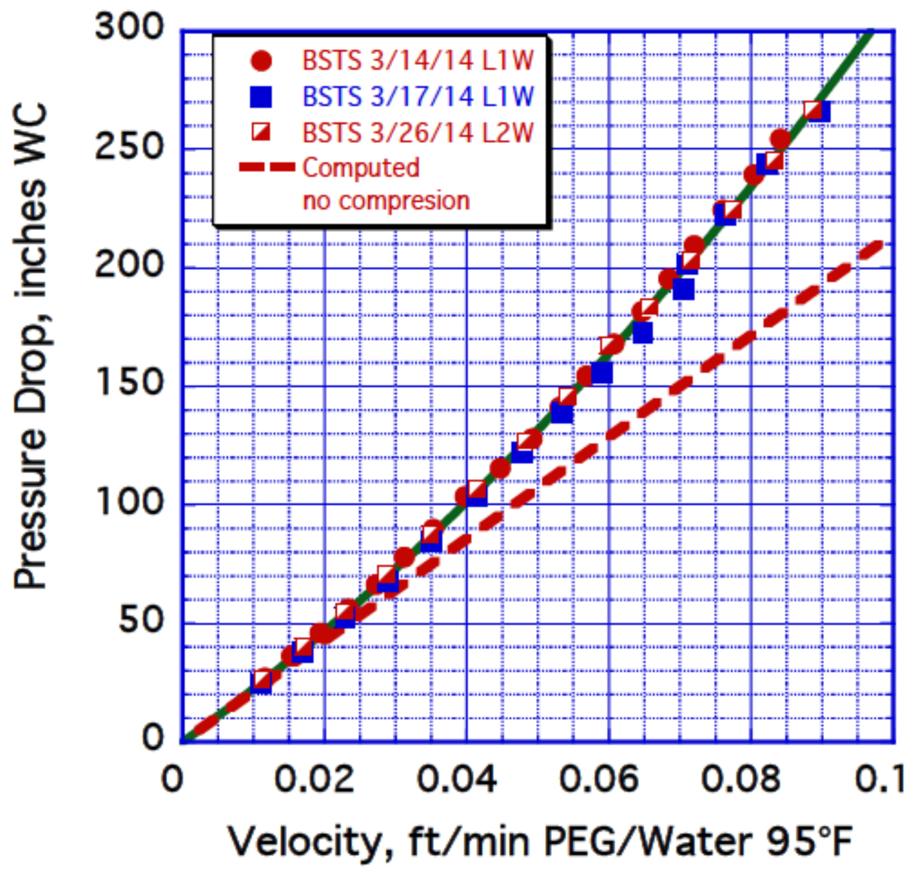

Figure 25. Experimental data from Figure 24 plotted with the linear (first) term of the pressure drop curve in Equation 4 showing the increased pressure drop due to the medium compression at higher velocities (pressures). The viscosity of the PEG/water solution is computed to be 186 cP.

A compilation of the graphs in Figures 22, 23, and 25 are shown in Figure 26. The slopes of the lines for PEG, water and air are 2145, 10.98, and 0.127 inch WC/(ft/min) respectively. Note that the PEG data deviates from the straight line at increasing velocity due to medium compression as seen in Figure 25. The deviation of the experimental data from the straight lines at low flows is due to low resolution of the pressure and flow instruments.

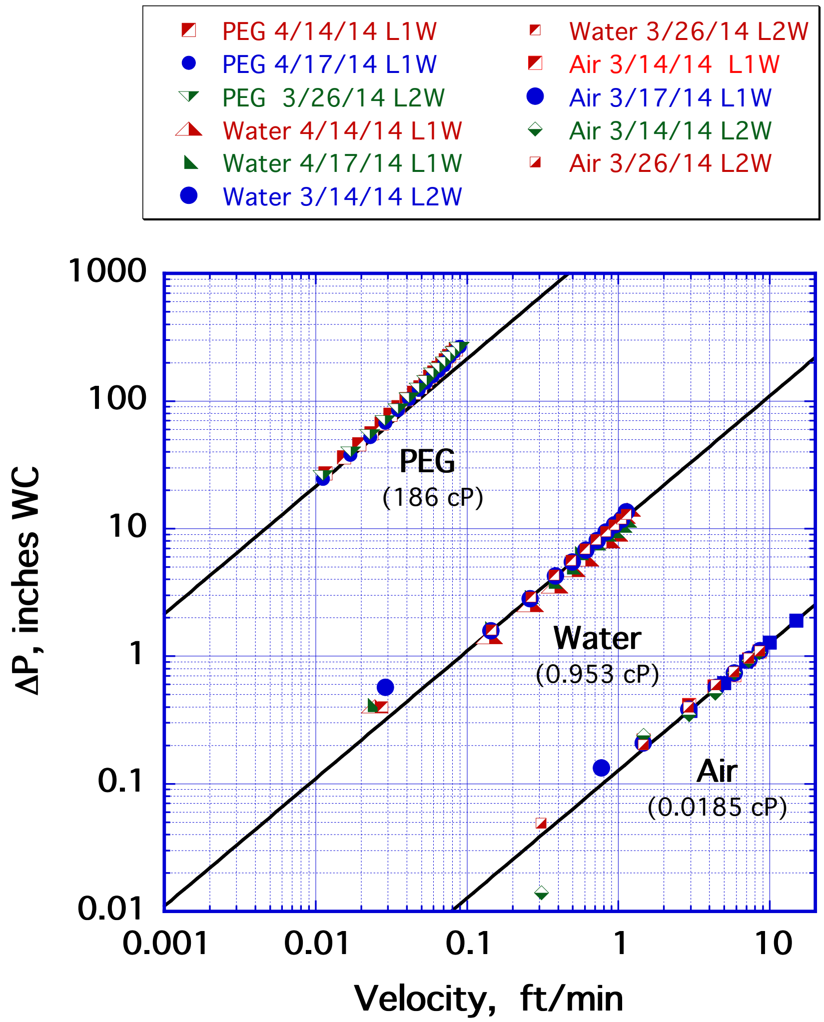

Figure 26. Measured pressure drops across flat sheets of Lydall 3398-L1W (no screens) and 3398-L2W (front and back screens) HEPA filter media as a function of fluid velocity for air, water and 50% by weight solution of PEG-8000/water. The viscosity values are shown in parenthesis. Tests were conducted using the tester in Figure 19. Note, the 186 cP for the PEG solution is computed from water tests.

MSU conducted a similar set of pressure drop measurements for metal fiber medium used by Porvair to construct metal HEPA filters. The medium consisted of two layers of Bekaert 3AL3 stainless steel fiber medium sandwiched between metal screens.

Vertical Test Stand (VTS) For Testing Flat Media Efficiencies and Pressure Drops

The second flat media tester used in the filter development project is the vertical test stand (VTS) shown in Figure 27. This test stand was used to measure the pressure drop and penetration of DOP aerosols as a function particle diameter for various air velocities. The test hardware and procedure for measuring filter efficiency was developed using the VTS and was used in the subsequent flat media testing. A similar system was built for the large scale test system (LSTS) to test full-scale HEPA filters. Although a dust feeder was initially installed in the VTS to obtain particle loading on flat media, this was not pursued after a preliminary test, since it was redundant with the isokinetic samplers, which had the added benefit of using the same aerosols as the full-scale filters and avoiding sample line losses.

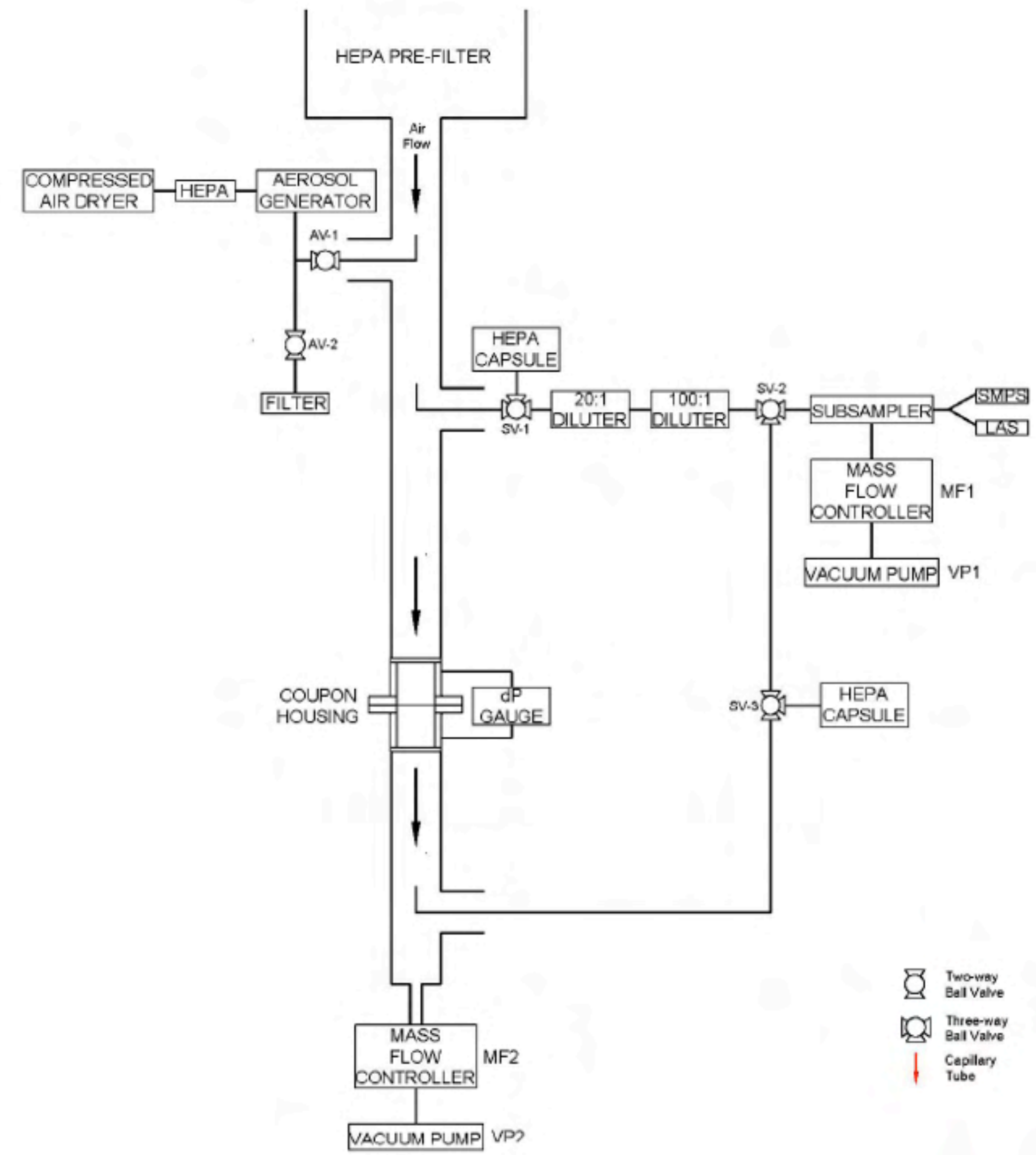

Figure 27. Schematic of the vertical test stand (VTS) with a 5.80 inch ID tube and filter holder for measuring the DOP efficiency and pressure drop of flat media samples at variable flow rates in air. A 6-jet Laskin nozzle (TSI) is used to generate DOP aerosols.

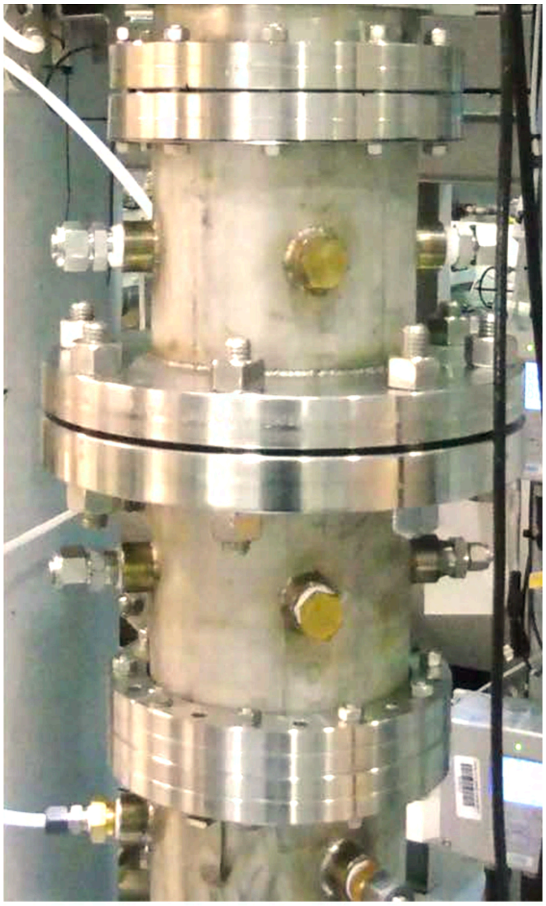

(A)

(B)

Figure 28. Detailed photograph of the VTS (A) at the filter holder flange and (B) with the top flange removed and exposing the test filter (7.10 inches diameter, 5.80 inches effective diameter), the lower and upper Teflon sealing gaskets, the supporting screen, and the O-ring. (Phillips et al, 2016)

The VTS in Figures 27 and 28 was used to measure the pressure drop and DOP efficiency for the Lydall 3398, 3398-L1W, and 3398-L2W filter media, that were used by the filter manufacturers in this project.

Figure 29 shows the pressure drop across the Lydall HEPA glass fiber media 3398 (standard with no glass cloth), 3398-L1W (glass cloth on one side) and 3398-L2W (glass cloth on both sides, but no additional screens). Note that the MSU pressure drop measurement for the 3398 media is significantly lower than the Lydall data sheet for the same filter and the 3398-L1W and 3398-L2W values in both Figure 29 for the VTS and Figure 22 for the BSTS. MSU also states the filter pressure drop has an uncertainty of +/- 0.16 inches WC. Based on the Lydall 3398 data sheet and the Lydall 3398-L1W Ricketts data, (Ricketts et al, 2008), one layer of the glass cloth increased the pressure drop at 10.5 ft/min by 0.06 inches WC at, a value that is comparable to other studies of pressure drop across glass cloths.

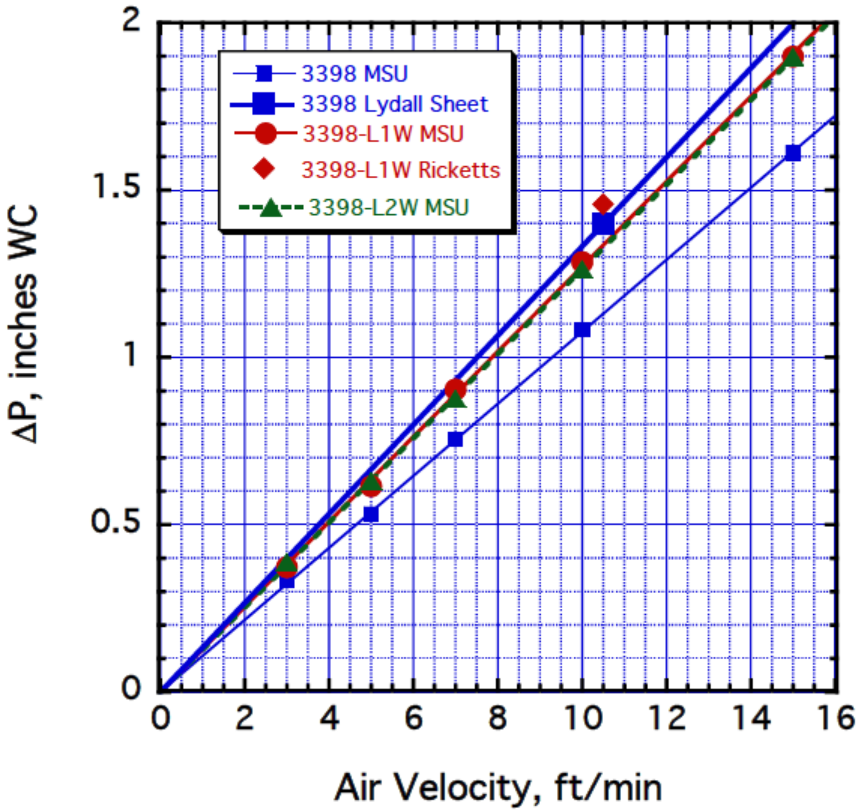

Figure 29. Experimental measurements of the pressure drop of the Lydall 3398, 3398-L1W and Lydall 3398-L2W HEPA media measured by MSU and others. The Lydall 3398-L1W medium has the glass cloth on the downstream side. The Lydall 3398 MSU data is suspect because of the deviation from the manufacturer's data and the remaining MSU data. Each MSU point is the average of three different samples with the variability range less than the size of the symbols used for the data points.

MSU also measured the pressure drop across the Lydall Ultra Low Penetrating Air (ULPA) filter media to enable the filter manufacturers to use a higher efficiency medium if needed. Figure 30 shows the results of the MSU tests along with the Lydall data sheet value.

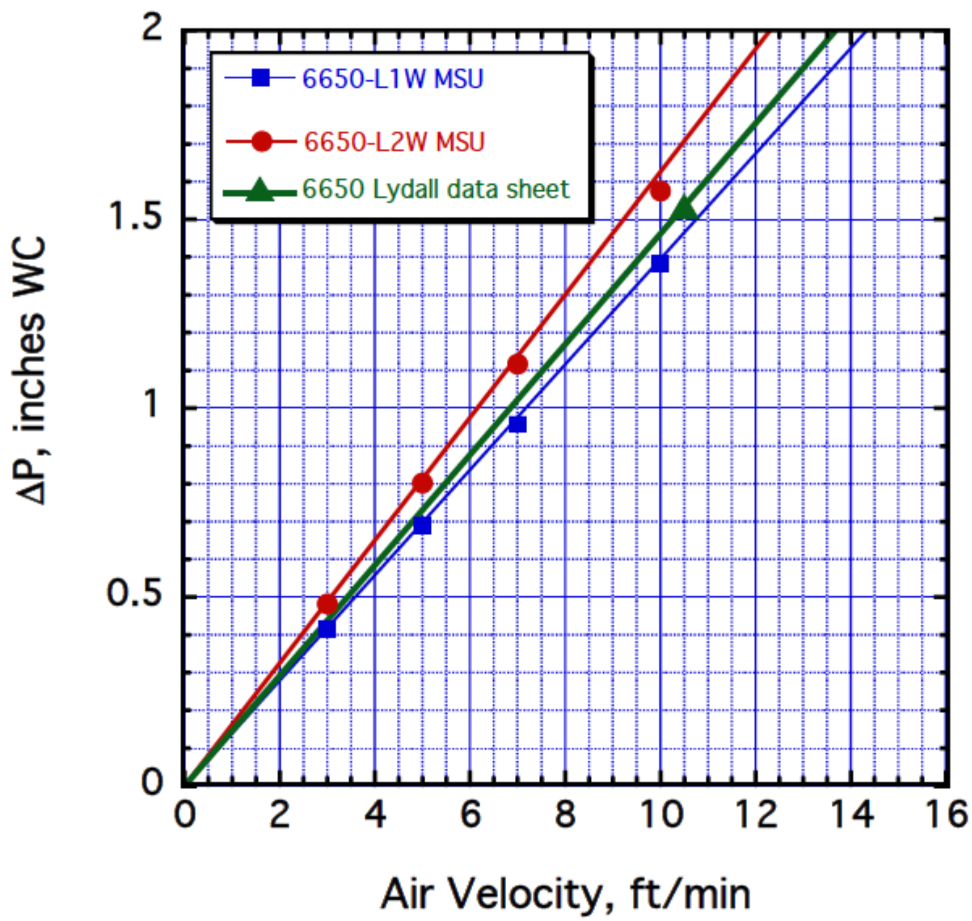

Figure 30. Experimental measurements of the pressure drop of the Lydall 6650, 6650-L1W and 6650-L2W ULPA media measured by MSU and others. Each MSU point is the average of three different samples with the variability range less than the size of the symbols used for the data points.

In-Duct Isokinetic Samplers (IDIS) for Particle Loading on Flat Media

A third, flat media tester was fabricated to allow direct comparisons of pressure drop increase during particle loading in both flat sheet and full-scale filters as shown in Figure 7. Although particle loading on flat media could be conducted in the VTS shown in Figure 27, Bechtel wanted the flat media and full-scale filter to be exposed to the same test aerosol and therefore required that several isokinetic sample holders be installed inside the test duct used for the full-scale filter (Garcia, 2012b).

MSU built four in-duct, flat filter holders to be able to measure the pressure drop increase across flat media during particle loading while simultaneously measuring the pressure drop across a full-scale filter using the same medium. Figure 31 shows one of the four in-duct filter holders that are mounted inside the test duct used for testing the full-scale filter. The inlet opening of the filter holder in Figure 31 is sized to obtain isokinetic sampling of the particles.

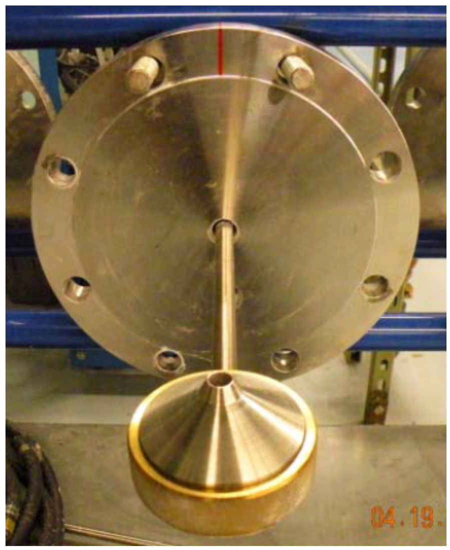

Figure 31. Photograph of the in-duct isokinetic sampler with the exhaust sampler tube attached to the plate that mounts on the large scale test duct (Wong et al, 2106)

By periodically interrupting the particle loading to remove the filter holders and weighing the isokinetic filters and the full-scale filter, MSU was able to measure the particle mass loaded on the flat media and on the filter corresponding to measured pressure drops. Although intermediate values of pressure drop between the weighings were measured, the corresponding intermediate weight values were computed using challenge aerosol concentrations. The pressure drop measurements were then divided by the medium face velocity to obtain DP/V and thus enable direct comparison of the flat medium values to those of the full-scale filter. Similarly, the particle mass accumulation was divided by the effective filter area to obtain M/A and thus allow the flat media values to be directly compared to those of the full-scale filter.

Unfortunately, most of the collected data from the isokinetic filter samples were not analyzed since a satisfactory HEPA filter had already been qualified, thus no longer requiring supporting studies that aid in filter design. A preliminary analysis of one of the fourteen tests was presented as a poster (Wong et al, 2016) shown in Figure 32 and illustrates the difference in particle loading in a filter and particle loading on the filter medium. Although the units in Figure 32 are incorrect, the graph shows the particle loading for the flat media has a linear response for the increasing $Al(OH)_3$ deposits during the entire loading test. The full-scale filter initially follows the same pressure curve as the flat medium, but then the pressure drop has an exponential rise with increasing deposits.

The particle deposits for the full-scale filter in the linear portion of the loading curve form the deposit on the medium and do not significantly alter the channel flow through the filter pleats. However, above a certain value the deposits begin to restrict the channel opening and eventually close it.

The points of the initial deviation from the flat medium and of the the final particle loading capacity are determined by the effective particle size (larger particles exacerbate the pleat closure) and the pleat spacing (smaller pleat spacing exacerbates the pleat closure). Theoretical models of the particle loading process in pleated filters have been developed to understand this process (Hettkkamp et al, 2012; Bergman, 2006, 2008, 2016).

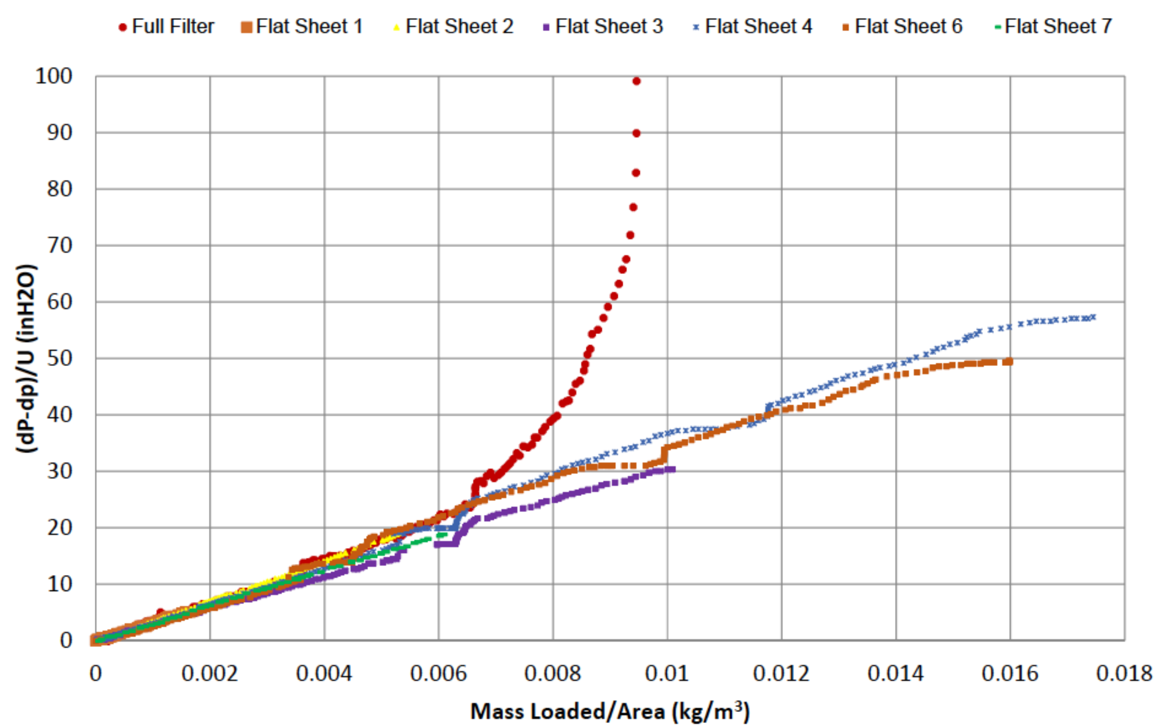

Figure 32. Loading of Al(OH)3 aerosols on flat media using the filter holders in Figure 31 and on the Porvair Safe-Change HEPA filter with the Lydall 3398-L2W medium. Note that the units are incorrect. (Wong et al, 2016).

Inertial Impactor for Particle Mass Size Distribution

An important instrument required in the Bechtel test plan (Garcia, 2012b) for analyzing filter loading data such as shown in Figure 33 is an inertial impactor, which is used to determine the mass distribution of particles as a function of particle size. This instrument is critical for establishing both the mass and density of the particles when analyzing the size distribution from the other instruments (SMPS, LAS, APS) that are used for size and concentration measurements. Each of the three instruments measure a unique particle property: the scanning mobility particle sizer (SMPS) measures the particle electrical mobility; the laser aerosol sizer (LAS) measures a light scattering signal dependent on the particle size and refractive index ; the aerodynamic particle sizer (APS) measures the particle aerodynamic diameter, which depends on the particle size, shape, and density. Figure 33 shows the Pilat impactor mounted inside the test duct upstream of the HEPA filter so that test aerosols can be measured directly without line loss as occurs with the other instruments used to determine particle size distributions for characterizing the challenge aerosol and for filter efficiency measurements (Pilat et al, 1970).

Figure 33. Photograph of Pilat impactor mounted inside the test duct upstream of the HEPA filter (Wong et al, 2016)

The particle size measurements using the Pilat impactor were taken along with the SMPS, APS and the LPS to characterize the aerosol challenge in 14 filter loading tests using $Al(OH)_3$, Arizona Road Dust, and acetylene soot. These measurements were intended to relate the aerosol challenge properties of the different test aerosols to the filter mass loading and pressure drop. Unfortunately, the planned analysis of the aerosol measurements were not performed once the 14 filter loading tests were completed and the filters qualified. A preliminary analysis (Cox et al, 2016) was conducted relating size distribution of the SMPS and the LAS.

Filter Efficiency Test System and Procedure

Another addition to the MSU test facility is the fabrication of an ASME AG-1 filter efficiency test system and the development of a filter efficiency test procedure (Bergman, 2014). MSU had previously measured HEPA filter efficiency using a TSI SMPS to measure the undiluted challenge particle concentration as a function of particle size and a TSI LAS to measure the downstream particle concentration as a function of particle size (Giffen et al, 2012).

The filter penetration was computed from the ratio of the downstream laser value to the upstream SMPS value, thus introducing small errors due to the aerosol size dependency of the laser. In addition, the filter efficiency data was computed as the total efficiency summed over the entire challenge aerosol diameter or the total efficiency for particles greater than 0.3 microns. (Giffen et al, 2012). These efficiency measurements do not correspond to the conventional HEPA filter test methods prescribed by ASME AG-1 and DOE Standard -3020 (2015) where the efficiency is measured at 0.3 micron DOP, or other recognized HEPA test standards such as the IEST-RP-CC007 (2007), ASTM-F1471 (2009) and EN-1822 (2009). Aerosol Science suggested a filter efficiency test system using the LAS to measure the upstream concentration after diluting the sample to about 2000:1 instead of the SMPS and to measure the downstream concentration undiluted with the LAS (Bergman, 2014).

The schematic in Figure 27 of the VTS shows the filter efficiency test system developed by MSU and AS for use in all of the flat sheet media and the full scale filter tests. This test system was designed to have minimal particle loss by using 3-way ball values and having short sample lines with equal lengths upstream and downstream. The sample flow is 5 L/min to match the required flow of the two TSI diluters in conductive plastic sampling lines 0.188 inches ID yielding a tube Reynolds number of 1,470 to minimize particle loss (Kulkami et al, 2011). The ball valve SV-2 has the straight through for the upstream sample and the right angle bend for the downstream sample. Particle loss in the TSI diluters are included in the dilution ratio as a function of particle size that is measured monthly. The accuracy of the filter efficiency is directly related to the accuracy of the diluter calibration, which uses a similar procedure to the filter efficiency measurements. (Bergman, 2015a).

Four different measurements are made for each filter efficiency measurement: (Step 1) instrument zero readings are obtained by switching the valves SV1 and SV3 to the HEPA capsule for the upstream and downstream lines using valve SV2, (Step 2) the downstream background reading is obtained with no aerosols generated in the test duct and valve SV2 set to the downstream, (Step 3) the upstream sample is taken with the valve SV2 set to the upstream and after the DOP aerosol generator is adjusted to have approximately 2,000 counts/s for the LAS, and (Step 4) the downstream sample is taken with the valve SV2 set to the downstream. Multiple measurements of the concentrations are taken for each setting and sufficient sweep time is included between the samples to clear the sample lines.

The filter penetration at each particle size is computed by the ratio of the difference in downstream minus the downstream background divided by the product of upstream times the dilution ratio (ASTM-F1471, 2009). The adjustment of the challenge aerosol concentration in Step 3 ensures that the LAS obtains the maximum number of particles for accurate measurements while keeping the LAS coincident error less than 1%. Although this requirement was generally achieved for HEPA grade filters in the VTS for flat media, this was not achieved for the full-scale tests in the large scale test system (LSTS), where a typical diluted concentration was only 20 counts/s instead of 2,000 counts/s. The result of the low challenge concentration was increased uncertainty and scatter in the efficiency determination for the Phase 2 full-scale filter tests.

The penetration curve for the HEPA filters can be approximated by using a log-normal curve given by Equation 10 (Bergman et al ,1984; 2004, 2016a).

$$P = \frac{k}{LOG(\sigma_g)} \exp\left(- \frac{(LOG(D) - LOG(D_{CM}))^2}{2\left(LOG(\sigma_g)\right)^2} \right) \tag{10}$$

where P = penetration fraction
D = particle diameter, micron
D_{CM} = particle count median diameter, micron
σ_g = geometric standard deviation
k = a constant for each penetration curve

Equation 10 is used when graphing the penetration on an abscissa with Log base 10 as shown in Figure 34. Slightly different equations are used when graphing on a linear abscissa or abscissa with a natural log base e. (Bergman 2016a).

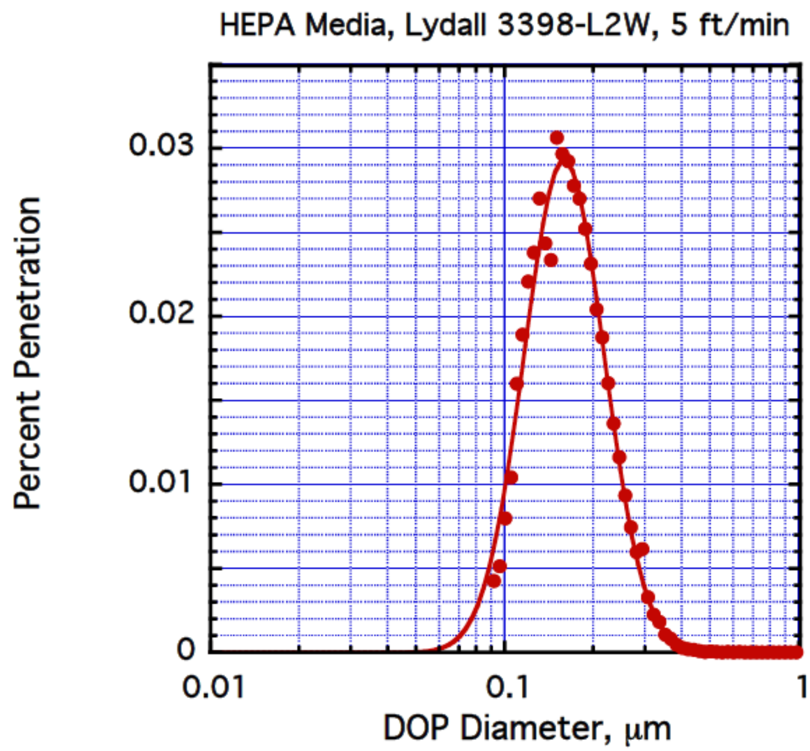

Figure 34. Experimental DOP penetration measurement of Lydall 3398-L2W flat medium using the LAS particle counter and the VTS in Figure 27. The curve through the experimental points is given by Equation 10 with $D_{CM} = 0.176$ and $\sigma_g = 1.367$.

The SMPS is also used in the filter penetration measurements, but since only a small fraction of the particles are measured in the instrument, the instrument is less sensitive for filter penetration measurements compared to the LAS. Figure 35 shows the penetration of another sample of the same medium used in Figure 27, but with penetration measurements with both the LAS and the SMPS at 15 ft/min instead of 5 ft/min as in Figure 34. Compared to the LAS, the SMPS shows considerable scatter, even for the ten times higher penetration values at 15 ft/min. This is an intrinsic feature of the SMPS, which measures only about 1% of the particles that the LAS measures. The data scatter for the SMPS penetration values increases significantly at lower face velocities, where the downstream particle concentration and thus the penetration is much lower.

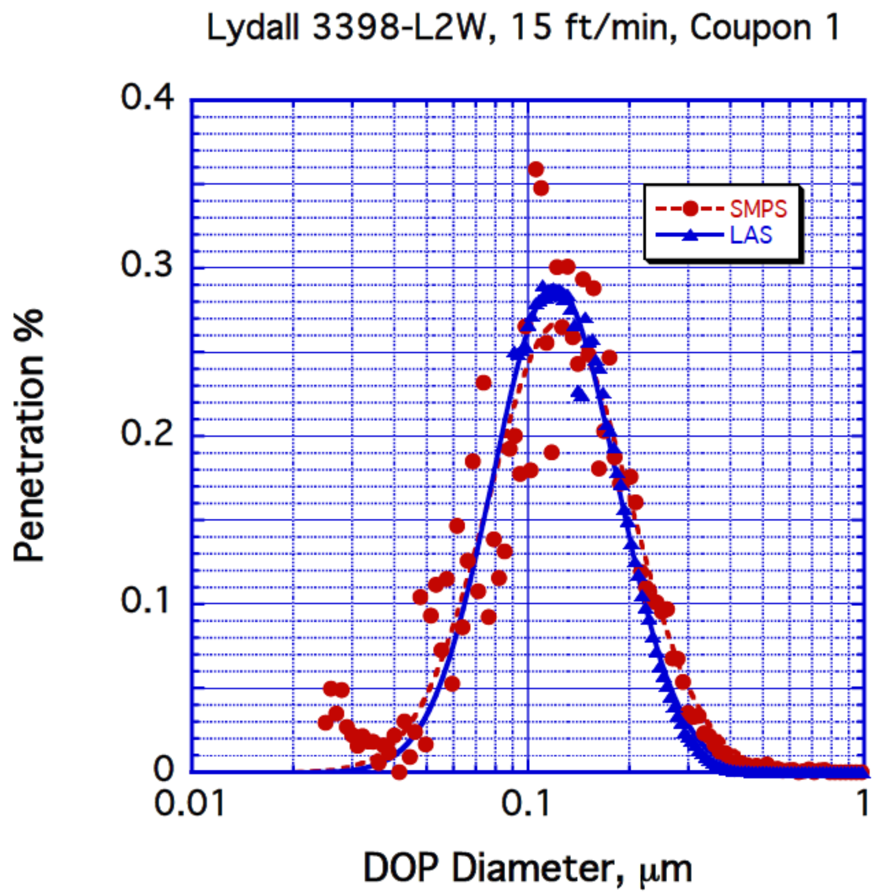

Figure 35. Experimental DOP penetration measurement of Lydall 3398-L2W flat medium using the LAS, the SMPS and the VTS in Figure 27. The curve through the experimental points is given by Equation 10 with D_{CM} = 0.144 and σ_g = 1.53 for the LAS and D_{CM} = 0.157 and σ_g = 1.62 for the SMPS.

Although the log-normal equation is a good fit of the central portion of the penetration curve, the equation fit to experimental data becomes poor in the tail of the penetration curve where the 0.3 micron aerosol penetration is reported. Figure 36 shows a magnified portion of the two curves in Figure 35 and the deviation of the curves from the data. Figure 36 also shows the penetration data generated from the SMPS is displaced to larger particle sizes compared the LAS data. This displacement introduces an error in the DOP penetration measurements using the LAS.

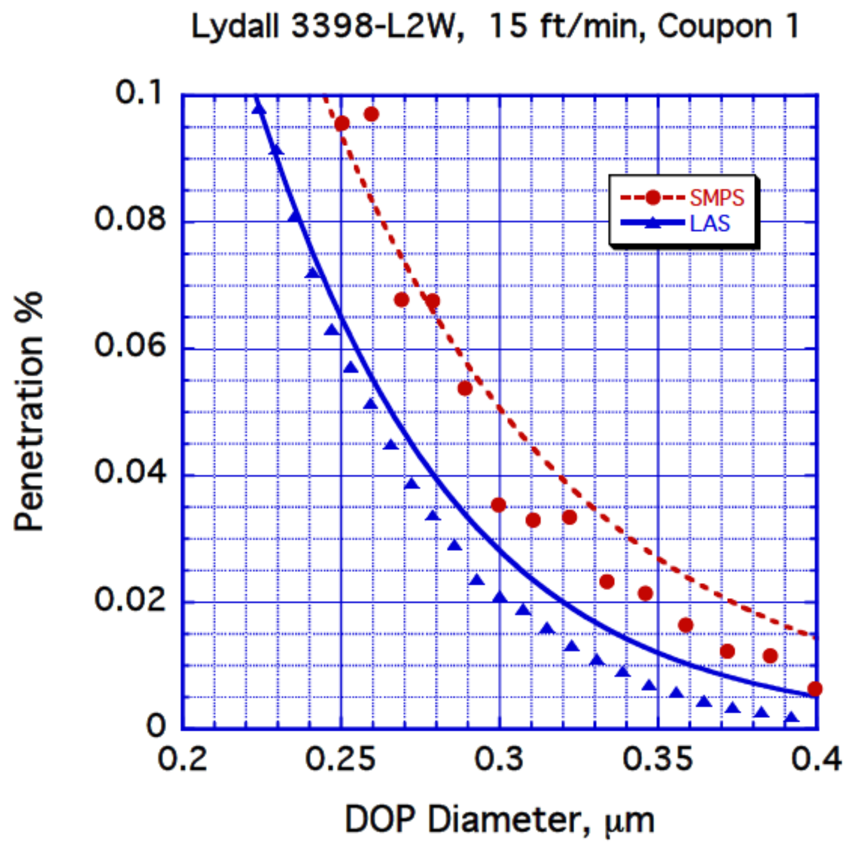

Figure 36. Magnification of Figure 35 showing the deviation of the log-normal fit to the experimental DOP penetration measurement of Lydall 3398-L2W flat medium using the LAS, the SMPS and VTS in Figure 21. (Bergman, 2016a)

The accuracy for determining the HEPA filter penetration at 0.3 microns using DOP aerosols was improved by fitting a range of data centered at 0.3 microns with an exponential curve as done in Figure 37. The best fit curves in Figure 37 remove the random fluctuation of data when using individual penetration points.

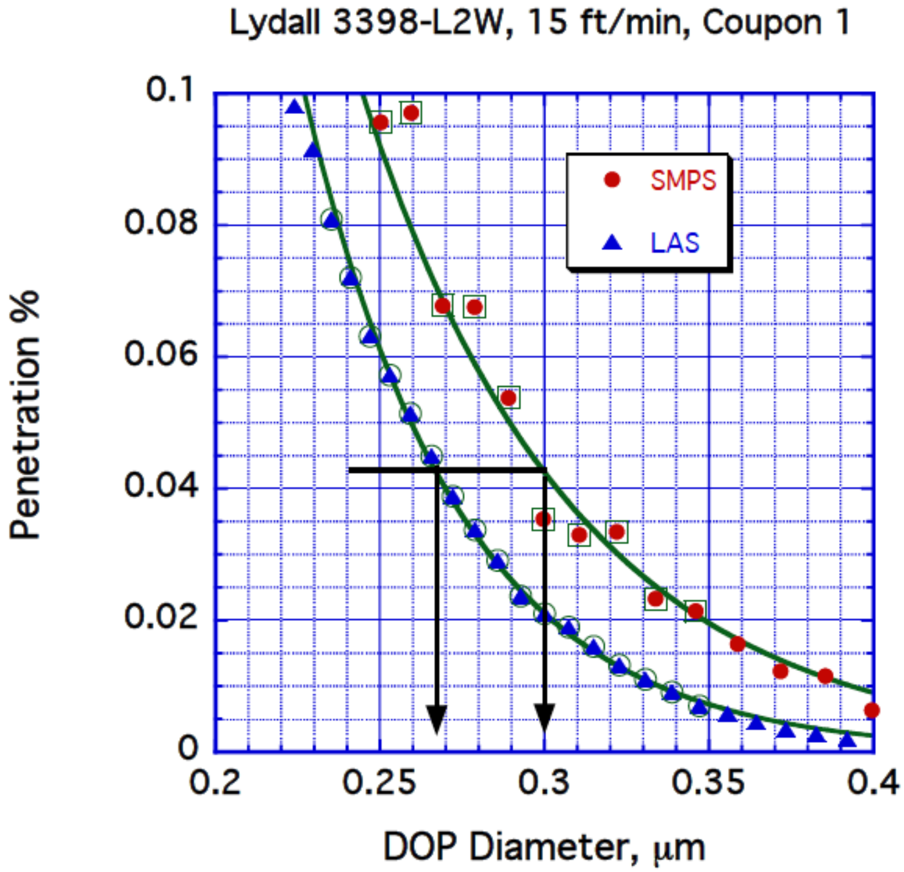

Figure 37. The penetration data from Figure 36 are fitted to exponential functions using the encircled data with squares for the SMPS data and the circles for the LAS data. Compared to the SMPS penetration at 0.3 microns, the LAS data are shifted to 0.27 microns because the LAS was calibrated with PSL spheres and not DOP (Bergman, 2016a; Phillips et al, 2016)

The accuracy for determining the HEPA filter penetration using DOP aerosols was further improved by correcting for the small shift in DOP particle size measured with the LAS compared to the SMPS as seen in Figure 37. This shift in particle size was due to calibrating the LAS with PSL spheres and not DOP (Bergman, 2015b, 2016a). The standard practice of calibrating optical counters with PSL spheres introduces an error when measuring DOP because the refractive index of DOP (1.49) is smaller than the refractive index of PSL (1.59). This difference makes a 0.3micron DOP particle appear like a 0.27 micron PSL particle.

For HEPA filter standards other than the US DOP test (ASME AG-1, DOE-STD-3020), the aerosol penetration is measured at the peak penetration, where the shift in the size has a negligible effect (IEST, 2007; EN-1822, 2009). This shift in DOP penetration can make the difference between passing and failing for filters with borderline efficiency. For example, the LAS penetration at 0.3 microns passes with

0.02%, but fails at 0.27 microns with 0.04%. Since the LAS is calibrated with PSL, the HEPA filter efficiency is determined at the LAS 0.27 micron size.

MSU was tasked with measuring the efficiency at air velocities ranging from 3 to 15 ft/min of candidate filter media for use by filter manufacturers (Garcia, 2012b). The MSU test results for the Lydall 3398-L2W medium are shown in Figure 38.

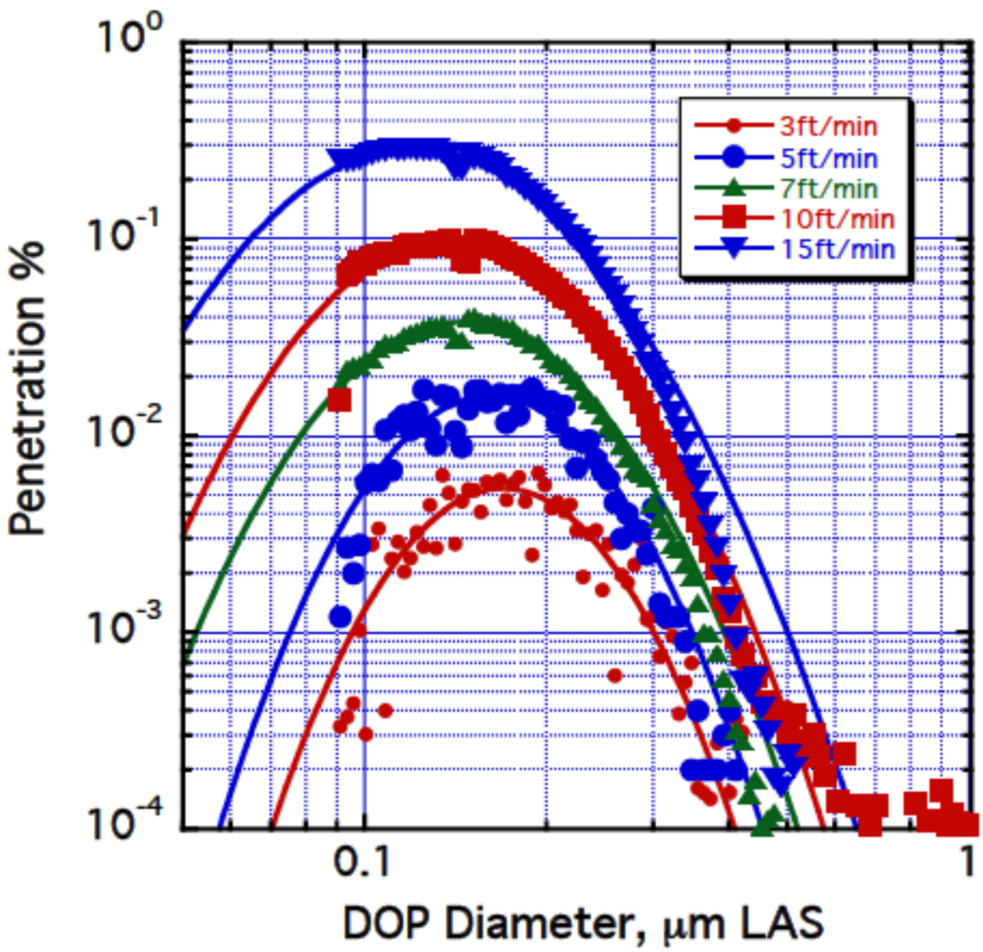

Figure 38. Penetration measurements of Lydall 3398-L2W medium in the VTS as a function of DOP diameter measured with the LAS for face velocities from 3 to 15 ft/min. The data for the 3 and 5 ft/min were preliminary data and show considerable scatter since very low DOP concentrations were used in these preliminary tests. Although MSU completed newer tests for the 3 and 5 ft/min using the final test procedure, the data were not available for use in this report. The curves represent best fits to log-normal curves given by Equation 10.

The portion of the penetration graphs around 0.30 microns was re-plotted on a log-linear scale in Figure 39 to determine the DOP penetration at 0.27 microns using exponential curves to smooth the data. The scatter of data for the 3 and 5 ft/min data is due to the very low DOP challenge concentration in these early measurements. Greatly improved data has been generated but not processed by MSU.

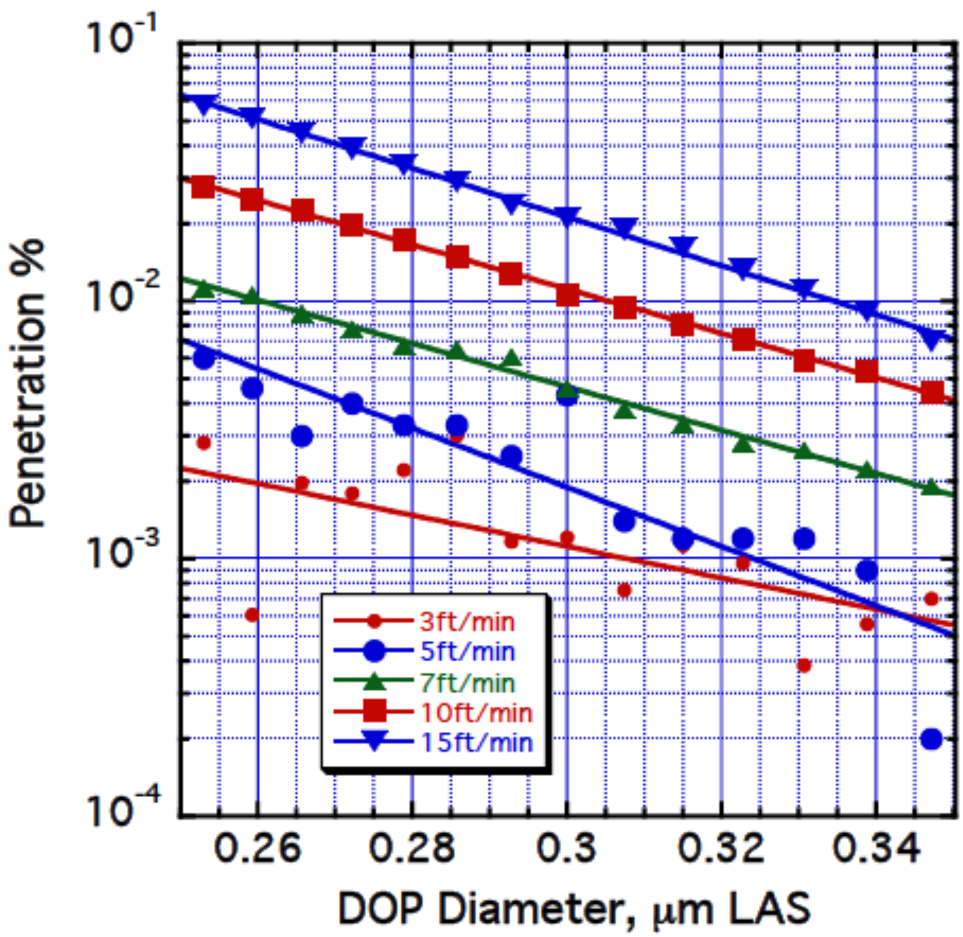

Figure 39. Magnified portion of Figure 38 showing the DOP penetration of 3398-L2W medium to compare the penetration at 0.27 microns and 0.30 microns. Note the scatter in the 3 and 5 ft/min are due to the very low challenge concentration in the two preliminary measurements. The curves are exponential functions fitted to the data between 0.25-0.35 microns.

The Lydall ultra-low penetrating air (ULPA) media designated Lydall 6650-L1W and 6650-L2W, were also tested for DOP penetration; however, only preliminary data at 3 and 15 ft/min using the Lydall 6650-L2W medium were available for this report.

Figure 40 shows the results of the tests conducted on the VTS in Figure 27. MSU conducted penetration tests at 7, 10 and 15 ft/min using Lydall 6650-L1W and

6650-L2W media but did not process the data. The 3 and 5 ft/min tests were eliminated in the final tests because the Lydall ULPA medium would only be used at the higher velocities.

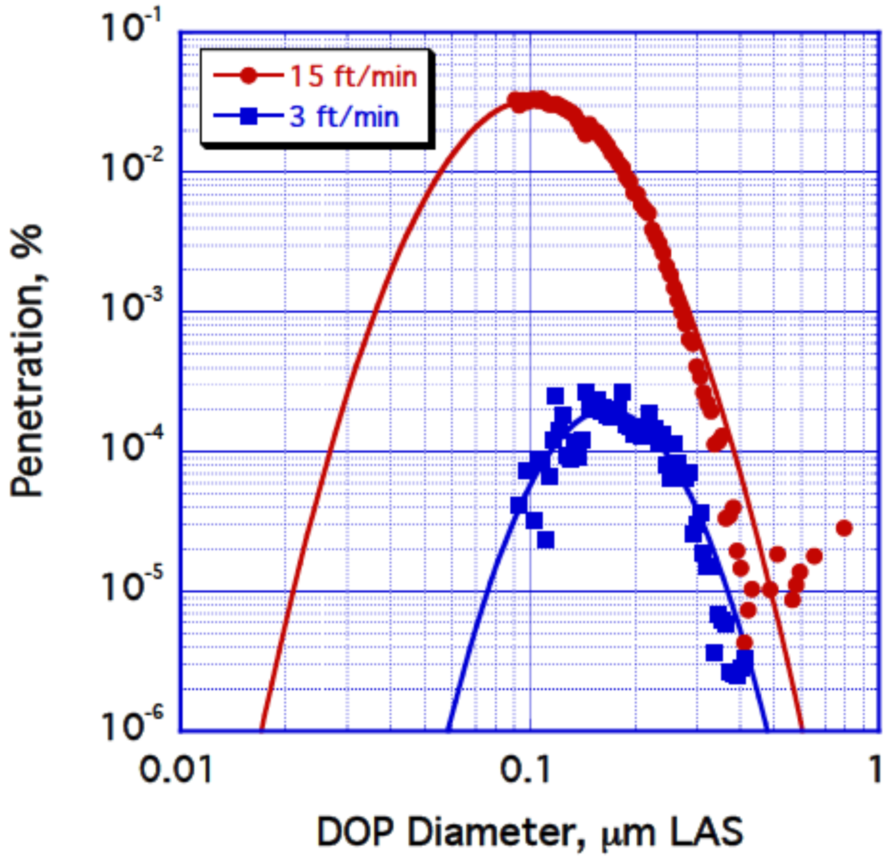

Figure 40. Preliminary penetration measurements of Lydall 6650-L2W medium as a function of DOP diameter measured in the VTS with the LAS at face velocities of 3 and 15 ft/min. The curves represent best fits to log-normal curves given by Equation 10.

The portion of the penetration graphs around 0.30 microns was re-plotted on a linear scale in Figure 41 to determine the DOP penetration at 0.27 microns using exponential curves to smooth the data.

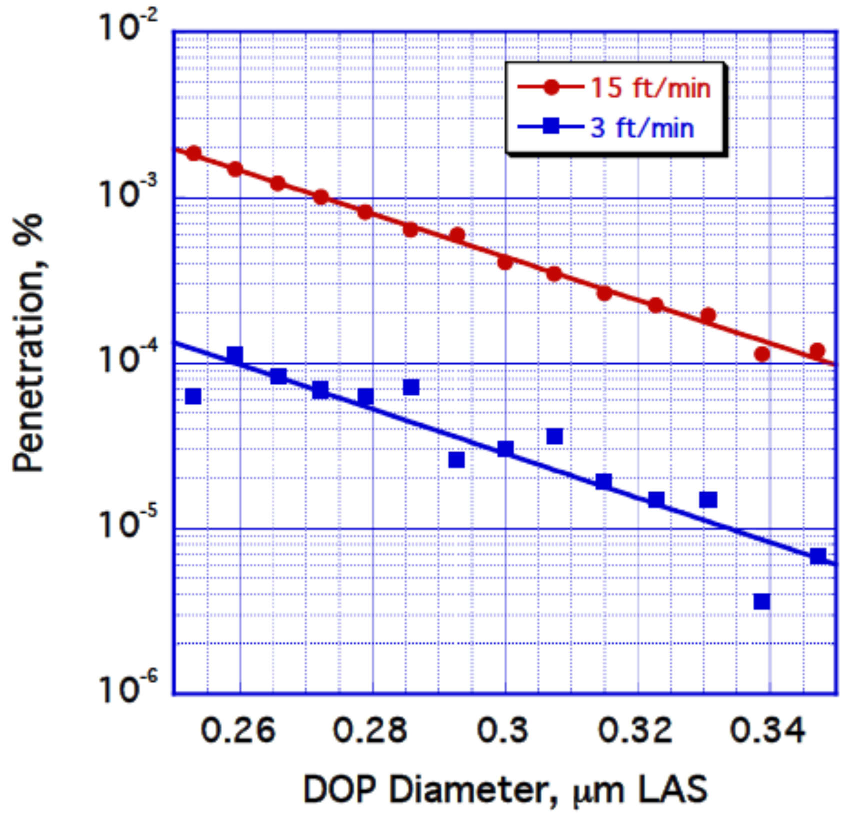

Figure 41. Magnified portion of Figure 40 showing the DOP penetration of 6650-L2W medium to compare the penetration at 0.27 microns and 0.30 microns. The curves are exponential functions fitted to the data between 0.25-0.35 microns. Note the scatter at 3 ft/min is due to insufficient challenge concentration

MSU measured the DOP penetration as a function of particle diameter as shown in Figure 38 for the following HEPA media: Lydall 3398, 3398-L1W, and 3398-L2W; and for the following ULPA media: Lydall 6650-L1W and 6650-L2W. However, only the single penetration values (assumed to be measured at 0.27 microns) were processed and are plotted in Figure 42. The two sets of curves in Figure 42 representing the LAS penetration at 0.27 microns and 0.30 microns for both the HEPA medium (Lydall 3398-L2W) and the ULPA medium (Lydall 6650-L2W) were taken from Figures 39 and 41.

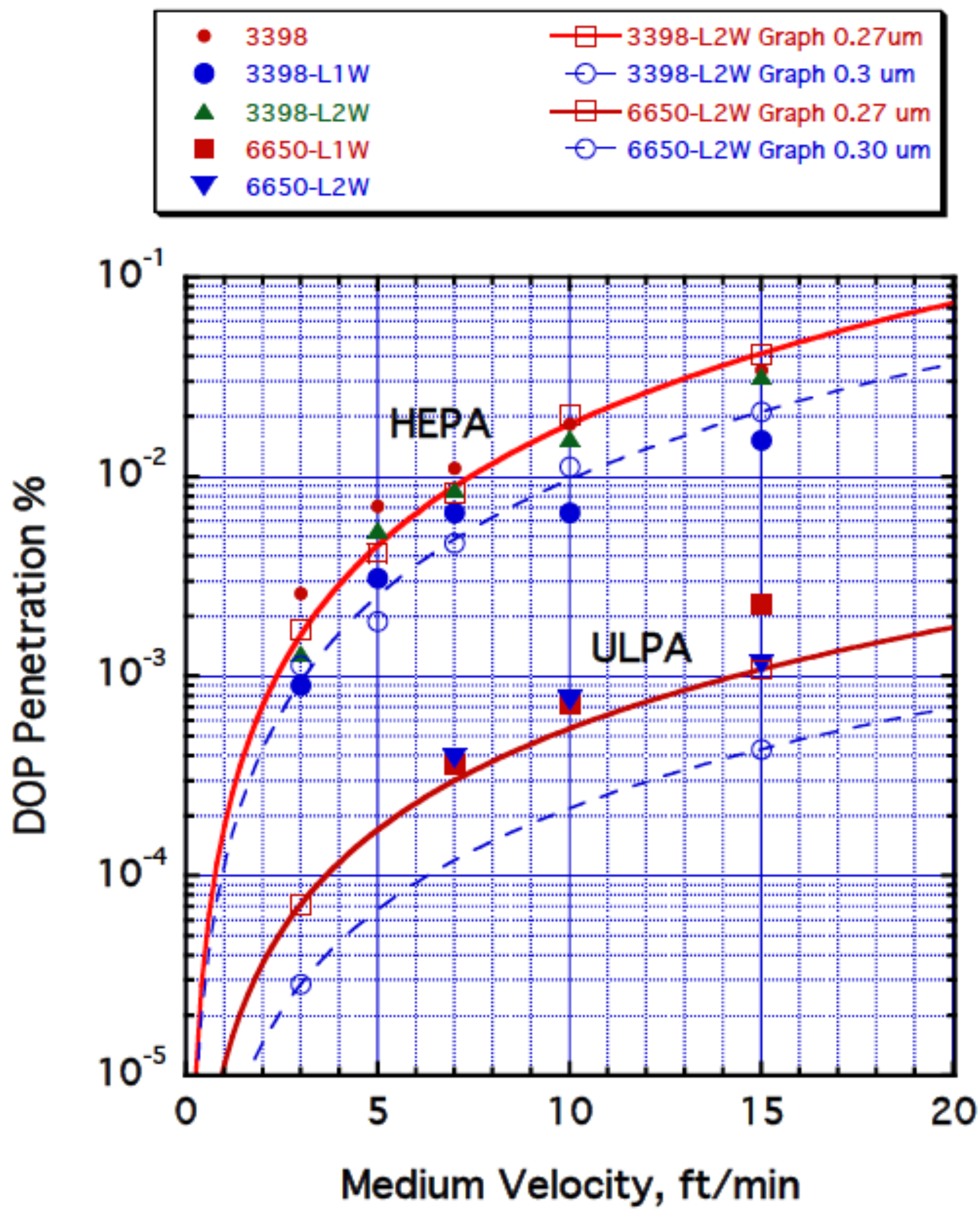

Figure 42. DOP penetration values measured by MSU at 0.27 microns for various HEPA and ULPA media measured using the VTS in Figure 27. The solid curves represent the measurements at 0.27 microns and are shown as open squares taken from Figures 39 and 41. The dashed curves represent the measurements at 0.30 microns and are shown as open circles taken from Figures 39 and 41.

Filter Leak Scan Test

During the initial filter testing, many of the filters showed significant DOP penetration suggesting leaks. To help the manufacturers correct the design or fabrication deficiency that created the leaks, Bechtel requested that MSU perform a leak scan test on all filters prior to any of the scheduled tests using a leak test system similar to that used in the clean-room industry (IEST-RP-CC034, 2009). MSU fabricated a test system shown in Figure 43 that consisted of a variable speed blower attached to a filter interface duct containing ports for aerosol injection and upstream sampling probe. The scan leak test system would be mounted on a filter, the blower and DOP aerosol injection turned on, and an operator would take a sampling probe connected to a photometer and scan the perimeter of the filter for aerosols. The location of a leak was identified by a large increase in photometer reading, and the magnitude of the leak was determined by the ratio of the photometer reading of the scan to the photometer reading of the upstream reference.

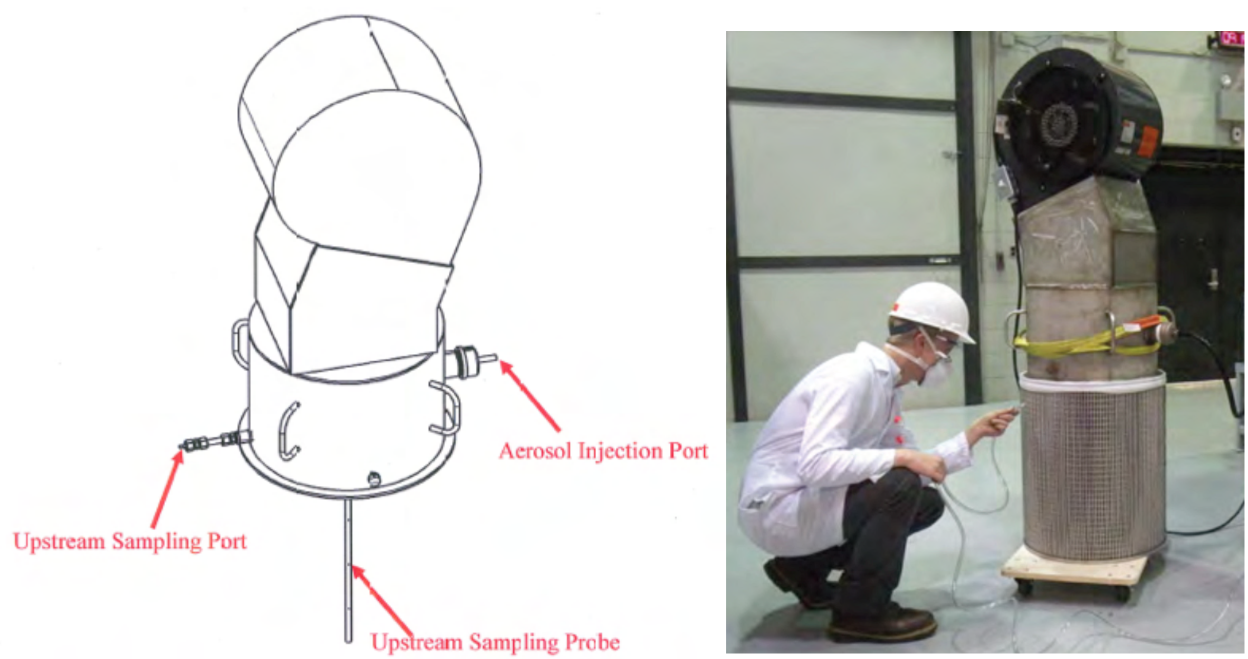

(A) (B)

Figure 43. Filter leak scan (A) tester consisting of a blower, aerosol injection and upstream sampling probe and (B) scan test with operator using a sampling probe to scan the surface of the filter for leaks.

Large Scale Test System (LSTS) for Measuring Filter Efficiency, Pressure Drop and Particle Loading

MSU built the LSTS shown in Figure 44 to measure the HEPA filter efficiency, pressure drop, and particle loading in the Phase 2 of the project (Wilson et al, 2016).

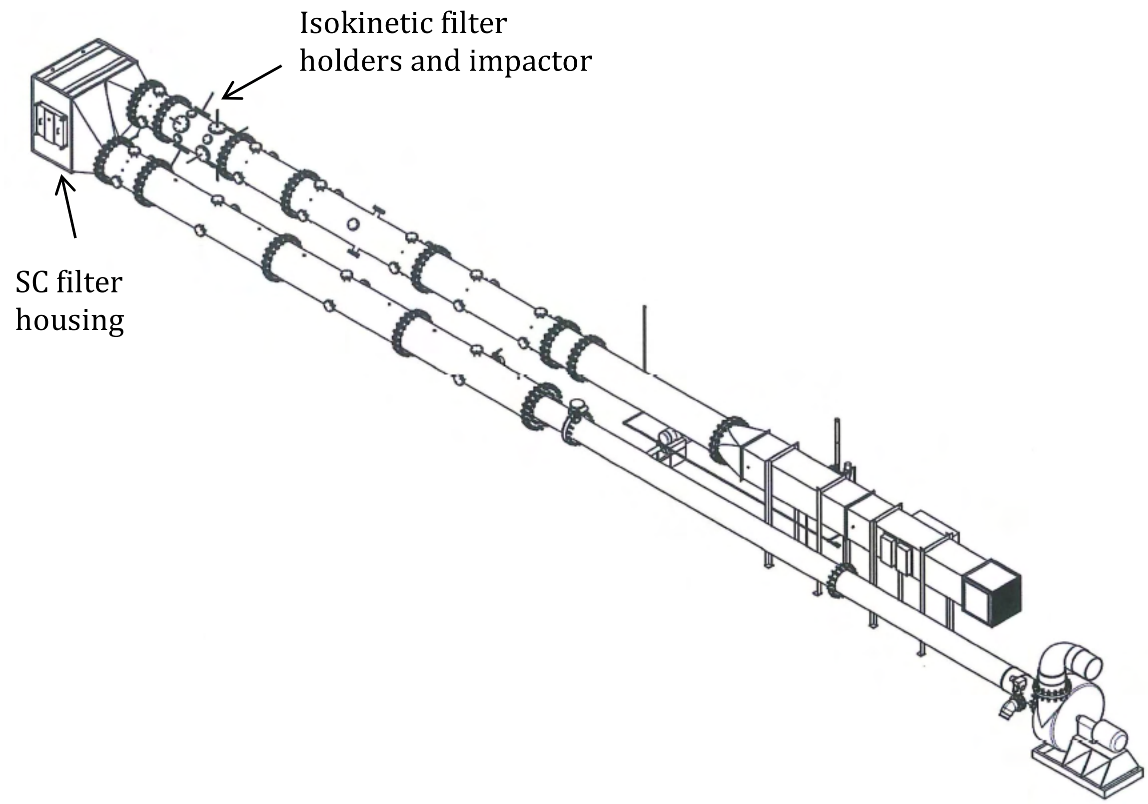

Figure 44. Schematic of the Large Scale Test System (LSTS) used for filter efficiency, pressure drop and particle loading studies. The test section housing the isokinetic filter holders and impactor is shown. (Wilson et al, 2016)

The LSTS is similar to the test system used in the DOE study that revealed the problems with the original radial flow HEPA filters shown in Figures 4 and 5. (Giffin et al , 2012). Additional features were added to the LSFTS to meet the requirements of the Bechtel contract: separate housings for the safe-change and remote-change HEPA filters to represent the WTP housings (Figure 45), isokinetic filter holders (Figure 31) and impactor (Figure 33) for particle loading characterization, filter efficiency test system (similar to that in Figure 27), oxygen starved acetylene flame soot generators to simulate smoke loading (Figure 46), and a larger blower capable of pulling 2,000 cfm at 50 inches of filter pressure drop. To enable particle loading tests at elevated temperature and humidity, a boiler with steam injection port is added to the upstream duct after the inlet filters (Wilson et al, 2016). The same powder injector used in the previous studies (Giffin et al, 2012) generates dry aerosols ($Al(OH)_3$ or A1 Arizona Road Dust) for filter loading (Wilson et al, 2016).

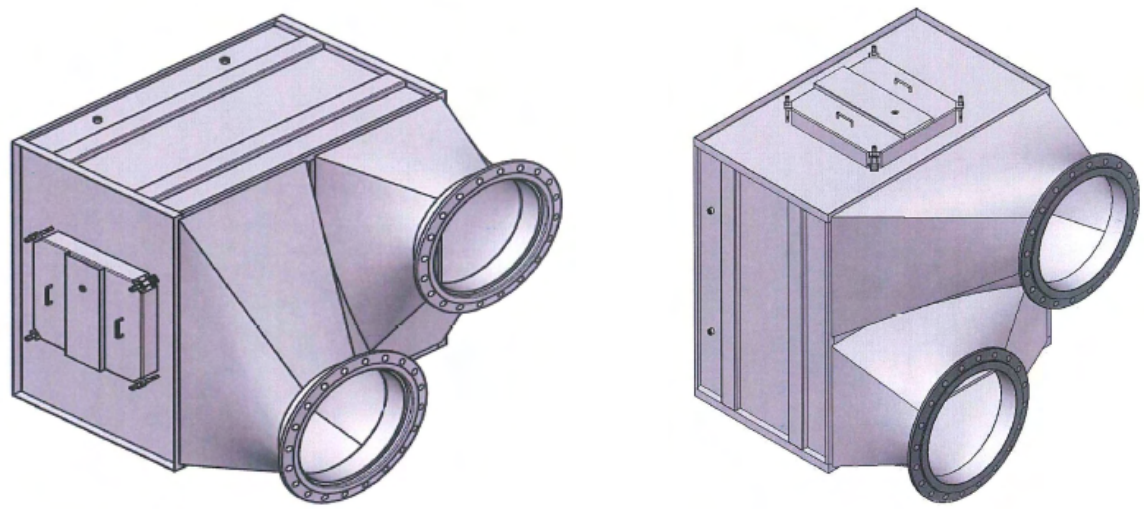

(A) (B)

Figure 45. Filter housings for (A) the safe-change filters mounted horizontally and (B) remote-change filters mounted vertically using the access doors shown. The diameters of the filter mounting inlets are 13.0 inches and 20.1 inches for the safe-change and remote-change housings respectively. (Wilson et al, 2016)

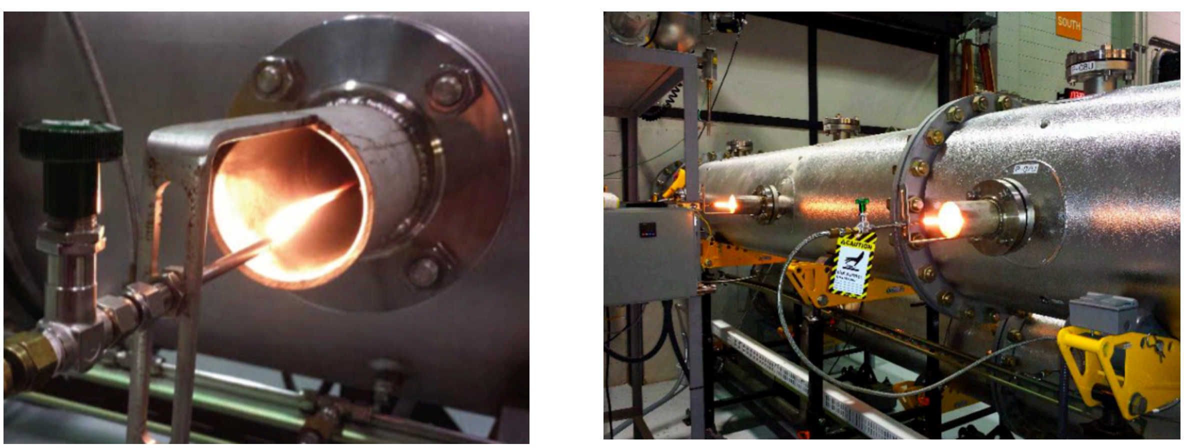

(A) (B)

Figure 46. Photograph of (A) oxygen starved acetylene burner for generating soot and (B) two burners injecting acetylene soot into the LSTS upstream of the HEPA filter. Up to 4 burners are used in filter loading tests.

RESULTS

Kurion Prototype 1 Filter With Proprietary Pleat Design, High-Strength Glass Fiber Medium and No Separators

Kurion fabricated prototype 1 filters using pleated Lydall HEPA media with glass scrim on one side (Lydall 3398-L1W), wire mesh on both sides of media to provide pleat support and a cylindrical wire grid around the exterior to hold the filter shape. The filters had very little medium area (125 ft2 total, 118 ft2 effective for the safe-change filter and 159 ft2 total, 150ft2 effective for the remote change filter). This resulted in very high medium face velocities of 16.9 ft/min for the safe-change and 13.3 ft/min for the remote-change filters compared to the standard 5 ft/min.   The filters used a proprietary pleat design in a cylindrical filter configuration with a nominal pleat depth of 3 inches. No separators were used. The parameters of the prototype 1 safe-change and remote-change HEPA filters are shown in Table 3.

Table 3. Parameters of Kurion Prototype 1 filters

Filter	Inlet ID, in.	Pack ID, in.	Pack OD, in.	Pleat* depth, in.	Effective area, ft2	Medium velocity ft/min	No. of pleats
Safe change	13.0	13.3	19.9	3.09	118	16.9	140
Remote change	11.0	12.6	18.8	2.93	150	13.3	176

*Proprietary pleat design

Unfortunately, the efficiency at different velocities for the HEPA medium (Lydall 3398-L1W) that Kurion used in their prototype 1 filters had not been determined prior to the fabrication of the filters. MSU had just completed the fabrication of the RLPTS in Figure 9 and used the Kurion filters as part of the shake-down tests. Had the media efficiency tests been available, they would have shown that the prototype 1 filters would fail the DOP penetration test due to the high medium velocity as seen in Figure 35.

Kurion Prototype 1 Safe-Change Filter With High-Strength Glass Fiber Medium and No Separators

The initial tests of the Kurion safe-change filter for DOP efficiency using the tester in Figure 8 in the air configuration mode showed that it is close to the threshold requirement of 0.03% penetration at 0.27 microns LAS at the rated flow of 2000 cfm as shown in Figure 47. However, the test used the original MSU filter penetration test method whereby the upstream was measured with the undiluted SMPS and the downstream with the LAS. This method did not yield accurate results because the LAS particle size measurements are displaced as shown in Figure 30. Using the penetration values for 0.27 microns in Figure 42 at 16.9 ft/min suggests that the penetration at 0.27 microns was 0.05%. No penetration measurements were taken at the 20% rated flow.

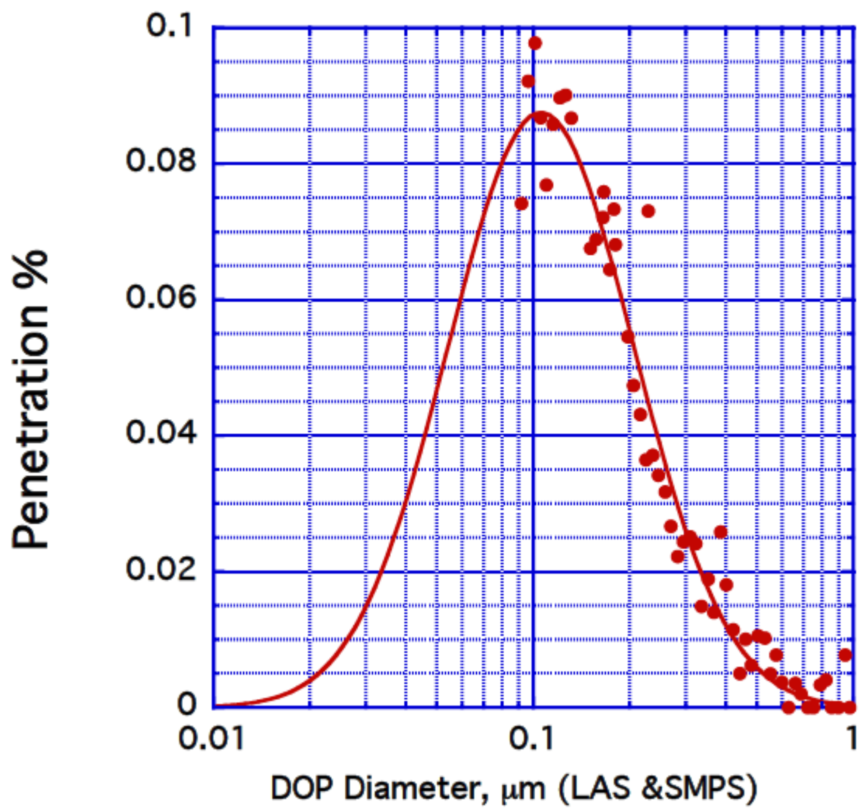

Figure 47. DOP penetration % at 2000 cfm for Kurion SC prototype 1 (K-SC-Pro-1) filter using Lydall 3398-L1W medium (16.9 ft/min medium velocity) and fitted to a log-normal curve. The penetration method used the original MSU test method of undiluted SMPS for upstream measurement and LAS for downstream measurement. The pressure drop at 2,000 cfm was 2.56 inches WC.

The pressure drop measurements of the Kurion safe-change filter at 1400 cfm (1.76 inches WC at 11.9 ft/min) and 2000 cfm (2.56 inches WC at 16.9 ft/min) are superimposed on the pressure drop curve for the Lydall 3398-L1W medium from Figure 22. Figure 48 shows that the filter pressure drop of the filter is slightly greater than that of the medium as would be expected to account for the added resistance from the channel flow in the full-scale filter. The laminar flow through the filter follows the expected performance of Filter B in Figure 6

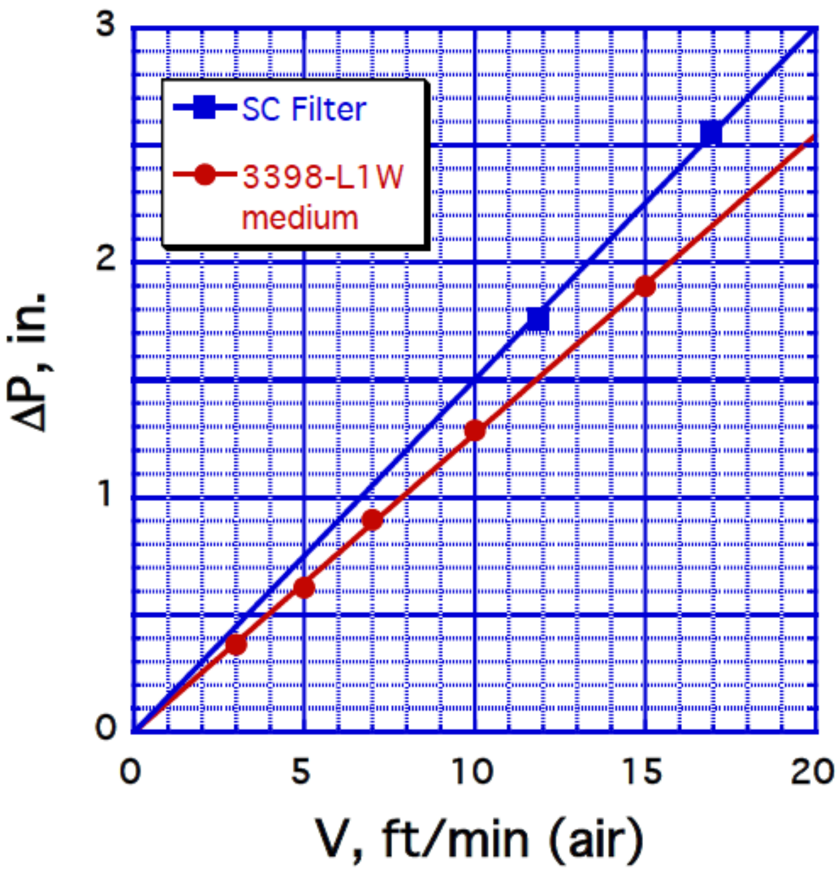

Figure 48. Initial pressure drop of Kurion SC prototype 1 filter using Lydall 3398-L1W medium. The two DP measurements of the full size filter were taken at 1400 and 2000 cfm. The slopes of the SC filter and 3398-L1W medium are 0.1502 in. WC/ft/min (7.365E3 Pa/m/s) and 0.1271 in. WC/ft/min (6.232E3 Pa/m/s) respectively.

The pressure drop across a pleated filter at typical flows is approximately the sum of the (1) media pressure drop, and (2) the pressure drop due to flow resistance through the pleat channels. Both of these flows are laminar and have the pressure drop proportional to the fluid velocity. The small pressure drop due to inertial flow where air is accelerated and decelerated into and out of the pleats is ignored here, especially for the high viscous fluids like PEG/water. Thus, the pressure drop across the pleated filter is given by Equation 11.

$$\Delta P_F = \eta V \left(K_M + K_P \right) \tag{11}$$

where ΔP_F = pressure drop across filter

η = viscosity of the fluid in the filter test

K_M = a constant dependent on the filter structure (eg. Thickness, fiber diameter, fiber packing density, etc)
K_P = a constant dependent on the pleat geometry (e.g. width, depth, medium surface roughness, presence of separator, etc.)

The constants K_M and K_P in Equation 11 can be determined from the pressure drop of the filter and medium in air in Figure 48. For the filter medium, the slope of the curve in Figure 48 is 0.1271 inch WC/ft/min. Using this slope and the air viscosity of 0.0185 cP in Equation 4, the value of K_M= 6.87 inch WC/(ft/min)/cP. For the filter in Figure 48, the slope is 0.1502 inch WC/ft/min. Using this slope, the air viscosity of 0.0185 cP and K_M = 6.87 in Equation 11 yields K_P = 1.25 inch WC/(ft/min)/cP. These constants cannot be used for the PEG/water flows due to slip flow, which results in lower K_M values. In addition, since water significantly softens HEPA filter media, it is unlikely that the pleat configuration and the K_P value will remain constant in going from gas to liquid.

If the filter pleats partially collapse with increasing differential pressure then the pressure coefficient for the filter pleat resistance, K_P , increases with increasing velocity in the first approximation by the following equation:

$$K_P = K_{P0} + c_P V \tag{12}$$

where K_{P0} = pressure coefficient of un-collapsed pleat
c_P = coefficient for increased pressure due to partial pleat collapse at increased velocity

Note that Equation 12 only applies for partial pleat collapse. If severe pleat collapse occurs as seen with the Flanders filters in Figures 4 and 5, then higher orders of V will be required in Equation 12. Also, for normal air velocities with clean filters, the pleats do not collapse, and $K_P = K_{P0}$.

Substituting Equations 9 and 12 into Equation 11 for the filter pressure drop yields

$$\Delta P_F = \left(K_{M0} + K_{P0}\right)\eta V + \left(c_M + c_P\right)\eta V^2 \tag{13}$$

Equation 13 is used in this report to analyze the pressure drop of the filter in terms of contributions by the medium resistance and the pleat flow resistance. At low velocities (low pressure drop) , only the first, linear term in Equation 13 is used as in Figure 48. The second term in Equation 13 becomes important at high pressure drops where the medium compresses and/ or the pleats collapse as seen in Figure 49 for the PEG/water solution.

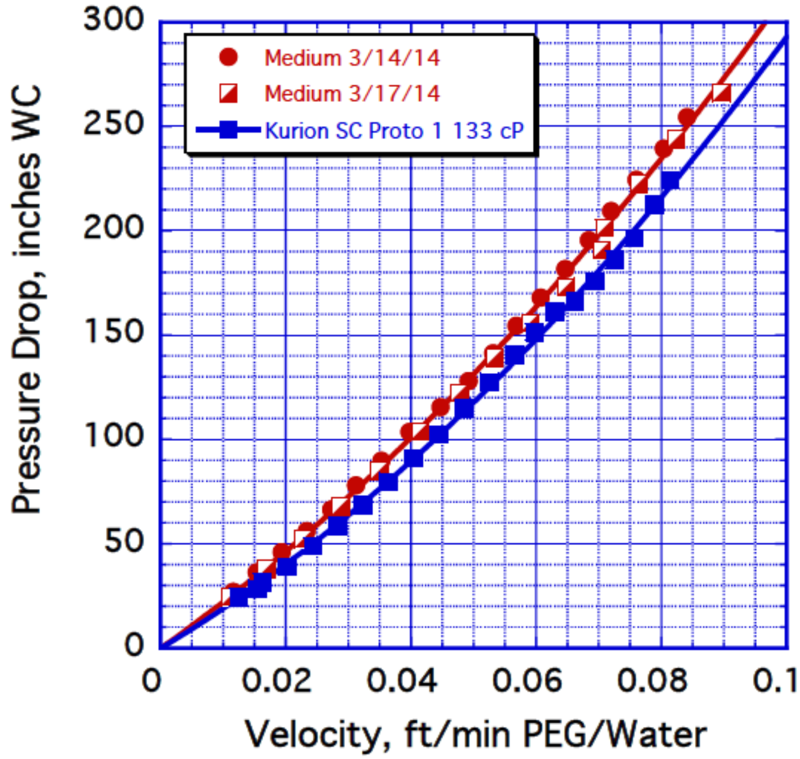

Figure 49. Measurements of the pressure drop versus medium velocity of the Kurion prototype 1 safe change filter tested with a PEG/water solution at 95°F (measured as 133 cP) in the full-scale tester in Figure 8 and the flat media samples of Lydall 3398-L1W tested with a PEG/water solution (computed 186 cP) in the bench-scale tester in Figure 19.

The higher pressure drop for the filter media tests in Figure 42 is due to the higher viscosity of the PEG-water solution used for the media (computed as 186 cP based on water tests) compared to the SC filter (133 cP). The media tests also have an uncertainty in the computed velocity due to the uncertainty of the medium diameter described previously.

The best fit curve for the Kurion SC prototype 1 filter with a PEG/water solution of 133 cP from Figure 49 is given by Equation 14

$$\Delta P_F = 1{,}782\, V + 11{,}478\, V^2 \tag{14}$$

To compare the pressure drop of the filter medium and of the full-scale filter, the viscosity of the PEG/water solution must be identical. Since the pressure drop of the medium and full-scale filter is directly proportional to the fluid viscosity as seen in Equation 13 (even for air with slip flow), the pressure drop of the medium or the filter tested with a fluid at one viscosity can be converted to a pressure drop with the fluid at a second viscosity.

$$\Delta P_2 = \frac{\eta_2}{\eta_1} \Delta P_1 \qquad (15)$$

Although the choice of the second viscosity is arbitrary, 186.2 cP is selected here because that is derived from comparing media tests with water in Figure 23 and with PEG/water in Figure 24 and using the water viscosity at 72 °F (0.953cP) as described previously. Converting the DP filter values to a constant viscosity has the additional benefit of allowing direct comparisons of different filters. Thus the pressure drop of the SC filter in Figure 49 is modified using Equation 15 with η_1 = 133 cP and η_2 = 186.2 cP and the data replotted in Figure 50.

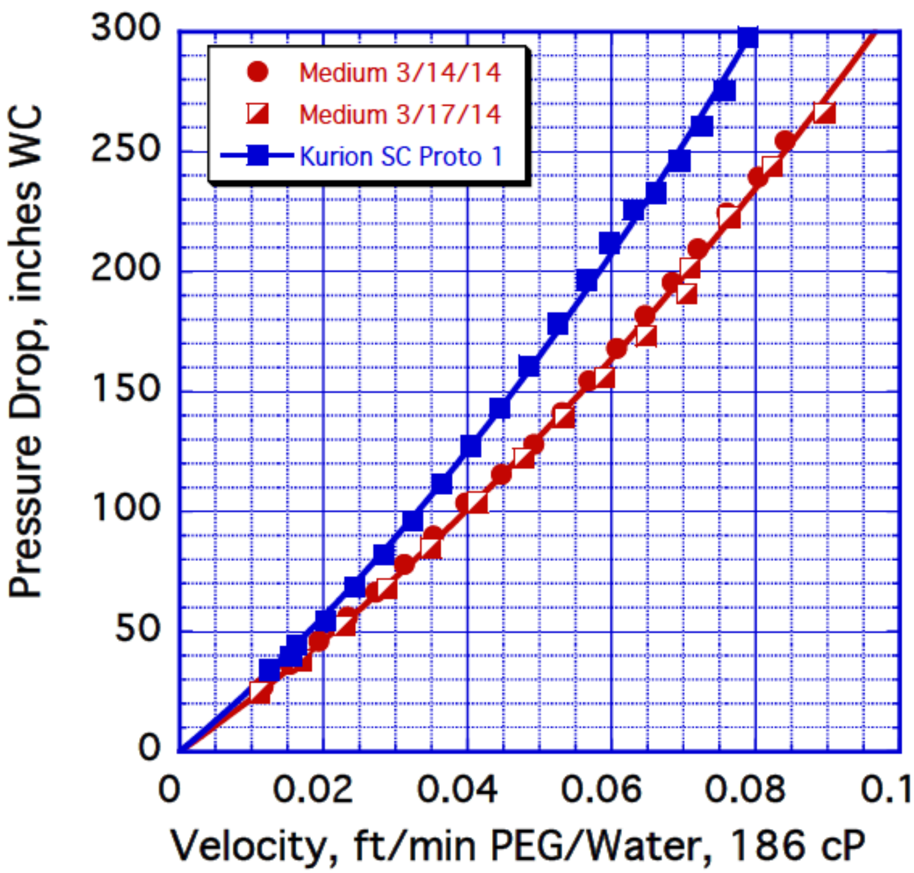

Figure 50 Computed pressure drop of the Kurion prototype 1 SC filter for a viscosity 186. cP from the experimental pressure drop at 133 cP in Figure 49 and the experimental pressure drop for the 3398-L1W medium at 186.2 cP.

The best fit curve to the SC filter data in Figure 50 is given by Equation 16

$$\Delta P_F = 2495\,V + 16069\,V^2 \qquad (16)$$

The coefficients of Equation 16 for the filter and Equation 7 for the medium, and the constant K_{M0}= 11.52 derived from the water test in Figure 23 are used to solve the remaining parameters in Equation 13: c_M= 52.81, K_{P0} = 1.877, and c_P= 33.49.

Using these coefficients and the appropriate portions of Equation 13, the contribution of the filter medium, pleat channel flow, medium compression and pleat compression on the filter pressure drop can be determined and are graphed in Figure 51.

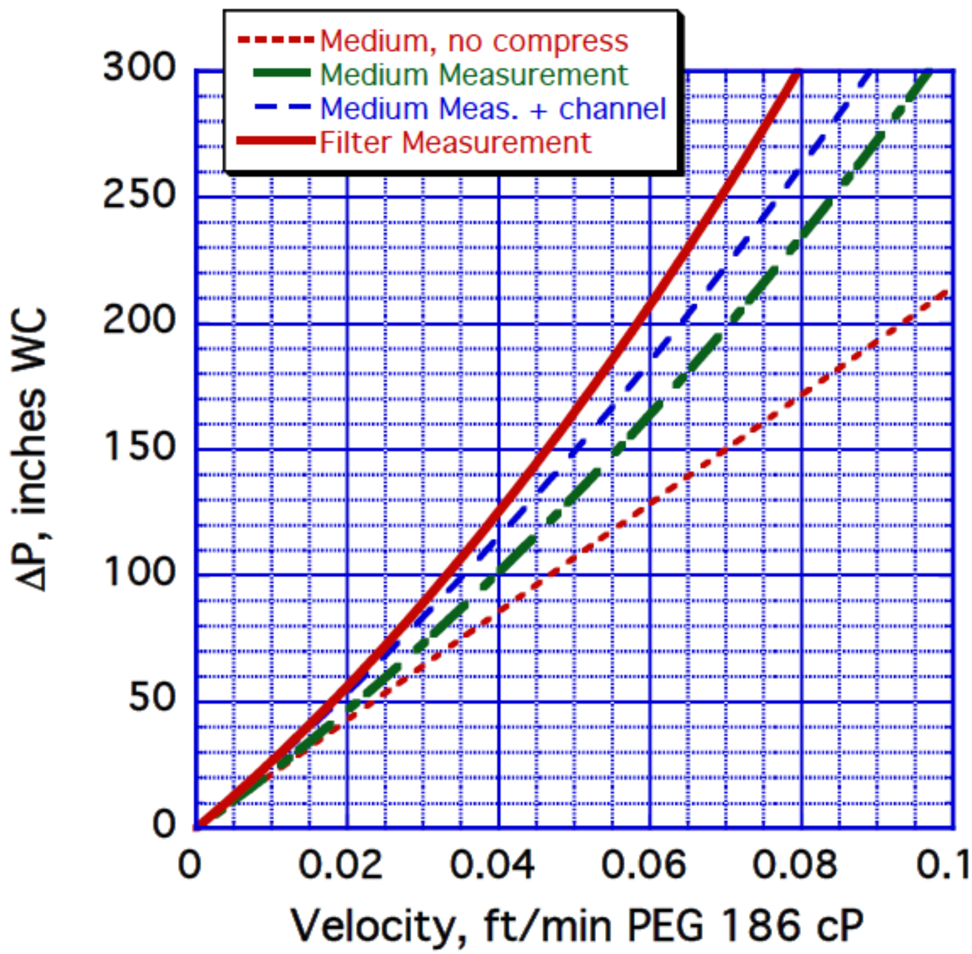

Figure 51. Pressure drop measurements as a function of fluid velocity of the K-SC-Pro-1 filter and filter medium from Figure 50, the computed pressure drop of the medium with no compression, and the pressure drop of the medium measurement plus the computed pressure drop of the pleat channel flow. The pressure due to pleat collapse is seen as the difference between the filter measurement and the medium measurement plus computed pressure drop of the pleat channel flow.

Figure 51 shows the greatest contribution to the filter pressure drop is the pressure drop of the filter medium. The compression of the filter medium is the next major portion of the filter pressure drop. The pressure drop of the pleat channel flow has a much smaller contribution. Finally, Figure 51 shows that the partial pleat collapse has the smallest contribution to the total filter pressure drop.

The large effect of the medium compression on the total filter pressure drop is explained by the lofty nature of the glass fiber medium. Figure 52 shows a cross section of the Lydall 3398-L1W medium used in the Kurion prototype 1 filters. Since the medium has about 95% porosity, the medium is easily compressed; and a compressed medium has significantly greater pressure drop than the uncompressed medium.

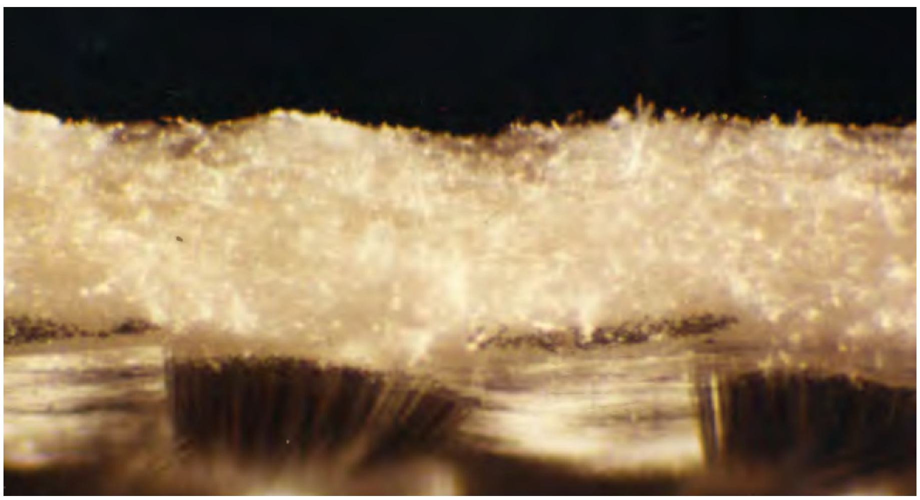

Figure 52. Photograph of the cross-section of the Lydall 3398-L1W medium used in the Kurion prototype 1 filters. The glass fiber mat is glued onto a glass cloth shown on the bottom

Following the high pressure test, MSU drained the PEG/water solution, added clean water and rinsed the filter. Heated air at 100°F was then passed through the water saturated filter beginning at 100 cfm where the DP=33 inches WC and then the flow was gradually increased to 400 cfm over 150 minutes. The filter DP continued to decrease at 400 cfm in an exponential fashion until the DP reached 10 inches WC. MSU attempted to measure the DOP efficiency at this point, but stopped the test when the LAS measurements showed excessive penetration, and MSU assumed the filter had major leaks.

This was the first experience with the liquid tester and the DP criterion for drying the filter had not yet been established. This criterion required the partially dried filter to have 2 times the pressure drop of the clean filter at 20% flow. For the

Kurion prototype 1 safe-change filter, this test DP is 1.02 inches WC. In contrast, the efficiency test was conducted with a pressure drop of 10 inches WC.

Assuming the increased pressure drop due to the water saturated filter is inversely proportional to the effective filter area, then the Kurion filter with a pressure drop of 10 inches WC at 20% flow (400 cfm) would have an effective medium velocity of 66.3 ft/min (3.38 x 10/ 0.51).

Extrapolating the DOP penetration in Figure 42 to 66.3 ft/min indicates that an undamaged HEPA medium would have a DOP penetration of almost 1%. Thus, the high DOP concentration measured downstream of the HEPA filter would occur even if the filter had no defects.

Examination of the Kurion prototype 1 safe-change (K-SC-Pro-1) filter following the high pressure test indicated that 8 of the approximately 140 pleats had ballooned as shown in Figure 53. This pleat ballooning had only a minor impact on the total filter pressure drop as seen by the minimal pleat collapse in Figure 51, but the defect was not acceptable to Bechtel.

(A) (B)

Figure 53. Photo of Kurion K-SC-Pro-1 filter (A) before and (B) after exposure to 225 inches WC and 95°F for one hour.

Kurion Prototype 1 Remote-Change Filter With Proprietary Pleat Design, High-Strength Glass Fiber Medium and No Separators

The Kurion prototype 1 remote-change filter (K-RC-Pro-1) was made with 159 ft2 of medium (150 ft2 effective) and had an initial DP= 3.69 inches WC and 0.35% DOP penetration at 2,000 cfm and 2.48 inches WC and at 1,400 cfm. These reported pressure drops represent the measured pressure drop of the filter in the RLPTS housing less the tare pressure drop of the 13.0 inches orifice in the tube sheet that the filter is mounted on (Figure 9). The pressure drop of the remote-change filter includes the additional pressure drop due to the 11.0 inches orifice, which is the inside diameter of the filter grab ring (Table 3).

Ideally, the pressure drop of the radial filter should be measured independent of the test housing and this generally implies the measurement of the filter pack (Bergman, 2017). Measuring the pressure drop of the filter pack is the implicit practice in testing AG-1 filters and is the practice used to qualify HEPA filters at the US Army test facility (Bergman, 2017). However for the RC HEPA filters in this study, the 11.0 inches diameter grab ring is considered to be part of the filter and is more restrictive than the RC filter pack inside diameter of 12.6 inches (Table 3). In addition, the reported MSU pressure drop from the RLPTS included the subtraction of the tare corresponding to the 13.0 inches diameter orifice in the tube sheet. If the pressure drop for the two orifices (11.0 and 13.0 inches) are known, then the pressure drop of the RC filter pack, $\Delta P_{RC,Pack}$, is given by (Bergman, 2017)

$$\Delta P_{RC,Pack} = \Delta P_F + \Delta P_{13"} - \Delta P_{11"} \tag{17}$$

where ΔP_F = reported pressure drop after subtracting the 13" orifice tare
$\Delta P_{13''}$ = tare pressure drop of 13" orifice in tube sheet
$\Delta P_{11''}$ = tare pressure drop of 11" grab ring

Note that the impact of various orifices in the test fixture or in the filter (e.g. grab ring, channel for gel seal) on the filter pressure drop for tests using air does not apply to tests with liquid. No corrections to the experimental pressure drop measurements as shown in Equation 17 are required. This follows because the pressure drop in air for flow through an orifice is due to fluid inertia, which is negligible in liquid systems used here. The inertial pressure due to air flow through an orifice is proportional to the square of the volume flow rate.

Although the pressure drop equation for the 13 inch orifice in the RLPTS was not available, the filter housing configuration for the RLPTS in Figure 9 (B) is similar to the configuration of the SC housing with the 13 inch orifice in Figure 45 (A). This similarity would yield a similar discharge coefficient for the orifice and thus allow the pressure drop equation developed for the SC housing to be used for the RLPTS (Bergman, 2017).

$$\Delta P_{13''} = 2.057x10^{-7}\,Q^2 \quad (18)$$

From the orifice flow equation, the pressure drop is inversely proportional to the square of the orifice area (Bergman, 2017). Thus Equation 18 for the 13 inch orifice can be converted to Equation 19 for the 11 inch orifice.

$$\Delta P_{11''} = 2.873x10^{-7}\,Q^2 \quad (19)$$

Using Equations 17-19, the pressure drop for the RC filter at 1400 and 2000 cfm decreased from 2.48 and 3.69 inches to 2.32 and 3.36 respectively. A comparable adjustment to the SC prototype 1 filter resulted in a negligible increase since the filter pack inlet diameter of 13.3 inches was close to the tube sheet orifice of 13 inches.

The measured pressure drop corresponding to the RC filter plus the grab ring orifice is graphed in Figure 54 along with the corrected pressure drop of the filter pack and the medium. The corrected pressure drop for the remote change filter at 2000 cfm is 3.36 inches WC (3.69 inches uncorrected). Note that the measured pressure drop is slightly non-linear with velocity due to the added orifice flow. When the pressure drop of the grab ring orifice is subtracted, the resulting pressure drop of the remote-change filter is linear.

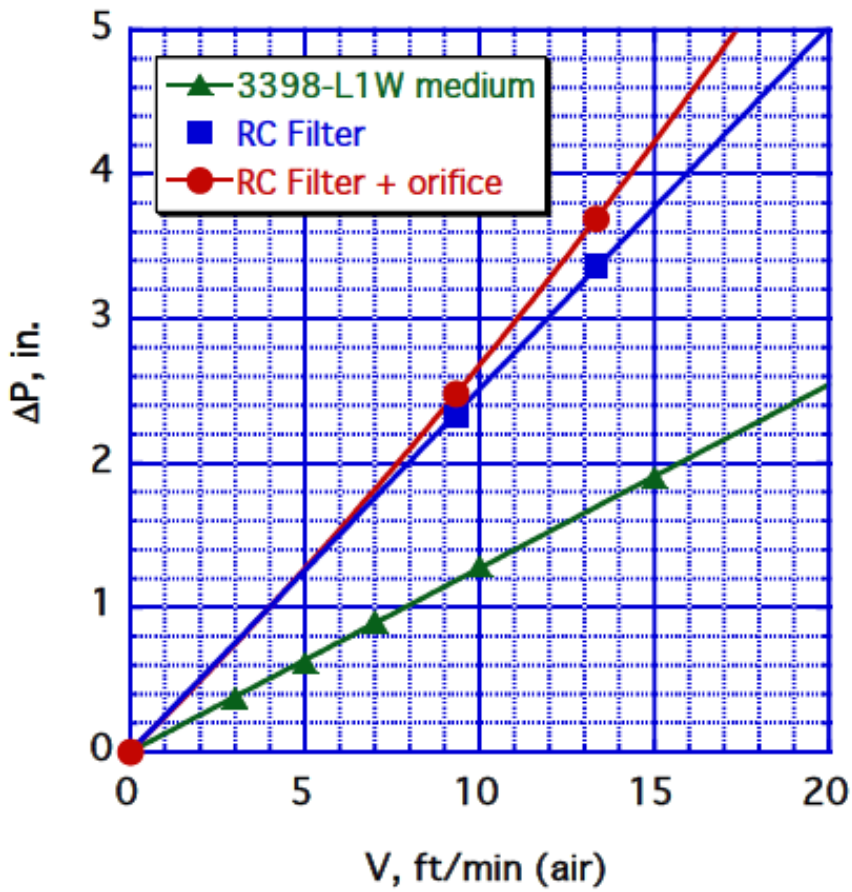

Figure 54. Pressure drop of the Kurion prototype 1, remote-change, HEPA filter, the filter plus the grab ring orifice, and the filter medium as a function of the medium air velocity under ambient conditions. The slopes of the RC filter and 3398-L1W medium are 0.2511 in. WC/ft/min and 0.1271 in. WC/ft/min respectively.

The analysis of the pressure drop of the remote-change filter and medium in air and in PEG/water solution follows the same process used for the safe-change filter. The constants K_{M0} and K_{P0} in Equation 13 can be determined from the pressure drop of the filter and medium in air in Figure 54. Since the filter medium in Figure 54 is the same as that used for the safe-change filter in Figure 51, the coefficient, K_{M0}= 6.87 inch WC/(ft/min)/cP. For the filter in Figure 54, the slope is 0.2511 inch WC/ft/min. Using this slope, the air viscosity of 0.0185 cP and the K_{M0} value of 6.87 in the first term of Equation 13 yields K_{P0}= 6.70 inch WC/(ft/min)/cP (0.2511/0.0185 – 6.87).

The remote-change filter was then tested using a PEG/water solution at 150 cP and 88.2 °F at increasing flows as shown in Figure 55. The best fit curve through the data is given by Equation 20.

$$\Delta P_F = 3{,}185\, V + 41{,}629\, V^2 \tag{20}$$

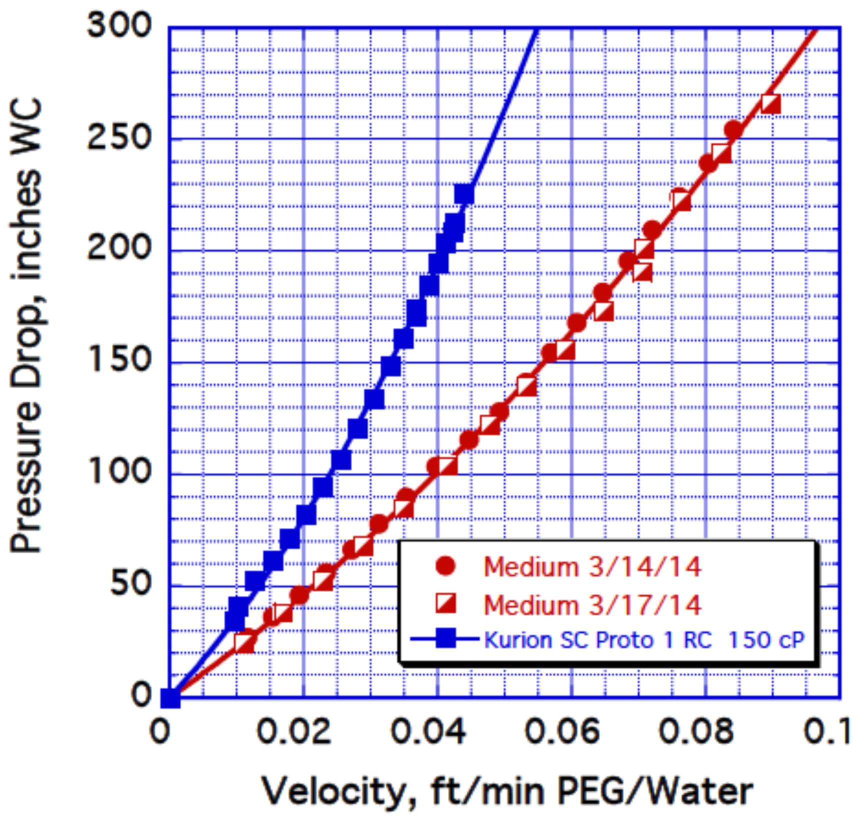

Figure 55. Measurements of the pressure drop versus medium velocity of the Kurion prototype 1 RC filter tested with a PEG/water solution in the full-scale tester in Figure 8 with an average PEG/water viscosity of 150 cP and an average 88.2 °F (87.1 – 91.6 °F). The medium measurements at 186.2 cP from Figure 50 are included for reference.

The pressure drop curve for the SC prototype 1 filter measured with the PEG/water solution at 150 cP was converted to the pressure drop corresponding to 186.2 cP using Equation 15 to allow direct comparisons of the filter and the medium and the results plotted in Figure 56.

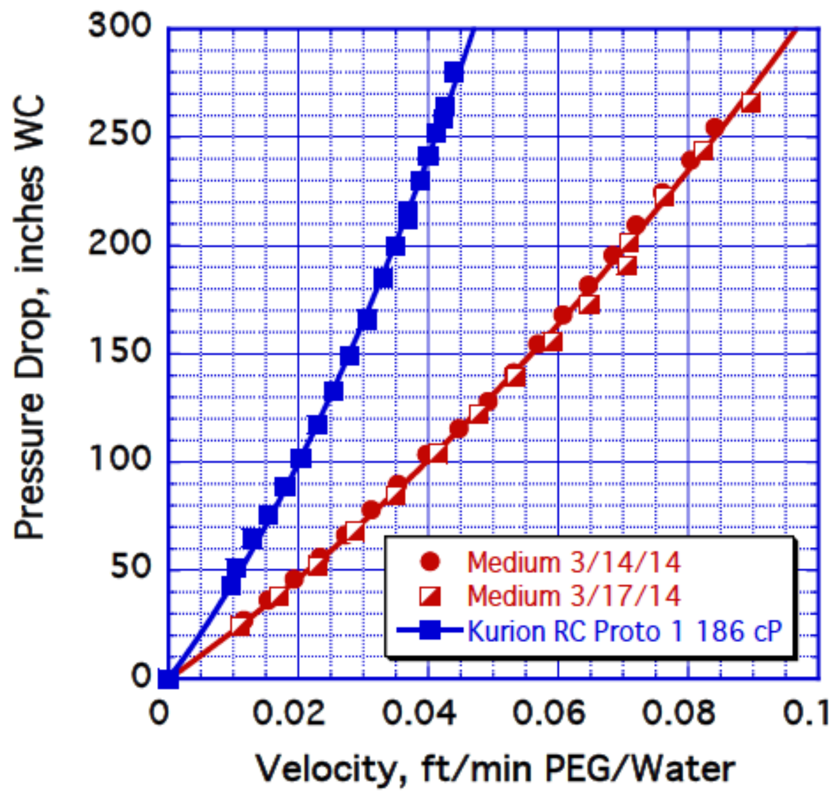

Figure 56. Computed pressure drop of the Kurion prototype 1 RC filter for a viscosity 186 cP from the experimental pressure drop at 150 cP in Figure 55 and the experimental pressure drop for the 3398-L1W medium at 186 cP.

The best fit curve through the points for the Kurion prototype RC filter in Figure 56 is given by Equation 21.

$$\Delta P_F = 3{,}953\, V + 51{,}668\, V^2 \tag{21}$$

The coefficients of Equation 21 for the filter and Equation 7 for the medium, and the constant K_{M0}= 11.52 derived from the water test in Figure 23 are used to solve the remaining parameters in Equation 13: c_M= 52.81, K_{P0} = 9.71, and c_P= 224.7.

Using these coefficients and the appropriate portions of Equation 13, the contribution of the filter medium, pleat channel flow, medium compression and pleat compression on the filter pressure drop can be determined and are graphed in Figure 57.

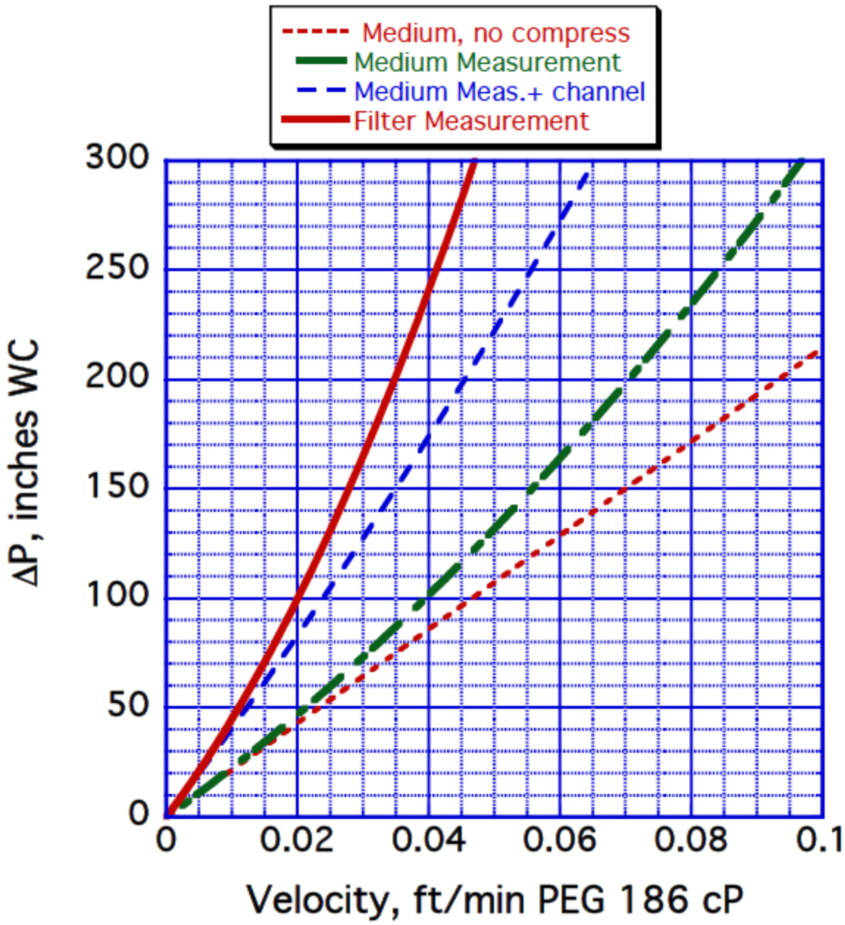

Figure 57. Pressure drop measurements as a function of fluid velocity of the prototype 1 RC filter and the filter medium from Figure 56, the computed pressure drop of the medium with no compression, and the pressure drop of the medium plus the pleat channel.

Comparing the RC filter in Figure 57 with the SC filter in Figure 51, shows the experimental DP measurements for the medium and the computed DP measurements for the medium with no compression are the same since the SC and RC filters use the same medium. However, the computed pressure drop for the pleat channel flow plus the medium is much greater for the RC filter than for the SC filter. This increased pressure drop results from the much tighter packing of the medium in the RC design compared to the SC design. The RC filter has 150 ft2 of effective medium configured in about 176 pleats compared to the SC filter, which has 118 ft2 configured in about 140 pleats. Both filter designs used a proprietary pleating design.

The RC filter also has a much greater pleat collapse than does the SC filter as seen by the difference between the DP of the filter measurement and the DP of the computed pleat channel flow pressure plus the measured filter pressure drop. Figure 57 shows the DP difference for the remote-change filter is much greater than the DP difference for the safe-change filter in Figure 51.

Following the liquid pressure tests, Kurion had pointed out an error in the criterion that Bechtel included in the initial version of the filter test specification, whereby a filter would fail the resistance to pressure test if the non-linearity of the DP versus velocity curve is greater than 20%. Kurion demonstrated that the criterion was ill-defined because there was no baseline reference for the linear portion of the curve.

In addition, Kurion pointed out the filter medium had extensive non-linearity due to medium compression. Although Bechtel included a reference medium test in all filter efficiency, particle loading and pressure drop measurements in both air and PEG/water solutions, this was overlooked in the criterion for pleat collapse.

This criterion was dropped in subsequent testing specifications. From Figure 57, a better reference pressure drop would be the filter medium pressure drop plus the computed pressure due to pleat channels. Figure 57 shows the filter pressure drop of 225 inches WC has a corresponding pressure drop of 164 inches WC for the combined medium pressure drop plus the pleat channel pressure drop. In this case, partial pleat collapse represents the difference, 61 inches WC, between the two values, or 27% of the total 225 inches WC.

The DOP penetration tests on the K-RC-Pro-1 filter indicated very large leaks before and after the high pressure PEG/water test. Figure 58 shows not only the large magnitude of the penetration, but also the near-flat profile of the penetration curve that is an indicator of a leaking filter (Bergman et al, 1997b). The DOP penetration test after the liquid test had a more conventional penetration curve, although the penetration value greatly exceeds the HEPA limit. The increased pressure drop of the filter after the PEG/water test suggests residual PEG deposits may have plugged some of the leaks. However, since the penetration of the HEPA media at 13.3 ft/min is about 0.03% in Figure 42, the high penetration at 0.3 microns in Figure 58 indicates a large leak. The leak scan test in Figure 43 was not available to determine the source of the leak

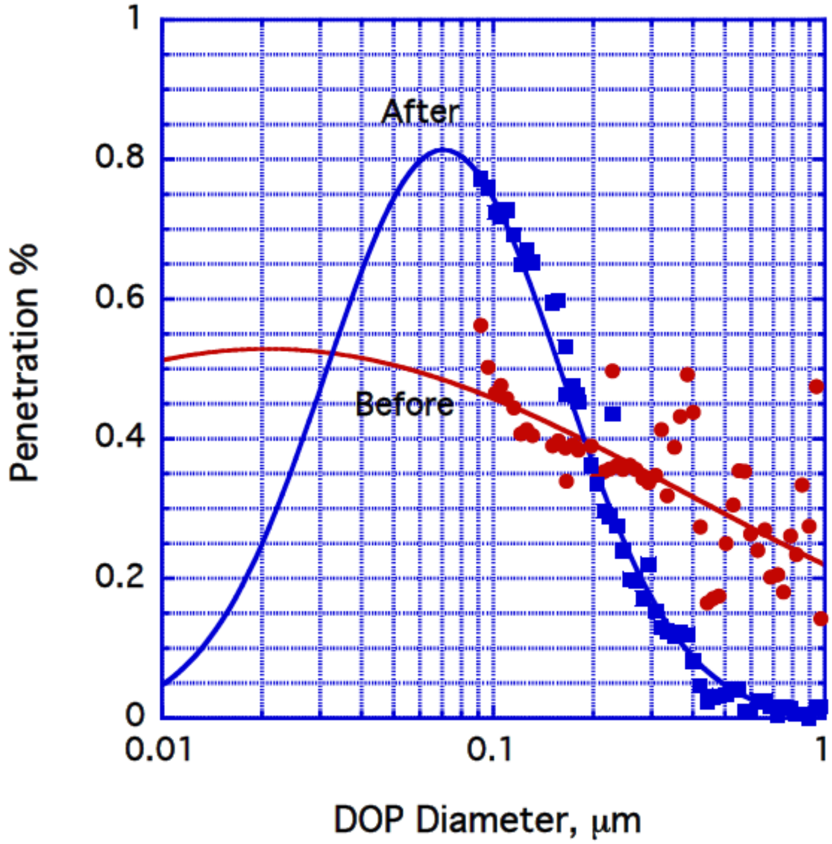

Figure 58. DOP penetration % at 2000 cfm for the Kurion RC prototype 1 (K-RC-Pro-1) filter using Lydall 3398-L1W medium (13.3 ft/min medium velocity) before and after the high pressure liquid test and fitted to log-normal curves. The RLPTS DP for the filter before test was 3.69 inches WC and after rinsing and drying the filter was 4.41 inches WC. The penetration method used the original MSU method of undiluted SMPS for upstream measurement and LAS for downstream measurement.

The photograph of the Kurion prototype 1 remote-change filter in Figure 59 shows no structural damage or deformed pleats as was seen for the safe-change filter in Figure 53. The increased strength of the remote-change filter is due to the tighter pleat packing compared to the looser safe-change filter. However, the tighter pleat packing comes with a price of significantly higher pressure drop as seen in Figure 57 compared to the safe-change filter in Figure 51.

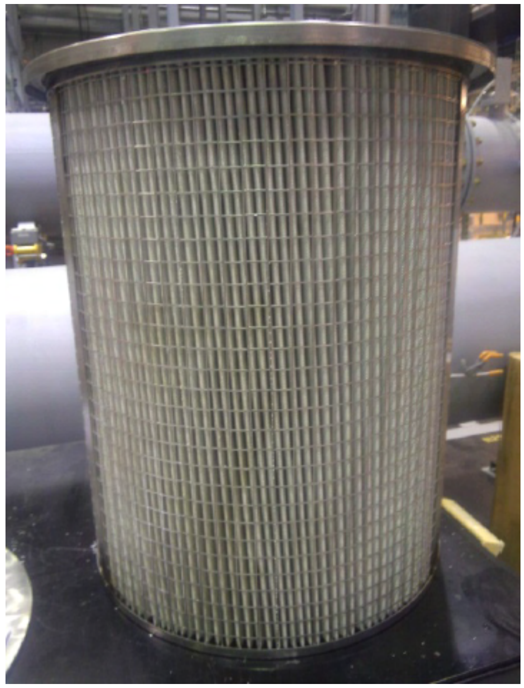

Figure 59 Photograph of Kurion prototype 1 remote-change HEPA filter following the high pressure liquid test.

Table 4. Summary of Kurion Prototype 1 Filter Tests

Filter	Rating, in. WC	Initial /Final	DP[1], in. WC	Penetration, %			Pass/ Fail	Mass gain, g
				2000 cfm	400 cfm	100 cfm		
K-SC-Pro-1	225	Initial	2.56	0.03	--	--	Pass	
		Final		--	--	--	Fail	--
K-RC-Pro-1	225	Initial	3.69	0.35	--	--	Fail	
		Final		0.20	--	--	Fail	--

[1]DP values represent the measured DP in the RLPTS minus the tare for the 13 inches orifice.

Kurion Prototype 2 Filter With High-Strength Glass Fiber Medium and Conventional Pleat Design With 3 Inch Pleats and Separators

Following the tests on the prototype 1 filters with the proprietary pleat design and no separators, BNI requested Kurion increase the filter area so that the filter efficiency would improve by lowering the medium velocity and use separators to improve pack stability and mitigate pleat collapse in their new radial-flow filter units. Kurion selected the higher strength Lydall 3398-L2W medium, added a wire mesh screen on the downstream side of the medium and selected aluminum separators with a corrugation height of 0.11 inches.

Because of the curvature of the radial filter, the separators did not cover the full depth of the pleat and were in contact with the filter medium on the inside portion of the pleats but not the outside portion of the pleats. This issue is greatly reduced when the separator height is reduced below 0.05 inches. The specific design features of the safe-change and remote-change HEPA filters are given in Table 5.

Table 5. Parameters of Kurion Prototype 2 filters

Filter	Inlet ID, in.	Pack ID, in.	Pack OD, in.	Separator height, in.	Pleat* depth, in.	Effective area, ft2	Medium velocity ft/min	No. of pleats
Safe change	13.0	13.3	19.3	0.11	3.00	141	14.2	154
Remote change	11.0	12.8	18.8	0.11	3.00	141	14.2	149

*Standard pleat design

Comparing filter areas in Table 5 for the prototype 2 filters to the previous prototype 1 filters in Table 3 shows a small increase in medium area for the SC filter (118 to 141 ft^2) and a small decrease in medium area for the RC filter (150 to 141 ft^2). Thus the filter efficiency for the Prototype 2 filters would not significantly change from the Prototype 1 filters.

Unfortunately, Kurion fabricated their new HEPA filters before MSU was able to test the penetration of the medium used in the manufacturers filters. Although the original test plan (Garcia, 2012b) did not require separate media tests, such tests were later deemed necessary for the filter development effort and were included in the revised test plan (Garcia, 2015). Had the media penetration data in Figure 35 been available, Bechtel would have informed Kurion that all of their prototype 2 filters would fail the DOP penetration test due to inadequate medium area and excessive medium velocity.

The Bechtel plan called for Kurion to submit two RC filters rated at 45 inches WC, two RC filters rated at 225 inches WC and two SC filters rated at 20 inches WC. However, since Kurion did not have laboratory facilities to measure DOP filter efficiency and pressure drop, Kurion submitted a PRE-test SC and RC filter to provide feedback in the filter design and fabrication.

Kurion Prototype 2 PRE Safe-Change Filter With High-Strength Glass Fiber Medium and Conventional Pleat Design With 3 Inch Pleats and Separators

Figure 60 shows a close-up of a portion of the prototype 2 safe-change HEPA filter designated as K-GFR-SC-001-PRE with the aluminum separators and the pleated Lydall 3398-L2W medium having a wire screen on the downstream side.

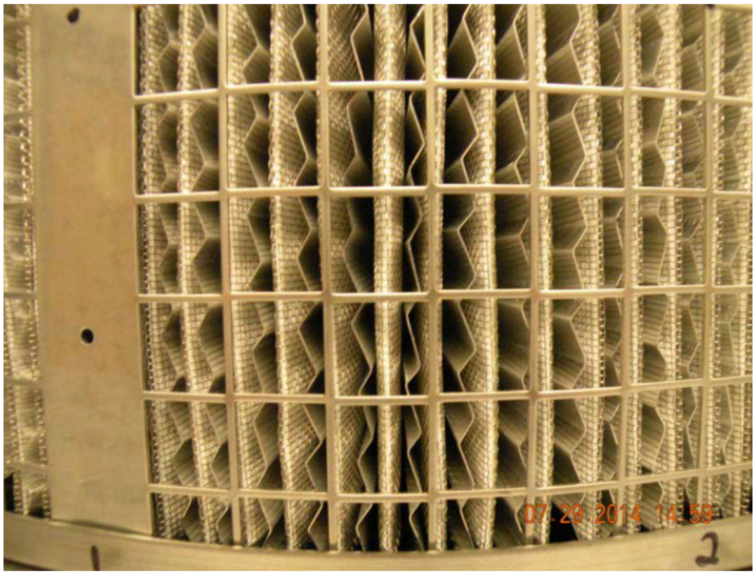

Figure 60. Close-up photograph of the K-GFR-SC-001-PRE filter showing the pleated 3398-L2W medium with a downstream wire screen and aluminum separators.

The SC prototype 2 filter was installed in the tester shown in Figures 8 and 9 configured for air flow to measure the pressure drop and DOP efficiency. The pressure drop of the filter was measured at increasing air flow, but the data was not reduced and available for analysis. MSU reduced the pressure drop at 2000 (14.2 ft/min), and this value is graphed in Figure 61 along with the pressure drop data for the medium 3398-L2W taken from Figure 29. Note that the 3398-L1W and 3398-L2W media have the same pressure drop curve. The pressure drop of the filter in Figure 61 is only slightly greater than the medium pressure drop and indicates that the air resistance in the pleat channel flow with the aluminum separators is very low.

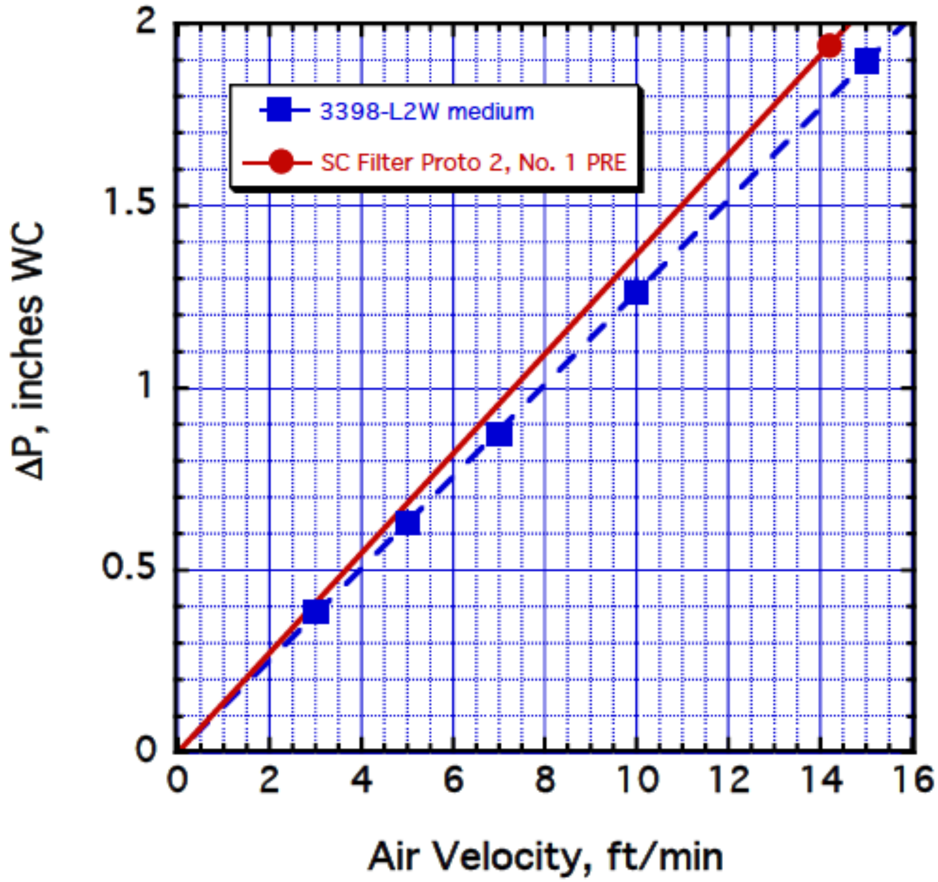

Figure 61. Pressure drop measurements for the SC prototype 2 (K-GFR-SC-001-PRE) filter and the medium, 3398-L2W, used in the filter plotted as a function of air velocity. Note the slope for 3398-L2W (0.1263 in. WC/ft/min) is identical within experimental accuracy to 3398-L1W (0.1271 in. WC/ft/min)

The slopes of the medium (0.1263 in. WC/ft/min) and filter (0.1366 in. WC/ft/min) pressure drop curves in Figure 54, ambient air viscosity (0.0185 cP) and Equations 9 and 13 are used to determine the coefficients K_M and K_P for medium and pleat channel pressure drop, respectively. Using the same procedures as previous yielded $K_M = 6.83$ and $K_P = 0.557$.

The DOP penetration measurements at 2000 cfm and 400 cfm are shown in Figure 62.

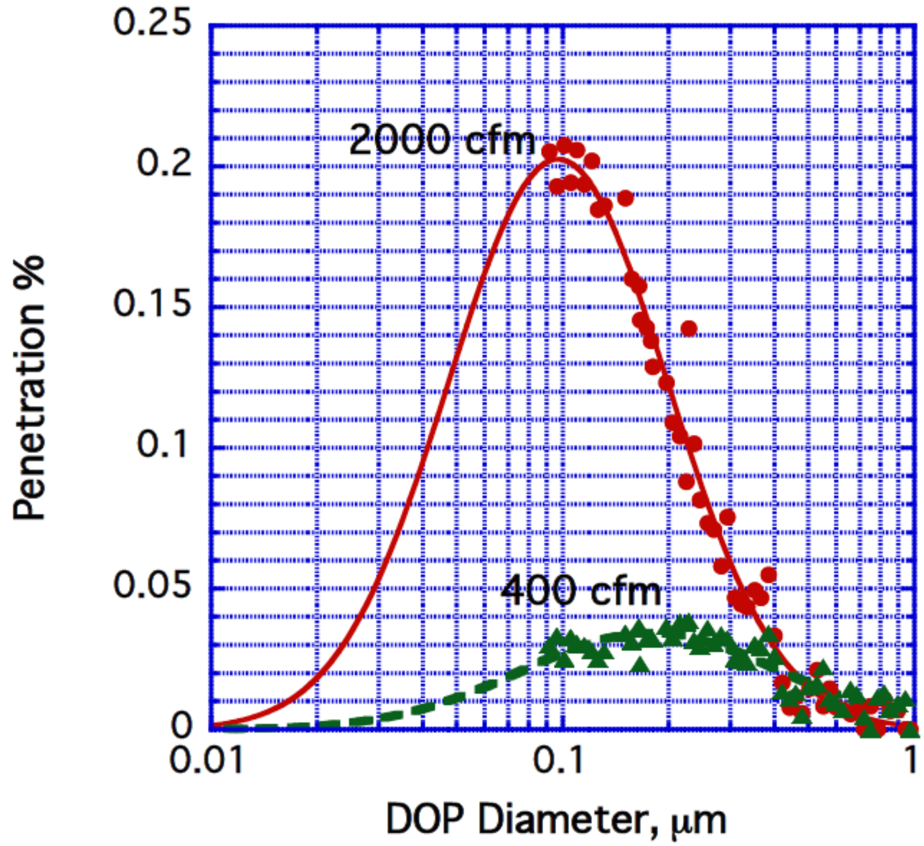

Figure 62. DOP penetration of the prototype 2, K-GFR-SC-1 PRE, filter at 2000 and 400 cfm corresponding to a medium velocity of 14.2 ft/min and 2.8 ft/min respectively and fitted to log-normal curves. The penetration method used the original MSU method of undiluted SMPS for upstream measurement and LAS for downstream measurement. The pressure drop of the clean filter at 2000 cfm was 1.94 inches WC.

Figure 62 shows the filter failed the DOP penetration test at 2000 cfm (0.074% at 0.27 microns), but barely passes at 400 cfm (0.03% at 0.27 microns). If the filter had no leaks as measured by the media tests in Figure 42, the penetration at 2000 and 400 cfm would be 0.038% and 0.0015% respectively. Even without any leaks, the filter failed the DOP penetration test due to the high medium velocity. The location of the leak was not determined since the scan test in Figure 43 was not available.

Following the DOP efficiency test, the RLPTS system was configured for the liquid flow and a PEG/water solution added. The flow through the filter was then incrementally increased to produce the experimental pressure drop versus velocity data in Figure 63.

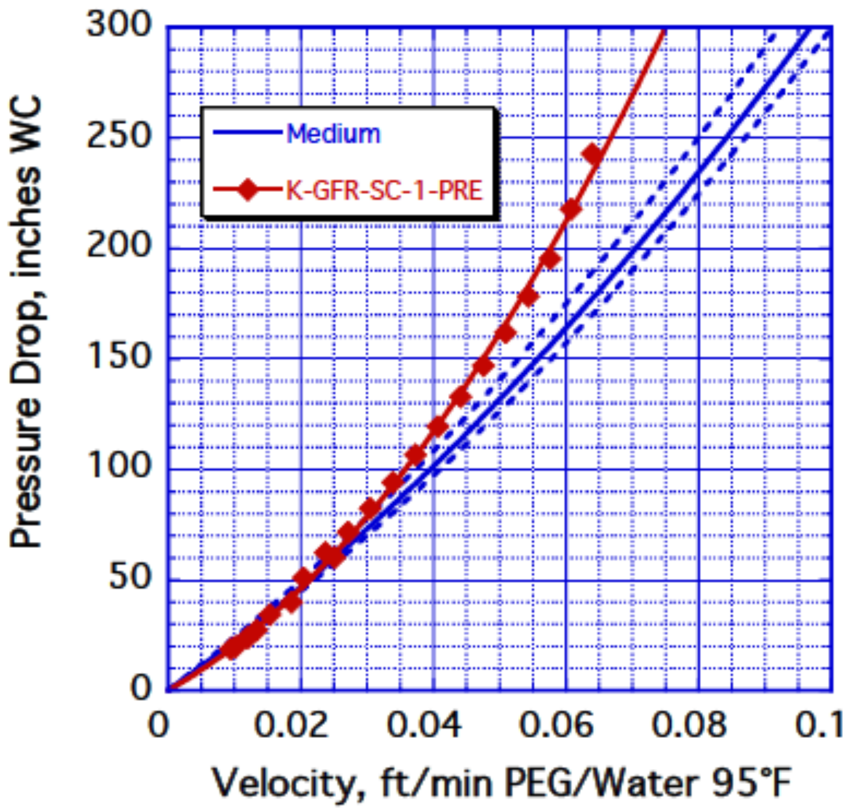

Figure 63. Measurements of the pressure drop versus medium velocity of the Kurion prototype 2 SC filter (K-GFR-SC-1-PRE) tested with a PEG/water solution measured as 186 cP at 95°F before and after the test in Figure 65. The pressure drop of the medium from Figure 24 with a computed viscosity of 186 cP is superimposed.

The dashed lines in Figure 63 represent the uncertainty of the medium pressure drop computed from the uncertainty of the PEG/water viscosity derived from the extremes of the water data in Figure 23. Since no direct measurement of the viscosity were made on the PEG/water solution for the medium test, the filter constant, K_{M0}= 11.52 inch WC/ft/min/cP , from the water tests was used to compute the PEG viscosity from the medium pressure drop using Equation 9 and the coefficients of the medium pressure drop in Equation 7.

The small pressure drop difference between the filter and medium in Figure 63 for the PEG/water solution is in general agreement with the measurements of the pressure drop difference for the filter and medium in Figure 61 for air up to about 60 inches WC. At higher filter pressure drops, the filter shows indications of partial pleat collapse as the filter pressure drop becomes increasingly greater than the medium pressure drop. Although no photographs were available of the final filter to determine any structural deformation, the increased filter pressure drop could result from reversible medium deflection between the ridges of the corrugated separators and thereby reduce the channel opening. This hypothesis is supported by the lack of a hysteresis in the pressure drop when the liquid flow was reduced during the pump shut down as shown in Figure 64.

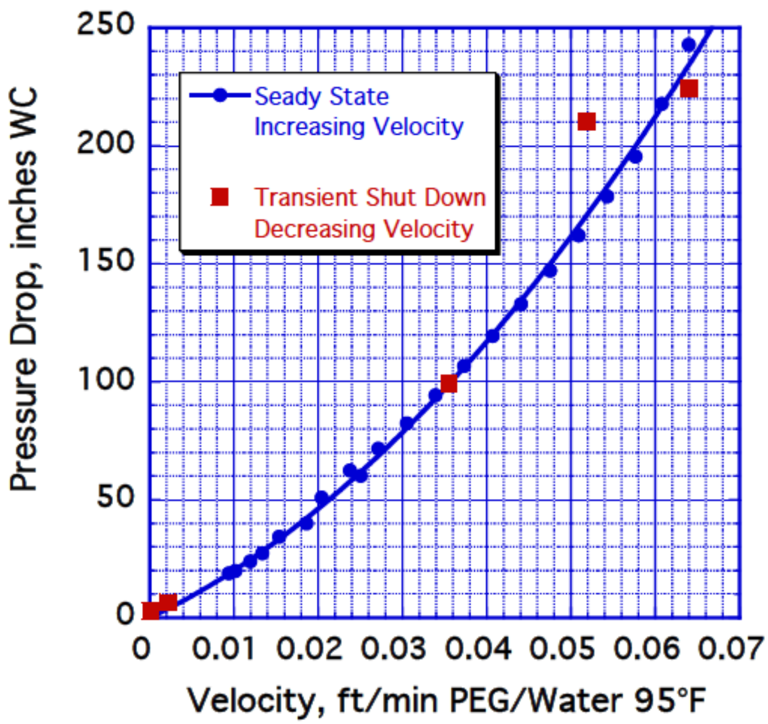

Figure 64. Pressure drop measurements for the prototype 2 filter, K-GFR-SC-1-PRE, from Figure 63 during steady state flow conditions and during the transient shut down. Each of the transient measurements were taken at 10 seconds intervals.

Except for the single data point at 0.052 ft/min, the remaining four data points during the pump shut down match the steady state measurements. This single point represents the first measurement following the pump shut-down and may include fluid inertia effects. Steady state measurements were not included in the test plan to examine hysteresis effects on the filter pressure drop.

Figure 65 shows the measured viscosity as a function of temperature for the PEG/water samples taken before and after the pressure test shown in Figure 63.

Since the samples have virtually the same viscosity before and after the test, the measured viscosity at 95°F will be a constant 186 cP during the test. The data and repeatability of the before and after tests are typical for the viscosity measurements made in support of the filter pressure tests.

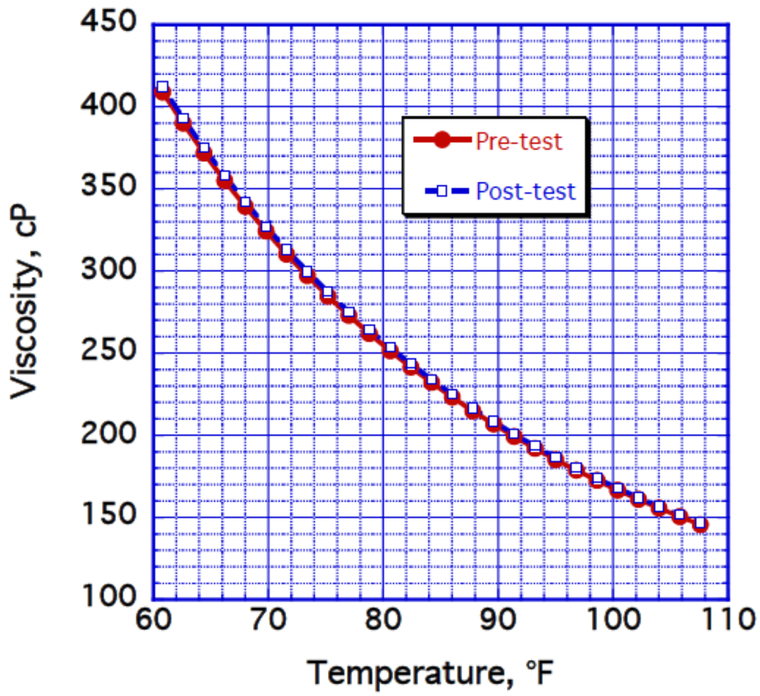

Figure 65. Viscosity measurements as a function of temperature taken from liquid samples before and after the pressure test on the prototype 2 filter, K-GFR-SC-1-PRE. The test results are typical for all of the samples taken for the filter tests in the RLPTS.

The PEG/water solution was then drained and the K-GFR-SC-1-PRE filter, rinsed with 100°F water at 35 gal/min for one hour, dried with air, and tested for DOP efficiency at 2,000 cfm. Figure 66 shows the DOP penetration has increased significantly following the high pressure liquid test.

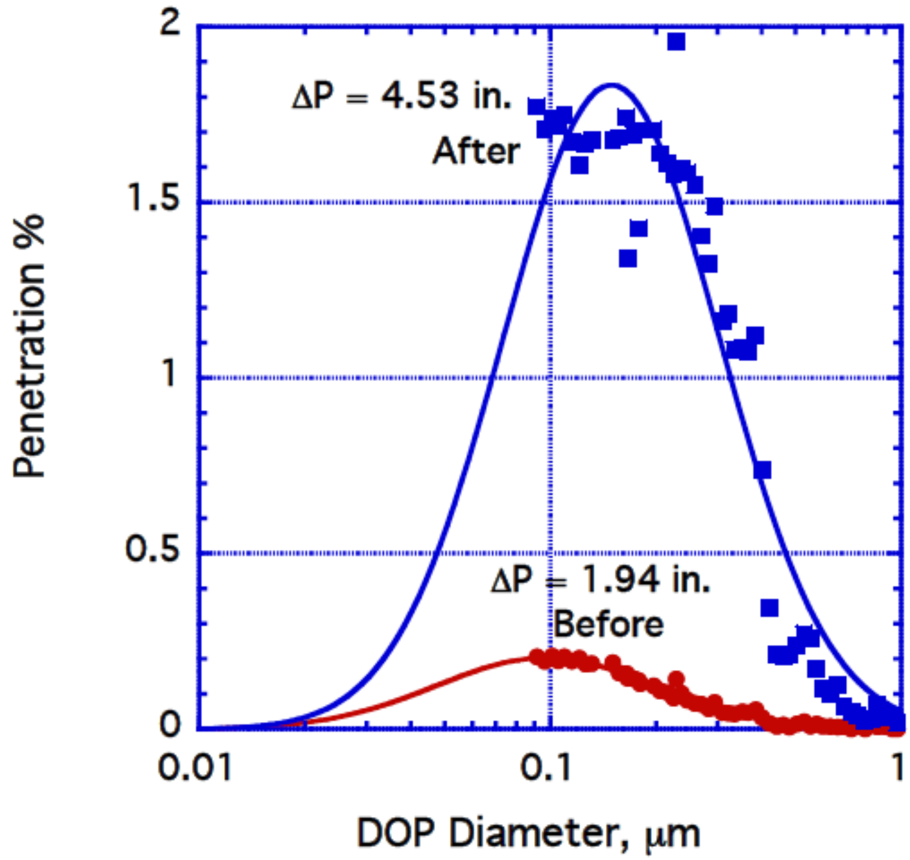

Figure 66. DOP penetration of the prototype 2 filter, Kurion K-GFR-SC-1-PRE, at 2,000 cfm before and after exposure to 225 inches WC in the RLPTS fitted to log-normal curves. The penetration method used the original MSU method of undiluted SMPS for upstream measurement and LAS for downstream measurement.

Figure 66 shows the filter leakage has increased significantly (from 0.074% to 1.2%) following the high pressure liquid test. The increase in pressure drop also suggests that the filter was not sufficiently rinsed with water, and residual PEG remained in the filter. The practice of weighing the dried filters to determine residual mass of PEG was implemented later in the program.

Kurion Prototype 2 PRE Remote-Change Filter With High-Strength Glass Fiber Medium and Conventional Pleat Design With 3 Inch Pleats and Separators

The first remote-change filter K-FS-RC-001-PRE had shipping damage with a visible dent on the filter pack. Since the initial DOP filter efficiency was only 98.5% , and because of the damage, no further tests were conducted. A replacement filter, K-GFR-RC-002-PRE, was then tested in the similar fashion as the SC filter. Figure 67 shows a photograph of a portion of the filter showing the pleated 3398-L2W medium with wire screen on the outside and the corrugated aluminum separators. The unit is similar to the safe-change filter shown in Figure 60.

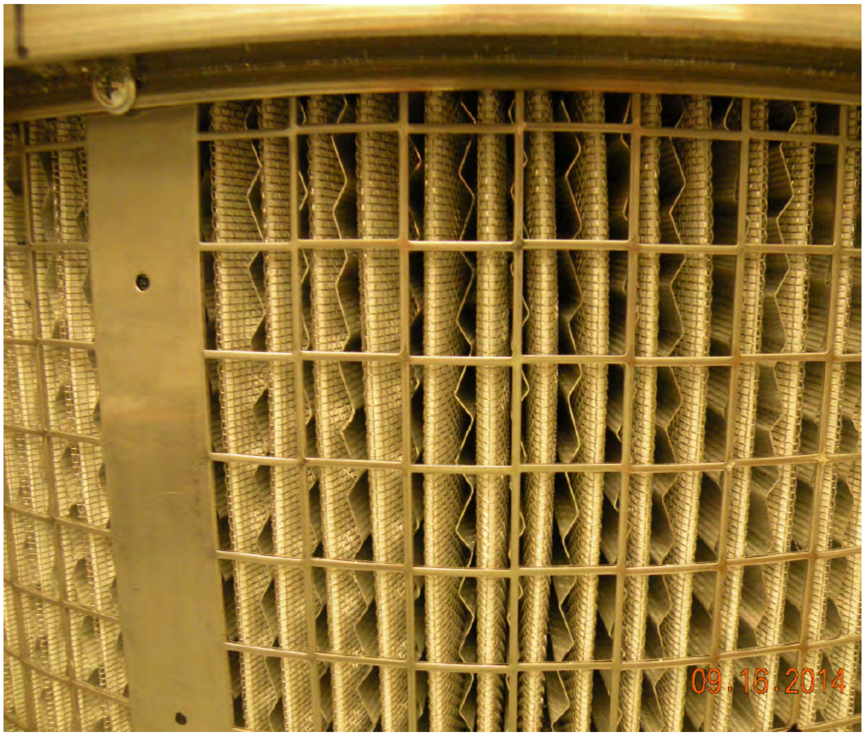

Figure 67. Close-up photograph of the K-GFR-RC-002-PRE filter showing the pleated 3398-L2W medium with a downstream wire screen and aluminum separators. The restraining strap is fastened to the endcap with a screw.

The filter was installed in the RLPTS using the air configuration to measure the filter pressure drop and DOP efficiency. Figure 68 shows the results of the initial pressure drop measurements of the filter and the medium used in the filter. No corrections were made to the reported pressure drops to subtract the added pressure drop due to the grab ring as done with the prototype 1 RC filter in Figure 54 because the filter had a negligible inertial contribution (as is seen by a velocity square term in the curve fit). Subtracting the pressure drop of the grab ring using Equations 17-19 resulted in the filter having a lower pressure drop than the medium at 15 ft/min, a physical impossibility. This problem is most likely due to assuming the discharge coefficient for filter orifices in the RLPTS (Figure 9 B) is the same as in the LSTS SC housing (Figure 45 A)

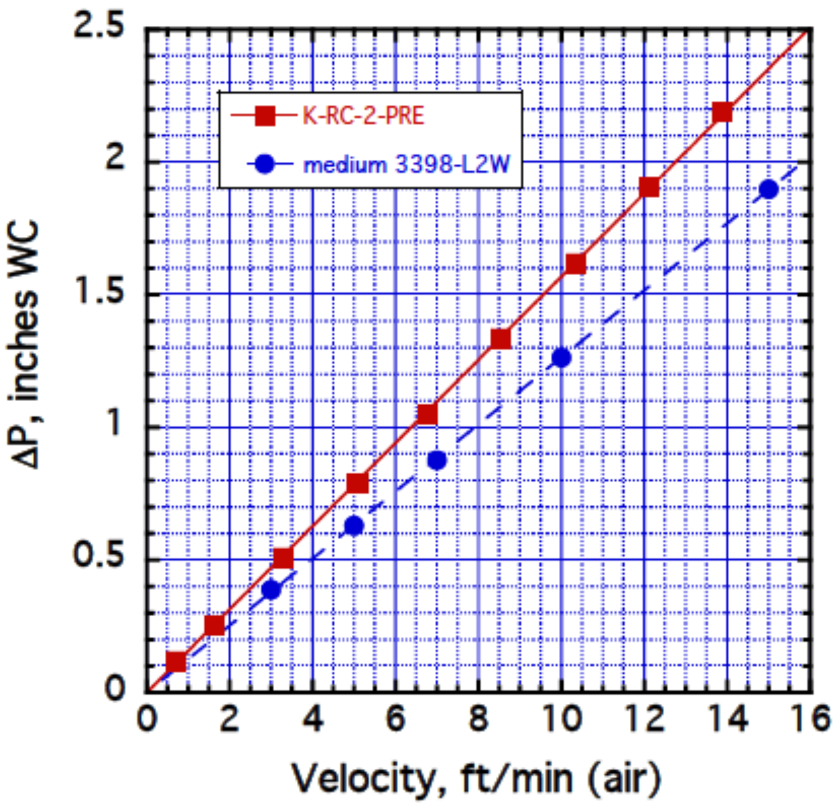

Figure 68. Pressure drop measurements for the RC prototype 2 (K-GFR-RC-002-PRE) filter and the medium, 3398-L2W, used in the filter plotted as a function of air velocity.

Figure 68 shows that the RC filter pressure drop is only slightly greater than the pressure drop of the medium due to the channel flow resistance.

The filter was then tested for DOP penetration using the instrumentation system shown in Figure 27 and a 6 nozzle, Laskin Nozzle DOP generator in the RLPTS. Figure 69 shows the DOP penetration measured at 2000, 400, and 100 cfm. All of the subsequent tests for the Kurion filters were tested using this efficiency test system.

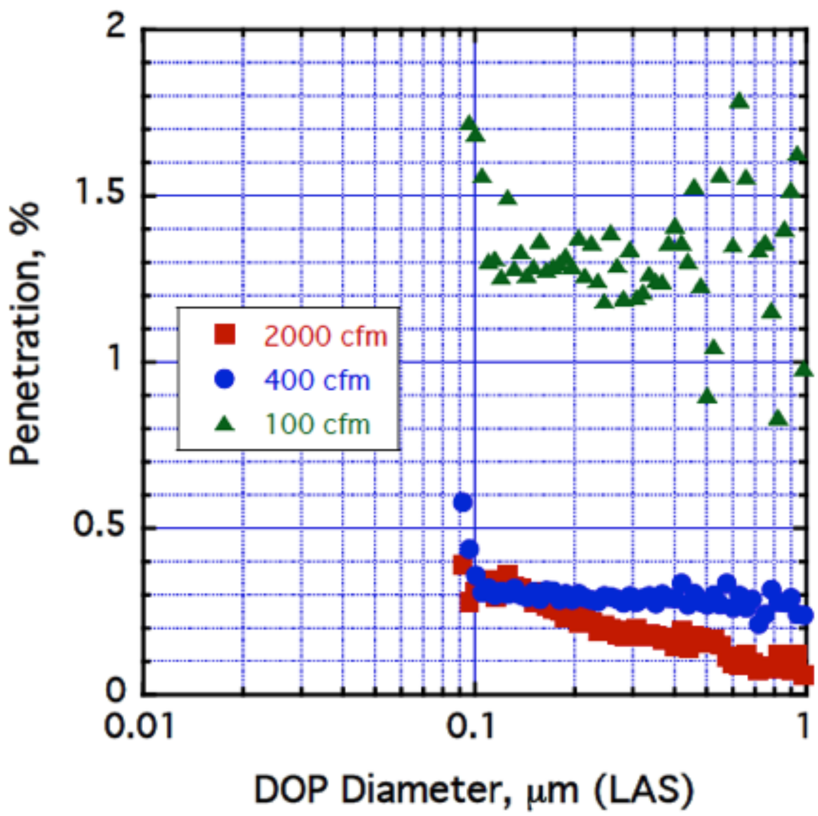

Figure 69. Penetration of DOP aerosols for the Kurion prototype 2 filter, K-GFR-RC-002-PRE, as a function of DOP diameter were 0.18%, 0.28% and 1.3% measured at 2000, 400 and 100 cfm respectively using the LAS (TSI) instrument. The penetration measurements were made using the measurement system shown in Figure 27 with the challenge concentration diluted by a factor of 1386 with two diluters. The pressure drop at 2,000 cfm was 2.19 inches WC with the grab ring.

Figure 69 shows the K-GFR-RC-002-PRE filter failed the DOP penetration requirement of less than 0.03% penetration at 0.3 microns and has a major leak at all flow rates. The penetration curves are approximately flat, independent of particle size as expected for significant leaks. In addition, the penetration increases with decreasing flow rate, another characteristic of leaks (Bergman et al, 1997b).

The RLPTS was then configured for the liquid resistance test; and, after filling the test system with 95°F PEG/water solution, the flow was increased incrementally to generate the pressure drop versus velocity curve shown in Figure 70.

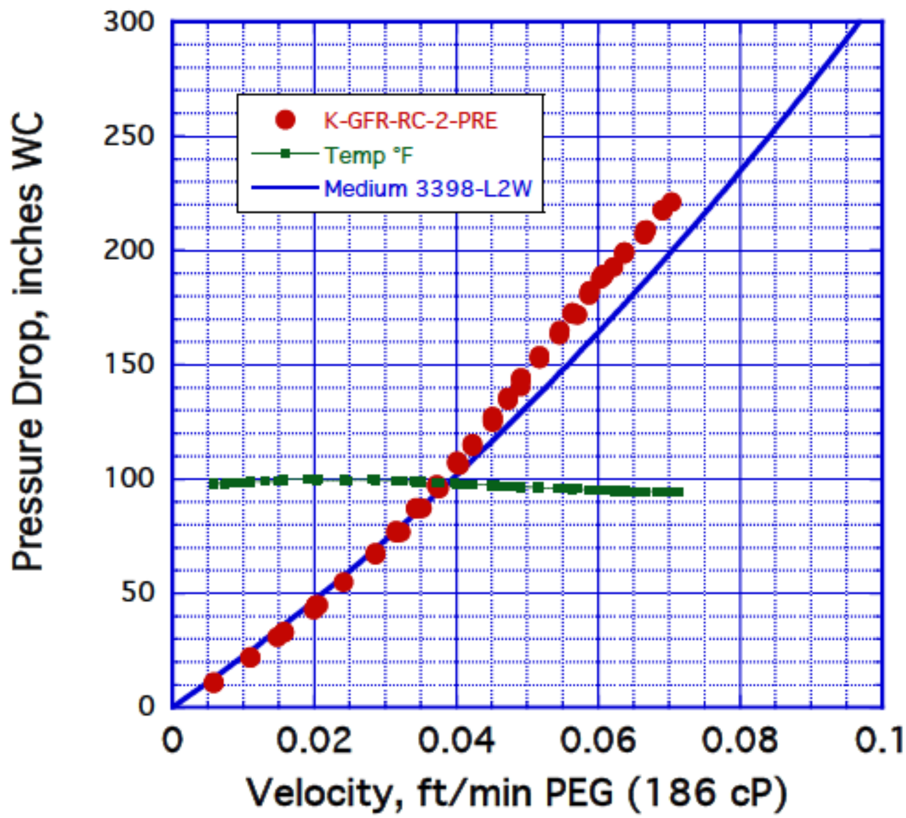

Figure 70. Measurements of the pressure drop versus medium velocity of the Kurion prototype 2 RC filter (K-GFR-RC-2-PRE) tested with a PEG/water solution. The pressure drop of the filter was corrected for the small temperature shifts using Equation 15 and the viscosity measurements that are similar to those shown in Figure 65 . The pressure drop of the medium from Figure 24 with a computed viscosity of 186 cP is superimposed.

Figure 70 shows that the pressure drop of the filter pack generally follows the pressure drop of the medium. The slight increase of the pressure drop for the filter pack with respect to the medium may suggest there is a small deflection of the medium between the corrugator peaks at pressure drops above 100 inches WC. The close agreement between the medium and filter pressure drops indicates that the filter pack structure has not changed significantly during the high pressure test and that the medium pleats and corrugated separators provide a robust design for pressures up to at least 225 inches.

However, after 34 minutes of the planned 1 hour exposure at 225 inches, the filter pressure drop decreased abruptly, and the viewing port in the filter housing showed that the bottom end cap of the filter had separated away from the filter pack as shown in Figure 71. The three metal straps holding the top and bottom endcaps were still attached during the deflection.

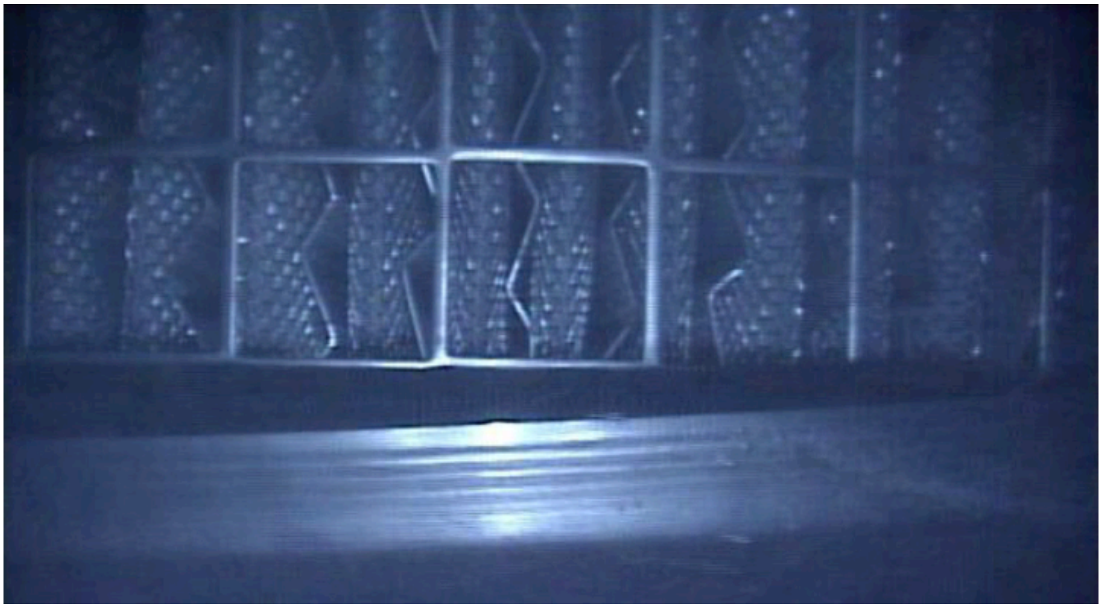

Figure 71. Bottom cap of K-GFR-RC-002-PRE filter popped off after 34 minutes of the planned one hour exposure to PEG/water solution at 95°F at 225 inches

The separation of the end cap seen in Figure 71 indicates that the high pressure was sufficient to break the urethane bond between the filter pack and the end cap. This separation also demonstrates that the three straps are not adequate to secure the two endcaps in place, without relying on the urethane sealant for structural integrity. If an adequate structural design were used to retain the endcaps, there would be no separation as seen in Figure 71, even with no urethane bond.

A post mortem of the failed filter revealed that the urethane sealant had not covered the end plate uniformly and may also be the source of the leaks in the filter . Figure 72 shows the residue of the PEG after the end cap was removed .

Figure 72. Photograph of the failed Kurion filter K-GFR-RC-002-PRE with the bottom endcap removed. The white deposits are from the dried PEG and suggest non-uniform sealing and potential leak paths.

The solution that Kurion pursued to correct the endcap deflection problem was to increase the urethane bond strength by using more sealant, selecting a urethane sealant with increased hardness and increasing the bonding surface using a proprietary technique.

Using the improved sealing methods, Kurion built and submitted four identical RC filters and two identical SC filters for testing at MSU. Two of the RC filters were to be tested as 45 inches rated filters and two as 225 inches rated filters. Neither of the two RC filters exposed to 225 inches WC experienced the problem of end plate separation as seen in Figure 71. The two RC filters tested and 45 inches WC and the two SC filters tested 20 inches performed well in the resistance to liquid to pressure test.

Although the solution of increasing the quantity and quality of the sealant to prevent end cap separation under high differential pressures was successful, future designs should have more robust mechanical support structure and not rely on the sealant to provide both sealing properties and mechanical strength. This approach will allow the high strength filter to retain its strength after exposure to more severe high temperature conditions than the standard AG-1 HEPA filters covered in AG-1 Sections FC and FK (Pratt, 1986) and after exposure to adverse environmental conditions (e.g. high moisture, chemicals, ozone) and age related deterioration.

Kurion Prototype 2 Remote-Change Filter With High-Strength Glass Fiber Medium and Conventional Pleat Design With 3 Inch Pleats and Separators and Rated at 45 inches WC

Two remote-change (RC) filters, K-RC-1 and K-RC-2 were tested for pressure drop and DOP efficiency before and after exposure to 45 inches of PEG/water solution for one hour using the RLPTS in Figure 9.

Figure 73 shows the initial DOP penetration of the K-RC-1 filter that had a pressure drop of 2.35 inches WC without correction for the filter grab ring. The DOP penetration at 100%, 20% and 5% flow is 0.02%, 0.02% and 0.007%. The lower penetration at lower flows indicates any leaks are negligible. However, the approximate constant penetration as a function of DOP diameter is a definite indicator of leaks. Figure 80 shows the pressure drop of the clean filter as a function of air velocity.

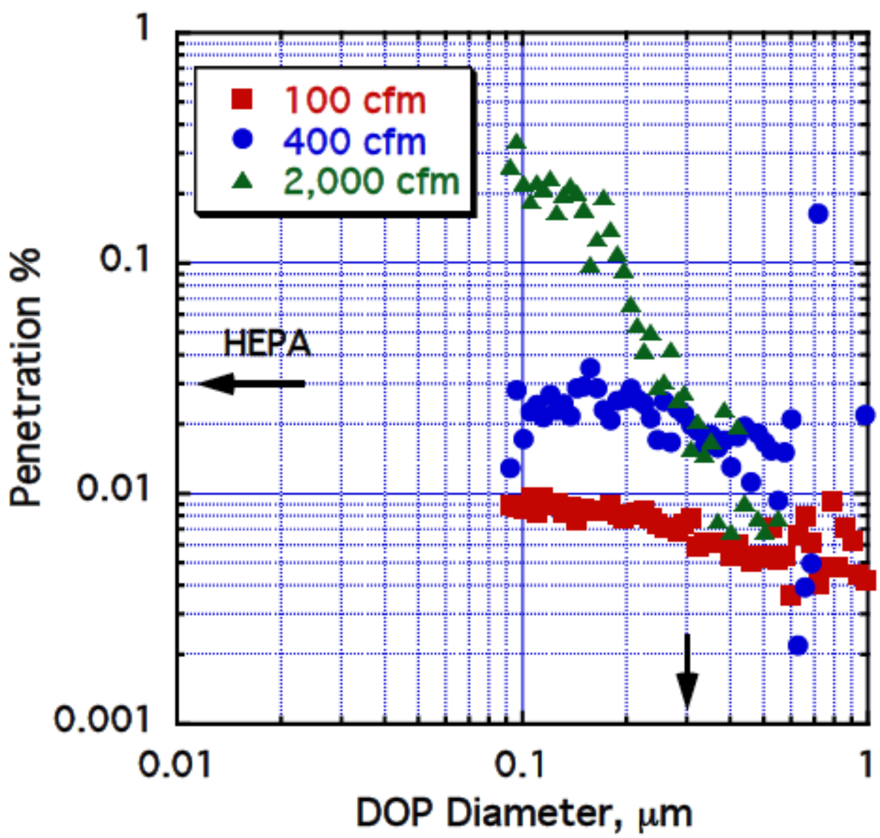

Figure 73 Initial penetration of the prototype 2 filter, K1-GFR-RC-001, shows the filter meet the HEPA filter requirement of less than 0.03% penetration at 0.3 microns DOP and had a pressure drop of 2.35 inches WC. The scatter in data is due to insufficient DOP challenge concentration. The new measurement system shown in Figure 27 was used with the challenge concentration diluted by a factor of 1823 with two diluters.

The RLPTS was then converted to the PEG/water system and the filter was tested for resistance to 45 inches WC PEG/water solution for one hour. The ramp-up pressure drop for the K1-GFR-RC-001 filter is shown in Figure 76.

The filter was then rinsed with heated water and the RLPTS drained and converted to the air system for filter drying. After the filter pressure drop reached the prescribed pressure drop, the filter was tested for DOP penetration. Figure 74 shows the filter failed the required penetration value at all flow rates tested.

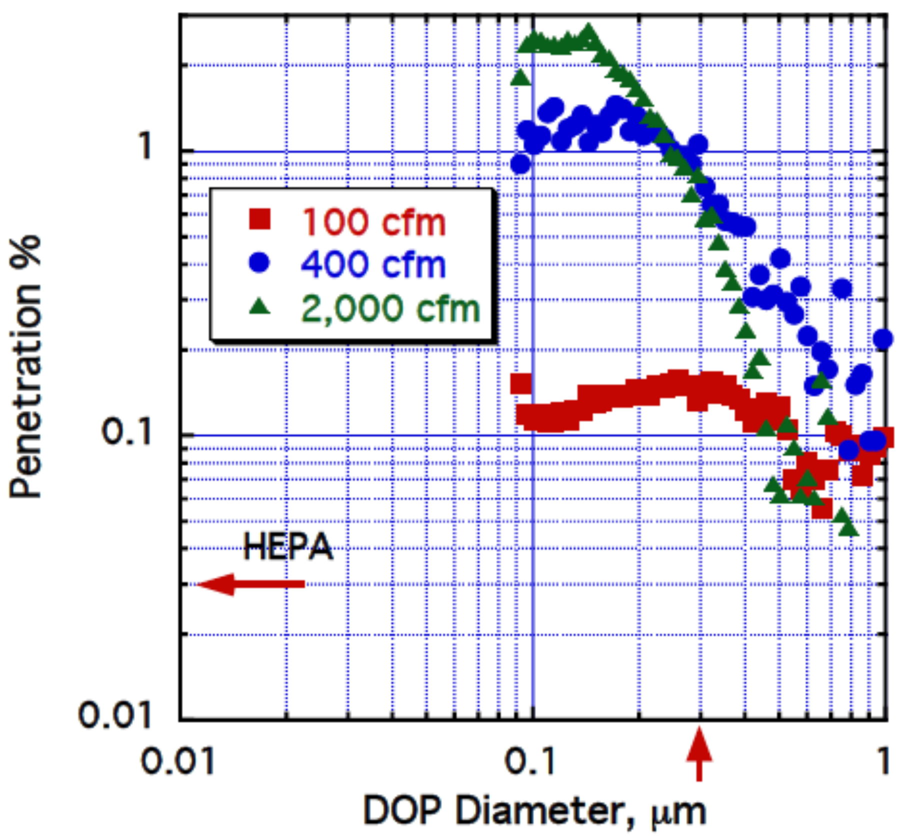

Figure 74 K1-GFR-RC-001 failed the final efficiency after 45 inch DP exposure to the PEG/water solution.

The second Kurion RC filter, rated at 45 inches WC, K1-GFR-RC-002 , was tested for filter efficiency and the results shown in Figure 75. The corresponding pressure drop curve for air flow is shown in Figure 80.

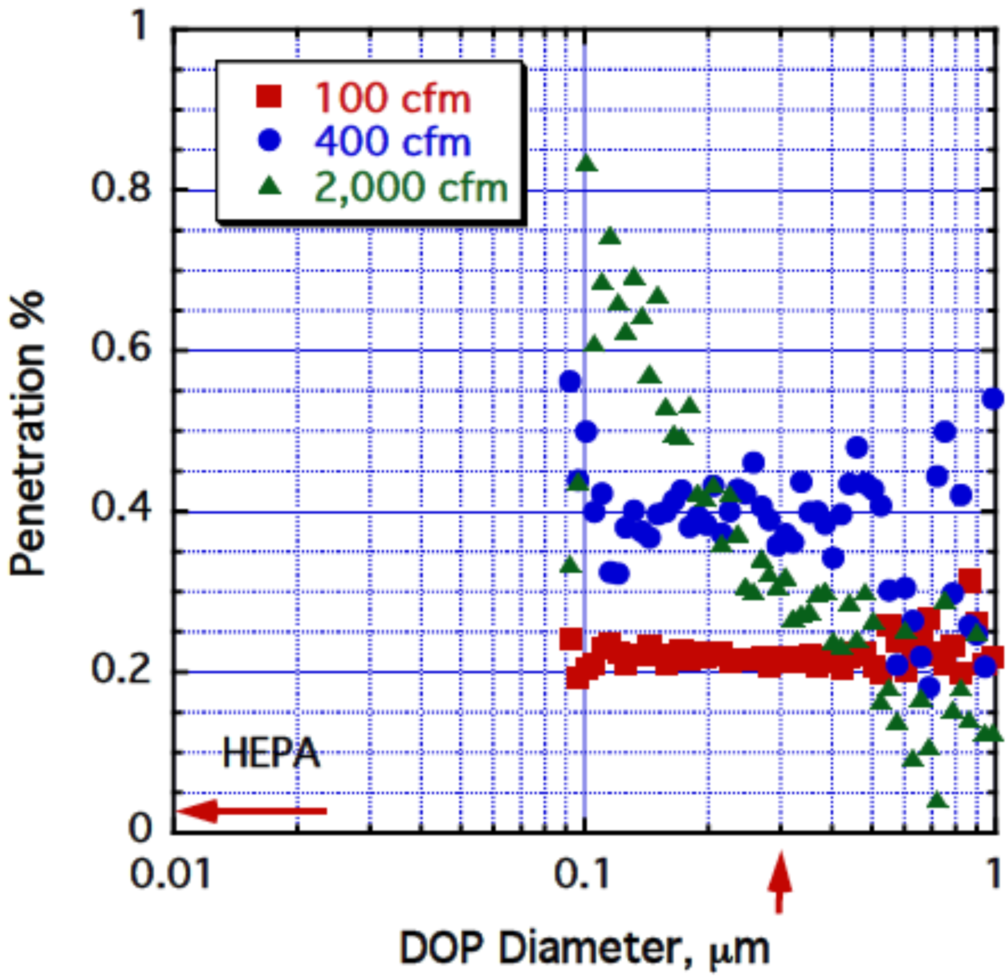

Figure 75. Initial DOP penetration of the K1-GFR-RC-002 filter as a function of DOP diameter. The filter failed the required penetration of 0.03% at all flow rates. The initial pressure drop at 2,000 cfm was2.37 inches WC uncorrected for the grab ring.

After converting the RLPTS to liquid, the K1-GFR-RC-002 filter was exposed to the PEG/water solution at 45 inches WC differential pressure for one hour. The ramp-up pressure drop is shown in Figure 76. The post exposure penetration test showed the leakage had increased.

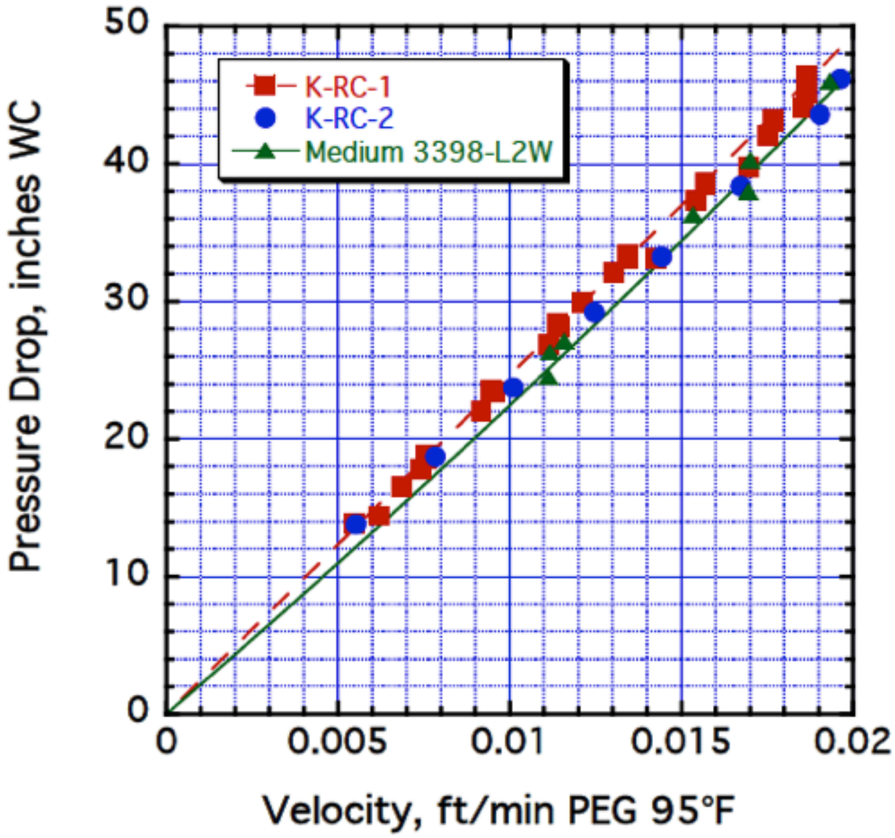

Figure 76. Pressure drop for RC filters K-RC-1 and K-RC-2 as a function of PEG/water velocity. The filter pressure drop is slightly greater than the 3398-L2W medium pressure drop.

Kurion Prototype 2 Remote-Change Filter With High-Strength Glass Fiber Medium and Conventional Pleat Design With 3 Inch Pleats and Separators and Rated at 225 inches WC

Two remote-change (RC) filters, K-RC-3 and K-RC-4 were tested for pressure drop and DOP efficiency before and after exposure to 225 inches of PEG/water solution for one hour using the RLPTS in Figure 9.

The K-RC-3 filter was installed in the RLPTS and tested for DOP efficiency and pressure drop. The initial pressure drop was 2.48 inches WC without correction of the filter grab ring. Figure 77 shows the filter failed the initial efficiency requirement of less than 0.03% penetration at 0.3 µm DOP. The initial air flow resistance curve is given in Figure 80.

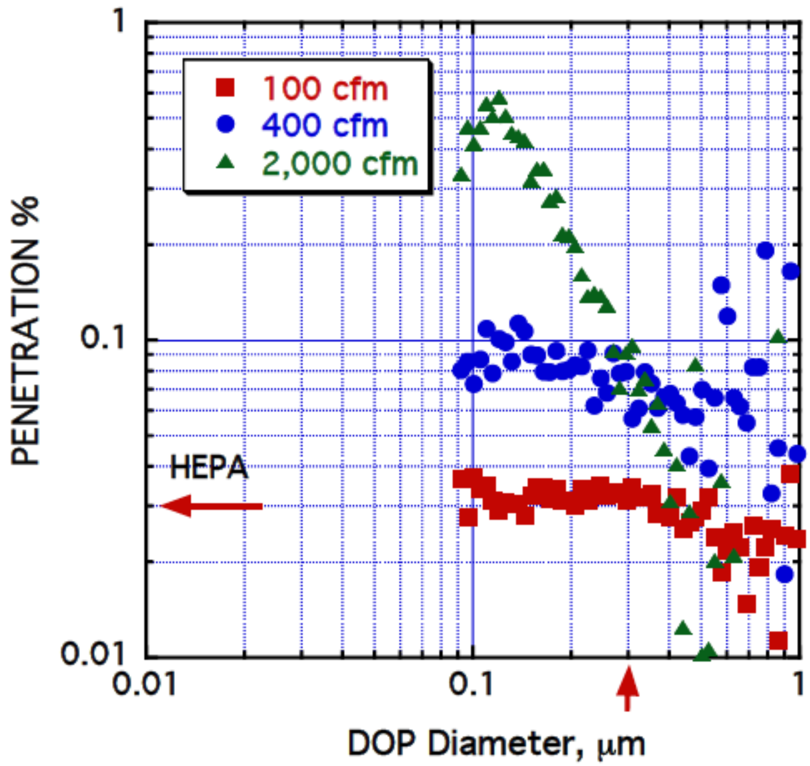

Figure 77. The DOP penetration of the K-GFR-RC-3 filter failed the required penetration at 2000 and 400 cfm and was at the limiting penetration of 0.03% at 100 cfm. The initial pressure drop at 2,000 cfm was 2.48 inches WC with no correction for the grab ring.

The K-GFR-RC-3 filter was then tested for resistance to a differential pressure of 225 inches WC for one hour. The ramp-up differential pressure is shown in Figure 79. After rinsing and drying the filter, the penetration was measured and showed an increase in leakage.

The second RC filter rated at 225 inches WC, K-GFR-RC-4, filter was installed in the RLPTS and tested for DOP efficiency and pressure drop. The initial pressure drop was 2.41 inches WC without correction of the filter grab ring. Figure 78 shows the filter failed the initial efficiency requirement of less than 0.03% penetration at 0.3 µm DOP at all flow rates. The initial air flow resistance curve is given in Figure 80.

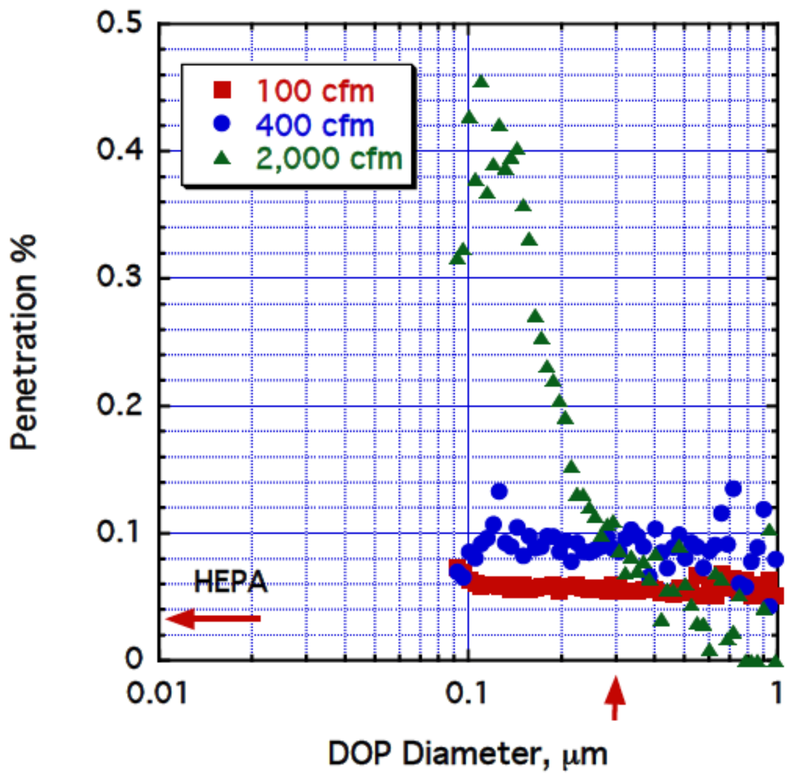

Figure 78 The DOP penetration of the K-GFR-RC-4 filter failed the required penetration at all flow rates. The initial pressure drop at 2,000 cfm was 2.41 inches WC with no correction for the grab ring.

The K-GFR-RC-4 filter was then tested for resistance to a differential pressure of 225 inches WC for one hour. The ramp-up differential pressure is shown in Figure 79. After rinsing and drying the filter, the penetration was measured and showed an increase in leakage.

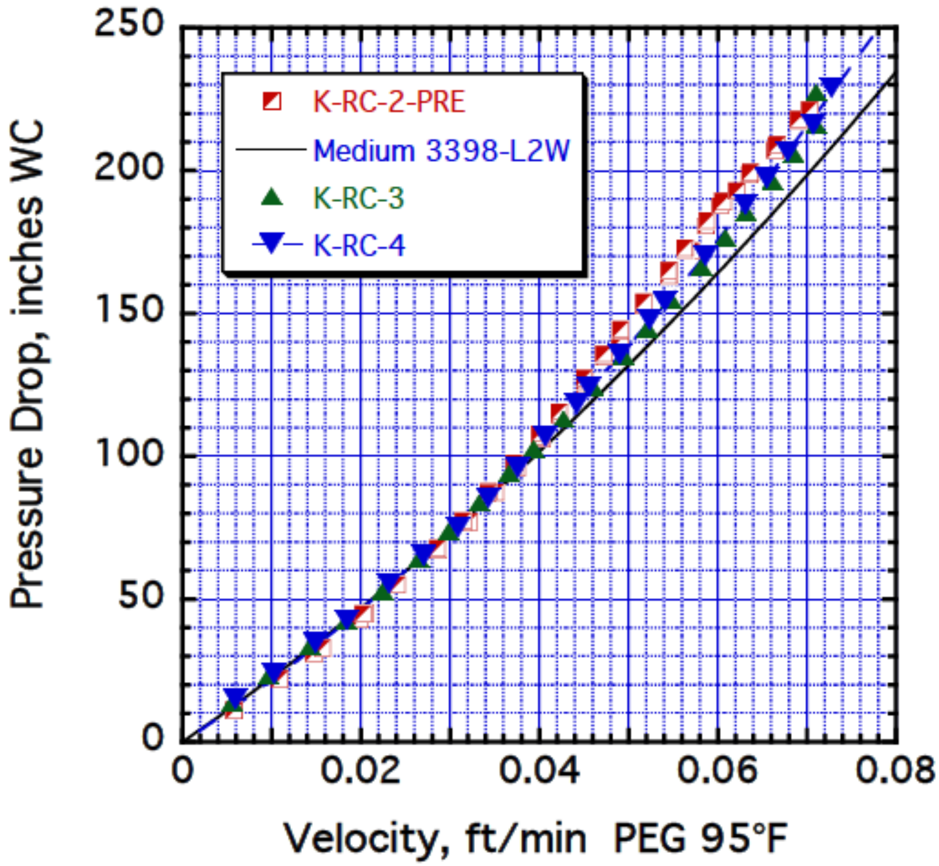

Figure 79. Pressure drop of K-RC-2-PRE, K-RC-3 and K-RC-4 filters as a function of PEG/water velocity. The filter pressure drop of the filters are about the same as the pressure drop of the medium at velocities up to 0.04 ft/min. At greater velocities, the filter pressure drop increases slightly compared to the medium pressure drop. Viscosity measurements were conducted before and after each filter test as shown in Figure 65.

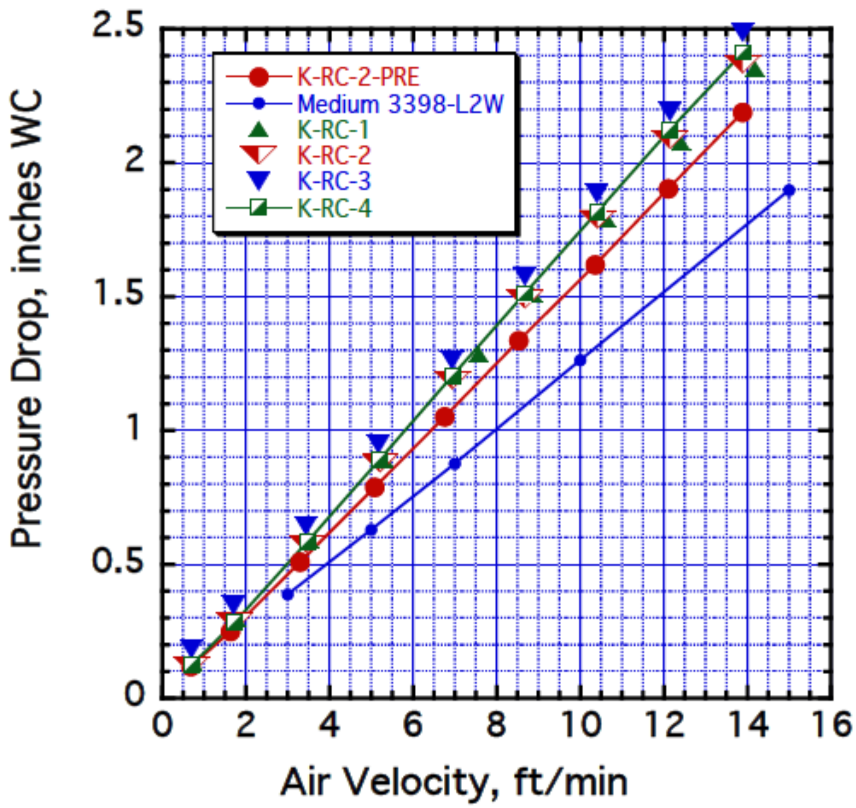

Figure 80. Pressure drop of the RC filters and the 3398-as a function of air velocity. No correction was made for the added pressure drop due to the grab ring.

Kurion Prototype 2 Safe-Change Filter With High-Strength Glass Fiber Medium and Conventional Pleat Design With Separators and Rated at 20 inches WC

Kurion fabricated and submitted two SC filters for testing at MSU. The construction of the two filters was the same as for the RC filters except for the filter pack dimensions shown in Table 5. The testing was similar to that for the RC filters, except that the exposure to high pressure in the RLPTS in Figure 9 only went to 20 inches.

The first RSC filter rated at 20 inches WC, K1-GFR-SC-001, was installed in the RLPTS and tested for DOP efficiency and pressure drop. The initial pressure drop was 1.95 inches WC. Figure 81 shows the filter had a major leak and failed the penetration requirement of less than 0.03% penetration at 0.3 μm DOP at all flow rates. The initial air flow resistance curve is given in Figure 84.

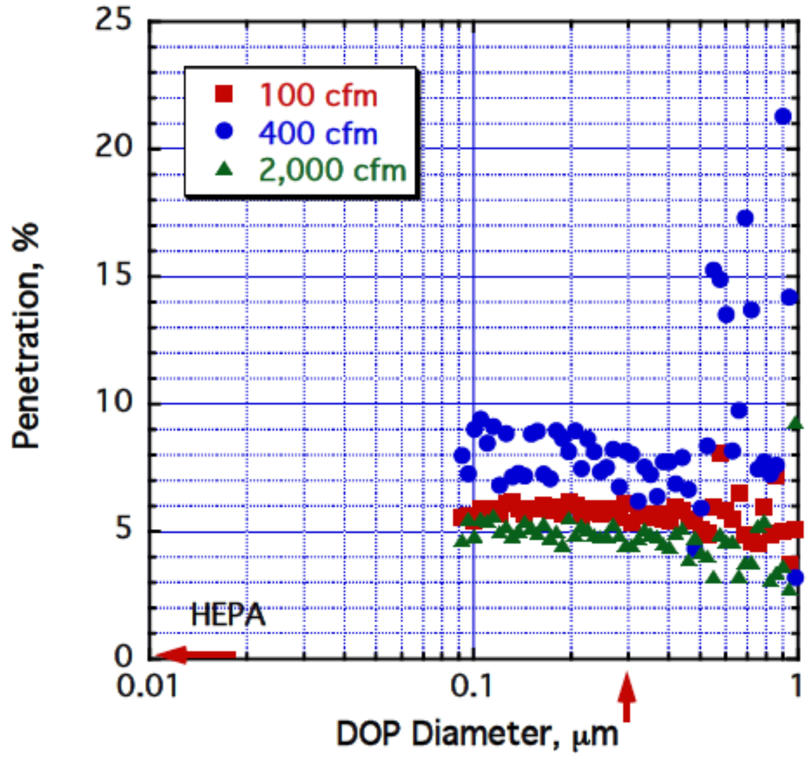

Figure 81. The DOP penetration of the K1-GFR-SC-001 filter had a large leak and failed the required penetration at all flow rates. The initial pressure drop at 2,000 cfm was 1.95 inches WC.

The K1-GFR-SC-001 filter was then tested for resistance to a differential pressure of 20 inches WC for one hour. The ramp-up differential pressure is shown in Figure 82. After rinsing and drying the filter, the penetration was measured and showed an increase in leakage.

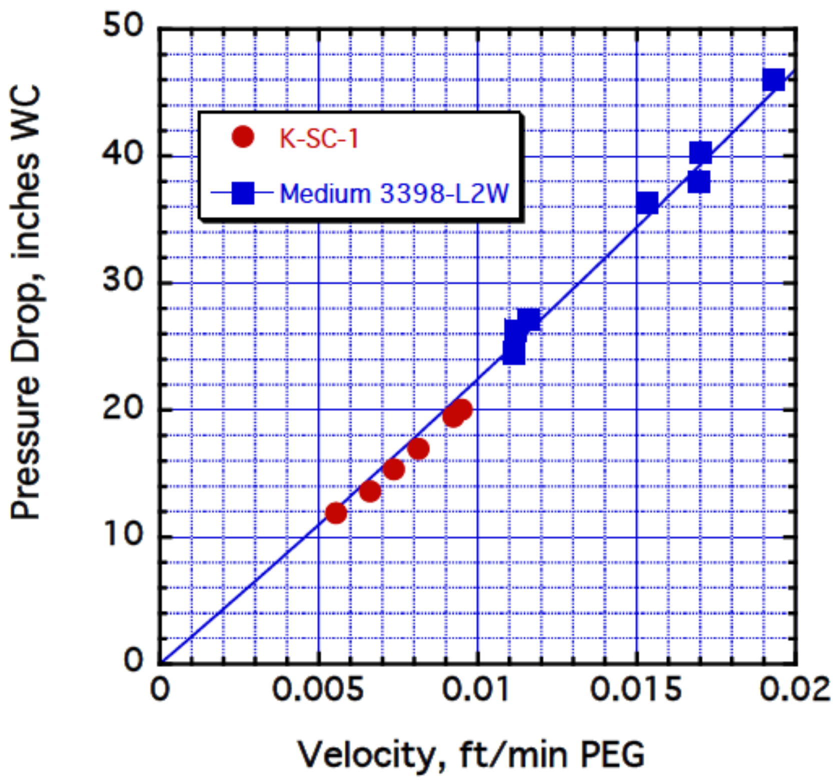

Figure 82. Pressure drop of the K1-GFR-SC-001 filter as a function PEG/water solution (95°F) velocity. The pressure drop of the 3398-L2W medium is also shown. Viscosity measurements were conducted before and after the filter test as shown in Figure 65.

The second SC filter rated at 20 inches WC, K1-GFR-SC-002, was installed in the RLPTS and tested for DOP efficiency and pressure drop. The initial pressure drop was 2.00 inches WC. Figure 83 shows the filter failed the penetration requirement of less than 0.03% penetration at 0.3 μm DOP at all flow rates. The initial air flow resistance curve is given in Figure 84.

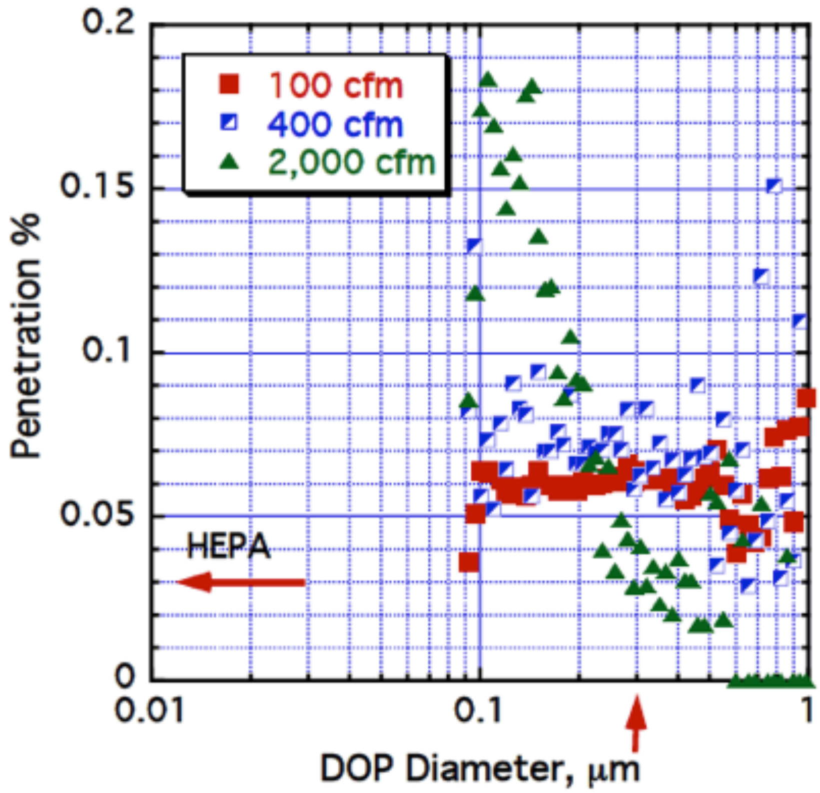

Figure 83. DOP penetration of the K1-GFR-SC-002 filter shows the filter failed the required 0.03% penetration at all flow rates. The pressure drop at 2,000 cfm was 2.00 inches WC.

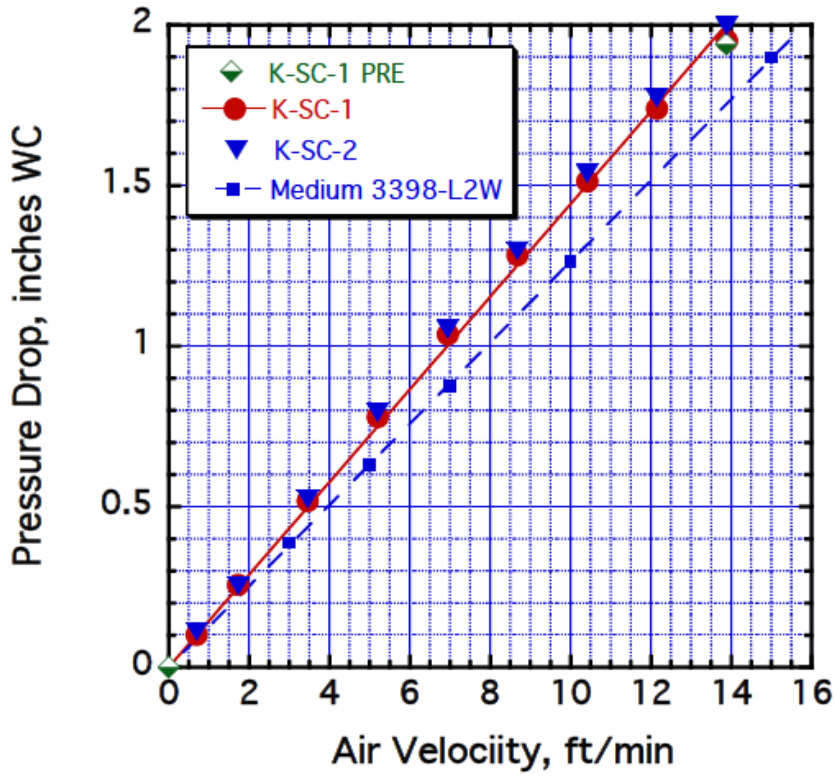

Figure 84. Pressure drop of the SC filters (K1-GFR-SC-001-PRE, K1-GFR-SC-001, and K1-GFR-SC-002) and the 3398-L2W medium as a function of air velocity.

Since the K1-GFR-SC-002 filter failed the DOP penetration test and since test data was available on the flow resistance to liquid PEG, no further testing was done on this filter.

Summary of the Kurion Prototype 2 Filter Tests

Kurion demonstrated that a high strength radial flow HEPA filter can be made using HEPA filter medium reinforced with glass cloth and aluminum separators with a pressure drop about 2 inches WC. Unfortunately, only 1 of the 8 filters were able to meet the DOP penetration requirement of 0.03% at 100 % and 20 % flow. The primary problem was the inadequate filter medium area that results in a high medium velocity and thus a failing penetration. The prototype 2 HEPA filters had an effective area of only 141 ft2, thus yielding a face velocity of 14.2 ft/min instead of the required 5 ft/min. Figure 42 shows that the medium 3398-L2W has a penetration of 0.03% at 14 ft/min. Since the lowest penetration that a filter can have is the penetration of the medium, and since all filters have a statistical number of leaks, the high medium velocity would cause nearly all of the filters to fail the required penetration as was seen in the Kurion tests (Bergman, 2016c).

The Kurion tests also illustrated the problem of insufficient structural strength of the metal support components to maintain the integrity of the urethane bond between the filter pack and the end-caps under high pressure. All of the tests showed increased DOP penetration following the exposure to high pressure. In one test, a photograph taken during the high pressure test captured the separation of the end-cap from the filter pack in Figure 71. DOP leak scans were not available to help confirm the breaking of the urethane bond was the source of the leaks in the other filters.

Table 6 summarizes the test results of the prototype 2 filters. Although the initial pressure drop was satisfactory, only one of the eight filers were able to meet the DOP penetration requirement of less than 0.03%. The weight gain of the filters is attributed to residual PEG that was not washed out of the filter.

Table 6. Summary of Kurion Prototype 2 Filter Tests

Filter	Rating, in. WC	Initial /Final	DP[1], in. WC	Penetration, %			Pass/ Fail	Mass gain, g
				2000 cfm	400 cfm	100 cfm		
GFR-RC-2-PRE	225	Initial	2.19	0.18	0.28	1.3	Fail	
GFR-RC-1	45	Initial	2.34	0.02	0.02	0.007	Pass	
		Final		0.73	0.76	0.15	Fail	730
GFR-RC-2	45	Initial	2.37	0.31	0.40	0.22	Fail	
		Final		0.65	1.3	0.6	Fail	147
GFR-RC-3	225	Initial	2.48	0.08	0.07	0.03	Fail	
		Final			4.8	1.7	Fail	74
GFR-RC-4	225	Initial	2.41	0.09	0.09	0.06	Fail	
		Final		0.28	0.27	0.12	Fail	257
GFR-SC-1-PRE	225	Initial	1.94	0.05	0.03		Fail	
		Final		1.2				
GFR-SC-1	20	Initial	1.95	0.035	0.065	0.062	Fail	
		Final		0.09	0.1	0.04	Fail	53
GFR-SC-2	20	Initial	2.00	4.7	7.3	5.7	Fail	

[1]DP values are the direct DP measurements from the RLPTS and subtracting the tare for the 13.0 inches orifice.

The compilation of the pressure drop versus air velocity for all of the prototype 2 filters is given in Figure 85.

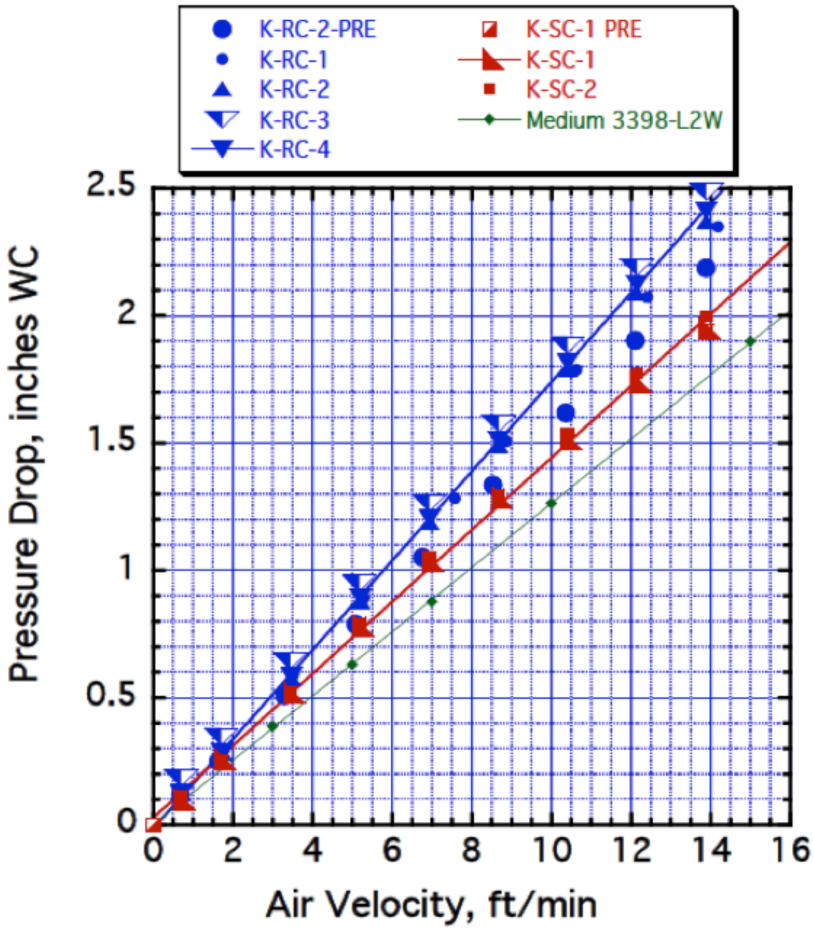

Figure 85. Pressure drop versus air velocity for all of the Kurion prototype 2 filters tested. The RC filters have a slightly greater pressure drop compared to the SC filters. Part of this increase is due to the tighter pleat packing for the RC filters compared to the SC filters. A portion of this increase is also due to the added pressure drop from the grab ring on the RC filters.

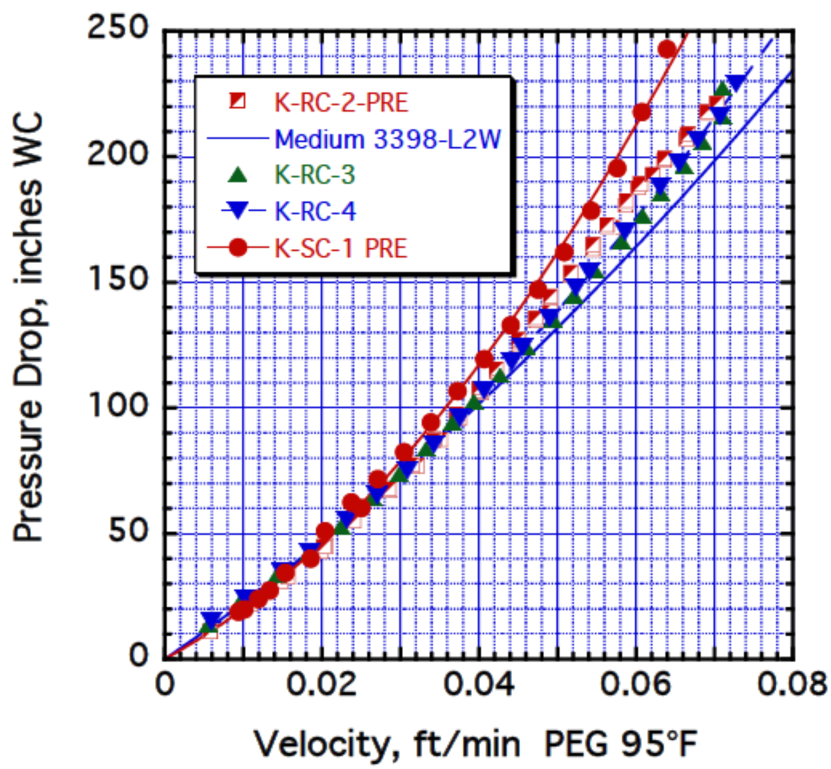

Figure 86. Summary of all of the Kurion prototype 2 filters tested to 225 inches WC in the PEG/water by combining Figure 63 for the SC-1-PRE filter with the RC filters in Figure 79. The tests at 45 inches and 20 inches are given in Figures 76 and 82 respectively and follow the medium, 3398-L2W, curve.

Figure 86 shows that the pressure drop of the RC filters is only slightly greater than that of the medium. This suggests that the filter structure does not change significantly during the high pressure exposure. The medium may deflect slightly at higher pressures and restrict the pleat channel flow. The higher pressure drop for the SC-PRE filter is due to the less compact filter pack, where the pleats have more room to distort and restrict the pleat channel flow.

Porvair Prototype Filters With High-Strength Glass Fiber Medium or Metal Fiber Medium, 1.5 Inch Pleats and No Separators

Porvair fabricated three prototype filters with no separators using different fiber media composites: (1) GF (glass fiber) consisting of Lydall 3398-L2W HEPA filter medium sandwiched between wire screens, and , (2) GFR (glass fiber-reinforced) consisting of the GF composite plus an additional wire screen (for pleat reinforcement) between the Lydall medium and the downstream wire screen, and (3) MM (metal fiber medium) consisting of two layers of Bekaert 3AL3 stainless steel sintered fiber mesh sandwiched between wire screens. The key filter parameters for the GF, GFR, and MM filters are shown in Tables 7-9 respectively.

Table 7. Parameters of Porvair prototype GF Filters

Filter	Inlet ID, in.	Pack ID, in.	Pack OD, in.	Pleat depth, in.	Effective area[2], ft2	Medium velocity ft/min	No. of pleats
Safe change	13.0	16.9	19.9	1.50	194	10.3	429
Remote change	11.0	15.9	18.9	1.50	190	10.5	404

Medium is reinforced glass fiber, Lydall 3398-L2W plus wire screens on both sides of medium

[2]MSU measurements indicated filter area is 146 ft^2

Table 8. Parameters of Porvair prototype GFR filters

Filter	Inlet ID, in.	Pack ID, in.	Pack OD, in.	Pleat* depth, in.	Effective area, ft2	Medium Velocity ft/min	No. of pleats
Safe change	13.0	16.9	19.9	1.50	152	13.2	333
Remote change	11.0	15.9	18.9	1.50	147	13.6	314

Medium is reinforced glass fiber, Lydall 3398-L2W plus wire screens on both side of medium and an additional reinforcement screen on the downstream side.

Table 9. Parameters of Porvair Prototype MM filters

Filter	Inlet ID, in.	Pack ID, in.	Pack OD, in.	Pleat* depth, in.	Effective area, ft2	Medium velocity ft/min	No. of pleats
Safe change	13.0	16.9	19.9	1.50	168	11.9	372
Remote change	11.0	15.9	18.9	1.50	166	12.0	352

Medium is 2 layers of Bekaert 3Al3 sintered stainless steel fiber mat

During the initial design review meeting with Porvair, AS and Bechtel engineers voiced strong concerns about the extremely tight packing of the filter pleats and the lack of separators. The filter medium area in the Porvair designs ranges from 1-1.4 times the area used in the Kurion filters (141 ft2), and the filter pack is squeezed into about half the volume compared to the Kurion design. Porvair used pleat depths of 1.5 inches compared to 3.0 inches for the Kurion designs. AS and Bechtel engineers were concerned that the tight medium packing would result in unacceptable high pressure drops and inadequate particle loading. Despite the concerns raised, Porvair continued with their filter designs as specified in Tables 7-9.

The computed medium velocity of the three prototype filters in Tables 7-9 ranged from 10.3 to 13.6 ft/min assuming the full medium is available for air flow. However, because the pressure drops of the filters are extremely high, the extreme compaction of the pleats must have increased the effective medium thickness and concurrently increased the efficiency of the transformed medium. As a result, the DOP penetration values in Figure 42 cannot be used as a guide for interpreting the DOP penetration of the Porvair prototype filters.

MSU conducted tests on seven filters representing the filters shown in Tables 7-9. However detailed data was provided to Bechtel for only three of the seven filters while summary data was provided for the remaining four filters. The analysis of the available test results is shown in this section.

Porvair (GF) Glass Fiber Filter With High-Strength Glass Fiber Medium and No Separators and Rated at 45 inch WC

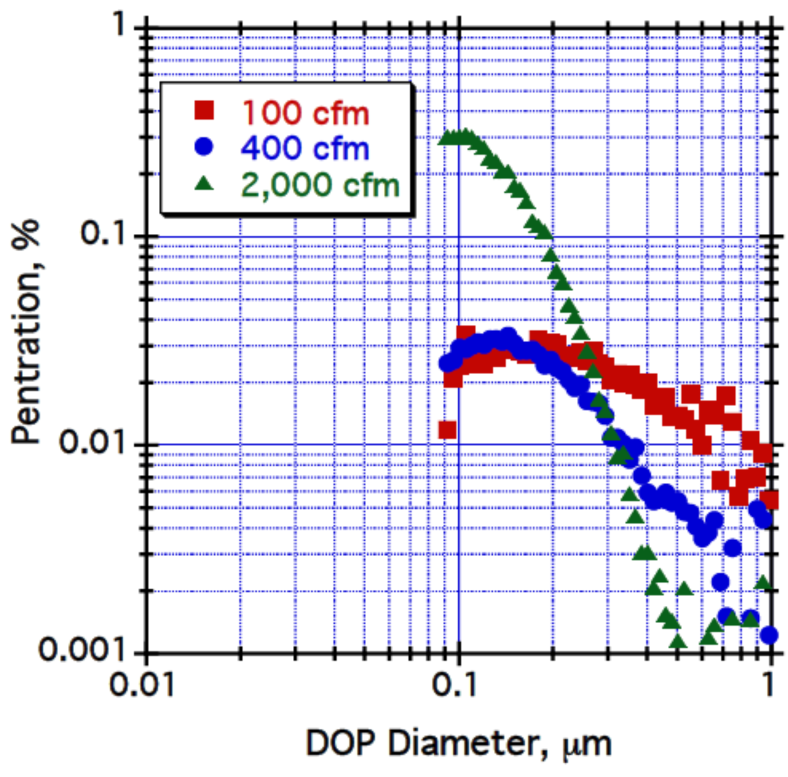

Figure 87. Initial penetration of P1-GF-RC-001 filter shows the filter penetration at 2,000, 400 cfm and 100 cfm was 0.013%, 0.013% and 0.023% respectively. The initial pressure drop at 2,000 cfm was very high at 10 inches WC. Thus the HEPA filter met the requirements for DOP penetration, but had unacceptable high pressure drop.

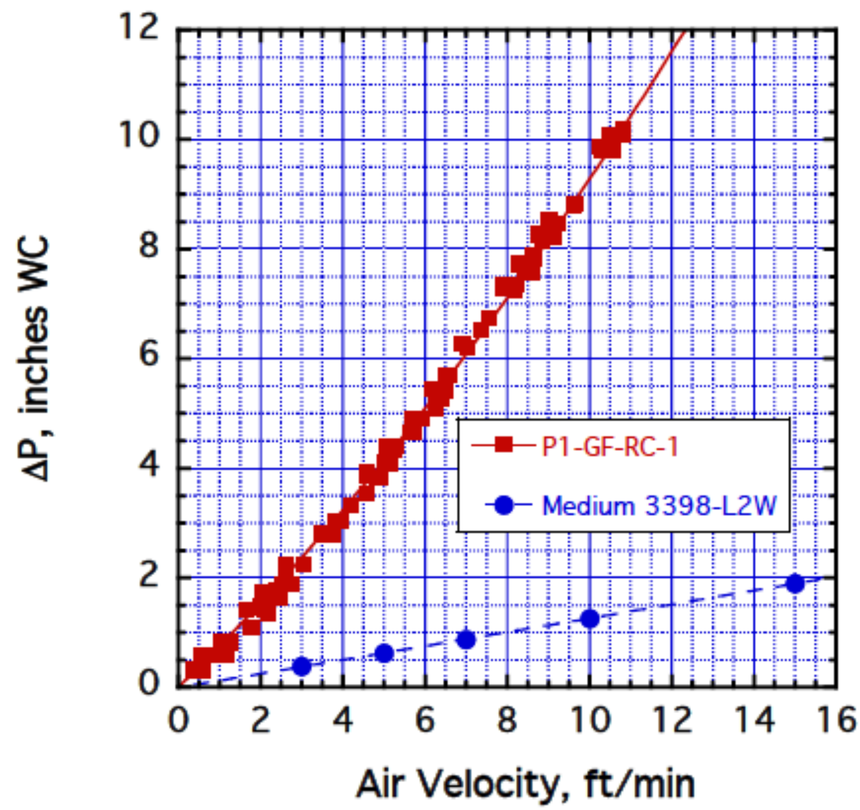

Figure 88. Pressure drop measurements for the Porvair RC filter, P1-GF-RC-1, and the medium, 3398-L2W, used in the filter plotted as a function of air velocity. The filter has a large increase in pressure drop compared to the medium.

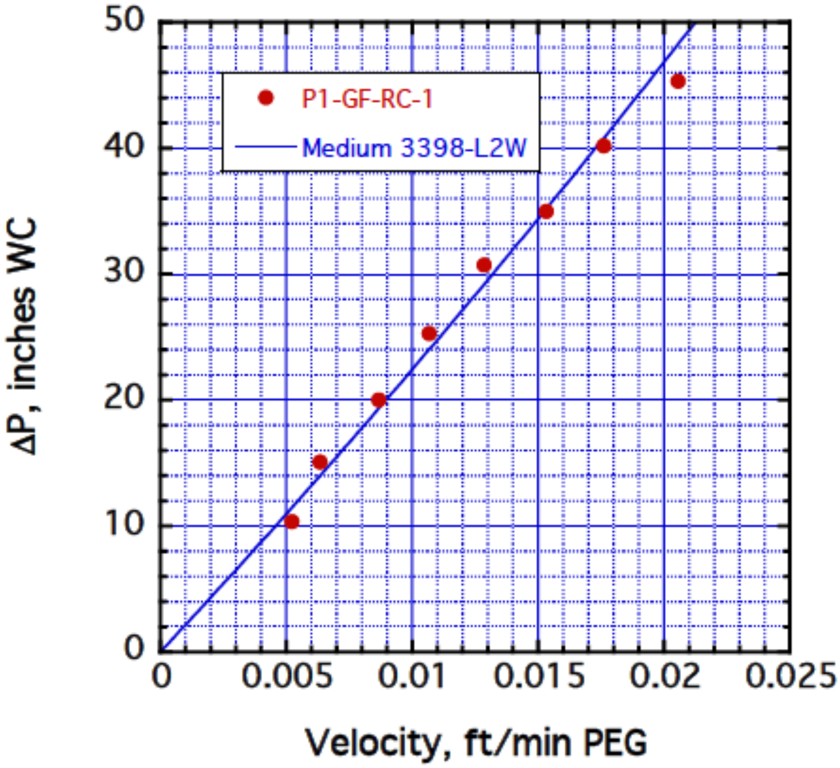

Figure 89. Pressure drop measurements for the Porvair RC filter, P1-GF-RC-1, and the medium, 3398-L2W, used in the filter plotted as a function of PEG velocity. The filter unexpectedly has about the same pressure drop as the medium and suggests a major leak.

The unexpectedly similar pressure drop of the filter and medium may be due to a large leak that developed during the test as was seen for the Kurion filter in Figure 71. Based on the air tests in Figure 88 , there should have been a much larger pressure drop for the filter than for the medium at the same fluid velocity. This suspicion is enforced by the very large aerosol penetration seen in the post test penetration test in Figure 90 .

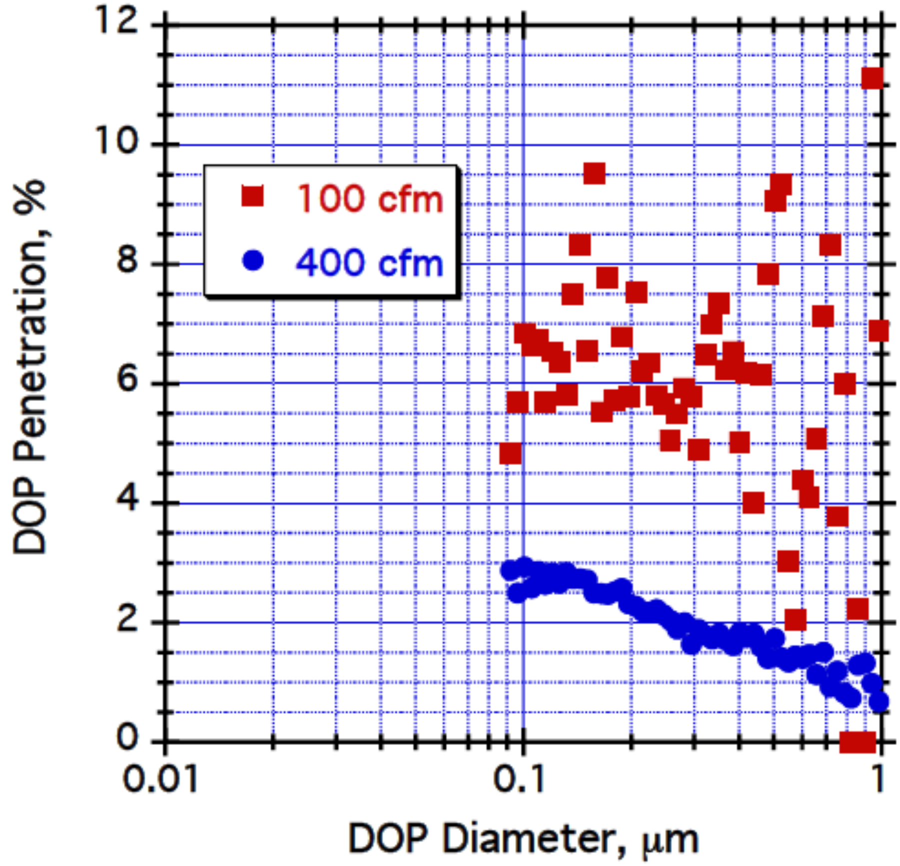

Figure 90. The final DOP penetration for the P1-GF-RC-001 filter following exposure to a differential pressure of 45 inches WC was 1.9% and 6% at 400 and 100 cfm respectively. The data for the 2,000 cfm was missing. The filter failed the penetration due to a large leak.

Porvair (GFr) Glass Fiber Filter With High-Strength Glass Fiber Medium, Wire Screen Reinforcement, No Separators and Rated at 225 inch WC

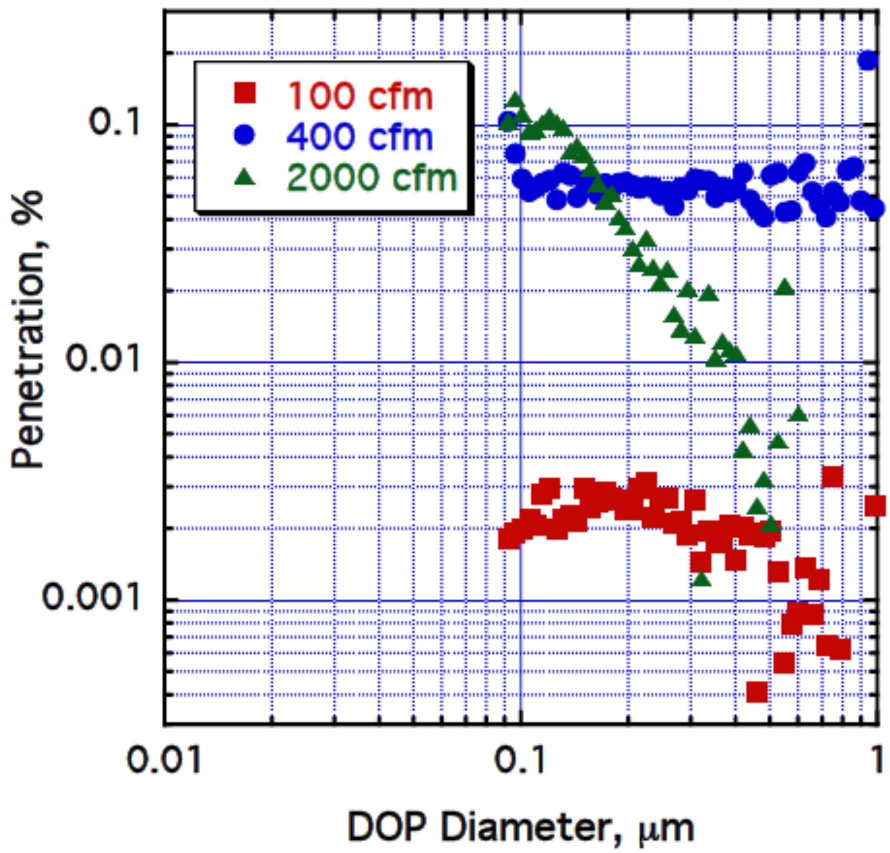

Figure 91. Initial penetration of P1-GFR-RC-001 filter shows the filter penetration at 2,000, 400 cfm and 100 cfm was 0.015%, 0.05% and 0.002% respectively. The 0.05% penetration at 400 cfm indicates the filter failed the required DOP penetration test. The initial pressure drop at 2,000 cfm was very high at 13 inches WC.

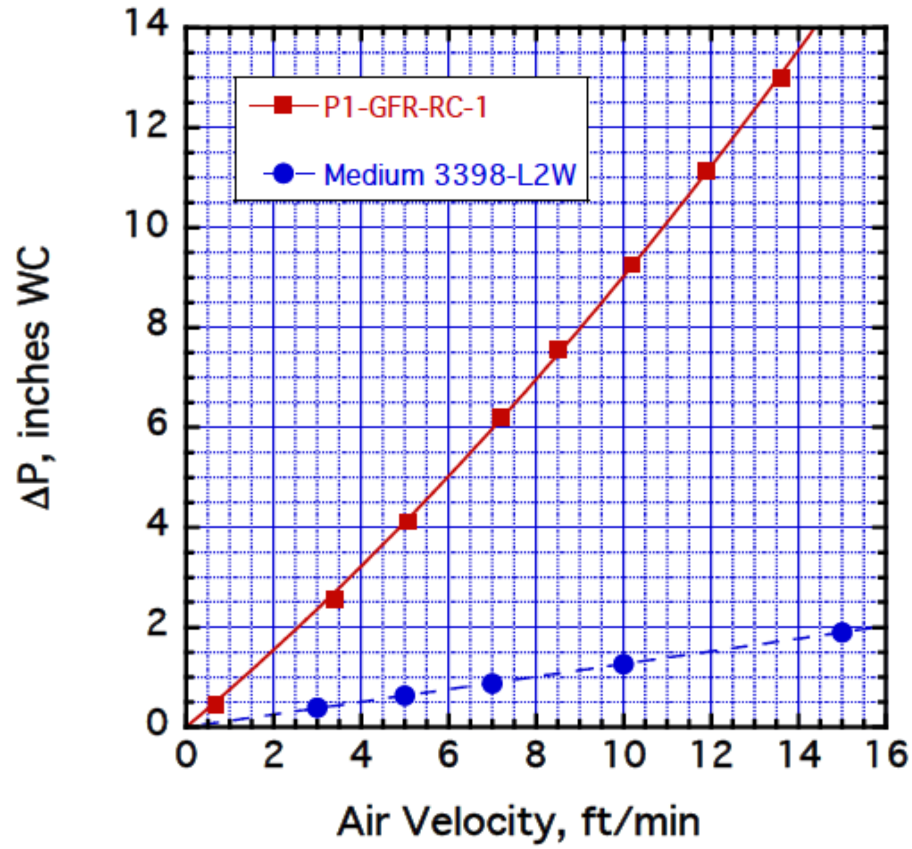

Figure 92. Pressure drop measurements for the Porvair RC filter, P1-GFR-RC-1, and the medium, 3398-L2W, used in the filter plotted as a function of air velocity. The filter has a large increase in pressure drop compared to the medium.

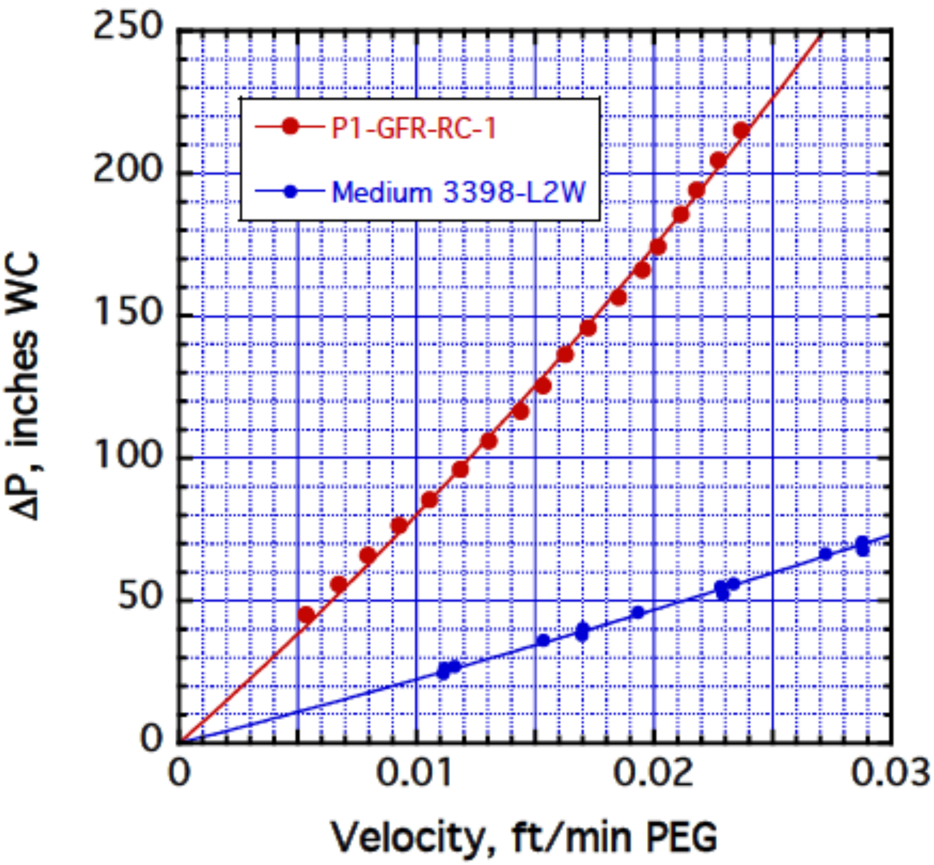

Figure 93. Pressure drop measurements for the Porvair RC filter, P1-GFR-RC-1, and the medium, 3398-L2W, used in the filter plotted as a function of PEG velocity.

Note the large difference in pressure drop between and filter and medium for the PEG/water solution is similar to that for the air test in Figure 92. This is the expected behavior for filters that do not develop major leaks during the high pressure PEG/water test.

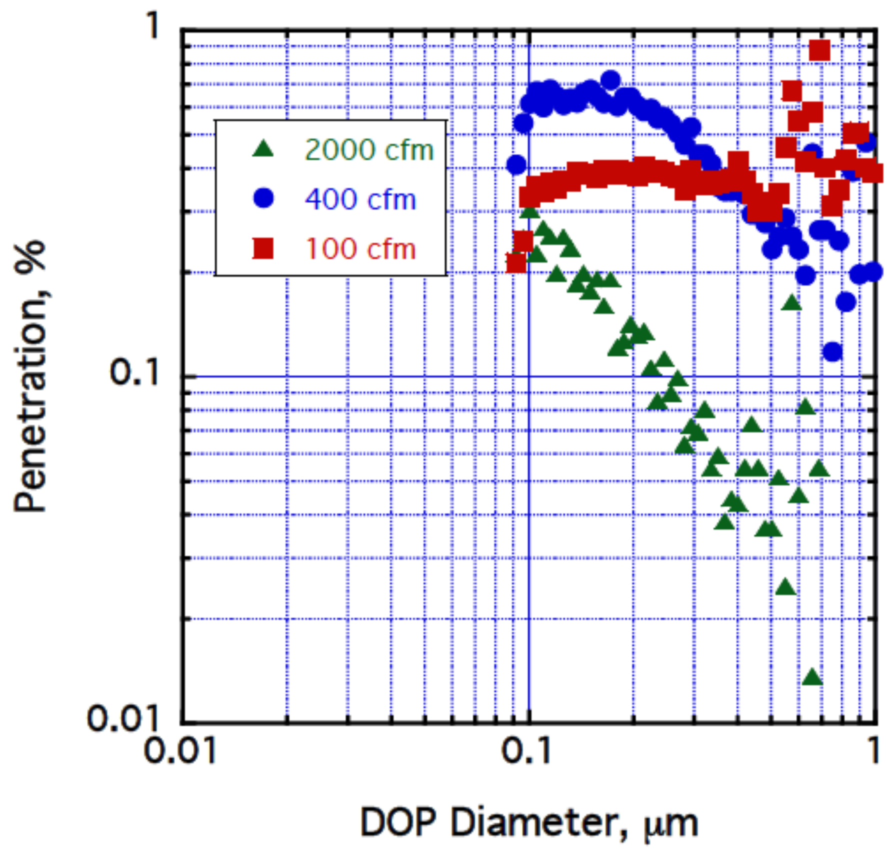

Figure 94. Final penetration of P1-GFR-RC-001 filter shows the filter penetration at 2,000, 400 cfm and 100 cfm was 0.08%, 0.46% and 0.37% respectively. These penetrations show the filter failed the required DOP penetration test but not as great as the P1-GF-RC-001 filter in Figure 90.

Porvair (MM) Metal Fiber Filter With No Separators and Rated at 225 inch WC

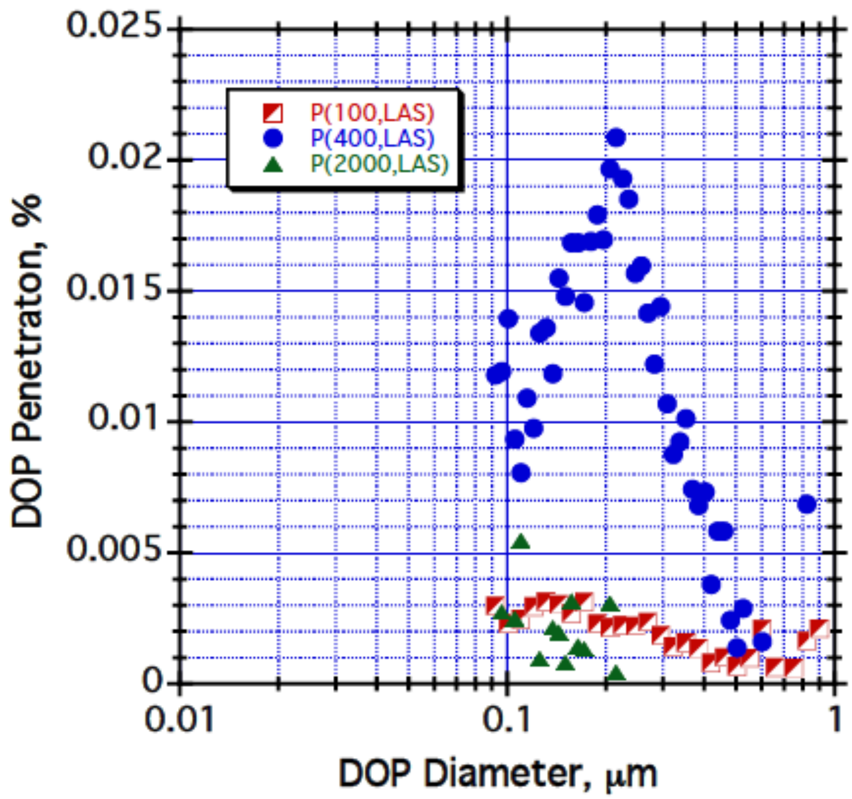

Figure 95. Initial DOP penetration of the Porvair P1-MM-RC-001 filter shows the filter penetration at 2,000, 400 cfm and 100 cfm was 0.001%, 0.012% and 0.002% respectively. The initial pressure drop at 2,000 cfm was very high at 22.3 inches WC.

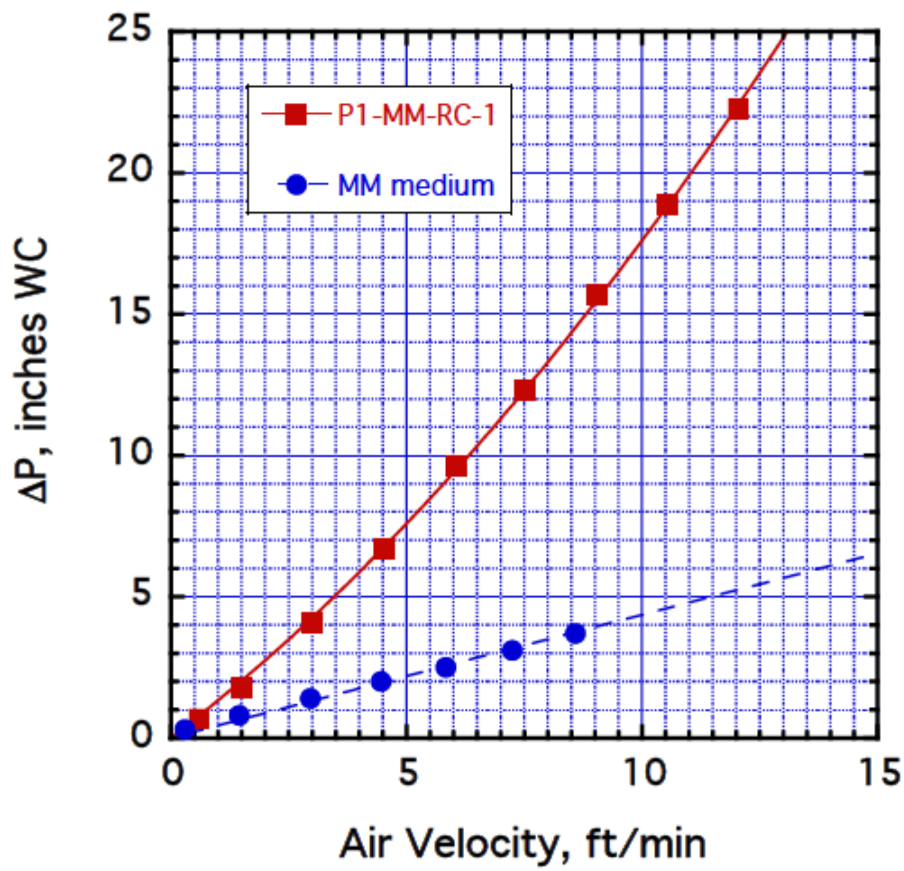

Figure 96. Pressure drop measurements for the Porvair MM filter, P1-MM-RC-1, and the MM medium, two layers of Bekaert AL3 sandwiched between screens, used in the filter plotted as a function of air velocity.

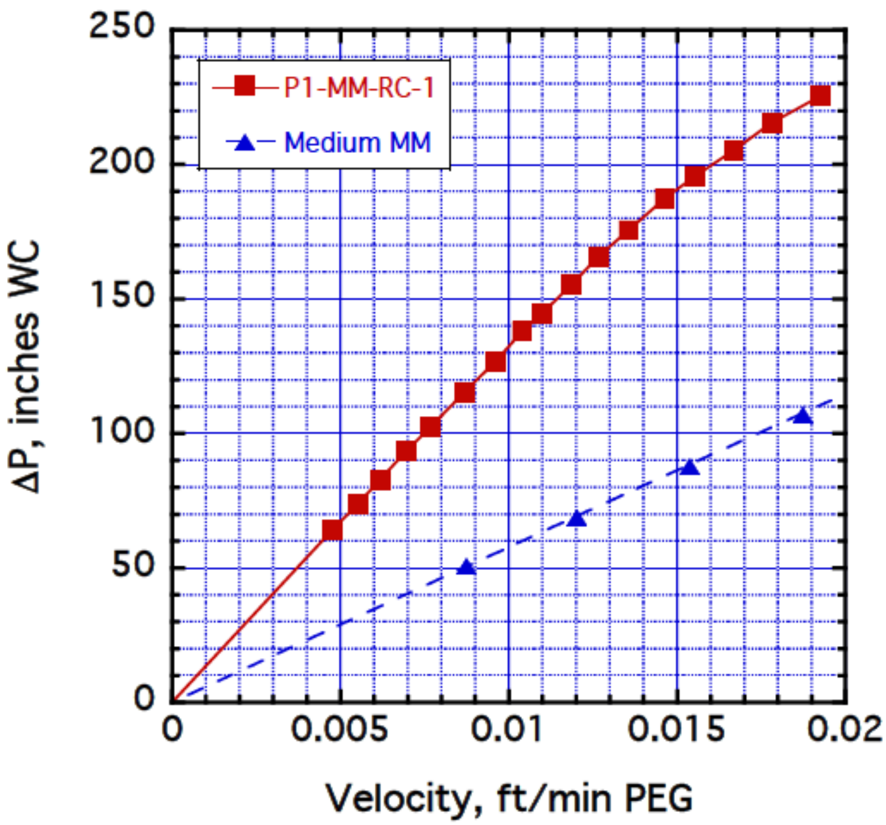

Figure 97. Pressure drop measurements for the Porvair RC filter, P1-MM-RC-1, and the MM medium, two layers of Bekaert AL3 sandwiched between screens, used in the filter and plotted as a function of PEG velocity. The decreasing pressure at higher velocities for the filter is likely due to the opening of previously compressed pleats.

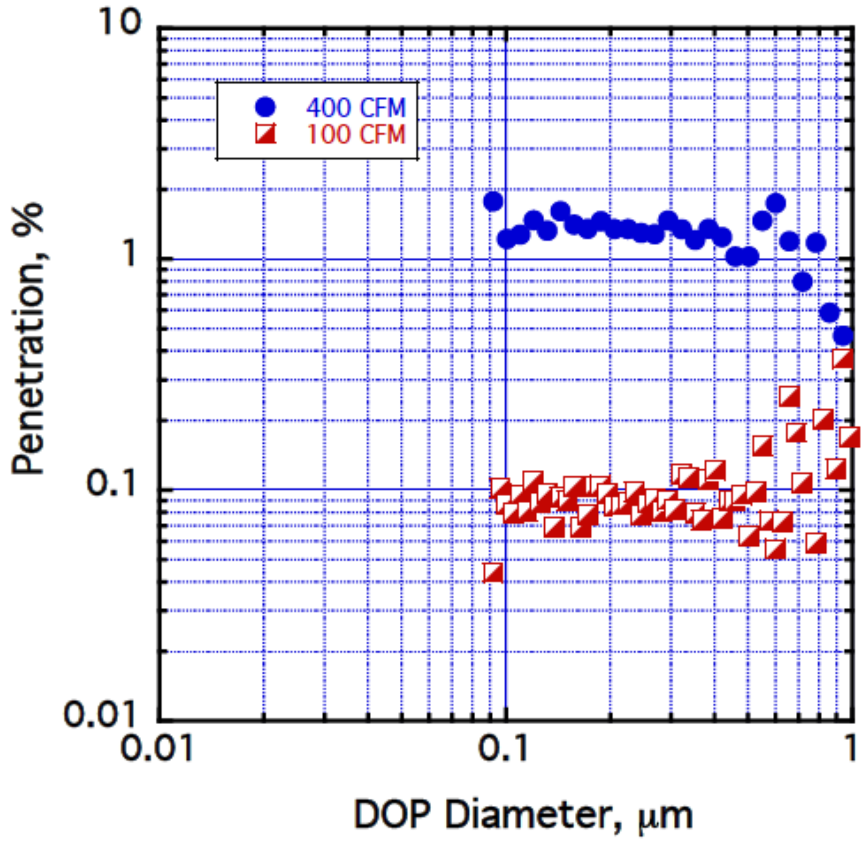

Figure 98. Final penetration of P1-MM-RC-001 filter shows the filter penetration at 400 cfm and 100 cfm was 1.3 % and 0.09% respectively. These penetrations show the filter failed the required DOP penetration test and had a significant leak.

Summary of Porvair Prototype Filter Test Results

Table 10 summarizes the test results of the three Porvair prototype HEPA filters. All of the prototype filters passed the initial DOP penetration test except for the P1-GFR-RC-1 filter where the penetration at 2000 cfm passed at 0.016% but failed at 400 cfm where the penetration was 0.055%. The DOP penetration tests following the exposure to 45 or 225 inches WC in the PEG/water solution for one hour showed that all of the filters had developed some leaks.

Although only limited data is available, the source of these leaks appears to be the breaking of the urethane bonds between the end-caps and the filter pack. This conclusion is supported by the observed bond breakage for a Kurion filter shown in Figure 71 and by a leak scan test of filter P1-MM-SC-1 where leaks ranging from 0.015% to 0.334% were observed around the circumference of the top, inlet side of the filter and leaks ranging from 0.019% to 0.075% were observed at a specific location on the opposite bottom side.

These leaks demonstrate that the steel filter support structure (end caps, three metal straps connecting the top and bottom end-caps, inner and outer grids) is not sufficiently rigid to prevent breaking the urethane bond that seals the filter pack to the end-caps during the high pressure exposure. The deflection or ballooning of the end caps under high pressure may cause the urethane bond between the filter pack and the end-cap to fail.

Despite the inability of the Porvair filters to withstand the high pressure challenge, the final average penetration of the 7 prototype filters tested at 2000 cfm and 400 cfm was 0.12% and 0.54% respectively. These penetration values provide a significant safety factor during unmitigated accidents in the WTP operations.

Table 10. Summary of Porvair Filter tests on prototype filters.

Filter	Rating, in. WC	Initial /Final	DP, in. WC	Penetration, %			Pass/ Fail	Mass gain*, g
				2000 cfm	400 cfm	100 cfm		
P1-GF-RC-1	45	Initial	10.0	0.013	0.013	0.02	Pass	
		Final			1.9	6.0	Fail	--
P1-GF-SC-1	45	Initial	8.75	0.028	0.025	0.006	Pass	
		Final	8.5	0.128	0.130	0.027	Fail	104
P1-GFR-RC-1	225	Initial	13.0	0.016	0.055	0.002	Fail	
		Final		0.075	0.46	0.36	Fail	--
P1-GFR-RC-2	225	Initial	13.8	0.018	0.017	0.006	Pass	
		Final	13.0	0.279	0.709	0.18	Fail	--
P1-GFR-SC-1	225	Initial	9.84	0.012	0.003	0.001	Pass	
		Final	10.0	0.068	0.172	0.020	Fail	155
P1-MM-RC-1	225	Initial	22.3	0.001	0.012	0.002	Pass	
		Final			1.3	0.09	Fail	--
P1-MM-SC-1	225	Initial	21.2	0.016	0.031	0.011	Pass	
		Final	21.5	0.058	0.067	0.029	Fail	461

*The mass gain represents the residual PEG on the filter.

The most significant observation from the test results is the excessive pressure drop of all of the filters. Figures 99 and 100 show photographs of the filter packs used in the GF and MM filters respectively prior to sealing the end-caps with urethane. The pleats are so tightly packed that they effectively restrict the air flow and create a high filter pressure drop. In addition, the compressed pleats on the inlet (inside) side of the filter restricts the available filter medium for particle deposits and would greatly reduce the filter particle loading capacity. The use of separators would have prevented these pleat closures.

Figure 99 Photograph of portion of Porvair filter pack prior to sealing the end-cap on the P1-GF-SC filter using Lydall 3398-L2W medium. The pleats block the air passage through the filter pack and create a high pressure drop. The pleat depth is 1.5 inches.

Figure 100.   Photograph of portion of Portion filter pack prior to sealing the end-cap on P1-MM-SC filter using two layers of Bekaert 3AL-3 stainless steel fiber medium. Note that the pleats on the inlet side (upper part of the photo) are tightly packed and block the air passage.

The DOP leak scan test used at MSU (Figure 43) generally correlated with the filter penetration measurements. The procedure called for scanning the filter with a probe from the top end-cap (inlet) to the bottom end cap parallel to the vertical pleats. Although this scanning technique is sensitive to detecting leaks within the filter pack, it is not sensitive to leaks in the urethane bond between the end-caps and the filter pack. A circumferential scan around the top and bottom end-caps would be more sensitive.

MSU provided Bechtel with leak scan tests on 4 of the 7 tests performed on the Porvair filters. Three of the four filters showed an increase in detected leaks following the high pressure test as was seen with the filter penetration tests. However, the filter, P1-GFR-RC-002 showed no leaks either before or after the high pressure test, yet the filter penetration in the post pressure test was 0.279% and 0.709% at 2,000 and 400 cfm respectively. The scan test procedure can be improved by to including a circumferential scan around the top and bottom end-cap seals.

Development of Improved gel-seal

The seal leak tests on the initial set of six glass fiber HEPA filters from Kurion tested in the RLPTS showed that the standard HEPA gel seals did not leak when tested at 20 inches and 45 inches, but showed major leaks at 225 inches WC. These tests coupled with the previous findings from Flanders confirmed that the Blu-Jel sealant fails at differential pressures above 70 inches WC (Peebels, 2003) and that a stronger gel was required to meet the leak requirement at 225 inches WC.

Kurion conducted preliminary tests to find alternative gel materials that are stronger and can resist the higher pressure and yet perform the sealing function using a knife edge. In general, stronger and harder gel materials can withstand the differential pressure of 225 inches WC but require a much greater force to insert a knife edge into the gel and may require modifications for remote installations that rely on gravity and also for manual installations. Additional concerns with a stronger gel material are how much gel adheres to the knife edge and whether the new gel material can meet the flammability and radiation resistance requirements. The development of the stronger gel-seal was discontinued pending the successful demonstration of a radial-flow HEPA filter that can withstand 225 inches WC. Although there is little doubt the stronger gel-seal can be developed, the increased force required to seal the filter may make conventional gaskets more attractive.

Assessment of Phase I Test Results

Neither Kurion nor Porvair were able to successfully demonstrate a HEPA filter that can withstand 225 inches WC in the liquid pressure test without structural damage or developing significant leaks. Each company also had prominent failures not related to the issue of resistance to the 225 inches WC. Kurion had only one of eight filters that passed the initial DOP efficiency test as seen in summary Table 5. Porvair could generally meet the efficiency requirements because the tight pleat packing effectively increased the thickness of the medium and also the pressure drop. The issue was insufficient medium area that resulted in high DOP penetration and also excessive leaks as seen in Figures 69, 73-75, 77, 78, 81 and 83. Porvair had unacceptable high pressure drops in all seven of their tested filters as seen in summary Table 10. This was an issue with pleat compression as seen in Figures 99 and 100.

The solution to these problems is well-known in the HEPA filter industry, and the problems should not have occurred. The use of inadequate medium area (120-190 ft^2) resulted in excessive medium velocity (10-17 ft/min instead of the required 5 ft/min) and failed DOP penetration. Porvair was limited in its prototype filters by using pleats with only 1.5 inches depth due to lack of adequate pleaters. The Flanders filter, that was being replaced had a medium area of 310 ft^2, about twice that used in the Kurion and Porvair prototype filters. Similarly the use of corrugated separators to prevent pleat collapse is a standard practice in the industry.

The need to develop a stronger gel-seal that can withstand 225 inches WC was another problem that emerged during the prototype filter development. Although the preliminary studies by Kurion indicted that a solution was feasible, the changes to the manual and remote filter change operations due to the stronger gel were not analyzed.

These problems were overshadowed by the issue of insufficient structural strength of the steel support elements to withstand high pressures. A glaring example of the insufficient structural strength of the filter hardware is the separation of the bottom end-cap from the filter pack seen in Figure 71 for the Kurion filter and the leaks developed in the Porvair filters in Table 10. The inadequacy of the structural strength of the steel hardware in both the Kurion and the Porvair filters was seen in the failure of all the filters to meet the DOP penetration requirement following exposure to high pressure.

The summary Tables 6 and 10 show that the DOP penetration increases following the high pressure exposure. For the Porvair filters, Table 10 shows that the average DOP penetration following the high pressure tests for all the filters was 0.12% and 0.54% at 2000 cfm and 400 cfm, respectively. These are relatively small leaks and can be greatly reduced by increasing the filter structural support for the filter pack and urethane seals. As an extreme example, the two-stage steel fiber HEPA filter shown in Figure 1 was able to withstand a differential pressure of 1,000 psi (27,680 inches WC) because of the high strength of the media support cores (Bergman, 2018).

High strength supports for the filter packs and for the urethane bond between the filter pack and end-caps can be developed based on a structural stress analysis.

Kurion conducted an experimental and theoretical study of the pleat strength with corrugated separators in response to Bechtel's concern with pleat collapse. Both companies also performed weight compression tests to simulate a crane hoist dropping on a filter. However, neither company analyzed filter ballooning under high pressure. The indicated source of the HEPA filter leakage is the outward swelling or ballooning of the steel end-cap and breakage of the urethane bond due to curvature in the end-cap surface. The use of high strength supports for weaker media and medium packs is common in the filter industry. This is also the basis for the high strength Lydall HEPA media, whereby a strong glass cloth is glued to the weak HEPA fiber medium. The issue of improving the strength of the steel components of the filter was not addressed during the review of the unsuccessful phase 1 tests.

A major issue raised and analyzed during the review process was the insufficient filter medium area and the resulting high medium air velocity. Kurion prototype 2 filters had 141 ft2 of medium and a medium velocity of 14.2 ft/min. From Figure 42, the 3398-L2W medium has a penetration of 0.028% at 14.2 ft/min. Thus the unavoidable leaks introduced during filter manufacturing would force the penetration to exceed the 0.03% limit and fail most of the filters as was seen in this report. A similar analysis of the high medium velocities in the Porvair prototype filters was not possible because the extreme compaction of the filter pleats invalidated any computation of medium velocity. From the extremely high pressure drop, the compressed pleats effectively formed a medium with much greater thickness, which not only increased the pressure drop, but also increased the filter efficiency.

Although increasing the filter medium area and adding corrugated separators is the logical filter approach, another option was proposed for using higher efficiency media such as ULPA (ultra-low penetrating air) medium in place of the HEPA medium. The combination of increasing medium area and using ULPA medium yields the highest efficiency. From Figure 42, the ULPA medium has a DOP penetration at 14.2 ft/min of 0.0011% compared to 0.028% for the HEPA medium. The reinforced ULPA medium, Lydall 6650-L2W, has only a 15% increase in pressure drop compared to the HEPA medium, Lydall 3390-L2W (compare Figures 29 and 30). Thus, Kurion could substitute the ULPA medium in place of the HEPA medium, and readily meet the DOP penetration requirement for the filter.

However, the suggestion of using ULPA medium, which is typically used in clean-room ULPA filters, raised concerns at Bechtel and prompted a technology readiness assessment. Technically, ULPA medium is similar to HEPA medium, except that ULPA medium has a greater fraction of small diameter glass fibers to increase the efficiency. Moreover, ULPA media has typically been used in clean-rooms, while HEPA filters have been used in the nuclear industry and other areas. Lydall manufactures both HEPA and ULPA media reinforced with glass cloth.

Revised Project Plan

The failure of the Kurion and Porvair prototype filters to demonstrate the filters can retain the required HEPA efficiency following exposure to 225 inches WC for one hour prompted Bechtel to abandon the goal of a HEPA filter that can withstand the full fan pressure in unmitigated WTP operations and accept standard mitigation strategies. Bechtel revised the project plan with significant input from DOE (Garcia, 2015) by reducing the maximum filter pressure from 225 inches WC to 50 inches WC and thereby eliminating the high pressure tests in the RLPTS (Figure 9), requiring the HEPA filter to use the high-strength glass HEPA medium with pleats at least 3 inches deep and use corrugated separators, implementing an iterative filter development process with Bechtel selecting the key filter parameters to optimize the filter design, and conducting filter loading with $Al(OH)_3$ powder at two flow rates (1,200 and 2,000 cfm) and three different temperature and relative humidity conditions (100°F and 40% RH, 171°F and 7% RH, and 166°F and 50% RH) to represent the different operating conditions at the WTP. The filter would be loaded to 50 inches WC or to the failure point. Bechtel also selected Porvair as the filter manufacturer.

The iterative development approach was selected to avoid the problem in the previous tests where Porvair would submit the required number of filters as a batch and have the same deficiency repeated in each filter. The iterative approach was not used in the initial project plan because of the additional time required and because the high strength HEPA filter technology was commercially available for axial filters, and the same technology could be used for radial flow filters.

The initial step of the iterative development was for MSU to generate data of DOP penetration for HEPA (Lydall 3398) and ULPA (Lydall 6650) media, with and without reinforced glass cloth at medium velocities ranging from 3 to 15 ft/min. The results were used to generate curves of DOP penetration versus medium velocity as shown in Figure 42. These curves would then be used to determine if the filter medium velocity in the proposed Porvair design were sufficiently low to achieve HEPA filter efficiency.

The iterative approach began with the default filter design having the Lydall 3398-L2W medium with a minimum pleat depth of 3 inches and corrugated separators. Porvair would submit a filter design with the proposed medium area. Bechtel would then determine if the filter medium velocity were sufficiently low for the medium DOP penetration plus a factor representing production leaks would be less than 0.03%. If Bechtel determined the proposed filter would meet the 0.03% DOP requirement, then they would approve the fabrication of the filter. If the proposed filter design indicated a DOP penetration exceeding 0.03%, then Porvair would have to increase the filter area to the required area, or if this were not possible, then the Porvair would have to use ULPA media to increase the efficiency and the iteration repeated with the new parameters. The fabricated filter would then be tested at MSU and depending on the results, another iteration of the process would begin.

Instead of fabricating full-scale filters for the iteration optimization, Porvair urged the use of filter segments called quadrant packs to save time and money. Figure 101 shows a photograph of the quadrant filter element that represents 4.55% of the full-scale filter. This recommendation was then included in the revised test plan.

After a successful filter design was confirmed with testing of the quadrant pack at MSU, Porvair would fabricate full-scale SC filters using the same design parameters for testing of pressure drop, DOP efficiency, and particle loading with $Al(OH)_3$ at MSU.

Determination of Filter Parameters Through Iterative Testing With Quadrant Pack Filters

Porvair fabricated several quadrant pack filters (Duvekot et al, 2017) like that shown in Figure 101 using the Lydall 3398-L2W medium, corrugated separators, and pleat depth of 3.27 inches and designated the design as D4 to distinguish it from other designs described in the revised project plan (Garcia, 2015). The D4 design was the standard HEPA filter design of pleated reinforced medium and corrugated separators as successfully developed for axial flow HEPA filters (Rudinger et al, 1990) and now adapted for radial flow HEPA filters.

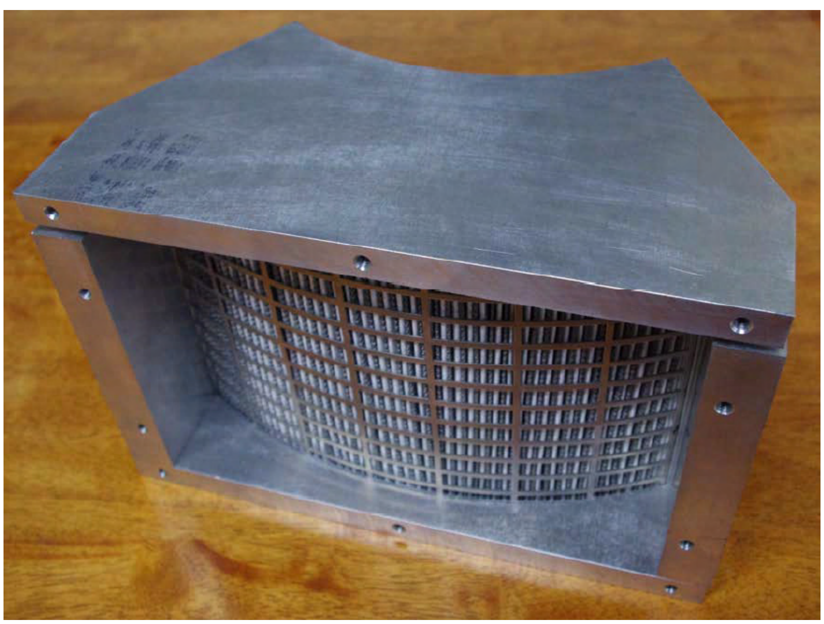

Figure 101 Exit side of Porvair quadrant filter used for optimizing the filter pleat and medium. The quadrant filter represents a 60° arc or 1/6 of the filter circumference and 4.55% of the full-scale filter.

The initial pressure drop measurements of the first two D4 quadrant filters, shown in Figure 102, indicated that the full-scale filter would have a pressure drop of 1.55 inches WC and would easily meet the initial target of less than 2.0 inches WC.

Porvair had developed and used corrugated sintered wire screens instead of the standard corrugated aluminum as the pleat separators in the quadrant filter packs (Amey et al, 2020). Porvair claimed that the corrugated sintered wire screens resulted in a filter pressure drop 25% lower than the same quadrant filter design using conventional corrugated aluminum separators but provided no experimental data to support its claim. Their explanation for the lower flow resistance was that air within the pleat channel could flow through the screen separator but not the solid aluminum (Duvekot et al, 2017; Amey et al, 2020). They claimed that the solid separator constrains the fluid flow to the longitudinal channels between the separators and the filter medium and would allow "little or no fluid flow across the [filter medium] sheets...except near the entrance and exit" of the filter pack. "The results is less flow across the filtration element sheets, which can result in greater pressure loss...." This argument is inconsistent with theoretical and experimental studies that show air flows through the filter media all along the pleat channel and not just at the pleat ends. The authors are not aware of any study suggesting that there is an unequal air flow on opposite sides of the separator within a pleat as would be required for the Porvair hypothesis.

Although there is research on reducing the skin friction of smooth surfaces by introducing surface modifications such as riblets or grooves (Kuhnen et al, 2018) the published drag reduction data ranges from 5-10% (Filippone, 2001) and only under limited conditions. However, no studies were found using screens for reducing skin drag. The claimed 25% reduction in filter pressure drop switching from solid separators to screen separators is most likely due to experimental differences between the two quadrant filter units. However, without experimental data and description of the test system it is only possible to refute the Porvair hypothesis for the claimed reduction in pressure drop.

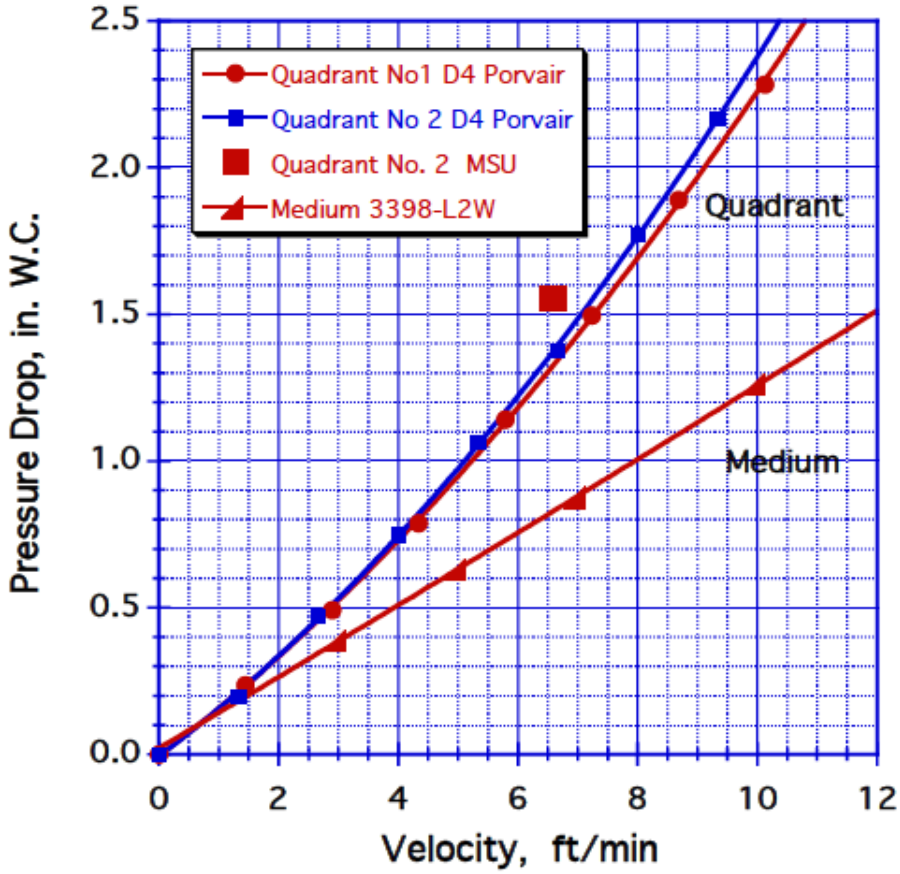

Figure 102. Pressure drop measurements of Porvair quadrant pack filter and Lydall 3398-L2W medium as a function of air velocity. The MSU point for the D4-2 quadrant pack is 1.55 inches WC at 6.58 ft/min and represents the pressure drop measured at MSU at 90 cfm flow corresponding to 2,000 cfm for a full scale filter.

The computed areas of the quadrant packs 1 and 2 are 12.6 ft2 and 13.7 ft2 respectively. The increased DP at MSU is believed to be due to accumulation of oil from efficiency testing.

Comparing the pressure drop of the quadrant filter (1.37 inches WC) to the medium (0.835 inches WC) at 6.58 ft/min corresponding to the full-scale filter shows the medium represents 61% of the filter pressure drop. The remaining 39% of the pressure drop is due to the pleat channel flow resistance.

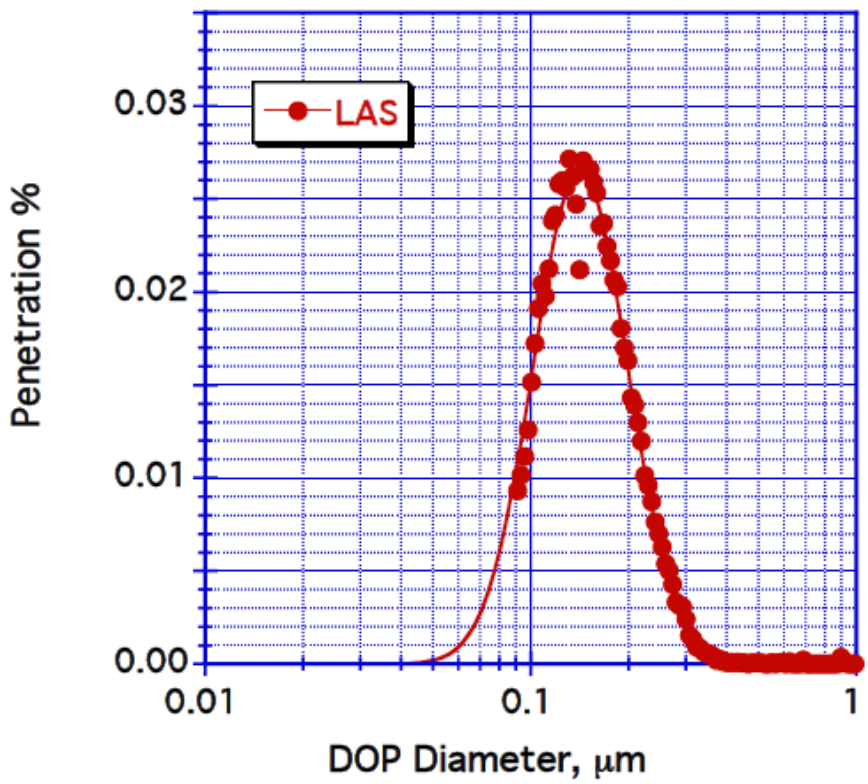

Figure 103. Penetration of Porvair quadrant pack filter D4-2 using 3398-L2W medium and corrugated separators and fitted to a log-normal curve. The filter had been partially loaded with oil deposits from previous filter testing. The penetration at 0.27 microns is 0.004% at 90 cfm (6.57 ft/min).

The pressure drop had increased from 1.36 inches WC measured for a clean filter by Porvair to 1.55 inches WC when received by MSU and 1.88 inches WC at the time of DOP testing. This pressure drop increase suggests deposits of test oil have accumulated on the filter and would lower the penetration

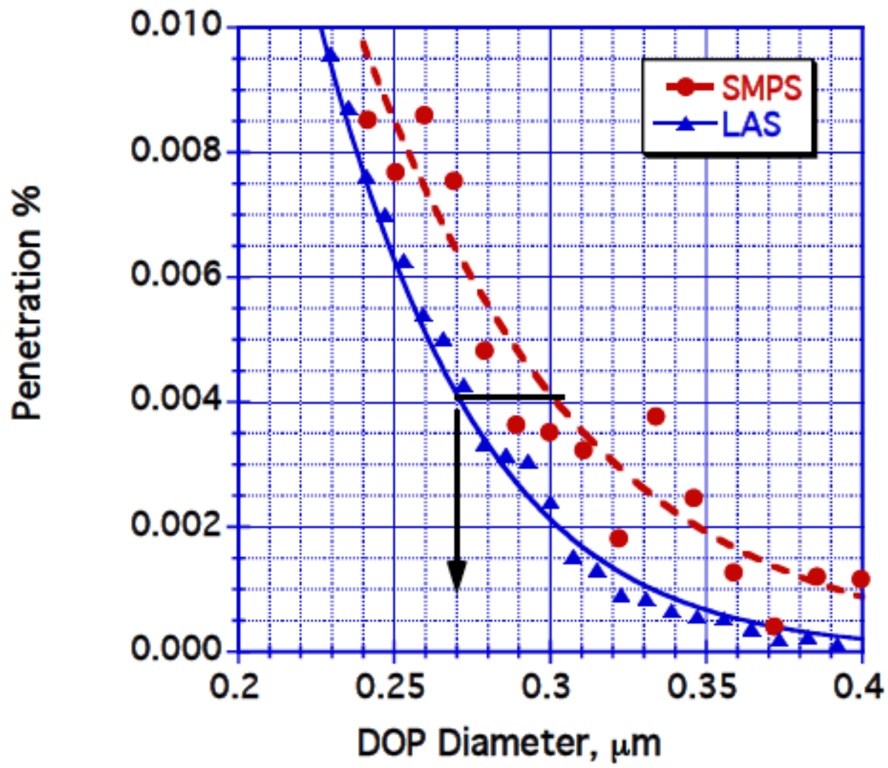

Figure 104. Magnified portion of Figure 96 showing the percent penetration for the quadrant pack D4-2 using the LAS and SMPS instruments. The penetration for for LAS instrument is shifted from the actual DOP diameter as measured with the SMPS because the LAS is calibrated with PSL and not DOP.

Porvair also tested other media and pleat separation methods, but the results were not useful for Bechtel (Duvekot et al, 2017).

Full Scale Porvair Filter Tests

Based on the successful tests with the quadrant pack, Porvair fabricated several SC filters for testing at MSU. The design parameters for the pre-qualification filters described in this section, P-SC-1 and P-SC-2, were not determined, but they were close to the final Porvair filters shown in Table 11

Table 11. Design Parameters of final Porvair filters

Filter	Inlet ID, in.	Pack ID, in.	Pack OD, in.	Sep. height in.	Pleat* depth, in.	Effective area, ft2	Medium Velocity ft/min	No. of pleats
Safe change	13.0	13.4	19.9	0.05	3.27	310	6.45	311
Remote change	11.0	12.3	18.9	0.05	3.27	310	6.45	301

Medium is reinforced glass fiber, Lydall 3398-L2W with no additional screens.

Figure 105 shows photographs of one of the filters, P-SC-3, used in the MSU tests to determine the final Porvair filter parameters.

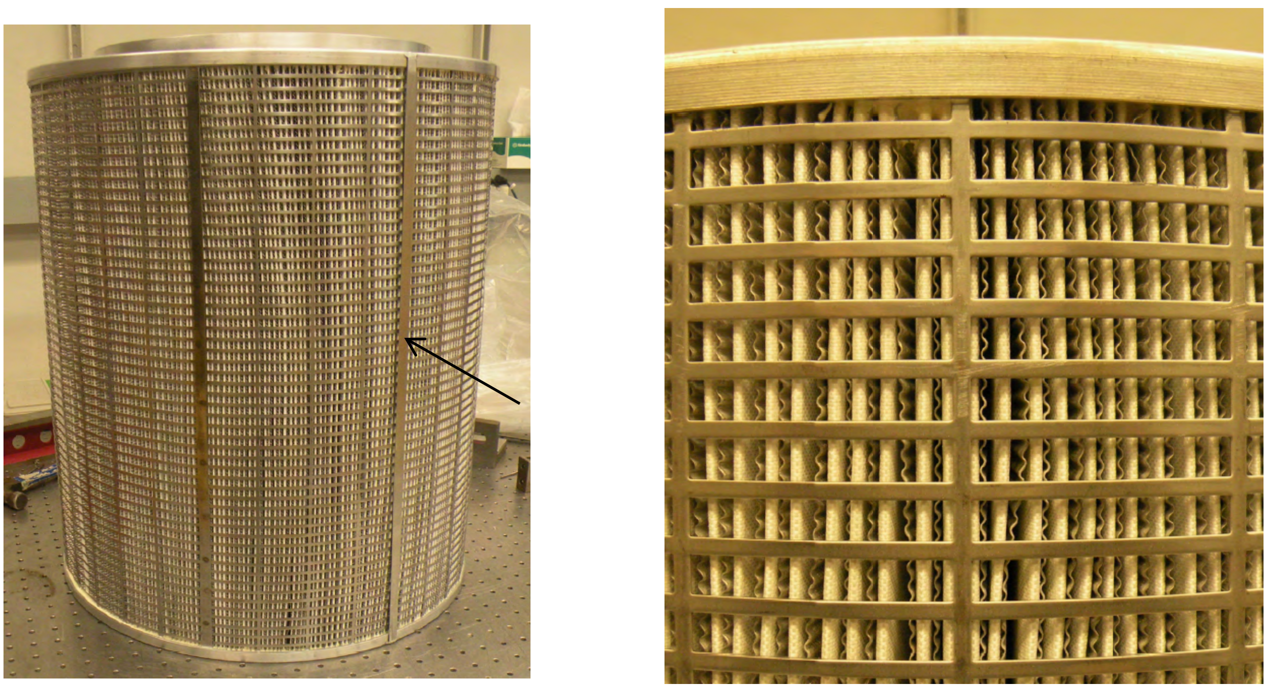

(A) (B)

Figure 105. Photograph of (A) the Porvair SC filter, P-SC-3, with arrow showing one of three end-cap support band and (B) magnified portion of the filter to show the pleats and corrugated separators.

Porvair Filter P-SC-1 Test Results

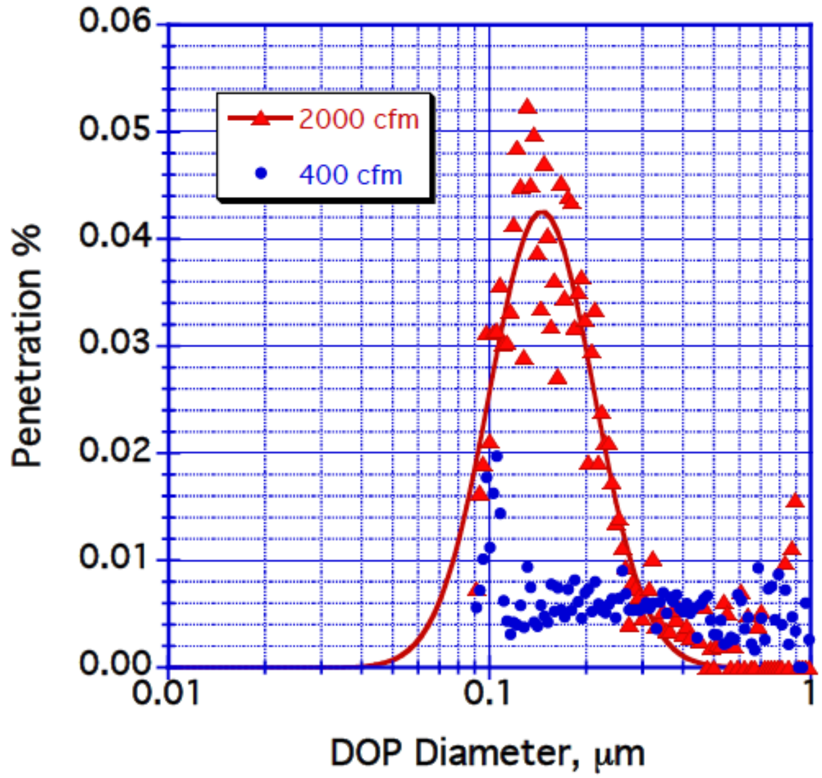

Figure 106. Percent penetration versus DOP particle diameter for P-SC-1 filter at 2000 and 400 cfm. 12/16/15 Test. At 0.30 micron DOP (0.27 micron measured with the LAS) the penetration is 0.009% at 2000 cfm and 0.006% at 400 cfm. The pressure drop was 1.27 inches at 2,000 cfm. The penetration at 100 cfm is similar to that at 400 but is not shown due to the scatter of data. The curve represents the best fit log-normal curve through the 2000 cfm points.

The scatter of all the data is due to insufficient DOP challenge. The LAS has only 16-17 counts/s at 2000 cfm and 55-68 counts/s at 400 cfm instead of the target 2000 counts/s.

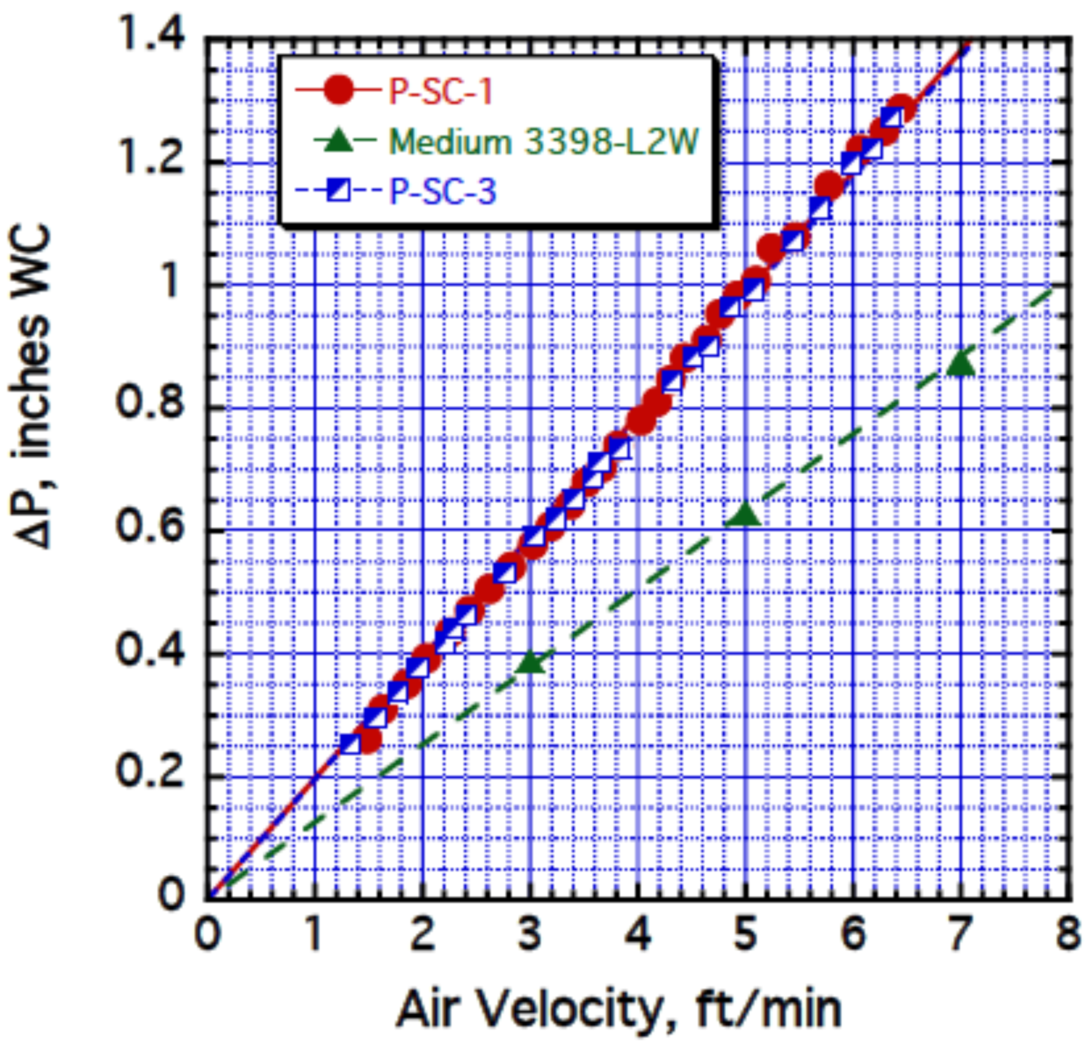

Figure 107. Measurement of pressure drop for filers P-SC-1 and P-SC-3 and medium 3398-L2W as a function of air velocity. The slopes for the P-SC-1, P-SC-3 and medium are 0.197, 0.196, and 0.126 respectively. The filter ΔP at 2,000 cfm is determined at a velocity of 6.45 ft/min.

Following the DOP penetration and pressure drop measurements, the filter was subjected to the rough handling test per ASME AG-1Code Section FK, Subarticle FK-5130. This test (Figure 18) consists of subjecting the filter to 0.75 inch amplitude of 200 cycles per second for 15 minutes. No visible damage was seen. The DOP penetration following the rough handling test is shown in Figure 108.

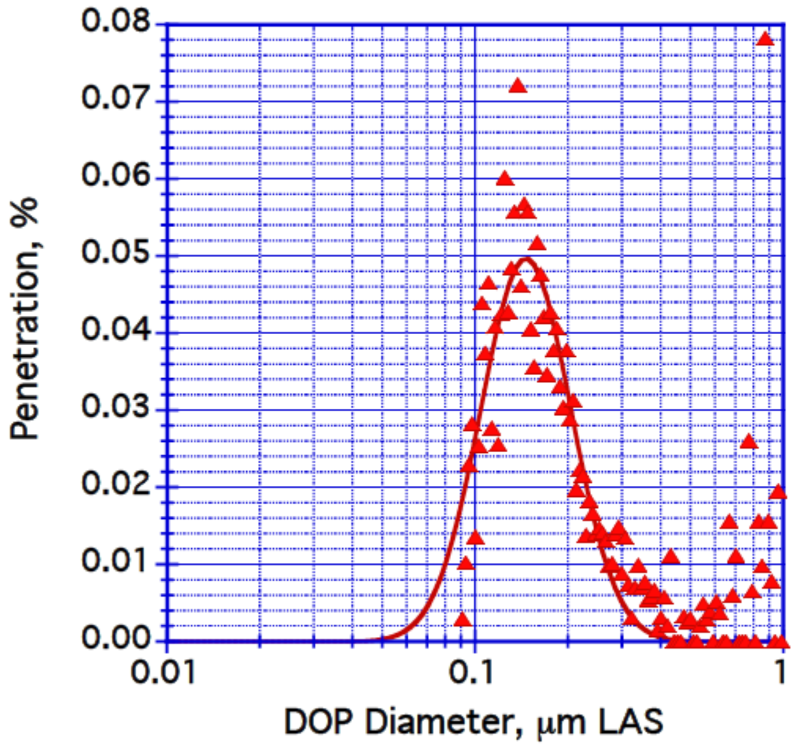

Figure 108. DOP percent penetration for P-SC-1 filter at 2000 cfm after the rough handling test. The penetration at 0.27µm is 0.012%; and, therefore, the filter passed the test. The curve represents the best fit log-normal curve.

The filter was then subjected to a particle loading test using Al(OH)3 powder at 1,200 cfm and 166°F and 50% RH since this represented the most severe of the three different test conditions in the revised Bechtel project plan (Garcia, 2015). The particle loading would at 4 and 10 inches WC and the air was returned to ambient temperature and relative humidity to allow for filter penetration measurements since the aerosol instrumentation could not operate under the high moisture content of the air. Figure 109 shows the filter DOP penetration prior to particle loading at 1200 cfm (100% rated flow), 240 cfm (20% rated flow), and 60 cfm (5% rated flow).

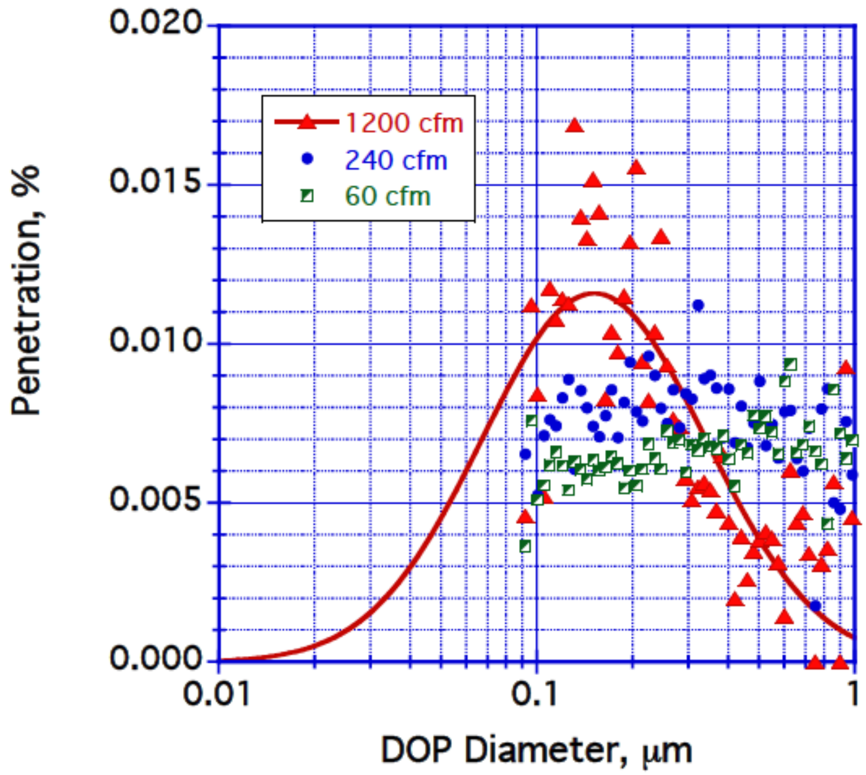

Figure 109. Penetration of P-SC-1 filter prior to particle loading measured at 1200, 240, and 60 cfm. The extensive scatter is due to very low DOP challenge concentration. The curve through the 1200 data is the best fit log-normal curve.

Although the scatter of data in Figure 109 is severe , the data at 1200 cfm can be fitted to a log-normal curve and somewhat resemble the typical penetration curves of filters seen in the flat medium tests and the quadrant pack tests. The penetration data at 240 and 60 cfm are clearly flat indicating significant leaks at the lower flows. Despite the large data scatter, the filter clearly has a penetration at all flows much less than the limit at 0.03%.

Filter penetration measurements were also conducted using $Al(OH)_3$ powder at various air flows, but the challenge concentration was far too low to obtain any meaningful data. The intent of these measurements was to demonstrate the much lower penetration with $Al(OH)_3$ and other solid aerosols than with DOP aerosols because of the higher particle density. However, the additional effort required for such tests would be significant and such data was not needed for the filter development project and was discontinued.

The filter was then subjected to a particle loading test using $Al(OH)_3$ powder at 166°F and 50% RH at a flow rate of 1070 cfm. The loading was intended to be conducted at 1200 cfm, but a calculation error in the set point caused the discrepancy. Theory and previous experiments on filter loading show that this flow deviation would not impact the filter medium mass loading. However, the increased pressure drop due to the filling and obstructing the pleat channels is poorly understood and is likely dependent on the challenge air velocity (Bergman, 2006, 2016b). The small difference of 130 cfm is not expected to cause significant changes in filter loading.

Figure 110 shows the pressure drop of the P-SC-1 filter as it is loaded with $Al(OH)_3$ powder for almost 80 hours. The intervals at 0 pressure drop represent times at which the test stand was turned off to remove the isokinetic filters (Figure 31) or to remove the test filter for weighing. The Pilat impactor (Figure 33) was also removed during the shut down.

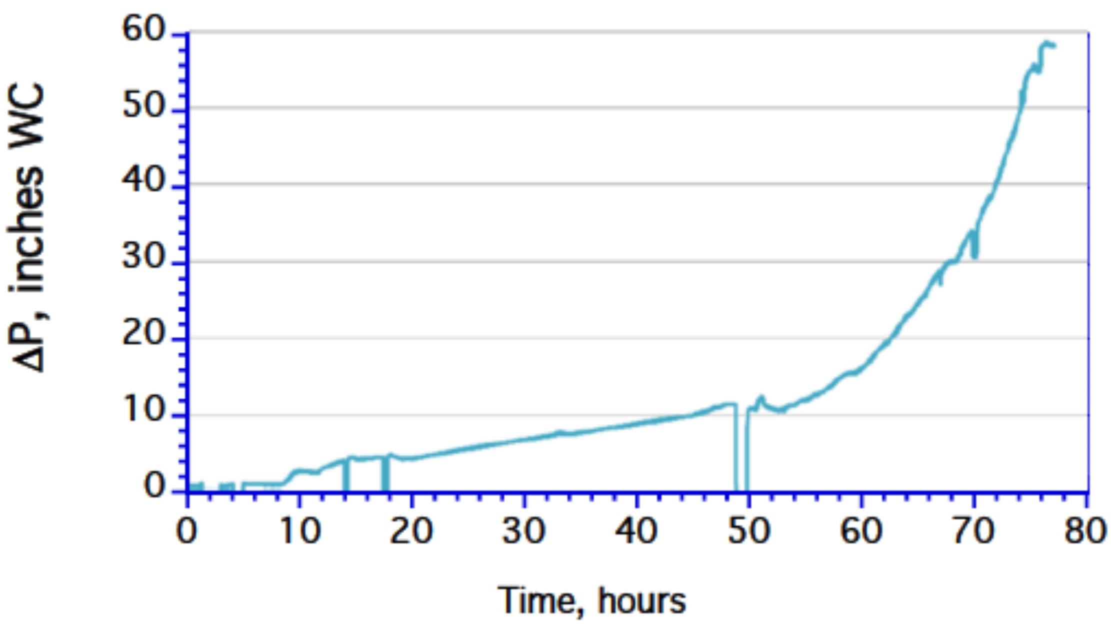

Figure 110 . Loading of P-SC-1 filter with $Al(OH)_3$ powder at 1,070 cfm to nominal 50 inches WC at 166°F and 50% RH.

Figure 111 shows the pressure drop increase of the P-SC-1 filter as a function of accumulated mass of $Al(OH)_3$ powder. The P-SC-3 filter loading is also included for comparison.

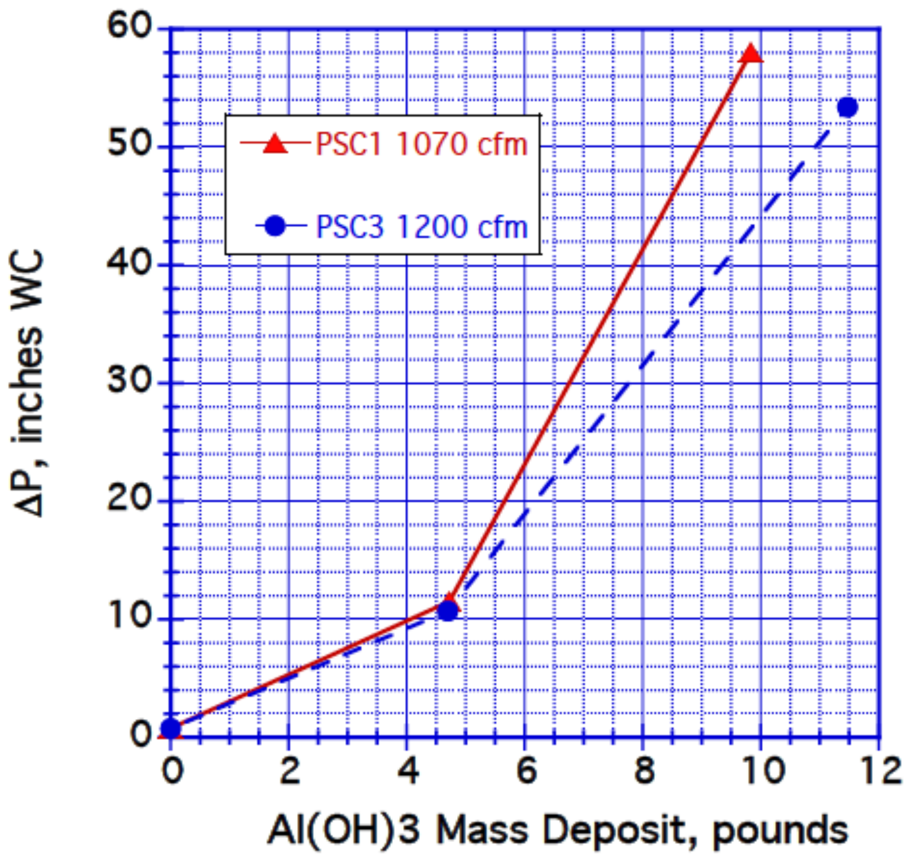

Figure 111. Pressure drop of P-SC-1 and P-SC-2 filters with increasing loading of $Al(OH)_3$ powder. Data points are based on mass measurements of the filter. Both filters readily meet the WTP minimum particle loading requirement of 830 g (1.8 pounds) of 2.5 μm particles at 10 inches WC.

The DOP penetration measurements at 1200 cfm before loading (0.76 inches WC) and at 4, 10 and 58 inches WC are shown in Figure 112. The data for the clean filter (0.76 in.) in Figure 112 was taken from Figure 109.

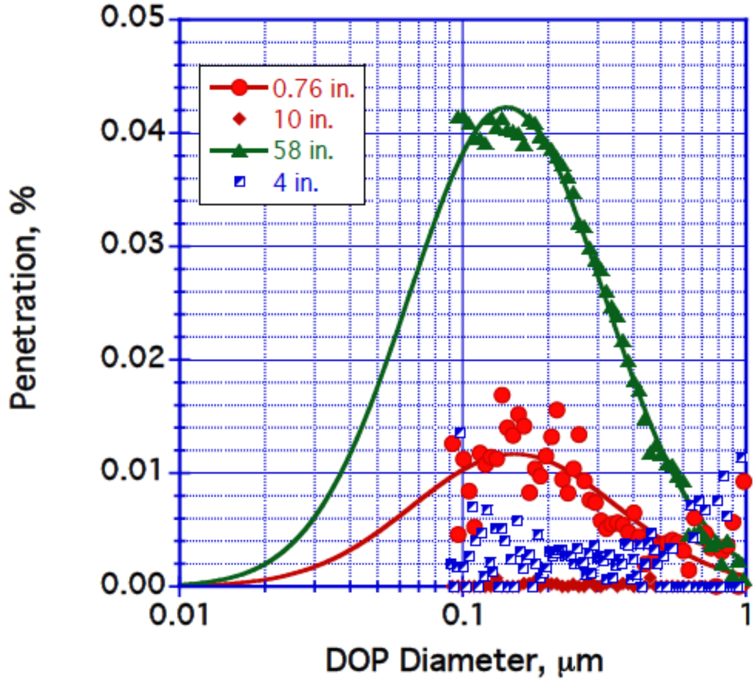

Figure 112. DOP penetration % as a function of DOP diameter for the P-SC-1 filter at 1,200 cfm when clean (0.76 in. WC) and at increasing loading with Al(OH)3 powder measured at 4, 10 and 58 inches WC. Note the penetration at 58 inches WC is 0.03% at 0.27 μm LAS and still meets the HEPA

The large scatter in the data is due to the very low DOP challenge concentration. The challenge concentration in terms of particles/second counted by the LAS is 17-21 for the 0.8 in. data, 13-15 for the 4 in. data, 21-23 for the 10 in. data, and 510-515 for the 58 in. data. As reference, the target challenge concentration is 2,000 counts/second.

The issue of low challenge concentration was raised and a recommendation made to replace the 6 jet Laskin nozzle with an ATI thermal DOP generator used in field tests of HEPA filter banks . This option was explored, but it was not used because of the additional project delay required to develop the proper controls and procedures. The ATI 5C thermal DOP generator was designed for air flows above 6,500 cfm and would have to be re-designed or a dilution system designed and fabricated for the generator. Since the Laskin nozzle generator currently used in the MSU LSTS (Figure 44) was sufficient to detect filter failure at 0.03% penetration, Bechtel concluded the project delay was not warranted.
Figure 112 shows that as the pressure drop increase on the filter, from the clean filter at 0.76 to 4 to 10 inches WC, the penetration decreases as expected for increasing particle deposits. However, by the time the filter pressure drop reaches

58 inches WC, the DOP penetration has increased to higher than the original penetration for a clean filter. This increase indicates that, although the filter still meets the penetration requirement of less than 0.03%, the high pressure has created leaks.

A video of the interior of the filter was taken when the filter was at 10 inches WC and also at the end of the loading at 58 inches WC. Figure 113 is a video still frame of the P-SC-1 filter after the DOP test while still subjected to 58 inches WC.

Figure 113. Video still frame of the P-SC-1 filter after the final DOP test at 58 inches WC and while subjected to the same pressure drop. The filter shows extensive pleat separation.

The P-SC-1 filter was then removed from the test housing and dried for 4 hours at 248°F (120°C) and then weighed, loosing 51 grams in the drying process. Figure 114 shows photographs of the interior of the P-SC-1 filter after drying. It shows that the pleat separations in Figure 113 have closed, thus indicating that the pleat separation occurs in a reversible fashion as high pressure is applied to the filter. Figure 114 also shows that $Al(OH)_3$ particle deposits have filled most of the pleat channels by the end of the test. Note the dark cracks along the pleats that indicate the regions where the pleats have separated.

Figure 114. Photograph of P-SC-1 filter showing the inside of the filter with the $Al(OH)_3$ deposits after heating and drying the filter. Note that the pleat separations seen with air flow in Figure 113 are not seen with 0 air flow. No damage to the filter was seen from the outside.

The filter was then installed in the test fixture (LSTS in Figure 44) and a video taken of the inside filter when operated at 1800 cfm. Figure 115 shows a still frame of the video.

Figure 115. Video still frame of P-SC-1 filter after drying and operating at 1600 cfm in the LSTS showing multiple pleat separations.

Figure 115 shows that that pleat separations have formed again after the filter is reinstalled in the LSTS and the air flow increased to 1600 cfm prior to DOP testing. The P-SC-1 filter was then tested for DOP penetration at 1,000 cfm, 1,200 cfm, and 1,600 cfm and the results shown in Figure 116.

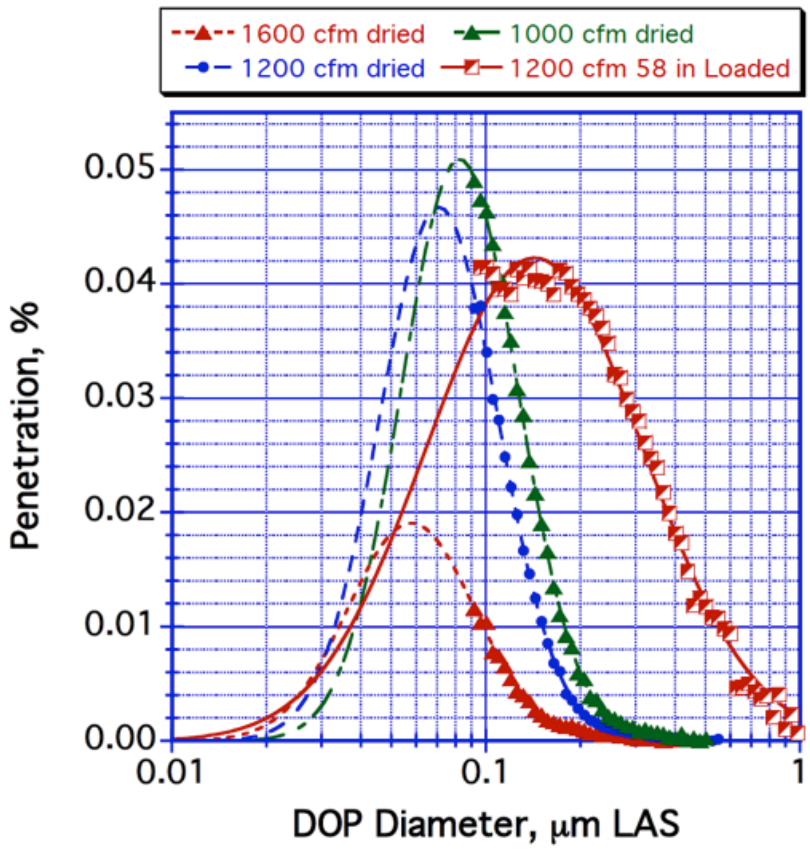

Figure 116. DOP penetration as a function of DOP diameter for the dried P-SC-1 filters at 1000 cfm, 1200 cfm and 1600 cfm. The final penetration at 1200 cfm and 58 inches DP following loading with Al(OH)3 is also shown and was taken from Figure 112. The extrapolated curves at smaller particle sizes should be treated with caution since there are no supporting data.

The three penetration measurements at 1000 cfm, 1200 cfm, and 1600 cfm on the dried filter show the particle capture mechanism is dominated by particle inertia since increasing air velocity results in increasing particle capture and decreasing penetration.

When the P-SC-1 filter was dried and re-tested for DOP penetration, the DOP penetration decreased dramatically from the initial test at 1200 cfm loaded to 58 inches WC as seen in Figure 116. The significant leak in the original test was sealed after the heating operation, even though the pleat separations form as the filter is pressurized with air flow as seen in Figures 113 and 115 or the pleat separations disappear with no air flow as seen in Figure 114. The penetration curve of the dried P-SC-1 filter at 58 inches WC and 1200 cfm in Figure 116 looks similar to the un-dried P-SC-3 filter at 50 inches WC and 1200 cfm in Figure 113. Thus one can infer that the filter drying did not alter the structure of the particle deposit as measured with DOP penetration.

Porvair Filter P-SC-3 Test Results

A second filter, P-SC-3, was tested in the same fashion as the previous P-SC-1 filter. Figure 117 shows the initial DOP penetration measurements at 2,000, 400, and 100 cfm air flow.

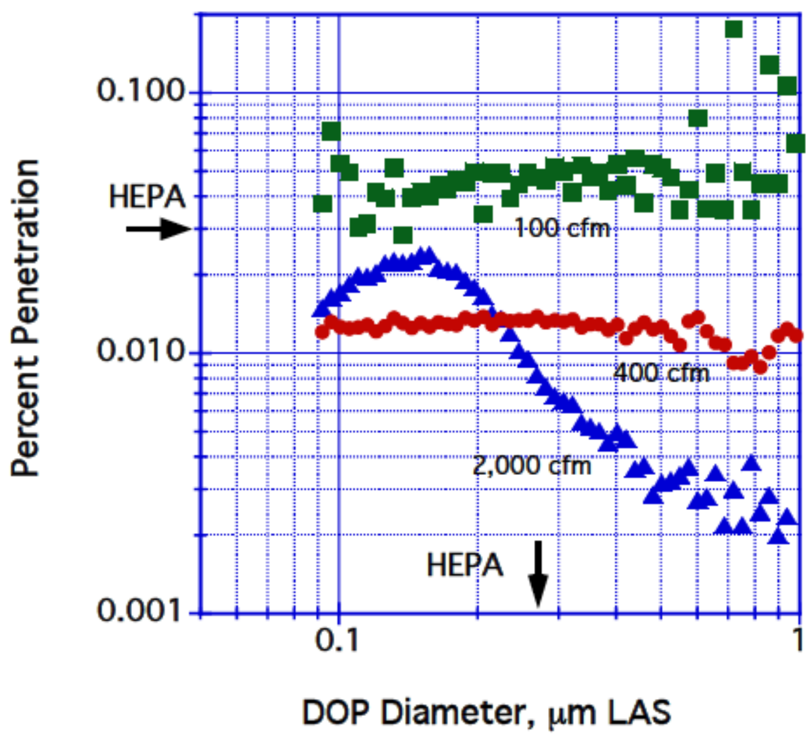

Figure 117. Percent penetration for clean Porvair P-SC-03 filter is 0.0085% at 2,000 cfm and 0.013% at 400 cfm. There are significant leaks as seen by the increased penetration at 400 cfm and by the flat penetration vs diameter profile. Also note that the penetration at 100 cfm exceeds the HEPA limit at 0.03%, but the ASME AG-1 Code only considers 100% and 20% flows.

Figure 117 shows the filter passes the required DOP penetration at 2,000 cfm and 400 cfm and therefore meets the requirements of the ASME AG-1 Code. However, the penetration at 100 cfm is 0.045% at 0.27 microns. The filter has a significant leak.

Figure 118 shows the same data from Figure 117 re-plotted on a linear penetration scale. The best fit log-normal curve through the 2,000 cfm data shows a poor fit due to the filter leakage, especially for large particle sizes where leaks are especially apparent.

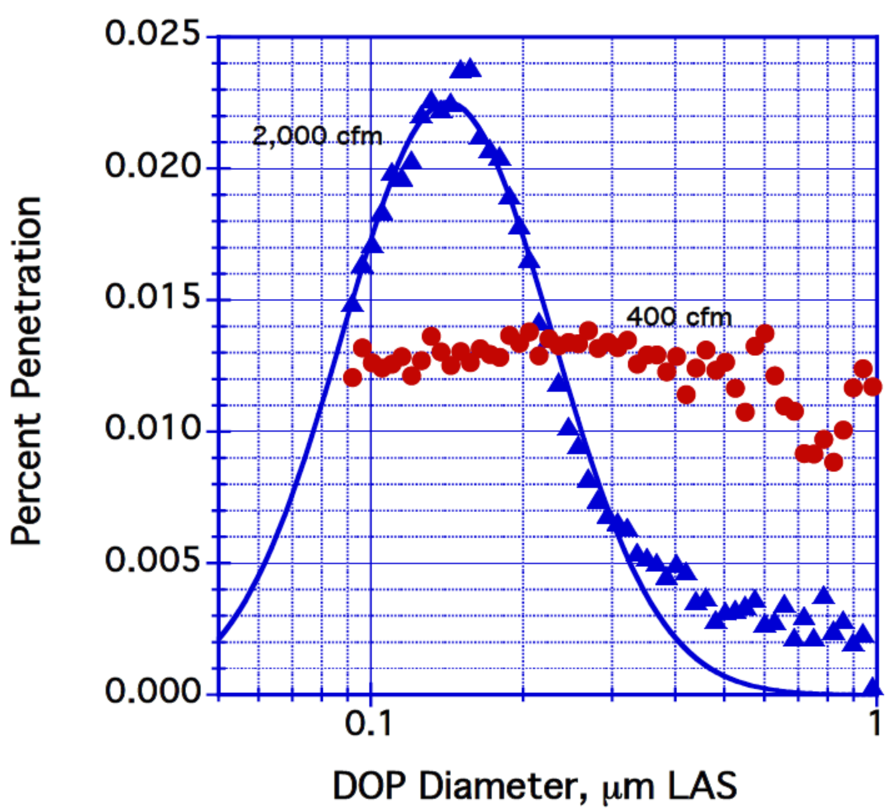

Figure 118. Percent penetration of P-SC-3 filter versus DOP diameter taken from Figure 117 and plotted on a linear penetration scale is 0.0084% at 2,000 cfm and 0.013% at 400 cfm at 0.3 μm DOP (0.27 μm LAS). The curve represents the best fit log-normal curve given by Equation 10 using data less than 0.4 μm. The data for 100 cfm is off the scale at values greater than 0.03%.

After the initial DOP penetration test, the filter was subjected to the rough handling test. One of the end-cap retaining straps had broken loose from the end-cap as seen in Figure 109.

Figure 119. Filter P-SC-3 suffered a broken strap during the rough handling test. MSU continued with the remainder of the tests despite the structural failure. Porvair improved the strap fastening method in subsequent filters, and the problem never occurred again.

The filter was tested for DOP penetration at 2,000 cfm and at 1,200 cfm following the rough handling test as required by ASME AG-1 Code to verify the filter still passed the DOP test at 0.3 microns. Figure 120 shows the percent penetration along with the best fit log-normal Equation 10. The filter easily passed the DOP penetration test where the DOP penetration at 0.3 μm DOP must be less than 0.03%.

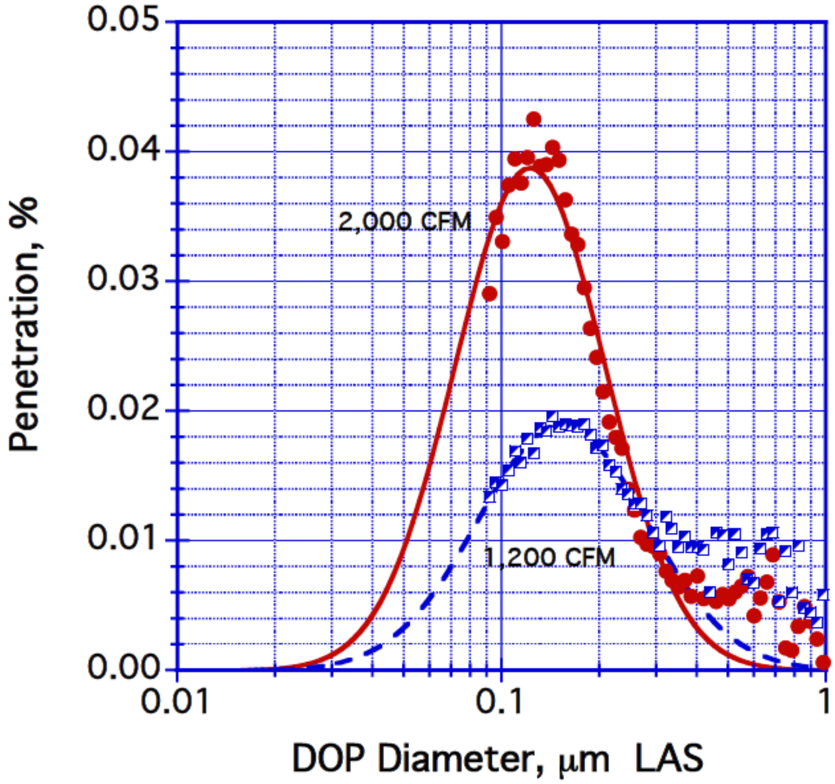

Figure 120. DOP percent penetration at 2,000 cfm and 1,200 cfm of P-SC-3 filter following the rough handling test. The filter passed the required penetration limit of 0.03% at 0.3 µm DOP (0.27 mm with LAS) . The additional test at 1,200 cfm was performed to have an initial penetration prior to commencing the loading of $Al(OH)_3$ powder at 1,200 cfm.

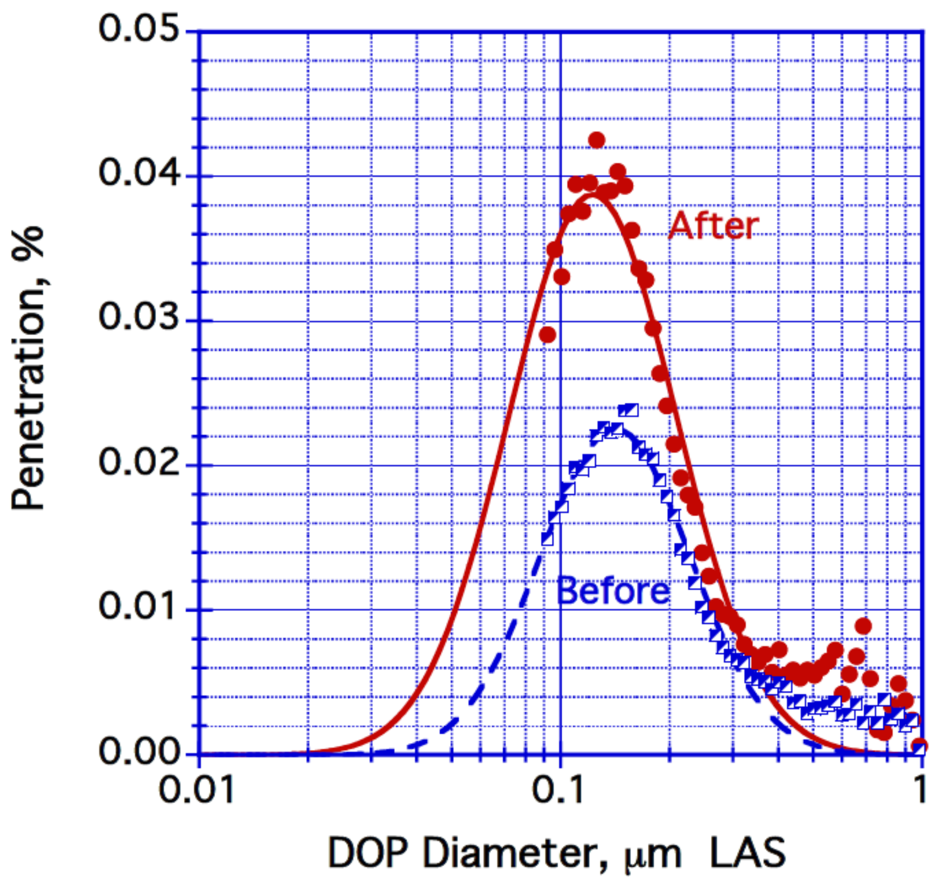

Figure 121. Penetration % of P-SC-3 filter at 2,000 cfm before and after the rough handling test. The before data is taken from Figure 118 and after data from Figure 120. The curves represent the best fit log-normal Equation 10.

Figure 121 shows that the rough handling had created a small leak in the filter as seen by the increased penetration after the test. However, the filter penetration for 0.3 µm DOP (0.27 µm with the LAS) had only increased from 0.0084% to 0.011% and therefore passed the ASME AG-1 requirement of less than 0.03% penetration.

The P-SC-3 filter was then loaded with $Al(OH)_3$ powder at 1,200 cfm and 166°F and 50% relative humidity in the similar fashion as the test on the previous filter, P-SC-1. Figure 122 shows the increasing pressure drop on filter during the particle loading.

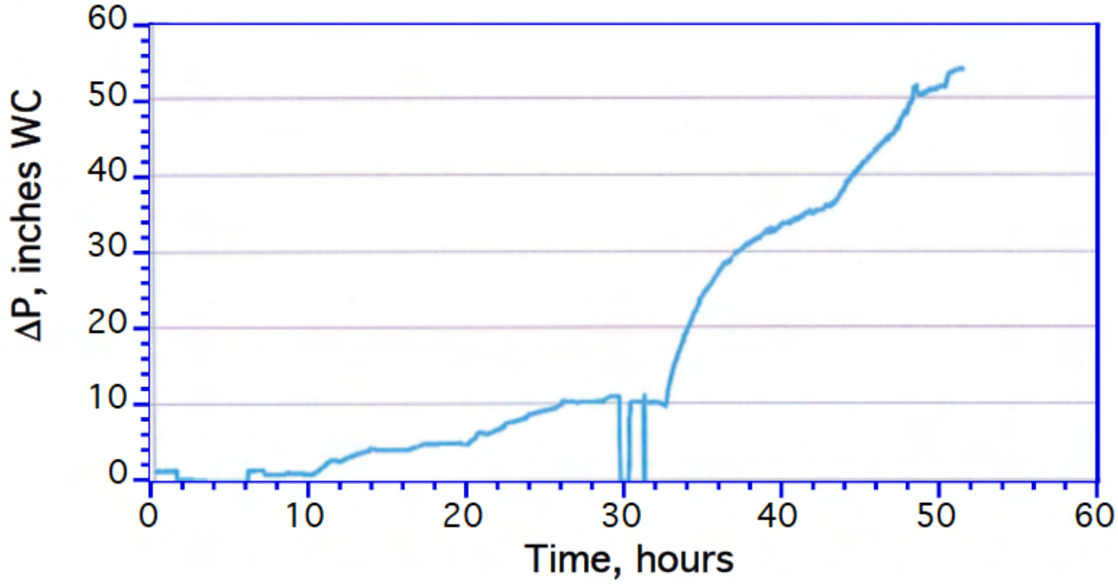

Figure 122. Loading of P-SC-3 filter at 1,200 cfm with $Al(OH)_3$ powder at 166°F and 50% RH. The 0 pressure drops represent the time the test stand was shut down to replace isokinetic filters and to weigh the test filter. The corresponding curve for ΔP versus mass deposit is shown in Figure 111.

Filter penetration measurements using DOP and $Al(OH)_3$ aerosols were made when the filter pressure drop reached 4, 10 and 50 inches WC. The temperature and relative humidity were returned to ambient conditions during the penetration measurements. However, the challenge concentration of the $Al(OH)_3$ was far too low for any meaningful penetration calculations, and the data was not reported. The DOP challenge concentration was also too low in some of the tests and that data is also not reported here. The resulting DOP penetration at 1,200 cfm for the three valid tests for the clean filter at 0.76 inches WC and when the filter reached 10.6 and 50 inches WC are shown in Figure 123.

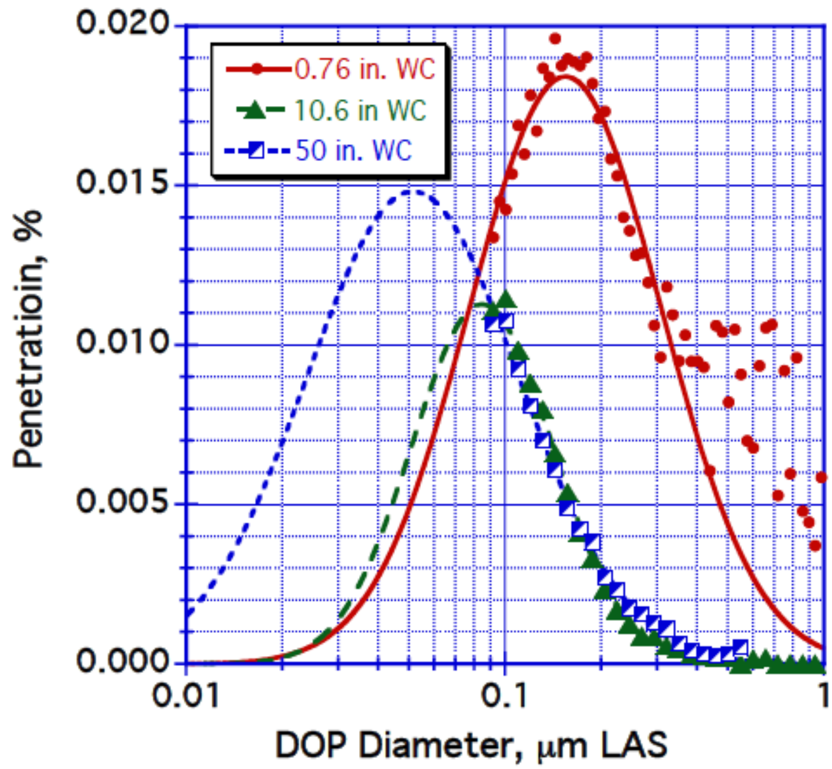

Figure 123. Percent penetration of DOP aerosols at 1200 cfm as a function of DOP diameter for P-SC-3 filter loaded with $Al(OH)_3$ powder at increasing loading as measured by the filter DP. The 10.6 inch WC data was generated after the filter was removed and re-installed in the housing. The curves represent best fit log-normal curves; and the extrapolations in the small size region are not reliable, especially the curves at 10.6 in. WC and 50 in. WC. The 4 inch loading data had insufficient DOP challenge concentration for meaningful measurements. The final penetration at 0.27 µm LAS was 0.0014%

Comparing the DOP penetration curves for the P-SC-3 filter in Figure 123 with those in Figure 112 for the P-SC-1 filter show similarities and differences. Both filters have approximately the same initial DOP penetration and show decreasing penetration with increasing particle deposits as the filter loads to 10 inches. The curves in Figure 112 have increased scatter due to the low DOP challenge concentration while the curves in Figure123 has little scatter due to sufficient DOP challenge concentration. Another difference is that the P-SC-1 filter in Figure 112 at 58 inches WC has an increased penetration due to a significant leak, although the filter still passes the 0.03% DOP requirement. In contrast, the P-SC-3 filter in Figure 123 has only a small leak since the DOP penetration was expected to be lower than the DOP penetration for the 10 inch curve. Theory and previous experiments predict the penetration at 50 inches would be much less than the penetration at 10 inches. A final difference in the penetration curves in Figures 112 and 123, is that there were no DOP penetration measurements after the P-SC-3 filter was dried at 248°F for 4 hours.

The filter penetration data generated by MSU is presented in both graphical form as shown in Figure 123 and in numerical tables of penetration at 0.3 microns DOP as measured by the LAS. The MSU computation of the penetration numbers consists of taking the average of three size bins centered about 0.3 microns. For the LAS, the mid points of the three bins are 0.294, 0.308 and 0.336 microns for deriving the penetration at 0.300 microns when using the full LAS scale to 7.5 microns.

A potential problem with the 3 point average can occur with increased scatter in the data. In that case, a curve fitted through a range of sizes containing many points about a mid-point would yield a better average as illustrated in Figure 104. The DOP penetration using the two methods were computed and tabulated in Table 12. For the P-SC-3 filter penetration data, Table 12 shows excellent agreement between the two methods, with only the 10 in. loading after weighing showing a small difference.

Table 12. Comparison of percent penetration for 0.27 μm and 0.30 μm DOP aerosols measured with the TSI Laser Aerosol Spectrometer (LAS) using a curve fit and the MSU 3 point average centered on 0.27 μm or 0.30 μm for the tests on filter P-SC-3.

Filter Test	Penetration % from Curve fit		Penetration % from MSU 3 point average	
	0.27 μm	0.30 μm	0.27 μm	0.30 μm
Initial 2000 cfm	0.0084	0.0066	0.0084	0.0066
Initial 400 cfm	0.013	0.013	0.013	0.013
Inititial 100 cfm	Low conc.	Low conc.	Low conc.	Low conc.
Repeat Initial 100 cfm	0.049	0.049	0.048	0.048
Post RH 2000 cfm	0.011	0.0089	0.011	0.0088
Post RH 1200 cfm	0.012	0.011	0.012	0.011
4 in. loading	Low conc.	Low conc.	Low conc.	Low conc.
10 in loading before weighing	Low conc.	Low conc.	Low conc.	Low conc.
10 in. loading after weighing	0.0010	0.00078	0.0010	0.00071
50 in. loading	0.0015	0.0012	0.0015	0.0011

Another issue with reporting the penetration of 0.3 μm DOP particles using the LAS is the small shift in particle size introduced by calibrating the LAS with polystyrene latex (PSL) instead of with DOP. This industry practice results in a shift in the LAS size from 0.30 μm to 0.27 μm as shown in Figures 37 and 104. Table 12 shows excellent agreement between the penetration values obtained from the fitted curves and from the three point average centered about 0.27 μm. Although the reported MSU penetration data is based on the three point average centered on the 0.30 μm LAS measurements, the difference between the DOP penetration at 0.27 μm and 0.30 mm is small and is only important for filters with penetration close to the limit 0.03% .

Photographs were taken of the P-SC-3 filter interior (upstream side) at the end of the $Al(OH)_3$ loading and while the filter was still subjected to 50 inches WC of differential pressure and are shown in Figure 124.

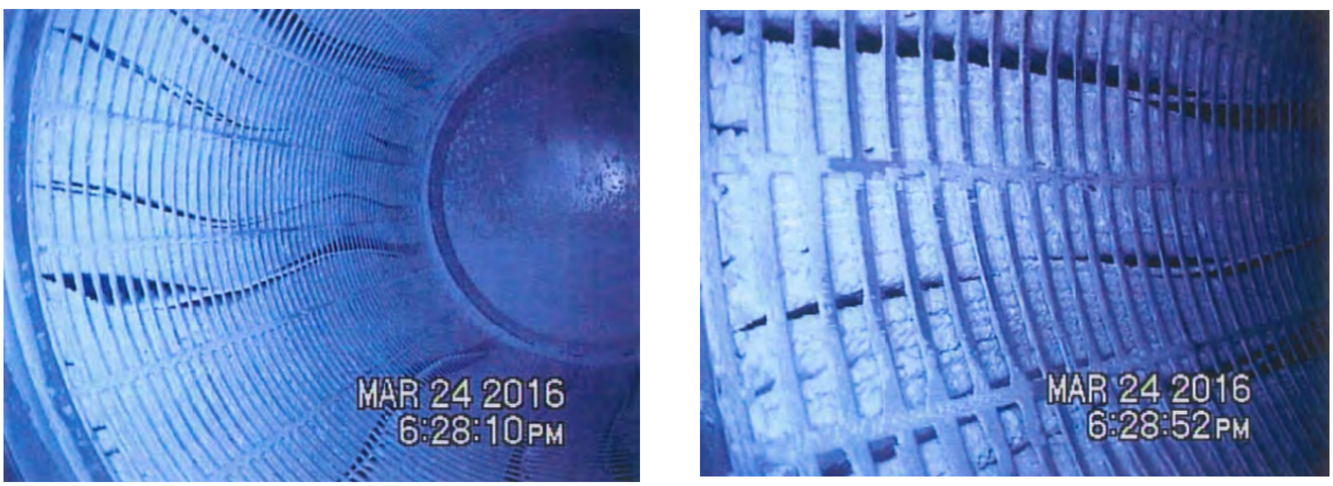

Figure 124. Photographs of the interior of the P-SC-3 filter after the end of the $Al(OH)_3$ powder loading while the filter is still subjected to 50 inches WC of differential pressure. No damage was observed on the exit side of the filter.

Figure 124 shows that large separations have formed between some inside pleats under the high temperature (166°F) and high moisture conditions (50% RH). These pleat separations would suggest a serious damage to the filter and high DOP penetration. However, the DOP penetration curves in Figure 123 and the penetration values in Table 12 show only a small increase in the penetration at 0.3 μm DOP.

The filter was then removed from the test system, weighed and then dried for 4 hours at 248°F and reweighed. No additional post-test penetrations were made as done with the P-SC-1 filter. However, the interior of the filter was photographed again.

Figure 125 (A) shows that the pleat separations seen in Figure 124 are no longer visible. The close-up of the deposits in Figure 125 (B) show cracks that were the likely locations of the pleat separations seen in Figure 124. The pleat separations from Figure 124 where the filter was under 50 inches WC of differential pressure have closed in Figure 125 when the filter was removed from the test housing. The ability of the filter to withstand such drastic pleat deformation and return to its original form is a testament to the strength of the reinforced Lydall medium 3398-L2W.

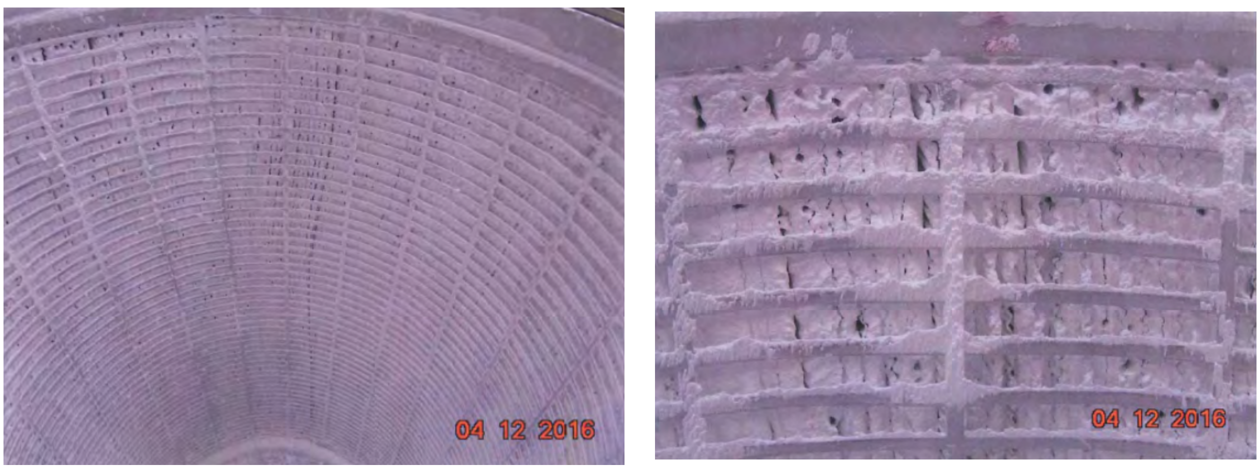

(A) (B)

Figure 125. Photograph (A) of the interior of the P-SC-3 filter after removal from the test system and (B) a close-up showing the deposits of $Al(OH)_3$ powder.

Based on the test results from the two Porvair filters, P-SC-1 and P-SC-3, the pre-qualification phase of the filter development project was declared a success and is summarized in Table 13. Both filters had an initial pressure drop of less than 1.3 inches WC at 2,000 cfm (Figure 107), P-SC-1 had an initial DOP penetration of 0.009% at 2,000 cfm and 0.006% at 400 cfm (Figure 106), and P-SC-3 had initial DOP penetration of 0.0084% at 2,000 cfm and 0.013% at 400 cfm (Figure 117). Also both filters had particle loading capacities of 4.7 pounds of $Al(OH)_3$ powder at 10 inches DP when operated at 1,200 cfm. This loading also exceeded the goal of 1.8 pounds (830 g) of 2.5 micron Arizona Road Dust. Finally, both filters were subjected to particle loading up to 50 inches WC at 166°F and 50% RH and passed the HEPA filter DOP penetration: the penetration at 0.27 μm LAS was 0.03% and 0.0013% for the P-SC-1 and P-SC-3 filters respectively.

Table 13. Pre-qualification efficiency, particle loading, and rough handling tests on Porvair SC filters

Filter	DP at 2000 cfm, inches WC	Initial DOP Pen%			Loading with Al(OH)3				
					Flow at loading cfm	at 10 in		at 50 in	
		2000 cfm	400 cfm	100 cfm		Mass, lb	DOP Pen %	Mass lb	DOP Pen%
P-SC-1	1.27	0.009	0.006	0.006	1070	4.7	<0.001	9.0	0.03
	after rough handling	0.012							
P-SC-3	1.27	0.0084	0.013	0.05	1200	4.7	0.0010	11.0	0.0013
	After rough handling	0.011							

Phase II Tests: Qualification of the Povair SC and RC Filters

With the successful demonstration of the prototype filters, Porvair fabricated SC and RC filters for submission to the US Army test facility for the efficiency, resistance to air flow and resistance to pressure tests; to the Underwriter's Laboratory for the spot flame test and resistance to temperature test; and to Mississippi State University for the efficiency, resistance to pressure and rough handling test. Porvair also submitted the Lydall 3398-L2W medium to the US Army test facility for qualification. These tests are prescribed by the ASME AG-1 Code and are required by the WTP. In addition, MSU performed particle loading tests specific for WTP requirements using acetylene soot (oxygen starved flame in Figure 46), AlOH)$_3$ powder (SpaceRite S-3 from J.M. Huber Corp), and Ultra-fine Arizona Road Dust (A1 Ultrafine from Powder Technology Inc) at 177°F and 40% relative humidity up to 50 inches WC as a WTP requirement .

When the filters to be qualified first arrived at MSU for testing they were inspected for quality per ASME FK-5000, plus additional parameters of the filter were measured or estimated and are tabulated in Table 14. The filters were then tested for resistance to airflow (FK-5110), test aerosol particle penetration (FK-5120), resistance to rough handling (FK-5130), and WTP specific particle loading tests.

Table 14. Estimated Parameters of q Porvair filters* Used for Qualification

Filter Type	Filter ID	Pack ID, in.	Sep. height in.	Pleat* depth, in.	Effective area, ft2	No. of pleats
Safe change	12784-1	13.45	0.0125	3.26	344	338
	12784-2	13.41	0.016	3.35	342	325
	12784-3	13.46	0.0095	3.25	329	326
	12784-4	13.09	0.0375	3.57	364	329
	12784-5	13.15	0.023	3.55	346	310
	12784-6	13.1	0.022	3.57	369	329
	13109-2	12.7	---	3.43	346	319
	13109-1	12.85	0.0225	3.68	359	313
	12784-1	13.45	0.0125	3.26	344	338
Remote change	13554-2	12.29	0.0195	3.3	297	290
	13554-3	12.37	0.0185	3.22	309	301
	13554-4	12.37	0.0135	3.24	318	306
	13554-5	12.35	0.0135	3.24	318	306
	13554-6	12.38	0.0245	3.23	308	297
	13554-7	11.95	0.0275	3.43	324	291

*Medium is reinforced glass fiber, Lydall 3398-L2W with no additional screens.

Resistance to Airflow at MSU and the US Army: AG-1 FK-5110

Tables 15 and 16 show the reported test results from MSU and the US Army test facility. Based on the US Army results, the Porvair SC filter meets the AG-1 Section FK-5110 pressure drop requirement of 1.3 inches WC, but the Porvair RC filter does not since the measured pressure drop was 1.92 inches WC. To use the Porvair RC filter in the WTP, Bechtel had to prepare an exception to the WTP safety documents

Table 15. Reported DP Values for Porvair Safe Change Filter

MSU Filter No.	MSU ΔP in. WC at 2000 cfm[1]	Army Filter No.	Army ΔP in. WC at 2000 cfm[2]
12784-1	1.08		
12784-2	1.09		
12784-3	1.20	12719-1	1.25
12784-4	1.16	12719-2	1.23
12784-5	1.22	12719-3	1.22
12784-6	1.20	12719-4	1.27
13109-2	1.13	Avg	1.243
13109-1	1.20	Std Dev	0.022
Avg	1.160		
Std. Dev.	0.054		

[1]The tare DP (0.900 inches WC) is based on the old MSU tare data.

Table 16. Reported DP Values for Remote Change Filter

MSU Filter No.	MSU DP in WC at 2000 cfm	MSU DP in WC at 2500 cfm[1]	MSU DP in WC at 3000 cfm[1]	Army Filter No.[2]	Army DP at 2000 cfm[2]
13554-2	2.64	3.81	5.05	13682-7	1.84
13554-3	2.72	3.94	5.25	13683-1	1.94
13554-4	2.77	3.74	4.88	13682-6	1.94
13554-5	2.60	3.72	4.95	13683-2	1.94
13554-6	2.64	3.81	5.05	Avg	1.915
13554-7	2.68	3.86	5.15	Std Dev	0.050
Avg	2.675	3.813	5.055		
Std. Dev.	0.062	0.080	0.133		

The safe change filter ΔP measurements from MSU and the US Army in Table 15 show reasonable agreement. The slightly lower ΔP value for MSU (6%) is primarily due to the slightly smaller opening in the MSU filter housing compared to the opening of the US Army filter housing. The smaller opening in the MSU housing creates a larger ΔP tare value that is subtracted from and lowers the experimental filter measurement.

However, there is a large difference in ΔP values for the remote change HEPA filters seen in Table 16. The much larger ΔP value for MSU (39.6%) is primarily due to the much larger opening in the MSU filter housing compared to the opening of the US Army filter housing. The US Army has selected the correct housing orifice for qualifying the Porvair radial flow HEPA filter. In contrast, the MSU orifice was selected to duplicate the orifice in the WTP remote change housing without regard to The larger opening in the MSU housing creates a smaller ΔP tare value that is subtracted from the experimental filter measurement and creates a larger filter DP. In addition, both the US Army and MSU include the additional resistance of the grab ring in the RC filter as part of the filter. This grab ring acts as an orifice to increase the filter pressure drop and make the curve of pressure drop versus air flow non-linear.

Analysis of Pressure Drop For Different Applications

The pressure drop associated with the radial flow HEPA filters differs significantly from the standard axial flow HEPA filters. In contrast with the axial flow HEPA filter, which has only one ΔP for all applications because the housing tare is negligible, the radial flow HEPA filter can have three different ΔP values with different tare values depending on the application: (1) AG-1 qualification, (2) WTP operation, and (3) filter pack DP for theoretical and design analysis. The WTP pressure drop is the reported MSU pressure drop plus the tare reading from the MSU housing. Each of the applications have a corresponding housing tare ΔP that either requires an experimental measurement or theoretical computation. Since only one housing tare is measured, the remaining housing tares can be computed using the equation for orifice flow. The experimental filter ΔP measurements are adjusted using these multiple tare values.

The critical dimensions for the housing inlets for the safe change and remote change filters at the US Army and MSU test facilities are shown in Table 17. These values represent the configuration of the filter housing when measuring the tare pressure drop of the filter housing without a filter installed. The tare pressure drop is then subtracted from the pressure drop measurements with a filter installed in the housing to compute the pressure drop of the filter. The lack of repeated tare measurements was a source of error in the filter pressure drop measurements for the radial-flow HEPA filters (Bergman, 2017).

Table 17. Dimensions of orifice size and housing inlet for safe change and remote change filters.

Filter Type	Filter Inlet Diameter, inches for US Army	Housing Knife Edge Diameter, inches for MSU
Safe-change	13.6	13.0
Remote-change	12.0	20.1
Chamber dividing plate	45.9” x 46.3”	34” x 56.8”
Chamber hydraulic diameter	46.1”	42.5”

Table 18. Dimensions of filter housing openings for the three applications and for the filter pack.

Application	Safe Change Housing opening, inches	Remote Change Housing opening, inches
AG-1 compliance-Goal	13.4[1]	12.3[2]
AG-1 compliance US Army	13.6[1]	12.0[2]
WTP operations and MSU	13.0	20.1
Filter pack DP measurement	13.0	11.0

[1] Assumes the gel-seal ring inside diameter of 13” is part of the filter pressure drop.
[2] Assumes the grab ring inside diameter of 11” is part of the filter pressure drop.

Although not explicitly stated in the AG-1 Code or previous publications, the intent of the AG-1 DP standard is to measure the ΔP of the filter pack. For example, the encapsulated, axial flow, FK HEPA filters with nipples on the inlet and exhaust, does not have the ΔP measured with the nipples included (Arndt, 2005; Bergman et al, 2005). The nipples are removed prior to ΔP qualification measurement. In a similar fashion, the radial flow HEPA filter should not include the restrictive annular inlet when measuring the filter DP. To comply with the AG-1 Code, the filter housing should have an opening that is the same dimension as the filter pack ID opening.

However, the presence of the gel-seal ring and filter grab ring interferes with a direct interpretation of what constitutes the filter pack. Table 18 shows the safe change filter has a radial flow filter pack with inside diameter of 13.4 inches. The US Army selected a 13.6 inches diameter, which corresponds to the diameter of the knife edge of the filter housing. Although the MSU housing also has the knife edge between 13.6-13.9 inches, it has a smaller 13.0 inch opening in the housing wall that extends beyond the knife edge to match the WTP housing design. Thus the MSU SC tare allows for a direct determination of the filter pack ΔP. In contrast, the Army tare includes the ΔP of the gel-seal ring of 13.0 inches that extends beyond the filter pack.

In a similar fashion, the US Army used 12.0 inches for the housing orifice for the remote change filter that has a filter pack with an inside diameter of 12.3 inches. However, the grab ring restricts the inlet to 11.0 inches and increases the tare pressure drop of the filter pack. In this case the resulting pressure drop measurement includes the resistance of the grab ring. These Army practices implicitly assume the grab ring and gel-seal ring are part of the filter for AG-1 compliance and result in small deviations in the measured filter pressure drop from that of the filter pack. This assumption is consistent with other AG-1 filter designs where the ΔP due to associated hardware (e.g the metal end plates in mini-pleat V-shaped filters, the metal support brackets in separatorless axial filters) have been considered part of the filter pack.

Note that the US Army dimensions are close (within 0.2-0.3 inches) to the design values for AG-1 compliance in Table 18. The selected 13.6 inches for the safe change filter and the 12.0 inches for the remote change filter differ only slightly from the design values of 13.4 inches and 12.3 inches respectively in Table 18.

The MSU orifice openings for the safe change and the remote change housings are the same as those in the WTP housings. Therefore the experimental pressure drop for the filters measured at MSU will be directly applicable for determining the filter load in the WTP plant and the pressure drop at filter change out.

Figure 126 shows the MSU experimental pressure drop data for the Porvair RC filters.

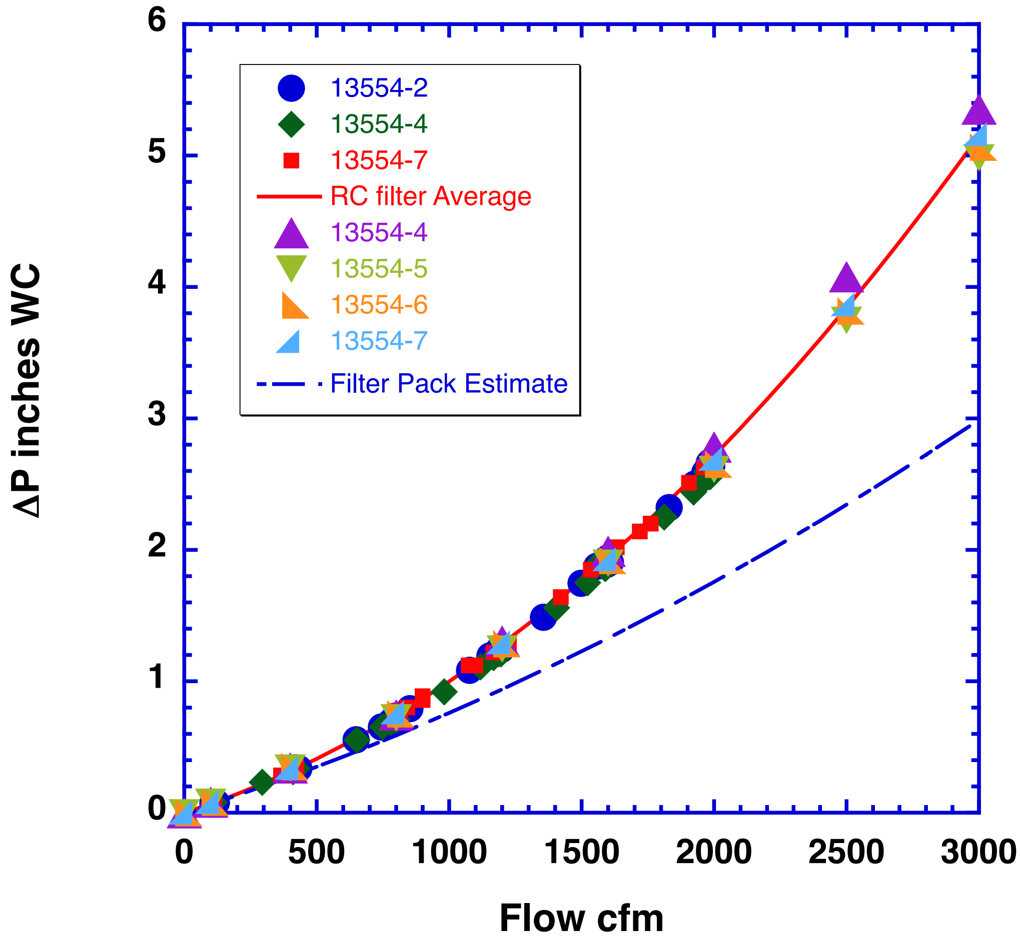

Figure 126. Experimental MSU data on Porvair RC filters with the best fit curve after subtracting the tare for the 20.1 inch orifice (Bergman, 2017). Also shown is the pressure drop of the filter pack.

The best fit curve through the filter data in Figure 126 is given by

$$\Delta P_{RC,MSU,Filt} = 6.408x10^{-4} Q + 3.585x10^{-7} Q^2 \tag{22}$$

A tare value for the 11 inches orifice in the MSU RC housing was computed using the orifice flow equation and data from the 20.1 inch orifice that was used in the MSU testing (Bergman, 2017). Although the preferred solution is to directly measure the pressure drop of the 11 inches orifice in the MSU RC housing, that was not done. Thus, the filter pack estimate is computed by first adding back the tare for the 20.1 inch orifice to the data in Figure 126 to obtain the original pressure drop and then subtracting the tare for the 11.0 inch orifice that represents the filter grab ring. The addition and subtraction of the equations for the 20.1inches orifice and the 11 inches orifice to Equation 22 yielded Equation 23.

$$\Delta P_{RC,Pack} = 6.408x10^{-4}Q + 1.185x10^{-7}Q^2 \tag{23}$$

Equation 23 represents the equation for the filter pack and is independent of the test facility. This equation was used to generate the DP curve for the filter pack in Figure 126.

The data in Figure 126 was converted to pressure drop as a function of velocity in Figure 127 to allow for a comparison with the filter medium, Lydall 3398-L2W.

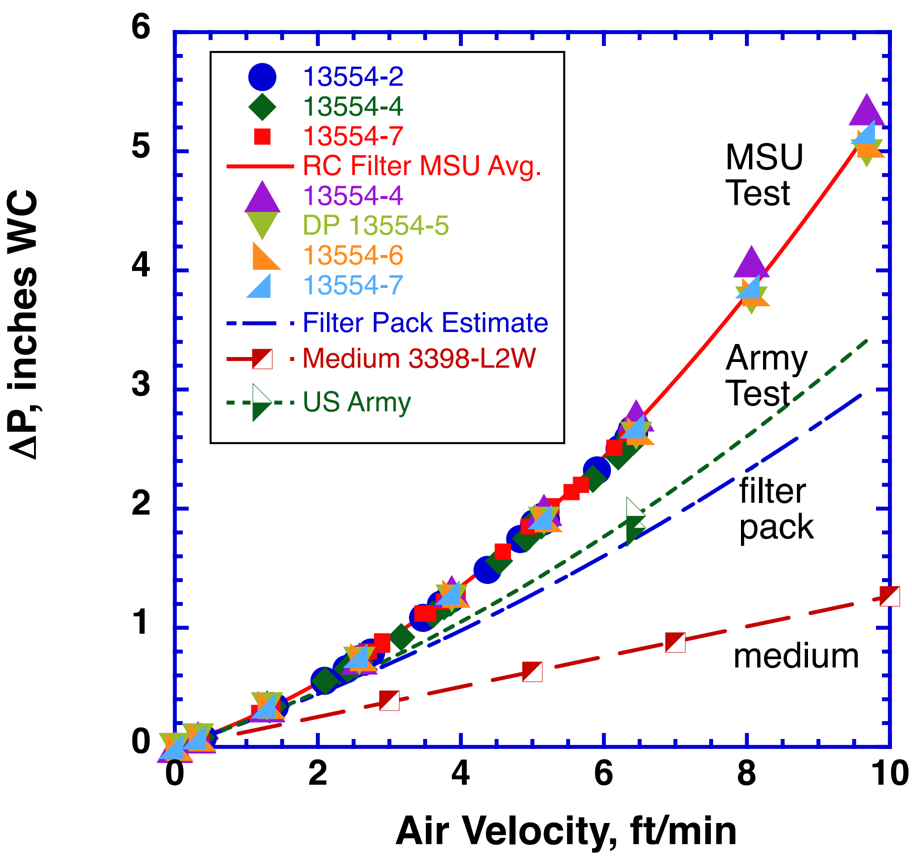

Figure 127. Pressure drop of Porvair RC filters, the filter pack, and the Lydall 3398-L2W medium as a function of medium air velocity . The pressure drop difference between the Army and MSU tests represent the differences in orifices in the two test fixtures (Table 14). The difference between the Army Test and the filter pack represents the added pressure drop of the 11 inches grab ring.

Figure 127 shows that the major fraction of the RC filter pressure drop is due to the 20.1 inches orifice size used in the MSU test fixture and the 11 inches diameter grab ring on the filter. The pressure drop of the RC filter at the WTP will be that shown for the MSU test plus a small (0.2 inches at 2000 cfm) addition due to the tare that is subtracted at MSU.

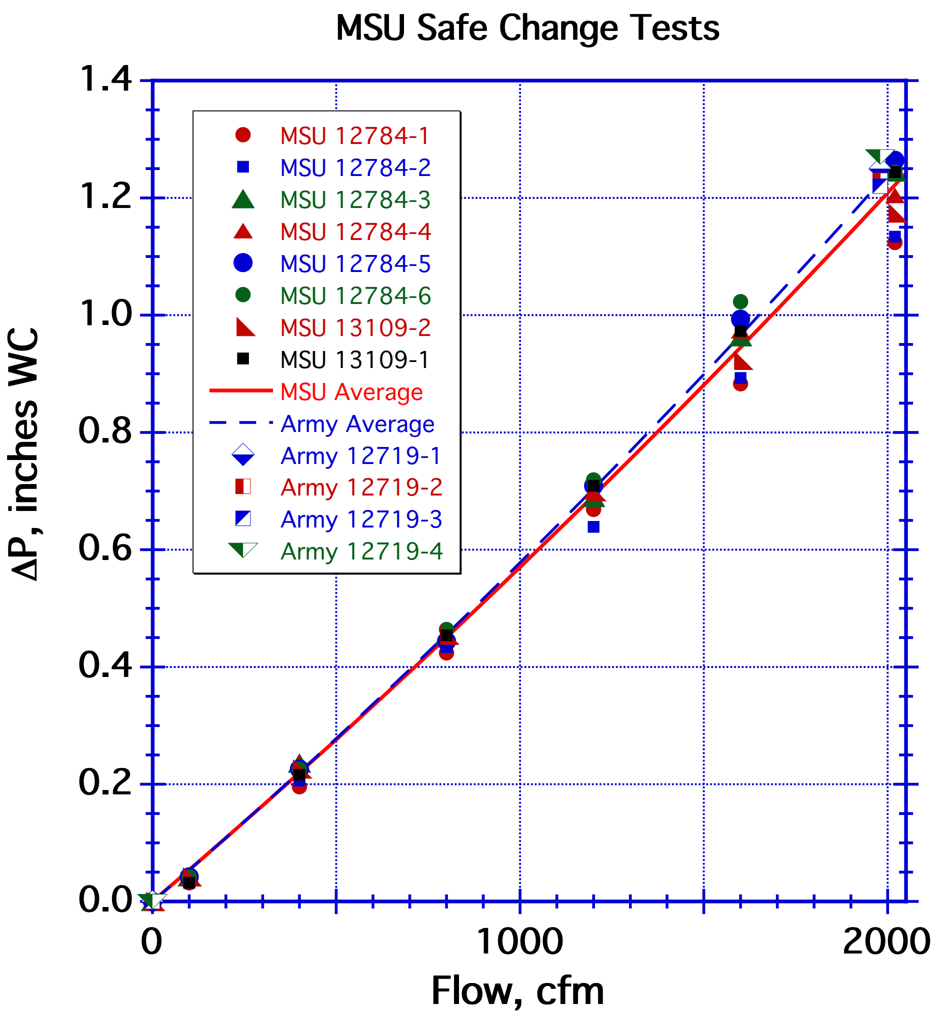

Figure 128. Pressure drop of the Porvair SC filters tested at MSU and at the Army Edgewood facility.

The best fit equation for the MSU pressure drop data in Figure 120 is given by Equation 24 that represents the best fit of the average pressure drop of the different filters.

$$\Delta P_{SC,Pack} = 5.359x10^{-4} Q + 3.418x10^{-8} Q^2 \quad (24)$$

Note that the MSU filter pressure drop is also the pressure drop of the filter pack since the 13.0 inches orifice of the MSU test fixture is the same as required for measuring the filter pack. The average pressure drop for the Army data is slightly higher because the filter orifice used in the Army test is 13.6 inches instead of 13.0 inches as used at MSU.

The data in Figure 128 is re-plotted as pressure drop as a function of air velocity in Figure 129 assuming an area of 310 ft^2.

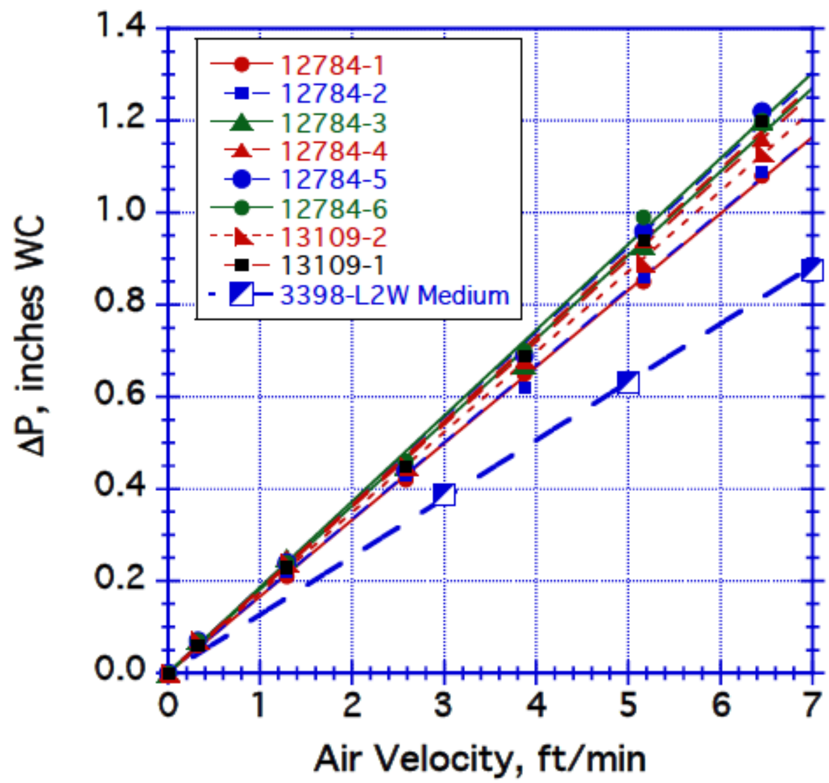

Figure 129. Pressure drop of the Porvair SC filters and the filter medium as a function of medium air velocity. Note that the pressure drops of the SC filters tested at MSU are a direct measure of the filter pack.

The difference between the pressure drop of the SC filter (also filter pack) and the medium at 6.45 ft/min (2,000 cfm) is 0.32 inches. The comparable difference for the RC filters in Figure 128 is 0.47 inches. These values represent the pressure drop of the pleat channel flow in the two filters. From this, one concludes that the RC filter is more tightly packed than the SC filter. This increased pleat packing for the RC filter compared to the SC filter reduces the effective volume of particles that can fill the pleats.

Additional ASME AG-1 Qualification Tests

Bechtel submitted SC and RC filters to the US Army Test facility for resistance to rated airflow, DOP efficiency and resistance to pressure tests. All of the filters passed the required tests except the RC filter failed the resistance to airflow test; the average pressure drop was 1.9 inches W.C. instead of the required 1.3 inches W.C. Bechtel obtained a waiver for this exception. In addition Bechtel submitted SC and RC filters to Underwriters Laboratory to qualify the filters for spot flame test and resistance to temperature. The resistance to rough handling tests were performed at MSU. All filters passed these tests.

Porvair submitted samples of the Lydall 3398-L2W medium to the US Army Test facility to qualify the medium. Not unexpectedly, the medium had approximately 8% combustible material and failed the requirement that HEPA media have less than 7% combustible material since adhesive is used to adhere the glass cloth to both sides of the HEPA medium. Bechtel sought and received an exception to this requirement for use in the WTP. Note that the high-strength medium qualifies in 2022 edition of AG-1 where the new section FM allows the high strength glass fiber media to have up to 10% combustibles.

MSU conducted the required AG-1 qualification tests for (1) resistance to air flow, FK-5110, (2) test aerosol particle penetration and (3) resistance to rough handling, FK-5130 prior to conducting the particle loading tests on each filter. Note that the MSU test sequence is more strenuous than what is specified in AG-1 because the same filter is subjected to both the rough handling and the high pressure particle loading in contrast to the AG-1 test where a separate filter is used for rough handling and the resistance to pressure test. The sequential testing of different challenges on the same filter follows that of the proposed qualification tests for metal filters (Section FI) and high strength filters (Section FM).

Particle Loading Tests to Meet WTP Operational Requirements

MSU conducted a series of particle loading tests on the SC and RC filters using acetylene soot, Al(OH)3 powder, and Arizona Road Dust test aerosols. Although not part of the ASME AG-1 filter qualifications, these particle loading tests were required by WTP to confirm the filters had a minimum loading capacity of 830 grams (1.8 pounds) of 2.5 micron particles. These loading tests were performed at elevated temperature (177°F) and water laden air (40% or 50% RH depending on the intended application.). All of the filters successfully met the loading requirements.

Each of the filter loading tests had 4 accompanying isokinetic flat filter medium samplers as shown in Figure 31 so that the same particle loading on the filter could be compared to particle loading on the filter medium as shown in Figure 32. This simultaneous determination of particle loading in the filter and filter medium enables the loading on the filter medium to be separated from the particle loading in the filter channels where filter design parameters such as pleat depth and pleat width influence the rise in pressure drop with accumulated particle mass. In general, larger diameter particles and tighter pleats result in more rapid increase in pressure drop of the filter compared to the medium. Thus, the tighter packing of pleats for the remote-change HEPA filter compared to the safe-change HEPA filter will result in greater pressure drop for the same mass loading. The filter design effects on particle loading in filters are added to the effects of particle size on particle loading on flat medium. Unfortunately, the analysis of this particle loading data was not completed since the high-strength radial-flow HEPA filers were qualified and this support analysis was not needed. Thus only the particle loading data for the filters were presented here.

Figure 130 shows the experimental measurements of the filter pressure drop as a function of particle mass deposits. The particle mass was determined by measuring the filter mass when clean, when the filter reached a nominal 10 inches WC and at the end of the test, where the pressure drop is a nominal 50 inches. The exact pressure drops at the 10 and 50 inches were measured but were not available for this report and introduces an uncertainty in the data in Figure 130 . The greatest uncertainty is in the nominal 50 inches, where the actual pressure drop may vary from 40 to 55 inches WC.

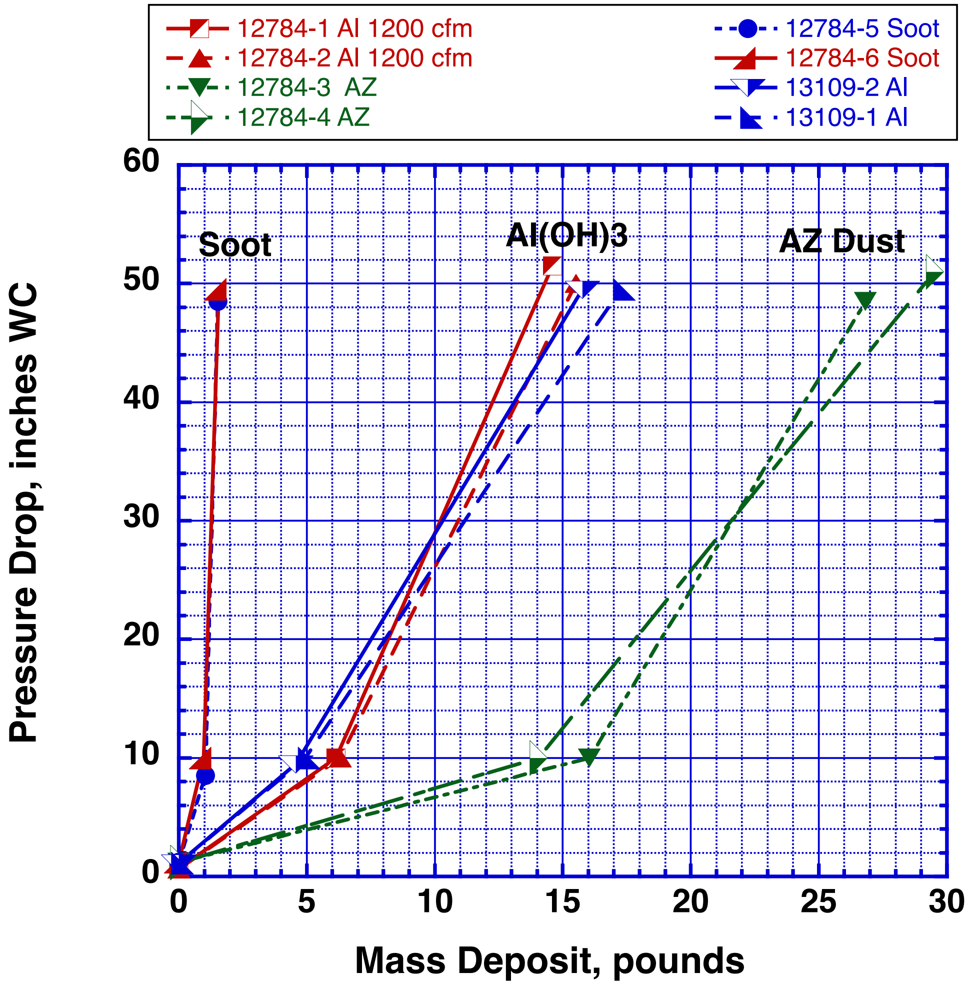

Figure 130. Particle loading on Porvair SC filters at 177°F and 40% RH using acetylene soot, $Al(OH)_3$ powder, and ultra fine Arizona Road Dust at 2,000 cfm. Two of the loading tests with $Al(OH)_3$ powder (12784-1 and 12784-2) were conducted at 1,200 cfm. The approximate mass median diameters for the soot, $Al(OH)_3$ powder, and Arizona Road Dust are 0.5, 1 and 5 microns, respectively. Note, that intermediate pressure drop vs mass data between the indicated data points could be derived from available MSU aerosol measurements but were not included here.

Figure 130 follows the well-established trend of smaller particles causing a more rapid increase in filter pressure drop than larger particles on a mass basis (Bergman, 2006, 2016b; Thomas et al, 2017). However, Figure 130 also shows that the filters loaded with about 15 pounds of $Al(OH)_3$ powder have approximately the same pressure drop (50 inches WC) at both 1,200 cfm and 2,000 cfm. This result is inconsistent with Darcy's Law, which states the pressure drop across a porous medium (e.g. a clean or particle loaded filter) increases linearly with increasing fluid (e.g. air) velocity assuming the filter or particle deposit structure does not change with increasing velocity (e.g. media or deposit compression, filter pleat collapse). A possible explanation is that the particle deposit structure within the pleats when loaded to very high pressure drop (50 inches WC) at 1,200 cfm is less permeable than when loaded at 2,000 cfm. This unusual behavior is not seen at lower particle loading. Figure 130 shows the loading below 10 inches WC follows the expected trend of lower pressure drop at lower flow rates for the same particle loading.

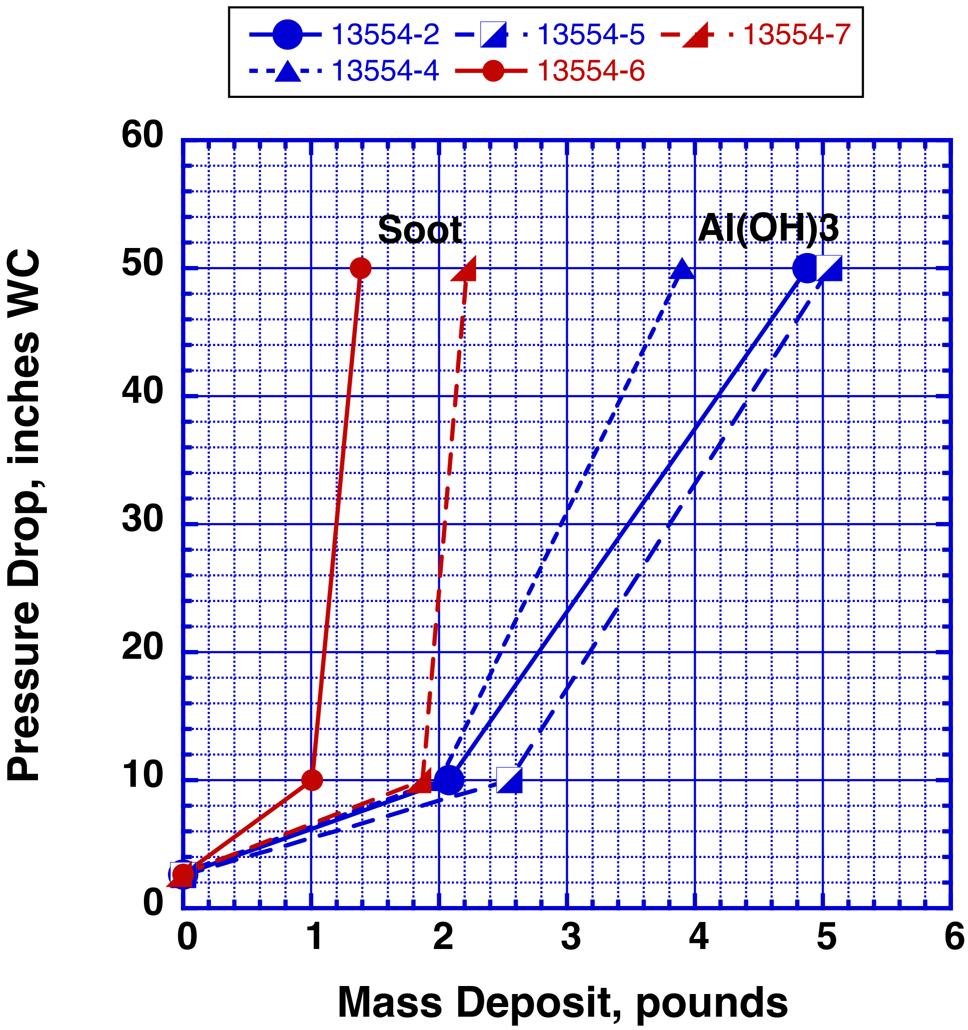

Figure 131. Particle loading on Porvair RC filters at 2,000 cfm and 177°F and 50% RH with soot and $Al(OH)_3$ aerosols on the RC filters. A fourth test using $Al(OH)_3$ powder was conducted, but the mass was not determined. Note, that intermediate pressure drop vs mass data between the indicated data points could be derived from available MSU aerosol measurements but were not included here. The planned test with Arizona Road Dust was dropped in the final Bechtel test plan.

Although the loading test with Arizona Road Dust was included in the original and revised test plan, it was dropped in the final filter qualification plan for RC filters because Bechtel engineers believed the RC filters would not be exposed to ambient dust as would the SC filters and because that would save time and money. However, the inclusion of the Arizona Road Dust test aerosol was to provide a large particle reference point to characterize particle loading in the RC filter as was done with the SC filter. The use of 3 different particle size aerosols enables a reliable prediction of particle loading for different size particles that may be generated in the WTP operations. Three different test particles also enables the relationship between particle size and filter design to be determined as illustrated in Figures 132 and 133 .

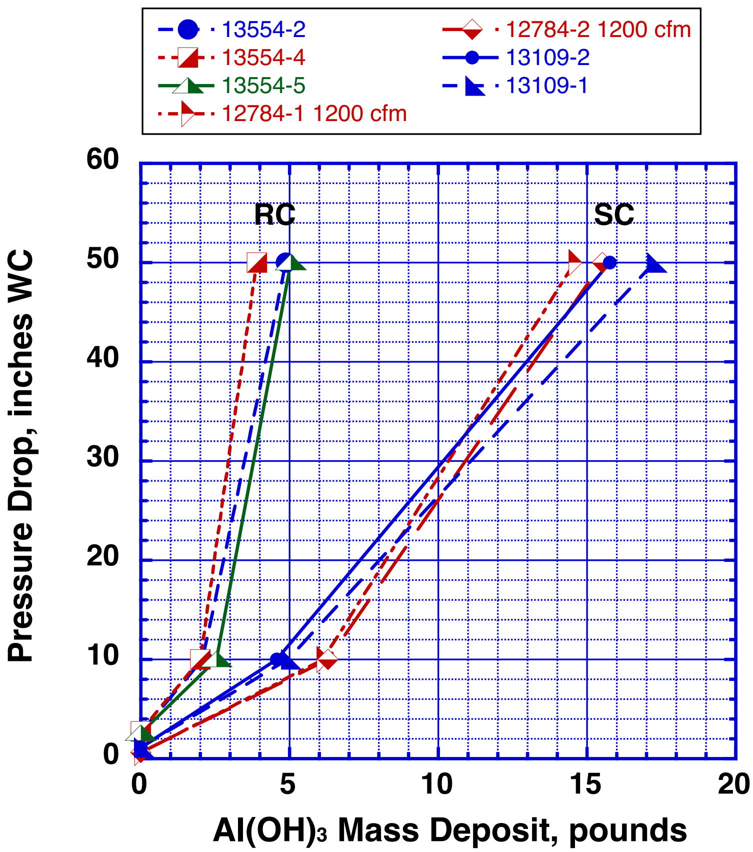

Figure 132. Comparison of Al(OH)3 particle loading on the remote-change (RC) and safe-change (SC) filters.

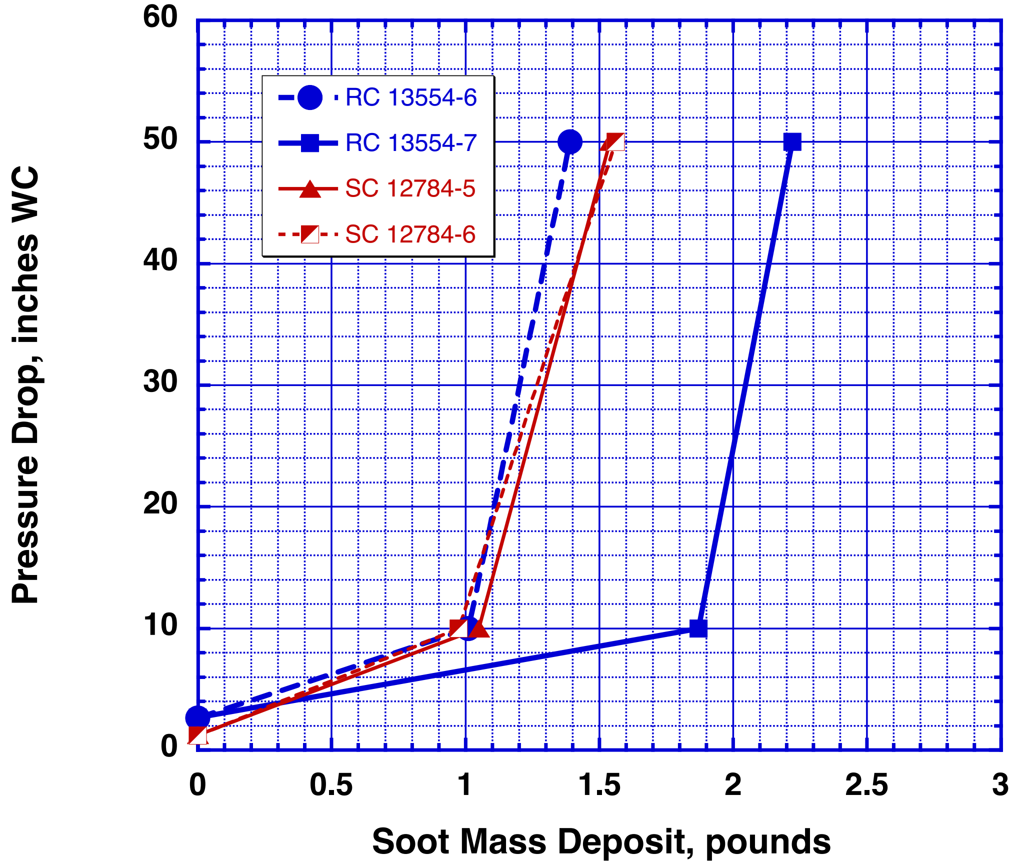

Figure 133. Comparison of soot particle loading on the remote-change (RC) and safe-change (SC) filters. The 13554-7 test is an anomaly believed to be due to larger particle size than the other tests.

Figure 133 shows that the 13554-7 test had substantially greater mass deposits than did the other three tests. This increase in mass deposit is most likely due to larger smoke particles formed in oxygen starved combustion. It is well-known that the mass and size of smoke particles from combustion of fuel increases with decreasing oxygen (Tewarson, 1995). It is also well-known that high concentration of small combustion particles rapidly coagulate into large soot agglomerates (Hinds, 1999). Together, these processes generate larger smoke particles that cause a lower pressure drop increase with the same mass of particles compared to the smaller smoke particles under oxygen rich conditions. Experiments have also shown that smoke from oxygen starved combustion do not plug HEPA filters as rapidly as smoke from oxygen rich combustion (Fenton et al, 1986). Although Fenton et al (1986) did not analyze their particle size measurements, their result agrees with the particle size hypothesis.

It is probable that the acetylene flames shown in Figure 46 were adjusted to richer conditions to increase the soot concentration and consequently also increase the soot size in test 13554-7 . Unfortunately, the size distribution measurements taken of the smoke aerosols were not provided for use in this report to resolve the issue.

The comparison of the RC and SC filter loading of Arizona Road Dust was not possible because the tests with the RC filter were eliminated in the final qualification test plan. Based on available theory (Bergman, 2006, 2008, 2016b), the decrease in particle loading capacity from the SC filter to the RC filter seen in Figure would be significantly greater for the large size Arizona Road Dust than for the smaller size $Al(OH)_3$ powder. Future loading tests with Arizona Road Dust could provide and missing data.

The current theory of filter loading (Bergman, 2008, 2016b) shows that filter loading is the combination of particle loading on the filter medium plus particle build-up in the pleat channels to block the air flow. All of the MSU filter loading tests in the Bechtel project plan (Garcia, 2012b, 2015) were designed to generate this data by measuring both the particle loading (i.e. pressure drop vs particle mass) on the medium using the isokinetic filter samples in Figure 31 plus the particle loading (i.e. pressure drop vs particle mass) on the filter. Figure 32 shows the experimental data of loading with Al(OH)3 powder on the Porvair SC filter. The difference in pressure drop between the isokinetic flat medium and the filter is due to the blockage of the pleat channels. All of the data for the particle loading tests have been generated but is not yet available for analysis.

On a qualitative basis, the trends in Figures 131 and 132 can be explained by the tighter filter pleat packing of the RC filter compared to the SC filter. The tighter pleat packing in the RC filter results in a smaller volume within the pleats where larger particles like Al(OH)3 can restrict the channel flow. Since the pleat channels in the SC filter are larger, the same mass of particles has less channel restriction. The pressure drop due to Al(OH)3 deposits on the filter medium is the same in both SC and RC filters and is small compared to the pleat channel restriction. In contrast to the larger Al(OH)3 powder, the deposit of small acetylene soot particles on the filter medium dominates the total pressure drop and is equal for the SC and RC filers as seen in Figure 133 (Except for the anomaly with filter 13554-7 believed to be due to larger smoke particles) . The small particles have a negligible effect of restricting the channel flow due to the small particle. Thus the particle loading with small diameter acetylene soot dominates media loading and is independent of filter structure (SC vs RC) while the loading with the larger diameter Al(OH)3 dominates pleat channel blockage and is dependent on filter structure (SC vs RC). These trends were seen in axial flow HEPA filters with differences in pleat packing (Dyment, 1997)

SUMMARY AND CONCLUSIONS

Bechtel National Inc (BNI) and its team of filter manufacturers (Kurion and Porvair), high-strength media manufacturer (Lydall), Aerosol Science (AS) and Mississippi State University (MSU) developed and tested a high-strength radial-flow HEPA filter for use in the new Waste Treatment Plant (WTP) in Hanford, Washington. The motivation for this development project was a prior Department of Energy (DOE) sponsored project at MSU that showed that the filter intended for the WTP, an ASME-AG-1 Section FK radial-flow filter, would not perform its intended function (Giffin et al, 2012; Waggoner, 2012; DOE 2013). In seeking a replacement filter, BNI first reviewed the operating conditions expected in the WTP and concluded that some HEPA filters had to withstand a differential pressure up to 225 inches W.C. (in contrast to 10 inches W.C. for standard HEPA filters) for one hour based on the maximum fan vacuum in some facilities.

Since test equipment and facilities for evaluating high-strength HEPA filter media and filters were not available at the start of this project, the test systems and the high-strength HEPA filters were developed concurrently. This concurrent development led to inefficiencies in the filter development since the test systems, especially the flat media test systems, BSTS and VTS, and the high pressure test system, RLPTS, were vital for guiding the filter design.

BNI explored two options for obtaining a high-strength HEPA filter by replacing the standard HEPA medium with either (1) a glass-cloth-reinforced HEPA filter medium from Lydall Inc. (Reudinger et al, 1990; Gilbert et. al., 1992) or (2) with a steel-fiber filter medium (Bergman et al 1991, 1997; Grenwal et al 1993). Both filter designs were constrained to have the radial-flow design to replace a conventional Section FK radial-flow HEPA filter in the existing filter housings. The filter development effort was divided into two phases: phase 1 for developing and successfully demonstrating prototype filters and phase 2 for qualifying the filters according to ASME AG-1 Section FK requirements plus additional requirements established by BNI. For the initial prototype filters, BNI allowed each of the two filter manufacturers to explore innovative designs.

A unique aspect of this filter development project was the reliance on flat medium tests to guide the filter design and to evaluate the filter performance. Three different flat media test systems were used in this study: the Bench Scale Test System (BSTS) to measure the pressure drop of filter media in both liquid and gas system, the Vertical Test Sand (VTS) to measure the efficiency and pressure drop of filter media, and the In-Duct Isokinetic Sampler (IDIS) to measure the particle loading (mass and pressure drop) of filter media. Comparing the pressure drop of the filter and of the filter medium as a function of medium velocity showed the contribution of the pleated filter structure to the total pressure drop. This was done extensively in this study. The BSTS was also used to design the high pressure liquid tester (RLPTS) by providing guidance on the liquid flow required to achieve pressure drops of 225 inches WC. In a similar fashion, a comparison of the filter efficiency of the filter and medium at the same medium velocity shows the degree of aerosol leakage introduced after fabricating the filter and after exposure to adverse conditions such as high pressure or rough handling. However, in this study, the primary use of media efficiency data was to investigate approaches for increasing the low efficiency in the initial prototype filters by increasing filter medium area and by using higher efficiency media. The least used flat media testing data was the particle loading data from the isokinetic samplers. Although all of the data were collected, they were not analyzed to show the effect of filter pleat design on the filter particle loading.

The first prototypes from both filter companies were not successful. Porvair manufactured prototype filters made from high-strength glass-fiber and steel-fiber media using the same design of 1.5 inch pleats and no separators (Tables 7-9). Aerosol Science and Bechtel engineers advised against this initial design due to the extreme overcrowding of the medium, but Porvair was confident it would work. Test results at MSU showed both glass-fiber and steel-fiber filters had very high pressure drops: 9-13 inches WC for the glass-fiber filters and 21-22 inches WC for the steel-fiber filters due to the overcrowding of the filter pleats (Figures 99 and 100). These prototype Porvair filters passed the initial efficiency tests but failed the efficiency test after exposure to high pressure (Table 10) and did not show any structural damage. The low efficiency in the Porvair filters following high pressure exposure were due to leaks as seen by the flat curves of penetration vs DOP diameter (Bergman et al, 1997b), especially at the lower air flow rates (Figures 90 , 94, 98), and were believed to be due to the separation of the sealant bonding the cylinder to the end-caps.

Kurion manufactured two different prototype glass-fiber filters: the prototype 1 filters with a proprietary filter pack design using the one sided reinforced medium (3398-L1W) and a pleat depth of 3 inches and no separators (Table 3) and the prototype 2 filters with a conventional filter pack using the two sided reinforced medium (3398-L2W) and a pleat depth of 3 inches and corrugated aluminum separators (Table 5). The prototype 1 SC filter met the initial efficiency requirement at 2,000 cfm but suffered pleat damage after exposure to 225 inches WC for one hour (Figure 53). The prototype 1 RC filter failed the initial efficiency test but showed no structural damage, presumably due to the tighter pleat packing (Figure 58, Table 4).

After these two failed tests, Kurion abandoned the prototype 1 design and submitted five RC and three SC filters with the prototype 2 design to MSU for evaluation. Most of the filters failed the initial efficiency test because of the insufficient medium that created high medium velocities plus leaks. Figure 42 shows that increasing the medium velocity above the required 5 ft/min significantly increases the DOP penetration. For the prototype 2 filters from Kurion, the medium velocity at 2,000 cfm was 14.2 ft/min (Table 5). At this velocity, the filter medium could barely meet the required penetration of 0.03% (Figure 35), making it unlikely that the filter ccould meet the HEPA penetration requirement. In addition to the high velocity, all of the prototype 2 filters from Kurion showed significant leaks as seen by the high initial DOP penetration and the flat curves of penetration vs DOP diameter. These leaks increased significantly following the exposure to high pressure.

One of the significant findings in the Kurion filter tests was the separation of the bottom end cap of one of the first prototype 2 filters, GFR-RC-002-PRE, filter during the high pressure test at 225 inches WC as seen in Figure 71. This separation occurred even with three metal straps connecting the two end caps together. A post mortem of the failed filter revealed that the urethane sealant had not covered the end plate uniformly and may also be the source of the leaks in the other filters. Kurion increased the urethane bond strength by using more sealant and increasing the bonding surface using a proprietary technique and did not encounter end-plate separation in their remaining filters, although aerosol leakage was still observed with the high DOP penetration and the flat penetration curves.

However, increasing the urethane bond strength is not optimum for high strength HEPA filters, since the bond is subject to weakening due to age and high temperatures. The preferred approach is to have more robust steel support structures for both end caps and for the straps or rods connecting the two end caps. The support straps connecting the two end-caps failed in some tests for both Kurion (Figure 71) and Porvair (Figure 119) and would require a more robust design for consistent performance. Another potentially weak component are the end caps where insufficient stiffness of the end-caps may also contribute to the filter leaks at higher pressures. A deformable end-cap could contribute to breaking the adhesive bond between the end-plate and the filter pack. With a more robust steel support structure, the urethane would function primarily as a sealing agent while the steel hardware would provide the filter strength. In addition, by replacing the urethane sealant with high temperature silicone, the filter would perform much better under high temperature conditions (750°F for 5 minutes) as previously demonstrated for such filters (Gilbert et al, 1992). Pratt (1986) showed the high-strength HEPA filters are not degraded after 10 minutes exposure to 500°C (932 °F). At this temperature, all of the medium binder is burned off, but the filter fiber pad retains it strength due to the glass support cloth. Thus, with a more robust steel support structure and silicone sealant, the high-strength glass fiber HEPA filter could operate under conditions considered for steel HEPA filters or ceramic HEPA filters at much lower costs and lower pressure drop.

Another issue that was addressed during the prototype development phase of the project was the gel-seal failure above 70 inches W.C.. Kurion conducted preliminary studies using test systems similar to what Flanders had used in Figure 13 A, and found that higher strength gels worked; however, the gel effectively became a semi-solid gasket and would require much greater force to seal and would potentially introduce operational problems when installing and removing filters. Although the motivation for continuing the use of gel-seals on high strength HEPA filters was the specific requirement to retrofit HEPA filters in existing filter housings at the WTP, the gel-seal concept is not consistent with a high-strength HEPA filter. A more reliable sealing for high-strength HEPA filters would be high-strength gaskets that are resistant to high temperatures.

Following the unsuccessful prototype tests on the Kurion and Porvair filters, Bechtel reassessed the goals and tasks of the project. The initial prototypes of the reinforced glass fiber HEPA filter failed from one or more of the following: high pressure drop due to overcrowding of the pleats from not using separators, structural failures from using insufficiently strong metal components, and low efficiency from insufficient medium area and from leaks. The Kurion prototype 2 filters had initial leaks which increased following high pressure exposure while the Porvair prototype filters developed leaks following the high pressure exposure. Adding corrugated separators along with sufficient area of the reinforced glass fiber medium corrected two of the three problems, but the prototype filters did not use higher strength metal components and thus were not reliable at 225 inches WC. During the reassessment, Aerosol Science conducted a supplemental study that showed that replacing the reinforced HEPA media with reinforced Ultra Low Penetration Air (ULPA) media would yield HEPA filters that could meet the efficiency requirements with only a small increase in filter pressure drop if filter manufacturers could not incorporate sufficient media area in their filters. Bechtel also reassessed the requirement of 225 inches filter DP to accommodate the full fan pressure during unmitigated WTP operations and found that using standard mitigation strategies enabled safe operations with a maximum filter DP of 50 inches WC.

Bechtel then developed a revised project plan that incorporated the findings from the project reassessment. The revised plan required the HEPA filter to use the high-strength glass HEPA medium with pleats at least 3 inches deep and use corrugated separators, implementing an iterative filter development process with Bechtel selecting the key filter parameters to optimize the filter design, and conducting filter loading with $Al(OH)_3$ powder at two flow rates (1,200 and 2,000 cfm) and three different temperature and relative humidity conditions (100°F and 40% RH, 171°F and 7% RH, and 166°F and 50% RH) to represent the different operating conditions at the WTP. The filter would be loaded to 50 inches WC or to the failure point using the LSTS air flow system in Figure 44 instead of testing at 225 inches WC using the RLPTS in Figure 8. Lowering the maximum pressure drop to 50 inches WC also allowed the filters to continue using the standard gel-seal and the standard ASME AG-1 FK hardware with straps connecting the two end-caps.

Porvair was contracted to fabricate pre-qualification filters based on the new design criteria, but they wanted to use model filters called quadrant packs, which are effectively a slice of the full filter, to experiment with the different filter design parameters (Figure 94, Duvekot et al, 2017). The initial default media was the Lydall 3398-L2W HEPA medium with glass support cloth on both sides of the medium. Porvair demonstrated that a high strength HEPA filter using reinforced

HEPA medium and corrugated separators could meet Bechtel requirements and could be successfully fabricated on the first iteration of the quadrant pack tests.

Although the successful filter design used by Porvair was the standard radial-flow HEPA filter with the Type A filter pack as described in ASME AG-1 Section FK, Porvair used an unusual separator consisting of a sintered wire screen that was corrugated (Amey et al, 2020) instead of the conventional corrugated aluminum separator. The wire screen had to be sintered because the wires in the screen would move during corrugation and not retain its shape. In addition, the pleated screen required conventional hemmed edges on both edges of the screen to prevent loose wires from puncturing the filter medium. Since the unique separator would be much more expensive and would require much longer production times compared to conventional corrugated aluminum separators, AS cautioned against this approach without first demonstrating that conventional aluminum separators would not work. However, since one filter design was already successful, Bechtel did not want to delay the project to explore using the conventional corrugated aluminum separators. The use of conventional aluminum separators would be a logical alternative to the sintered wire screen. Moreover, because the separator height is very small (nominal design height of 0.05 inches in Table 11 and measured heights of 0.01-0.04 inches in Table 14), the separators were not tapered.

Porvair then fabricated several full-scale filters and were tested at MSU. The MSU test results showed the safe-change filters had satisfactory efficiency and pressure drop and also passed the rough handling tests. MSU also conducted particle loading tests at 166°F and 50% RH on the filters and demonstrated the filters had adequate particle loading capacity that exceeded the WTP requirements.

With the successful demonstration of the prototype filters, Porvair fabricated SC and RC filters for submission to the US Army test facility for the efficiency, resistance to air flow and resistance to pressure tests; to the Underwriter's Laboratory for the spot flame test and resistance to temperature test; and to Mississippi State University for the efficiency, resistance to pressure and rough handling test. Porvair also submitted the Lydall 3398-L2W medium to the US Army test facility for qualification. These tests are prescribed by the ASME AG-1 Code and are required by the WTP. In addition, MSU performed particle loading tests specific for WTP requirements using acetylene soot, $Al(OH)_3$ powder, and Ultra-fine Arizona Road Dust at 177°F and 40% relative humidity up to 50 inches WC as a WTP requirement . DOP efficiency tests showed that all of the filters except the safe-change filter 12784-1 (post loading test was 99.60%) was able to meet HEPA efficiency of 99.97% following the loading tests to 50 inches WC.

The pressure drop associated with the radial flow HEPA filter is significantly higher than the standard axial flow HEPA filters since the inlet to the filter acts like a restrictive orifice prior to flowing into the filter pack. Since the common practice for determining the filter pressure drop is to subtract the tare pressure drop of the test housing from the measured total pressure drop, different values are obtained depending on the housing orifice diameter. In contrast with the axial flow HEPA filter, which has only one ΔP for all applications because the housing tare is negligible, the radial flow HEPA filter can have different ΔP values with different tare values depending on the application: AG-1 qualification, WTP operation, and filter pack DP for theoretical and design analysis. The WTP pressure drop is the reported MSU pressure drop plus the tare reading from the MSU housing. Each of the applications have a different corresponding housing tare due to different orifice diameters.

In addition to working with filter manufactures, BNI and AS worked closely with MSU to develop the test facilities and procedures for filter testing that were required for the filter development. BNI and AS provided the general guidance on the design and testing of the full-scale high pressure filter tester based on high viscosity water flow, while MSU developed the detailed design, test procedures and required infrastructure. AS also provided the detailed design and test procedure for dioctyl phthalate (DOP) aerosol filter efficiency measurements for MSU to comply with DOE and AG-1 test standards. Other testing details involving particle loading and aerosol measurements were given in the BNI testing specifications.

A number of project tasks were not completed once the primary objective of qualifying a high-strength HEPA filter was achieved. Some tasks required the analysis of data already collected but not analyzed such as integrating the aerosol measurements from the Pilot Impactor with the SMPS, LAS and APS to yield number size distributions and mass size distributions for characterizing the filter loading tests. Another task just requiring analysis was comparing the particle loading on the filter with particle loading on flat media as obtained with the isokinetic sampler.

Other incomplete tasks required additional experimental work to complete. An unresolved MSU testing issue for full-scale filters in the LSTS was the low DOP challenge concentration that yielded considerable scatter especially for low penetration measurements as seen in Figure 109. However, since the scatter was less significant at the higher penetrations near the HEPA failure (Figures 106, 108 and 112), optimization of the filter efficiency test was low priority.

An incomplete task, that remains important for testing all high-strength HEPA filters that are actively being developed such as the steel fiber filters (AG-1 future Section FI) and ceramic filters (AG-1 future Section FO) as well as the glass fiber filters (AG-1 Section FM) is the high pressure test system (RLPTS). Although the RLPTS (Figures 8 and 9) was successful in testing prototype high strength HEPA filters, the test system has not been optimized for avoiding precipitation of PEG on the filters and the requirement for rinsing and for the prolonged drying time. Decreasing the PEG concentration from the current 50% to a level that avoids significant precipitation would require greater liquid flows and larger pumps to compensate for the decreased viscosity. Another optimization effort would be to reduce the drying time for the wet filters. These optimization efforts could be conducted as part of an active filter test program for all of the high-strength filters being developed.

Although Bechtel and its team successfully developed a radial-flow HEPA filter that can withstand 50 inches WC and be installed in existing WTP housings, the original goal of resistance to 225 inches WC is feasible and would require relatively little effort. The primary cause of the observed filter failure to withstand the 225 inches WC challenge was the insufficient structural strength of the filter hardware (insufficient stiffness of the top and bottom end-caps and weak connecting straps holding the two end-caps together). The filter hardware used in this study was based on the AG-1 Section FK design that was only intended to withstand 10 inches WC. The likely cause of the increased DOP penetration was the breaking of the urethane seal between the filter pack and the end-caps and that allowed for aerosol leakage. By increasing the strength of the end-caps, they would not bend or balloon out under higher pressures. This would allow the urethane seal to function as a seal and not act as a structural support. In addition, the support straps connecting the two end-caps failed in some cases and should have a stronger design. Using stronger hardware support, the filter could potentially survive much higher pressures than 225 inches WC since the strength of the reinforced glass medium is much higher, although failure limits have not been established.

The fire resistance of the high-strength HEPA filter can also be increased significantly by replacing the urethane sealant with a high temperature silicone sealant as was shown by Gilbert et al (1992) for the high-strength axial-flow HEPA filter. This addition would allow the high-strength glass-fiber HEPA filter to operate continuously at 550°F (399°C) as suggested for steel-fiber filters in the draft AG-1 Section FI code. With ceramic sealants, the high-strength glass-fiber HEPA filter could potentially operate continuously at 750°F (399°C). Previous studies on high-strength glass-fiber HEPA filters have shown that these high-strength filters with ceramic sealants can withstand heated air flow at a differential pressure of 30 inches WC at 932°F (500°C) for at least 10 minutes with no structural damage or loss of efficiency (Pratt, 1986).

Thus, with improved structural support, the radial-flow high-strength glass-fiber HEPA could operate at 225 inches WC or even higher. Replacing the urethane sealant with silicone or ceramic sealant could allow the high-strength HEPA filter to operate at 550°F or 750°F respectively. These improvements would allow high-strength glass-fiber HEPA filters to be considered for applications where previously only steel-fiber or ceramic-fiber filters are used. In addition, since the glass fibers have smaller fiber diameters than the steel or ceramic fibers, they have a lower pressure drop at the same efficiency.

REFERENCES

Amey, C., Duvekot, E., Wilkinson, P. and Williams, A., (2020) US Patent 10,864,474 B2, Reinforced Filtration Apparatus.

Anderson,T. and Fergestrom, L. (2000) An offgas system for a low activity waste melter, Proceedings of the 26th Nuclear Air Cleaning and Treatment Conference, Richland, WA, Sept. 11-12, 2000, (www.isnatt.org)

ASME AG-1 (2019), American Society of Mechanical Engineer, Code on Nuclear Air and Gas Treatment, https://www.asme.org/codes-standards/find-codes-standards/ag-1-code-nuclear-air-gas-treatment/2019/drm-enabled-pdf

ASME N-511 (2017) In-Service Testing of Nuclear Air-Treatment, Heating, Ventilating, and Air-Conditioning Systems, https://www.asme.org/codes-standards/find-codes-standards/n511-service-testing-nuclear-air-treatment-heating-ventilating-air-conditioning-systems/2017/drm-enabled-pdf

ASTM-F1471 (2009) Standard test method for air cleaning performance of a high-efficiency particulate air filter system, https://www.astm.org/Standards/F1471.htm

Bao, L., Seki, K., Niinuma, H., Otani, Y., Balgis, R., Ogi, T., Gradon, L., and Okuyama, K., (2016) Verification of slip flow in nanofiber filter media through pressure drop measurement at low-pressure conditions, Separation and Purification Technology, 159, pp. 100-107 https://www.sciencedirect.com/science/article/pii/S1383586615304147?via%3Dihub

Bergman, W. and Biermann, A.(1985) Effect of DOP heterodisperson on HEPA filter penetration measurements, Proceedings of the 18th DOE Nuclear Airborne Waste Management and Air Cleaning Conference, M.W. First, Editor, Baltimore, MD, August 12-16, 1984, CONF-840806, pp 327-347. www.isnatt.org

Bergman, W., Conner, J., Larsen, G., Lopez, R., Turner, C., Violet, C., and Williams, K., (1991) "High efficiency steel filters for nuclear air cleaning" in Proceedings of 21st DOE/NRC Nuclear Air Cleaning Conference, San Diego, CA, August 13-16, 1990, pp. 732-761, NTIS, Springfield, VA, CONF-900813, or NUREG/CP-0116, 1991 (www.isnatt.org)

Bergman, W., Larsen,G., Weber, F., Wilson, P., Lopez, R., Valha, G., Conner, J., Garr, Williams, J.K., Biermann, Wilson, A.K., Moore,P., Gelner, C., Rapchun, D., Simon, K., Turley, J., Frye, L., and Monroe, D., (1993a), "Development and Evaluation of a Cleanable High Efficiency Steel Filter" in Proceedings of the 22nd DOE/NRC Nuclear Air Cleaning Conference, Denver, Co, August 24-27, 1992, UCRL-JC-1099769, January 1993. (available at www.isnatt.org)

Bergman, W., Wilson,K., Larsen, G., Lopez, R., (1993b), "Aerosol Filtration with Steel Fiber Filters" in Advances in Filtration and Separation Technology, Vol 7, Wallace W.F. Leung, Editor, American Filtration Society, Kingwood, Texas, April 1993.

Bergman, W., Larsen, G., Lopez, R., Wilson, K., Simon, K., and Frye, L., (1995) "Preliminary field evaluation of high efficiency steel filters" in Proceedings of the 23rd DOE/NRC Nuclear Air Cleaning and Treatment Conference, Buffalo, N.Y.,July 25-28, 1994, available from NTIS, Springfield, VA, CONF-940738 , pp 195-213, February , 1995 (available at www.isnatt.org)

Bergman, W., (1996), "Requirements for a Cleanable Steel HEPA Filter Derived From a Systems Analysis" Lawrence Livermore National Laboratory Report No. UCRL-ID-125048, June 1996.

Bergman, W., Larsen, G., Lopez, R., Wilson, K., Witherell, C., and McGregor, M., (1997a) "Further Development of the Cleanable Steel HEPA Filter, Cost/Benefit Analysis, and Comparison With Competing Technologies" Proceedings of the 24th DOE/NRC Nuclear Air Cleaning and Treatment Conference, CONF-960715, M.W. First, Ed., NTIS, Springfield, VA, pp. 708-742, August, 1997. (available at www.isnatt.org)

Bergman, W., Wilson, K., Elliott,J., Bettencourt, B., and Slawski, J.W. (1997b) In-place HEPA filter penetration test, Proceedings of the 24th DOE/NRC Nuclear Air Cleaning and Treatment Conference, CONF-960715, M.W. First, Ed., NTIS, Springfield, VA, pp. 649-670, August, 1996. (available at www.isnatt.org)

Bergman, W. (2004) Efficiency of HEPA filters in multi-stage filter systems, Proceedings of the 28th DOE/NRC Nuclear Air Cleaning and Treatment Conference, September 27-29, 2004, Albuquerque, NM. www.isnatt.org

Bergman , W.(2006) HEPA filter particle loading, Proceedings of the 29th Nuclear Air Cleaning and Treatment Conference, Cincinnati, OH, July 17-19, 2006. www.isnatt.org

Bergman, W. (2008), Assessment of 5 ft/min requirement for HEPA filters, Proceedings of the 30th International Nuclear Air Cleaning Conference, Seattle, WA, August 25-27, 2008. www.isnatt.org

Bergman, W. (2014) Recommended HEPA efficiency test system, Bechtel report, October 7, 2014.

Bergman, W. (2015a) Calibration of diluters and coupler in MSU tests on July 27, 2015, Bechtel report, August 23, 2015.

Bergman, W. (2015b) Correction of filter DOP penetration values when LAS is calibrated with PSL, Bechtel report, November 9, 2015.

Bergman, W. (2016a) Comments on MSU filter efficiency testing based on preliminary design 4 test results from November 11-13, 2015, Bechtel report, February 9, 2016.

Bergman, W. (2016b) Analytical model of HEPA filter loading for fire safety analysis, Proceedings of the 34th International Nuclear Air Cleaning Conference, San Antonio, TX, June 5-7, 2016. www.isnatt.org

Bergman, W. (2017) Pressure drop measurements of the WTP radial flow HEPA filters, Bechtel report, July 9, 2017.

Bergman, W (2018) Unpublished data on qualification test for steel HEPA filter described in Bergman et al (1991).

Cambo, W.H., Whitely, E.F., and Bond, L.E.(1987) US. Patent 4,687,697, Composite having improved transverse structural integrity and flexibility for use in high temperture environments.

Choi, H-J., Kumita, M., Seto, T., Inui, Y, Bao, L., Fujimoto, T., and Otani, Y. (2017) Effect of slip flow on pressure drop of nanofiber filters, J. Aerosol Science, 114, 244-249. https://www.sciencedirect.com/science/article/pii/S0021850217301702?via%3Dihub

Clarenburg, L.A. and Schiereck, F.C. (1968) Aerosol filters-II Theory of the pressure drop across multi-component glass fibre filters, Chemical Engineering Science, V. 23, pp. 773-781.
https://www.sciencedirect.com/science/article/pii/0009250968850122

Cox, S., Cho, H., and Waggoner, C.A. (2016) A review on real-time aerosol measurement techniques and their correlations, Proceedings of the 34th International Nuclear Air Cleaning Conference, San Antonio, TX, June 5-7, 2016. www.isnatt.org

Dahl, S. Biyani, R. and Holmes, E. (2012) Full focus needed on finishing Hanford's Waste Treatment Plant, Waste Management 2012,
www.wmsym.org/archives/2012/papers/12196.pdf

Defense Nuclear Facilities Safety Board (2012) Letter to DOE Secretary Chu recognizing Ms. Elaine Diaz as winner of DOE Safety System Oversight Annual Award https://www.dnfsb.gov/documents/letters/board-pleased-recognize-ms-elaine-n-diaz-hanford-site-office-river-protection-was

DOE (2013) Operating Experience Level 3: Laboratory tests indicate conditions that could potentially impact certain type of HEPA filter performance.
https://www.energy.gov/sites/default/files/2014/06/f16/OE-3_2013-02.pdf

Diaz, E. (2010) DOE Office of River Protection, Test plan for the Institute for Clean Energy Technology, Mississippi State University to determine particle loading and structural damage to Flanders radial flow HEPA filters developed with input from

Bechtel, DOE, Flanders, academia, users within the DOE complex, and the Defense Nuclear Facilities Safety Board. May, 12, 2010.

DOE-STD-3020 (2015) Specification for HEPA filters used by DOE contractors, https://www.standards.doe.gov/standards-documents/3000/3020-astd-2015/@@images/file

DOE-STD-3025 (2022) Quality assurance inspection and testing of HEPA filters https://www.standards.doe.gov/standards-documents/3000/3025-astd-2022/@@images/file

Duvekot, E., Amey, C., Wilsinson, P., and Williams, A. (2017) Development of high strength HEPA filters for use in demanding air and gas streams. Paper 17644 at Waste Management 2017 Conference, Phoenix, Arizona, March 5-9, 2017.

Dyment, J. and Loughborough, D.(1997) The effect of media area on the dust holding capacity of deep pleated HEPA filers. Proceedings of the 24th DOE/NRC Nuclear Air Cleaning and Treatment Conference, CONF-960715, M.W. First, Ed., NTIS, Springfield, VA, pp. 708-742, August, 1997. (available at www.isnatt.org)

EN- 1822 (2009) High efficiency air filters, European Standards, https://www.en-standard.eu/set-csn-en-1822-1-5-air-filters-epa-hepa-and-ulpa/

Filippone, A. (2001) Surface riblets for aerodynamic drag reduction, https://aerodyn.org/riblets.

Flour Daniel (1991) A conceptual study of metal fiber filters for nuclear air cleaning in the HWVP, US DOE Richland Operations Office, Contract DE-AC06-86RL10838 https://pdw.hanford.gov/arpir/pdf.cfm?accession=D196039033

Fenton, D.L., Gunaji, M.V., Tang, P.K. and Martin, R.A. (1986) Combustion aerosol loading of HEPA filters, in Gaseous Effluent Treatment in Nuclear Installation, G. Fraser and F. Luykx, eds. Graham and Trotman pp. 851-864.

Garcia, G. (2012a) Nuclear Grade High Efficiency Particulate Air (HEPA) Filters (ASME AG-1, Section FK Filters), Bechtel Report 24590-WTP-3PS-MKH0-T0002

Garcia, G. (2012b) High Efficiency Particulate Air (HEPA) Filter Test Specification, Bechtel Report 24590-WTP-3PS-MKH0-T0014

Garcia, G. and Kramer, Z. (2014) Development of a resistance to liquid pressure test system (RLPTS) for qualifying HEPA filters, Proceedings of the 33rd Nuclear Air Cleaning, St Louis, MO, June 22-24, 2014. www.isnatt.org

Garcia, G. (2015) HEPA Filter Qualification Test Plan, Bechtel Report 24590-WTP-ES-HV-15-001

Grewal, G., Milatovice, Z., Landon, F., and Harty, W.M. (1993) Application of high efficiency metal fiber filters in ventilation systems of non-reactor nuclear facilities, in Proceedings of the 22nd DOE/NRC Nuclear Air Cleaning Conference, Denver, Co, August 24-27, 1992, UCRL-JC-1099769, January 1993, pp. 574-585. (available at www.isnatt.org)

Giffin, P.K., Parsons, M.S., Wilson, J.A., and Waggoner, C.A. (2012) Performance comparison of dimple pleat and ribbon separated radial flow HEPA filters, Proceedings of the 32nd International Nuclear Air Cleaning Conference, Denver, CO June 17-19, 2012 (www.isnatt.org)

Gilbert, H., Bergman, W., and Fretthold, J.K. (1992) Development and evaluation of a HEPA filter for increased strength and resistance to elevated temperature, 22nd DOE/NRC Nuclear Air Cleaning and Treatment Conference, https://www.isnatt.org/

Gregory,W.S. and Smith,P.R. (1982) "Response to standard and high-capacity HEPA filters to simulated tornado and explosive transients." Los Alamos National Laboratory Report LA-9210-MS, http://lib-www.lanl.gov/cgi-bin/getfile?00307462.pdf

Gregory, W.S., Martin, R.A., Smith, P.R., and Fenton, D.E. (1983) Response of HEPA filters to simulated accident conditions, Proceedings of the 17th DOE Nuclear Air Cleaning Conference, M.W. First, Editor, Denver, CO, August 2-5, 1982, CONF-820833, pp. 1052- 1068. www.isnatt.org

Hedges, J. (2008) State Compliance Agreements: the Hanford Federal Facility Agreement and Consent Order, *http://www.ncsl.org/documents/environ/JHedges1009.pdf*

Hettkamp, P., Kasper, G., and Meyer, J. (2012) Simulation of pressure drop and capacity for pleated air filters loaded with dust, Filtration 12(3), p. 185-194. www.afssociety.org/about-afs/filtration-journal/

Hinds,W.C. (1999) Aerosol Technology: properties, behavior and measurement of airborne particles. John Wiley.

Horak,H.L., Gregory,W.S.,Ricketts,C.I.and Smith,P.R. (1982) "Structural performance of HEPA filters under simulated tornado conditions" Los Alamos National Laboratory Report LA-9197-MS, Nuclear Regulatory Agency Report, NUREG/CR-2565, http://lib-www.lanl.gov/cgi-bin/getfile?00312786.pdf

IEST-RP-CC007 (2007) Testing ULPA filters, Institute of Environmental Science and Technology, http://www.iest.org/Standards-RPs/Recommended-Practices/IEST-RP-CC007

Jennings, S. G., (1988) The mean free path in air, J. Aerosol Science, Vol.19, No. 2. Pp.159-166. https://www.sciencedirect.com/science/article/pii/0021850288902194

Kirsch, A.A., Stechkina, I.B., and Fuchs, N.A. (1973) Effect of gas slip on the pressure drop in fibrous filters, J. Aerosol Science, 4, pp. 287-293, https://www.sciencedirect.com/science/article/pii/002185027390089X

Kramer, Z., Dick, J., Wilson, R. (2014) Development of high strength HEPA filters for Hanford's Waste Treatment Plant (WTP), Proceedings of the 33rd Nuclear Air Cleaning, St Louis, MO, June 22-24, 2014. www.isnatt.org

Kuhnen, J., Scarselli, D., Schaner, M. and Hof, B., (2018) Relaminarization by steady modification of the streamwise velocity profile in a pipe, Flow Turbulence Combustion, Vol. 100, pp. 919-943.

Kulkarni, P., Baron, P.A., and Willeke, K. (2011) Aerosol Measurement: Principles, Techniques, and Applications, Third Edition, John Wiley & Sons

Loughborough, D. (1991) The dust holding capacity of HEPA filters, Proceedings of the 21st DOE/NRC Nuclear Air Cleaning Conference, M.W. First, Editor, San Diego, CA, Aug. 13-16, 1990, NUREG/CP-0116, CONF-900813, pp. 155-172 www.isnatt.org

Navennti, R. (2002) Bechtel National Inc. Waste Treatment Plant Project, Proceedings of the 27th Nuclear Air Cleaning & Treatment Conference, September 2002, Nashville, TN www.isnatt.org

Norton, O.P. (2013a) Notes on fluid selection for liquid pressure testing, Institute for Clean Energy Technology, MSU report, August 8, 2013

Norton, O.P. (2013b) Heater requirements for liquid pressure testing , Institute for Clean Energy Technology, MSU report, December 5, 2013

NQA-1 (2012) Quality Assurance Requirements for Nuclear Facility Applications, ASME, https://www.asme.org/products/codes-standards/nqa1-2012-quality-assurance-requirements-nucle-(1)

Okemgbo, A. (2009) Grout treatment facility regulatory closure final report, attachment to Washington Department of Ecology letter to DOE Office of River Protection, https://pdw.hanford.gov/arpir/pdf.cfm?accession=0908251097

Peebles, B. (2003) BLU-JEL Pressure Test, Flanders Job Number: 23-027, Flanders/CSC , July, 3, 2003.

Phillips, K, Rickert, J. and Waggoner, C.A. (2016) Proceedings of 34th Nuclear Air Cleaning Conference, San Antonio, TX, June 5-7, 2016. www.isnatt.org

Phillips, S., Cho, H., and Waggoner, C.A. (2016) Design and characterization of a test stand for performance evaluation of flat filter media, Proceedings of 34th Nuclear Air Cleaning Conference, San Antonio, TX, June 5-7, 2016. www.isnatt.org

Pilat, M.J., Ensor, D.S., and Bosch, J.C. (1970) Source test cascade impactor, Atmospheric Environment, Vol. 4, pp. 671-679, https://faculty.washington.edu/mpilat/Impactor.PDF

Pratt, R.P. (1986). The performance of filters under hot dynamic conditions, pp. 824-836, in Gaseous Effluent Treatment in Nuclear Installations, Graham & Trotman Limited, London, UK

Ricketts, C.I., Smith, P.R. and Jensma, N.R. (1998) A New Concept for Qualification and Quality Assurance of HEPA Filter Mechanical Reliability, Proceedings of the 25th DOE/NRC Nuclear Air Cleaning and Treatment Conference, MW. First Editor, NUREG/CP-0167, CONF-980803, Minneapolis, MN August 3-6, 1998 www.isnatt.org

Ricketts, C.I., Ricketts, P.H., and Smith, P.R. (2006) Filter performance specifications and a prototype test apparatus for the qualification of high-strength HEPA filter designs, Proceedings of the 28th Nuclear Air Cleaning Conference, Albuquerque, NM, September 7-29, 2004 www.isnatt.org

Ricketts, C.I., Cambo, W. H., and Stillo, A. (2008) Realization of filter performance specifications for the qualification of high-strength HEPA filters, Proceedings of the 30th Nuclear Air Cleaning Conference, Seattlle, WA, August 25-17, 2008* www.isnatt.org

Ricketts, C.I., Stillo, A., Cambo, W. H. (2010) Realization of performance specifications for the qualification of high-strength HEPA filters, Proceedings of the 31st Nuclear Air Cleaning Conference, Charlotte, NC, July 19-21, 2010 www.isnatt.org

Ricketts, C.I., Stillo, A., Cambo, W. H. (2012) Performance specifications and test protocols for the qualification of high-strength HEPA filters, Proceedings of the 32nd Nuclear Air Cleaning Conference, Denver, CO, June 17-19, 2012 www.isnatt.org

Rouse, J.K. (2000) Hanford RPP-WTP high-level waste vitrification offgas system, Proceedings of the 26th Nuclear Air Cleaning and Treatment Conference, Richland, WA, Sept. 11-12, 2000, (www.isnatt.org)

Rudinger, V., Ricketts, C.I., and Wilhelm, J.G. (1990) High-Strength High-Efficiency Particulate Air Filters for Nuclear Applications, Nuclear Technology, Vol. 92, Oct. 1990, pp. 11-38.

Stillo, A. (2015) Filter efficiency and pressure drop for clean HEPA filters at 100% and 20% flow measured at Camfil and at the US Army Aberdeen Proving Ground and the filter efficiency and pressure drop for the post wet pressure test at 20% flow measured at the US Army Aberdeen Proving Ground, Feb. 17, 2015.

Tewarson, A. (1995), "Generation of Heat and Chemical Compounds in Fires" Section, 3, Chapter 4, SFPE Handbook of Fire Protection Engineering, 2Nd Edition, National Fire Protection Association, Quincy, MA, 1995.

ter Kuile and Doing (1999) Circular HEPA filters for use in nuclear containment and ventilation systems, Minneapolis, MN, August 3-6, 1998, (www.isnatt.org)

Thomas, D., Charvet , A., Bardin-Monnier, N., and Appert-Collin, J.C. (2017) Aerosol Filtration, Elsevier, Oxford, UK.

Unz, R., Wilson, J.,McCown, J., and Waggoner, C. (2014) Infrastructure for testing and qualifying robust radial flow HEPA filters, Proceedings of the 33rd Nuclear Air Cleaning, St Louis, MO, June 22-24, 2014. www.isnatt.org

J. C. Urton (2005) Inverted use of Blu-Jel seal filter under vacuum, Flanders, F/CSC Job No. 23-027, June 7, 2005.

Van Beek, J.E. and Wodrich, D.D. (1990) Grout disposal system for Hanford Site mixed waste, Waste Management 1990, www.wmsym.org/archives/1990/V1/121.pdf

Waggoner, C (2012) Is a filter loading qualification test needed? Proceedings of the 32nd International Nuclear Air Cleaning Conference, Denver, CO June 17-19, 2012 (www.isnatt.org)

Weamer, J. (2012a) WTP HEPA Filter Data, e-mail on July 30, 2012.

Weamer, J. (2012b) Path forward for WTP radial HEPA filter issue, presentation to Bechtel and DOE, August 29, 2012

Wilson, J.A., Waggoner, C.A., Rickert, J., and McCowan, J. (2016) Infrastructure and test methods for evaluation of AG-1 Section FK 2000 cfm radial flow filters, Proceedings of 34th Nuclear Air Cleaning Conference, San Antonio, TX, June 5-7, 2016. www.isnatt.org

Wong, M., Cho, H., and Waggoner, C.A. (2016) Design and performance of an in-place flat media particle loading testing system, Proceedings of the 34th Nuclear Air Cleaning Conference, June 5-7, 2016, San Antonio, TX www.isnatt.org

ACKNOWLEDGEMENT

The authors gratefully acknowledge the financial and technical support from Bechtel National Inc. that made this study possible.

This project was a team effort by six organizations and many people who worked tirelessly for 5 years to its successful completion. A special acknowledgement is given to Elaine (Diaz) Porcaro from the Department of Energy, River Protection Project, Richland, WA. She had identified the problems with the commercial HEPA filters, initiated the project with Bechtel National Inc. to correct these problems and shepherded the project from its inception to completion. C. Ricketts provided valuable input to Ms. (Diaz) Porcaro and the project through his many reviews of technical issues.

The project was skillfully planned and executed by the following dedicated team of managers and engineers at Bechtel National, Inc., Richland, WA: J. Weamer, T. Houck, J. Dick, Z. Kramer, S. Crow, G. Dalton, S. Anderson, and D. Howard.

The following managers, scientists and engineers at the Institute for Clean Energy Technology, Mississippi State University, Starkville, MS developed new and improved filter test technologies and conducted extensive filter testing : J. Rickert, J. Wilson, J. Stormo, R. Unz, P. Norton, J. McCown, T. Wofford, H. Cho, S. Phillips, M. Wong,

We are grateful to the following engineers from Kurion Inc., Richland, WA, for developing prototype filters: J. Kriskovich, D. Roome, B. Carpenter, J. Parham, J. Frethold, R. Sexton, and A. Frost.

We also gratefully acknowledge the development of the high-strength HEPA filter by the following engineers from the Porvair Filtration Group, Fareham, UK and Ashland, VA, for developing and producing the final successful filter: E. Duvekot, C. Amey, P. Wilkinson, and A. Williams

Finally we acknowledge the critical role of Lydall Inc., Rochester, NH and its engineers, B. Cambo and S. Gross, for providing the high-strength HEPA media that was the basis of the high-strength HEPA filter and for providing supporting tests and advice. Bill Cambo was one of the inventors of the high-strength glass-fiber filter technology.